STRATEGIES TO EVADE IMMUNE RESPONSE AGAINST ADENO-ASSOCIATED VIRUS VECTORS DURING GENE THERAPY

SANGEETHA HAREENDRAN

PHD THESIS

2015

CENTRE FOR STEM CELL RESEARCH (A UNIT OF INSTEM, BENGALURU)
CHRISTIAN MEDICAL COLLEGE, VELLORE

SREE CHITRA TIRUNAL INSTITUTE
FOR
MEDICAL SCIENCES AND TECHNOLOGY, TRIVANDRUM
Thiruvananthapuram

STRATEGIES TO EVADE IMMUNE RESPONSE AGAINST ADENO-ASSOCIATED VIRUS VECTORS DURING GENE THERAPY

A THESIS PRESENTED BY

SANGEETHA HAREENDRAN

Centre for Stem Cell Research (A unit of inStem, Bengaluru)
Christian Medical College, Vellore

TO

THE SREE CHITRA TIRUNAL INSTITUTE FOR
MEDICAL SCIENCES AND TECHNOLOGY, TRIVANDRUM
Thiruvananthapuram

IN PARTIAL FULFILMENT OF THE REQUIREMENTS
FOR THE AWARD OF
DOCTOR OF PHILOSOPHY

2015

DECLARATION BY STUDENT

I, Sangeetha Hareendran hereby certify that I had personally carried out the work depicted in the thesis, entitled, “Strategies to evade immune response against adeno-associated virus vectors during gene therapy”.

No part of the thesis has been submitted for the award of any other degree or diploma prior to this date.

Signature: 

Name of the Candidate: Sangeetha Hareendran

Date: 17/06/2016

CERTIFICATE BY GUIDE

Dr.Alok Srivastava, MD, FRACP, FRCPA, FRCP
Professor of Medicine and Head,
Centre for Stem Cell Research (A unit of inStem, Bengaluru),
Christian Medical College Bhagayam Campus, Vellore
Tamil Nadu-632002

This is to certify that Sangeetha Hareendran in the Centre for Stem Cell Research of Christian Medical College, Vellore has fulfilled the requirements prescribed for the Ph.D degree of the Sree Chitra Tirunal Institute for Medical Sciences and Technology, Trivandrum.

The Thesis entitled, "Strategies to evade immune response against adeno-associated virus vectors during gene therapy" was carried out under my direct supervision. No part of the thesis was submitted for the award of any degree or diploma prior to this date.

*Clearance was obtained from the Institutional Ethics committee for carrying out the study.

Signature:

Date: 17/6/2016

ALOK SRIVASTAVA
Professor of Medicine
Head, Centre for Stem Cell Research,
(A Unit of inStem, Bengaluru)
Christian Medical College Campus,
Bagayam, Vellore - 632 002, Tamil Nadu, India.

CENTRE FOR STEM CELL RESEARCH
Christian Medical College Campus, Bagayam, Vellore - 632 002, Tamil Nadu, India.
CHRISTIAN MEDICAL COLLEGE

The Thesis entitled

Strategies to evade immune response against adeno-associated virus vectors during gene therapy

Submitted by

Sangeetha Hareendran

for the degree of

Doctor of Philosophy

of

SREE CHITRA TIRUNAL INSTITUTE

FOR

MEDICAL SCIENCES AND TECHNOLOGY, TRIVANDRUM

Thiruvananthapuram

Is evaluated and approved by

Dr. Alok Srivastava

(Guide)

Dr. Srikala Raghavan

(External examiner)

ACKNOWLEDGEMENTS

At this juncture of bringing an end to my PhD research, I acknowledge the people who have been instrumental in making this happen. I sincerely appreciate each of them who have contributed in one way or the other to make this study practically possible.

Foremost I would like to thank Dr. Alok Srivastava, my guide and mentor. His constant support, valuable suggestions and constructive criticisms have immensely helped me, right from the start of my research work till the completion of this thesis. I am deeply indebted to him for mentoring my scientific pursuits and for always encouraging me to do better. I owe the success of this study to Dr. Jayandharan GR, my supervisor. His generous efforts in guiding me through every aspect of this PhD work with patience and wisdom are greatly appreciated. I wholeheartedly thank him for inspiring me and helping me keep the spirits high at the face of obstacles during this endeavor. He has taken at most care to improvise my scientific skills and temperament, for which I am extremely obliged to him.

I wish to extend my gratitude to other faculty members of my department, Dr. Sanjay Kumar, Dr. Rekha Samuel and Dr. Aparna V for their encouragement and support. I am grateful to Dr. Shaji RV for his assistance and advice regarding the PhD programme and thesis submission. The efforts he took in successfully conducting our course work and exams are truly appreciated. I am grateful to Dr. Vikram Mathews, Department of Hematology, CMC and Dr. Solomon Satishkumar, Department of Physiology, CMC for all their guidance and support.

I sincerely acknowledge the funding support received from CSIR, Government of India towards my Senior Research Fellowship during PhD. I also

thank Bayer Hemophilia award and DBT, Government of India grants-in award to Dr. Jayandharan for providing financial support for this study.

My special thanks go to the animal facility in-charge, Dr. Pratheesh, former faculty, Dr. Sumathy and the Lab technicians, Satish, Esther and Pavithra for their helpful, supportive and friendly disposition. I am appreciative of the help and support rendered by the core- lab supervisor, Vaidhyanathan and technician, Saranya. Among the office staff, I express my gratitude to Tamilvanan, Selvi, Muthukrishnan, Shirley, Anu madam and Geetha for being friendly and always willing to help.

I take this opportunity to thank my friend Vaani Roshini, who stood by me through thick and thin. She has unhesitatingly helped me in many technical aspects of this study and above all, has always been dependable and friendly. I shared a special rapport both personally and scientifically with Nishanth and Dr. Sabna. Enthusiastic discussions with them have helped me gain valuable insights about science and life. I am obliged to Balaji, Dr. Sen, Dr. Ruchita and Akshaya for their support and friendship.

I am fortunate to have good friends like Ajay, Abbas, Sachin, Kannan and Nancy whose company made my PhD life breezy and a memorable one. I thank my dear friends Ansu and Divya, for their affection and encouragement, which helped me face many tough times with hope and confidence. My appreciation goes to Sumitha E, Saravanan,Sumitha PB, Thiagi, Musheer, Janaki, Suresh and Augustine for their help and motivation. Guiding and interacting with project students Mansoor, Ramya, Prachi, Shantoshini, Satish, Kayal and Prateepa was a fun-filled learning experience. I am indebted to all my other colleagues who have rendered their support and help during the course of my research.

I fall in short of words to thank my parents, who have been my pillars of strength and support throughout these persevering years of PhD. Without their unfailing love, sacrifice and encouragement, I would not have accomplished this feat. Their faith in my abilities fuelled my aspirations and inspired me to work with determination till the end. I am indebted to my brother Sooraj for his affection and encouragement. I fondly remember my late grandparents, for their nurturing love and support, which instilled in me the confidence to succeed.

My husband, Krishnakumar has been a source of constant love, support and motivation. I wish to thank and reciprocate my love to him for being a true definition of companionship. Our son, Aniketh has added infinite joy and meaning to life, whose mere presence is a fountain of blessing. All this has been possible only because of the grace and blessing of the Almighty. With at most gratefulness, I surrender all my deeds and actions at His holy feet.

TABLE OF CONTENTS

LIST OF FIGURES

Page

LIST OF TABLES

ABBREVIATIONS

AAP	Assembly activating protein
AAT	Alpha-1 antitrypsin
AAV	Adeno-associated virus
Ad	Adenovirus
ADA	Adenosine deaminase
ALT	Alanine transaminase
APC	Antigen presenting cell
AST	Aspartate transaminase
BDD	B-domain deleted
Cap	Capsid
TCR	T cell receptor
CFTR	Cystic fibrosis transmembrane conductance regulator
CPK	Creatine phosphokinase
CTL	Cytotoxic T lymphocyte
CTLA-4	Cytotoxic T lymphocyte associated protein 4
DC	Dendritic cells
DMD	Duchenne muscular dystrophy
DMSO	Dimethyl sulfoxide
dNTP	Deoxynucleotide triphosphate
EBV	Epstein-Barr virus
EGFP	Enhanced green fluorescent protein
ELISA	Enzyme-linked immunosorbent assay
FACS	Fluorescence activated cell sorter
GAPDH	Glyceraldehyde-3-phosphatedehydrogenase
HEK	Human embryonic kidney
HIV	Human immunodeficiency virus
HSC	Hematopoietic stem cells
HSPG	Heparin sulphate proteoglycan
HSV	Herpes simplex virus

hTERT	Human telomerase reverse transcriptase
HTLV	Human T celllymphotropic virus
IEE	Integration efficiency element
IFN	Interferon
Ig	Immunoglobulin
IKK	IκB kinase
IL	Interleukin
ITR	Inverted terminal repeat
IVIG	Intravenous immunoglobulin
LCA	Leber's congenital amaurosis
LPL	Lipoprotein lipase deficiency
MHC	Major histocompatibility complex
MMF	Mycophenolate mofetil
MTT	3-(4,5-Dimethylthiazol-2-Yl)-2,5-Diphenyltetrazolium Bromide
Nab	Neutralizing antibodies
NEMO	NF-κB essential modulator
NF-κB	Nuclear factor-κB
NHEJ	Non-homologous end joining
NHP	Non-human primate
NIK	NF-κB inducing kinase
ORF	Open reading frame
OTC	Ornithine transcarbamylase deficiency
PAMP	Pathogen associated molecular motif
PARP	Poly ADP-ribose polymerase
PBMNC	Peripheral mononuclear cells
PBS	Phosphate buffer saline
PCR	Polymerase chain reaction
PEG	Poly-ethylene glycol
PI3K	Phosphoinositide 3-kinase
PLA2	Phospholipase A2
PRR	Pattern recognition receptor

RBE	Rep binding element
Rep	Replication
RPE-65	Retinal pigment epithelium-specific 65kD protein
RSV	Rous sarcoma virus
S/T	Serine/ threonine
Sc	Self-complementary
SCID	Severe combined immunodeficiency
Ss	Single-stranded
TE	Tris-EDTA
TG	Triglyceride
TGF	Transforming growth factor
TLR	Toll-like receptor
TMV	Tobacco mosaic virus
TNFR	Tumor necrosis factor receptor
Treg	Regulatory T cell
Trs	Terminal resolution site
UPR	Unfolded protein response
Vgs	Viral genomes
VP	Viral protein

PhD SYNOPSIS

Background

Recombinant adeno-associated virus (AAV) has proven to be a promising gene therapy vector for treatment of diseases such as leber's congenital amaurosis, hemophilia B, α1- anti-trypsin deficiency, muscular dystrophy and Parkinson disease. One of the limitations noted in clinical trials is the T cell mediated immune response in patients administered with high vector doses.Hence strategies to attenuate the vector targeted- innate and/ or adaptive immune responses are a prerequisite to further improve the clinical outcome in AAV-mediated gene therapy.

Objectives

1. To study the role of NF-κB and associated proteins such as PARP-1 in AAV-mediated gene transfer both *in vitro* and *in vivo*
2. To test bio-engineered AAV vectors *in vitro* and *in vivo,* either in the presence or absence of NF-κB/PARP-1 inhibitors to achieve efficient gene delivery
3. Evaluate the optimal AAV vectors and NF-κB/PARP-1 modulation strategy in pre-clinical diseases models such as of hemophilia

Hypothesis

1. Inhibition of NF-κB pathway and associated proteins can modulate the host immune response against AAV vectors during gene therapy.
2. Targeted modifications on AAV capsid can generate vectors with improved efficacy.

Methods

Cell lines: Human cervical carcinoma cell line (HeLa) and the packaging cell line for the vectors, AAV293 (Stratagene, Santa Clara, CA, USA) were maintained in IMDM medium supplemented with 10% FBS and Penicillin-streptomycin at 37°C and 5% CO_2.

***Site-directed mutagenesis*:** Serine (S) →Alanine (A), Threonine (T) → A (Alanine) mutations were introduced on the AAV2 rep/cap plasmid by QuikChange II XL Site-Directed Mutagenesis Kit (Stratagene, La Jolla, CA, USA) and the presence of the desired point mutation was verified by restriction digestion analysis and DNA sequencing.

***Generation of recombinant vectors*:** AAV vectors containing enhanced green fluorescent protein (EGFP) gene or luciferase (luc) gene as transgene were generated by polyethylene-imine based triple transfection of AAV-293 cells.

Recombinant AAV vector transduction assays in vitro and in vivo: For *in vitro* studies, Hela cells were either mock infected or infected with appropriate AAV vectors. For PARP-1 and NF-κB inhibition assays, the inhibitors were added 24 hours prior to the virus infection. Forty-eight hours post transduction, the transgene expression was measured by flow cytometry or fluorescence microscopy. For *in vivo*studies, 8-12 weeks old mice were mock-injected (PBS) or injected with AAV vectors *via* the tail vein. Mice were euthanized 4 weeks after vector administration. To study the CD8+ T cell response, a booster dose of the inhibitor and the vectors was given at two weeks time point. At the end of 4 weeks, the transgene (EGFP or luciferase) expression in the hepatic lobes was analyzed by fluorescence microscopy or live animal imaging.

Gene-expression analysis by real-time quantitative PCR: Mice pre-treated with appropriate compounds (Bay11-7085, PJ34, Bo or ABT) were either mock-injected or injected with ~5 x 10^{10} vgs of AAV2 vectors and euthanized 2 hours later. The cDNA synthesized from liver tissue was profiled by the NF-κB RT-PCR Profiler array (Qiagen, SABiosciences, Frederick, MD, USA).

ELISPOT/ELISA assay: Mouse splenocytes were seeded in a 96 well plate pre- coated with anti- IFNγ antibodies (MABTECH) and ELISPOT assay was performed. After 12-48 hours of incubation, the ELISPOT plate was developed by BCIP/NBT ALP reaction and spots formed were enumerated in an ELISPOT reader system while for ELISA, standard curve analysis was performed to determine the concentration of IFNγ protein in the cell culture supernatant.

Major findings

It was reasoned that combined inhibition of NF-κB pathway and associated proteins such as PARP-1 can modulate the host immune response against AAV vectors during gene therapy. Of these the role of NF-κB in modulating innate immune response to AAV is known. We first screened for potent inhibitors of NF-κB, which could target both the canonical and alternate pathways apart from previously reported inhibitor Bay11-7082. Three of commercially available small molecule inhibitors, Bay 11-7085, Isohelenin and Ro106 were thus evaluated for their ability to down-regulate a focused panel of genes related to NF-κB signal transduction. Of the three compounds tested, Bay11-7085 performed the best in terms of repression of the various NF-κB associated genes (>2 fold). It was then examined if PARP-1, a known co-activator of NF-κB, can regulate the gene transfer efficacy of AAV. Our data showed that PARP-1 repression significantly enhances the transgene expression from single-stranded AAV vectors both *in vitro* and *in*

vivo(APPENDIX Figure1A/B). Further it was found that PARP-1 inhibition using PJ34, a pharmacological inhibitor was effective in regulating innate immune response against AAV vectors when targeted to murine liver. PARP-1 blockade resulted in marked attenuation of the expression of various NF-κB driven pro-inflammatory factors in the liver tissue. Since multiple stimuli activate NF-κB associated genes, and not just PARP-1, we were prompted to investigate the effect of a combined inhibition of NF-κB signaling and PARP-1 on the host immune response against AAV. Indeed, several of the AAV vector induced pro-inflammatory and cytokine genes were significantly down-regulated in mice subjected to synergistic inhibition of PARP-1 and NF-κB, as shown in APPENDIX -Figure 1C.

It was further hypothesized that AAV2 capsid could be phosphorylated by cellular kinases, and this could trigger the degradation of AAV particles by the ubiquitin/ proteasome machinery. We thus modified specific serine/ threonine residues, which could be potential kinase targets, by site directed mutagenesis (Stratagene). Our data shows that some of the S/T→A mutant vectors demonstrate significantly higher transduction efficiencies compared to the wild-type AAV2 (scAAV2-WT) vector in Hela cells. These mutant vectors also exhibited increased transgene levels in the liver when injected into mice (APPENDIX Figure 2A).

Next step was to evaluate the effect of synergistic inhibition of PARP-1 and NF-κB on AAV vector transduction *in vivo*and modulation of the host immune response against AAV vectors (wild-type and mutant). Mice were administered 1mg/kg Bortezomib (Bo, for NF-κB inhibition) and 12.5 mg/kg ABT-888 (ABT, for PARP-1 inhibition) followed by intravenous administration of either AAV2 wild-type or a mutant AAV2 vector carrying luciferase reporter gene followed by a booster dose two weeks later. At the end of 4 weeks, IFNγ ELISPOT analysis

showed that the capsid driven CD8+ T cell response in the AAV2 wild-type injected mice decreased significantly in the Bo plus ABT group compared to the drug untreated mice (APPENDIX Figure 1C2B). There was no significant change in the T cell response upon NF-kB –PARP inhibition in the AAV2 mutant groups. This data suggests that the combination of drugs tested could have potential immunomodulatory effect on AAV2 based gene transfer, particularly when high doses of vectors would be needed to achieve clinical benefit.

Finally, this immune- suppression protocol was evaluated in Hemophilia B mice. Consistent with our previous data in normal mice, CD8+ T cell response against AAV vectors was significantly down-regulated in hemophilia B mice upon synergistic inhibition of PARP-1 and NF-kB (APPENDIX Figure3).

Significance of the findings

It has been previously shown that AAV activates immune related signaling pathways such as Toll-like receptor 9 (TLR-9), NF-κB and unfolded protein response (UPR). Hence our primary objective was to inhibit NF-κB, a transcription factor strongly linked to immune and inflammatory responses, and associated proteins such as PARP-1 in the context of AAV gene delivery. It was found that inhibition of PARP-1, a co-activator of NF-κB improves the transduction efficiency of AAV vectors, particularly of the single stranded virus. PARP-1 blockade was further effective in down- regulating the expression of innate immune response markers in mice administered with AAV2 vectors. The repression of AAV vector induced pro-inflammatory and cytokine genes' expression was more profound in mice subjected to synergistic inhibition of PARP-1 and NF-κB.

High doses of conventional AAV vectors have mostly been associated with immune responses in patients undergoing clinical trials, irrespective of the serotype used. To this effect, AAV2 variants were generated by mutating specific serine/ threonine residues on the viral capsid that exhibited enhanced transduction compared to conventional AAV2 vectors. Targeted modifications of serine/ threonine residues on AAV capsid is a constructive strategy to develop superior vectors as they could be administered at relatively low doses.

It was further evaluated if synergistic inhibition of PARP-1 and NF-κB pathway would modulate the CD8+ T cell response directed against AAV. ELISPOT analysis revealed that AAV capsid specific IFNγ secretion by activated CD8+T- cells was also significantly down-regulated in mice when both NF-κB pathway and PARP-1 was blocked while the transgene expression remained unaffected. The immune-modulation achieved using inhibitors of NF-κB pathway and PARP-1 in the context of AAV gene transfer was finally validated in a therapeutic model of Hemophilia B mice. To conclude, the synergistic immune suppression protocol targeting NF-κB signaling and PARP-1 proteins, proposed in this study could effectively suppress both pro-inflammatory as well as adaptive immune responses against AAV vectors during gene transfer.

SYNOPSIS APPENDIX

Figure 1

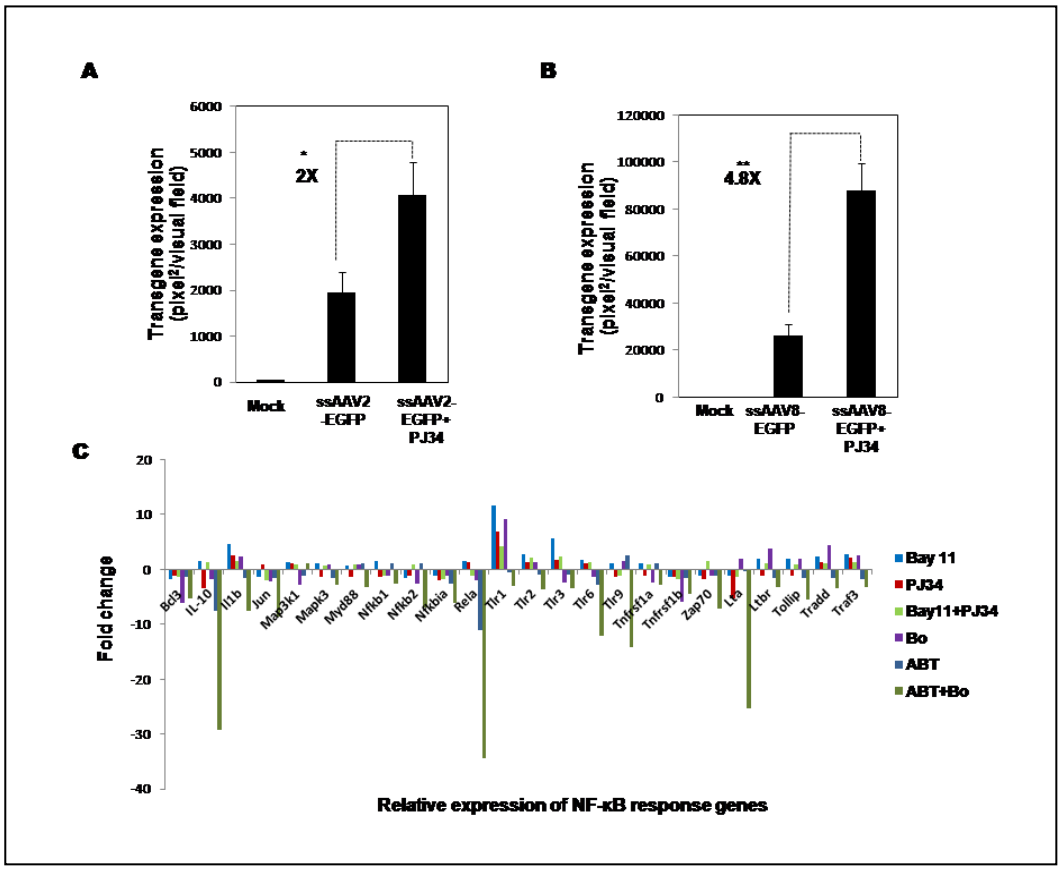

(A/B) *Pharmacological inhibition of PARP-1 during AAV-mediated hepatic gene transfer in vivo: Transgene expression was measured in liver sections of BALB/c mice 4 weeks after mock (PBS)-injection or administration of ssAAV2-EGFP/ ssAAV8-EGFP vectors alone or in the presence of PARP-1 inhibitor, PJ-34.* ***(C)*** *Combined inhibition of PARP1 and NF-κB down-regulates the expression of AAV vector-induced innate immune marker genes in murine liver.*

Figure 2

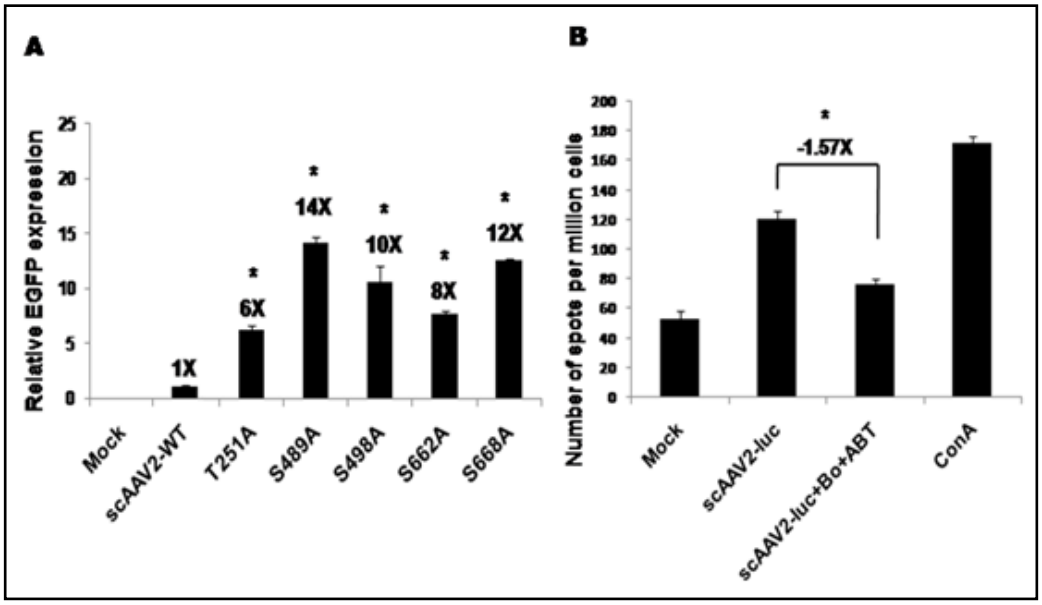

(A) *AAV2 serine/ threonine mutant vectors exhibit enhanced transduction upon hepatic gene transfer in vivo. Analysis of EGFP transcript levels by real-time quantitative PCR. Hepatic RNA isolated from animals injected with AAV2-WT, AAV2 S/T vectors were analyzed for EGFP expression and the data normalized to the GAPDH reference gene.****(B)*** *Combined inhibition of PARP1 and NF-κB modulates the CD8+ T cell immune response against AAV2 vectors. AAV2 capsid specific T cell response was quantitated by IFNγ based ELISPOT assay. The graph shows the number of spots generated per million splenocytes stimulated with AAV2 capsid specific peptide. Concanavalin A (ConA) was used as the positive control.*

Figure 3

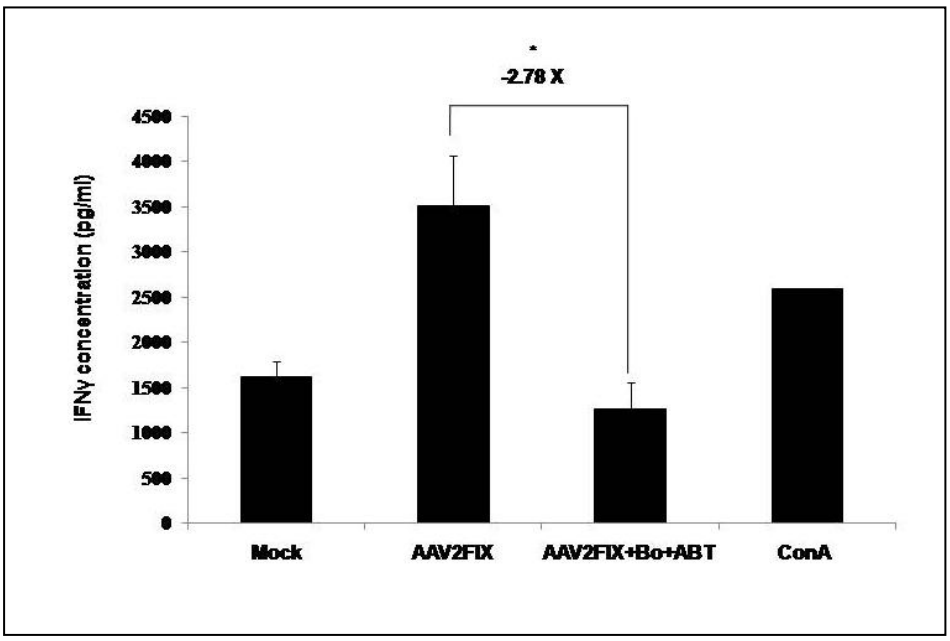

Modulation of AAV2 targeted CD8+ T cell immune response in hemophilia B mice upon combined inhibition of PARP1 and NF-κB. Graph shows the concentration of the IFNγ protein (pg/ml) secreted by activated T cells, and measured by ELISA. Splenocytes were isolated from mice under different treatment groups and stimulated with AAV2 capsid specific peptide in culture. Concanavalin A (ConA) was used as the positive control for T cell activation.

1. INTRODUCTION

The emergence of gene therapy in the late 1980s ushered in a new era of molecular genetic medicine. Progress in recombinant DNA technology and virus-based genetic manipulations gave momentum to this attractive treatment option. Gene therapy as the term suggests refers to the use of 'genes' as 'drugs'. It is a technology by which genes or small DNA or RNA molecules are delivered to human cells, tissues or organs to correct a genetic defect, or to provide new biological functions for the ultimate purpose of preventing or treating diseases(Lyon et al., 2008).Using an appropriate vehicle (vector), genes may be introduced into cells*ex vivo* (outside the body) and these modified cells could be subsequently re-administered to patients, or alternativelythe vector carrying the functional copy of gene could be directly administered to the patient (*in vivo*). In 1990, W.F Anderson and Michael Blaese conducted the first human gene therapy trial for treatment of adenosine deaminase-severe combined immunodeficiency (ADA-SCID) on a four-year-old patient by infusing retrovirus- modified T- lymphocytes expressing *ADA* gene(Blaese et al., 1995). Later, long term immune reconstitution was reported in other trials for ADA-SCID as well as X- linked SCID thus marking the success of gene therapy in correction of this disease phenotype (Cavazzana-Calvo et al., 2000, Aiuti et al., 2009)

Among the various indications addressed by gene therapy, success with monogenic disorders has been more evident(Ginn et al., 2013). Cystic fibrosis, SCID, muscular dystrophy, α-1 antitrypsin (AAT) deficiency, hemophilia, ornithine transcarbamylase (OTC) deficiency, lipoprotein lipase (LPL) deficiency, β-thalassaemia and Canavan disease are few examples of this disease category in

which gene therapy trials have been approved. A range of viruses including retrovirus, lentivirus, adenovirus, vaccinia virus, herpes simplex virus (HSV) and adeno- associated virus (AAV) have been used as vectors for gene transfer (Ginn et al., 2013). These viral vectors, engineered to be non-pathogenic and replication deficient are regarded as ideal gene transfer systems as they infect and deliver their genomes into the host cells, thereby enabling prolonged expression of any desired gene of interest (transgene). Nonetheless the risk of insertional mutagenesis and immune response in patients remain as major safety concerns while utilizing viruses for gene therapy. The unfortunate event of death of 18-year-old Jesse Gelsinger, treated for OTCdeficiency as a result of fatal inflammatory response to the adenovirus vector, lead to clinical disappointment and rendered a major setback to gene therapy (Raper et al., 2003). Further in 2002, four of the ten children in the French trial treated for X-linked SCID using autologous HSCs (hematopoietic stem cells) modified by murine retrovirus encoded IL-2 receptor γ chain developed leukemia following vector integration near the *LMO2* proto-oncogene promoter (Hacein-Bey-Abina et al., 2003). Non-viral gene delivery methods have gained attention as they can carry relatively large sized DNA, without being immunogenic. Despite this, their application in gene therapy is restricted due to relatively poor efficacy stemming from inefficient delivery of nucleic acids into target cells. Naked DNA/ plasmid and liposome- nanoparticles containing cationic lipid/ DNA complexes, delivered by electroporation or gene gun are the common non-virus based gene transfer systems explored for clinical application (Wang et al., 2013).

The adverse events noted in clinical trials advocated caution in the use of retrovirus and adenovirus as gene delivery vectors, and gave impetus to exploit alternative viruses such as AAV. AAV is classified under the genus *dependovirus* and belongs to the *parvoviridae* family. It is a small virus with a single stranded

genome of size 4.7Kb encased within an icosahedral non-enveloped protein capsid. The genome of AAV consists of 145bp long palindromic nucleotide sequences termed as inverted terminal repeats (ITR) flanking two ORFs (Open reading frames), *rep* and *cap*, genes of which encode for proteins involved in replication and virus structure (Daya & Berns, 2008). Some desirable features that make it attractive as a potential gene therapy vector are the lack of pathogenicity, low immunogenicity, infectivity in multiple cell types and more importantly, the stable integration of viral DNA into human genome at AAVS1 site thereby precluding incidence of cancer by insertional mutagenesis (Srivastava, 2008). Recombinant AAV (rAAV) is designed by replacing the two ORFs with the transgene in between the ITR sequences. Packaging of the rAAV vectors thus requires the *rep-cap* functions to be provided through a plasmid *in trans*. Traditional vector packaging of rAAV required co-infection with helper viruses such as adenovirus or herpes simplex virus, while currently the 'helper' gene functions are provided in the form of a plasmid (Xiao et al., 1998). Removal of *rep* genes in rAAV abrogate its ability to integrate to the host genome and therefore it exists as an episomal concatamer within the nucleus. For precisely this reason, it is more efficacious to use AAV to deliver genes into the post mitotic tissues such as liver, retina and brain, which exhibit relatively slow turnover than to rapidly dividing stem cells (Asokan et al., 2012).

Pre-clinical investigations in mice, dogs, non-human primates and other animals have yielded impressive results in the treatment of various genetic diseases using AAV. Cystic fibrosis was the first disease in which AAV-based gene therapy trial in human subjects was conducted (Wagner et al., 1998). Subsequently patients with hemophilia B, Parkinson disease, duchenne muscular dystrophy and AAT deficiency have been treated. In 2008-2009, a major milestone was achieved when sub-retinal administration of AAV2 expressing *RPE-65* (retinal pigment epithelium-

specific 65 kD protein) gene, restored vision and showed sustained improvement in patients suffering from Leber congenital amaurosis (LCA) (Bainbridge et al., 2008, Maguire et al., 2008). The first gene therapy product to receive approval for marketing by European commission is Alipogene tiparvovec (trade name Glybera), for treatment of LPL deficiency and is essentially an AAV1 vector expressing human *LPL* gene (Gaudet et al., 2013).

In a phase I/II dose escalation trial for hemophilia B, the patients who were infused high vector dose of AAV2 demonstrated *FIX* expression at therapeutic level of about 10% of normal. However, after 6- 8 weeks, a reduction of circulating FIX levels was observed which coincided with the asymptomatic elevation of serum transaminases. Later PBMNC analysis of one of the patients revealed CD8+ T cell response to the capsid that destroyed the vector transduced hepatocytes (Mingozzi et al., 2007). Capsid targeted CTL response, particularly in patients administered with high dose of virus particles, was also documented in trials for AAT and LPL with AAV1, and muscular dystrophy with AAV2 vectors (Hareendran et al., 2013). In the most recent trial for hemophilia B using AAV8 which showed long term efficacy in disease correction, the T cell response to the vector was moderated using glucocorticoid therapy(Nathwani et al., 2011).

In addition to CTL responses, pre-existing antibodies and presence of memory B cells or T cells in patients who had prior exposure to AAV infection can severely impact the outcome of gene transfer (Mingozzi & High, 2013). Natural infection of AAV early in life can cause anti-AAV antibodies to develop in the body. Epidemiology studies have estimated that ~70% of human population is seropositive for AAV2. Least seroprevalence (~38-40%) is noted for AAV5 and AAV8 serotypes, although there are concerns of cross- reactivity of neutralizing antibodies (Nab)

between serotypes (Calcedo et al., 2009, Boutin et al., 2010). The recently reported AAV trial for hemophilia B had excluded the patients who were seropositive for AAV8, projecting the limitation imposed by Nab(Nathwani et al., 2011). Taken together, these reports highlight that immune response directed against the infused vectors stands as a major obstacle to AAV gene therapy.

1.1 Rationale and Hypothesis

To realize the full potential of gene therapy using AAV vectors for the treatment of genetic disorders, it is necessary to minimize the immune response directed against them. The immune response documented in clinical trials clearly indicates a direct correlation to the vector dose administered. Vectors having enhanced transduction could possibly achieve therapeutic index even if delivered at lower doses, without causing immune activation. We reasoned that when AAV particles get internalized into the cell, they get phosphorylated at specific amino acids by kinases and this can signal the capsid ubiquination and their subsequent degradation by proteasome machinery. Improved efficacy of AAV2 vectors attained by introducing tyrosine to phenylalanine mutations on the capsid supports this line of thought (Petrs-Silva et al., 2009, Mowat et al., 2014). However, the effect of altering of capsid exposed serine/ threonine residues on AAV2 vector performance had not been explored. Therefore, in this study theselective modification of serine/ threonine (S/T) amino acids on AAV2 capsid was tested as an alternative approach to augment the transduction efficiency of these vectors.

AAV vector immunology can be regulated only if there is a better understanding of the mediators and signaling pathways associated with it. It has been previously shown that AAV infection activates the NF-κB pathway in murine

liver as a part of innate immune response (Jayandharan et al., 2011). On the other hand, the role of PARP-1, a DNA damage sensor protein and an NF-κB co-activator has not been studied before in the context of AAV transduction and immune response. Further the effect of blocking PARP-1 activity with concomitant inhibition of NF-κB on AAV-mediated gene transfer and modulation of host immune response is unknown. We thus aimed at developing a strategy for combined inhibition of PARP-1 and NF-κB pathwaysto suppress the innate and cytotoxic responses directed against the AAV vector.

Our study is highly relevant to the current scenario of AAV gene therapy, where immune challenges are major impediments for this treatment modality. We have investigated on two approaches to circumvent this complex problem. First by enhancing the transduction efficiency of AAV vectors by creating novel S/T →A mutations on the viral capsid and secondly, by directly addressing the vector targeted innate and cytotoxic responses.

1.2 Objectives of the Study

1. To study the role of NF-κB and associated proteins such as PARP-1 inAAV-mediated gene transfer both *in vitro* and *in vivo*.

2. To test bio-engineered AAV vectors *in vitro* and *in vivo*, either in the presence or absence of NF-κB/PARP-1 inhibitors to achieve efficient gene delivery.

3. Evaluate the optimal AAV vectors and NF-κB/PARP-1 modulation strategy in pre-clinical models of diseases such as hemophilia.

1.3 Brief Overview of the thesis chapters

1.3.1 Literature review and Material and methods

After introduction, the next major chapter in this thesis is the literature review, which elaborates on principles and practice of gene therapy describing its origin, the various tools used for gene transfer and the status of human clinical trials for various diseases. The description of basic biology of AAV vectors follows next. The problem of immune challenge towards AAV vectors during gene therapy is then described in detail followed by the various strategies tested to circumvent it. Brief descriptions on hemophilia disease, NF-κB signaling pathway and PARP-1 are also included in this chapter. In the next chapter, material and methods, the study design is outlined and the various techniques/ methods used for conducting experiments and analyzing data are described.

1.3.2 Results

The next main chapter is results obtained in the study. This chapter has been sub-divided into five parts.

1.3.2.1 Role of NF-κB in AAV-mediated gene transfer

In the first part, the effect of inhibiting NF-κB signaling pathway on the transduction efficiency of AAV2 was evaluated. As the activation of NF-κB pathway in response to AAV infection and its implications on gene transfer has already been described (Jayandharan et al., 2011), in this study only the effect of inhibiting this pathway on the vector transduction has been evaluated. A potent NF-κB inhibitor was further identified by screening commercially available inhibitors which target

the NF-κB pathway, by examining the modulatory effect on the expression of AAV vector induced pro-inflammatory marker genes associated with this pathway.

1.3.2.2 Role of PARP-1 protein in AAV- mediated gene transfer

In the second part, the effect of PARP-1 inhibition on AAV2 transduction has been assessed, both *in vitro* in cell line and *in vivo* during liver targeted gene delivery to mice. The regulatory effect of PARP-1 inhibition on the induction of pro-inflammatorycytokine/ chemokine gene expression in response to AAV2 infection was also examined.

1.3.2.3 Modification of AAV2 capsid at specific serine/threonine residues enhances the transduction efficiency of AAV2 vectors

Third section in this chapter deals with the bio-engineering of AAV2 capsid by selectively altering serine/ threonine (S/T) residues on it and further analyzing their effect on AAV2 transduction efficiency. Transgene expression of the AAV2 mutants relative to the wild-type vector was evaluated both *in vitro* in HeLa cells and*in vivo* in murine hepatocytes, after gene transfer. The effect of inhibiting S/T phosphorylating kinases in the host cells on AAV2 transduction was also examined.

1.3.2.4 Synergistic inhibition of PARP-1 and NF-κB pathway modulates immune response against AAV vectors in normal C57BL/6 mice

In the fourth section of results chapter, the modulation of immune response against AAV vectors by synergistic inhibition of PARP-1 and NF-κB in normal C57BL/6 mice, was investigated. Attenuation of both pro-inflammatory cytokine gene expression as well as CD8+ T cell responses against AAV2 was

evaluated. The effect on the *in vitro* transduction of AAV2 vectors upon combined inhibition of PARP-1 and NF-κB was also assessed. To determine if the immune modulation observed with AAV2 could be extended to other serotypes, similar studies using AAV8 vectors were conducted.

1.3.2.5 Evaluation of PARP-1 and NF-κB combined inhibition as an immunomodulation strategy against AAV2 vectors in hemophilia B mice model

Final part of this chapter provides proof of validation of the immune-modulation strategy in hemophilia B mice, administered with AAV2 vectors expressing human *FIX* gene. Data on the mitigation of the cytotoxic T cell response targeting the viral capsid and effect on AAV- mediated FIX expression, upon treatment with combination of drugs inhibiting PARP-1 and NF-κB is elaborated.

1.3.3 Discussion

The next main chapter is discussion wherein the significance of the major results obtained in this study has been described in detail. The data has been discussed in relation to the existing scientific knowledge on these subjects and with its implications of AAV gene therapy. In short, it has been explained how the transduction profile of AAV2 vectors could be improved by rationally modifying the serine/ threonine residues on the viral capsid and the relevance of this approach. For the first time, it is in this study that the role of PARP-1 in AAV- mediated gene transfer and in modulating the host immune response has been examined. A novel immune- suppression strategy of combined targeting of PARP-1 and NF-κB has been proposed and validated both in normal C57BL/6 mice and hemophilia B mice model

subjected to AAV gene therapy. At the end, the limitations and the future directions of the study have been outlined.

1.3.4 Summary and conclusions

In the final chapter, summary and conclusions, the major findings of the study and their implications in AAV gene therapy are summarized. In this study, two distinct approaches have been conceptualized and successfully tested, with the aim of moderating the immune response against AAV vectors.

2. LITERATURE REVIEW

2.1 Gene Therapy

2.1.1 Origin and evolution

In the early 20th century, Sir Archibald Garrod proposed the concept of chemical pathology on the basis of Mendelian laws of inheritance. According to this, human disorders result from the disruption of the normal metabolic pathways by inherited mistakes in the factors that regulate those pathways. Garrod termed these disorders as the 'inborn errors of metabolism' and the factors later came to be called 'genes'. This laid foundation for the modern understanding of genetic medicine, by not only expounding the mechanism of a genetic disease but suggesting a possibility of correcting it by providing the functional complement of the defective gene (Friedmann, 1992). In 1968, Stanfield Rogers demonstrated that viruses could be used for transferring foreign genetic material by infecting plants with poly(A)-modified tobacco mosaic virus (TMV) (Rogers & Pfuderer, 1968). Later in 1973, he reportedly attempted to treat two arginase deficient girls using an unmodified Shope papillomavirus (SPV), which has a viral arginase gene. However the clinical follow up of the trial is not documented (Rogers et al., 1973). The inception of recombinant DNA technology in 1972 facilitated the isolation and cloning of normal copies of disease causing genes to produce recombinant virus vectors (Shimotohno & Temin, 1981). The improved calcium phosphate transfection method described by Graham and van der Eb further lead to an upsurge in virus based genetic manipulation of mammalian cells (Graham & van der Eb, 1973). Martin Cline at the University of California applied this transfection method to modify bone marrow cells from two

patients with β- thalassemia with plasmids containing normal *β- globin* gene. Though technically it was the first human trial for gene therapy, it had not received regulatory approval and was terminated. The first approved gene therapy trial was conducted in 1990 by W.F Anderson and Michael Blaese on four-year-old Ashanti Desilva, who was suffering from ADA-SCID using T-lymphocytes modified *ex vivo*by retroviral vector expressing *ADA* gene (Blaese et al., 1995).

Dr Theodore Friedmann describes in his book, The Development of Human Gene Therapy, the following which emphasizes the tremendous relevance of the inception of this field:

'Interestingly, the birth and evolution of gene therapy have been, if not unique, certainly one of the more unusual scientific developments in modern biomedicine' (Friedmann, 1999).

Gene therapy has notably raised curative hopes for the treatment for two diseases, ADA-SCID and LCA, with amelioration of disease phenotypes in long term follow-up reports of patients enrolled in the clinical trials (Maguire et al., 2008, Aiuti et al., 2009). The growing interest of scientists and companies in this field can be reflected from the review publication by Ginn *et al* which collates information of more than 1800 clinical trials on gene therapy (Ginn et al., 2013). Gene therapy underwent a paradigm shift from being a genetic research domain to a clinical medicine in 2013 when Alipogene tiparvovec or Glybera (AAV1 expressing *LPL* gene) became the first gene therapy product to receive regulatory approval for marketing in Europe (Gaudet et al., 2013). Figure 1 shows the timeline of major events which contributed to the origin and evolution of human gene therapy.

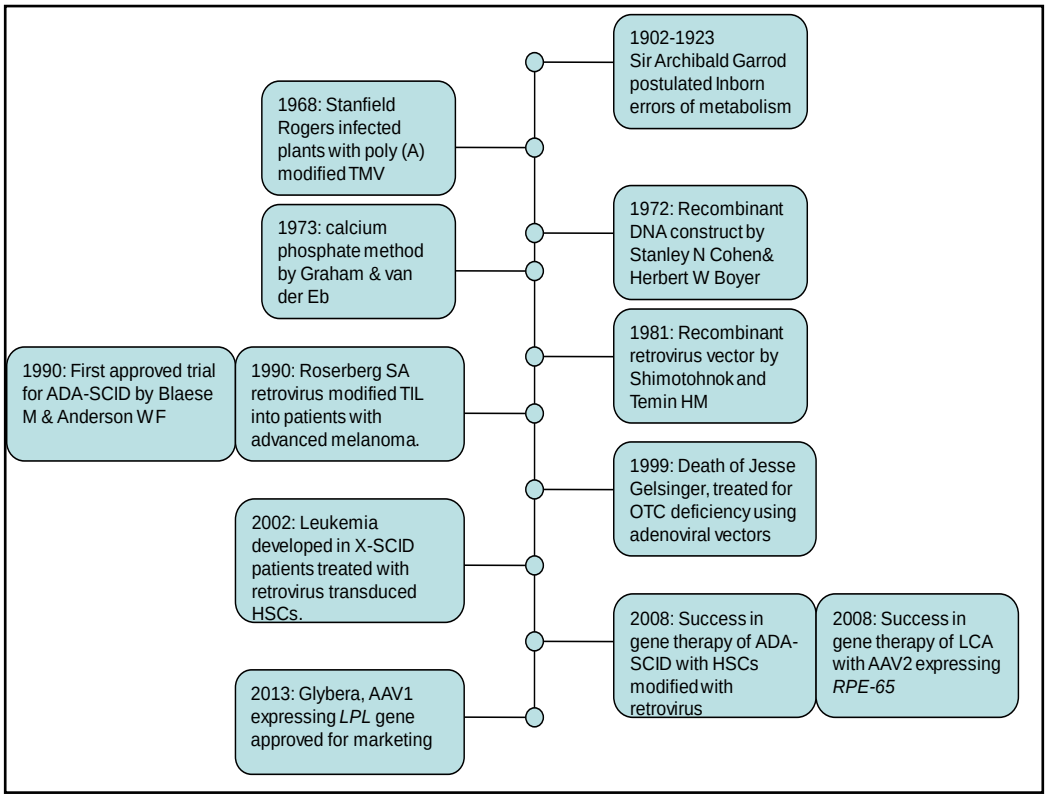

Figure 1: Timeline of milestones marking the origin and evolution of human gene therapy

2.1.2 Gene therapy vectors

Choosing the ideal vehicle or vector for gene delivery and expression is crucial to the success of gene therapy. The desirable features of efficient vector systems include the ability to achieve stable and sustained gene expression, tissue specific targeting, ease of production in large amounts and lack of pathogenicity or any kind of associated toxicity (Verma & Weitzman, 2005). Currently available vectors for gene therapy are broadly classified as non-viral and viral vectors. Non-viral gene transfer implicates delivery of naked DNA by physical methods such as electroporation, hydrodynamic, ultrasonic and biolistic gene guns or using synthetic DNA complexing agents like cationic liposomes (lipoplexes) or polymers

(polyplexes) (Wang et al., 2013). The cationic lipids (eg: DOTAP, DOTMA, DOSPA, DMRIE etc), cationic polymers (eg: Polyethyleneimine (PEI)), biodegradable cationic polysaccharides (eg: chitosan), or cationic polypeptides (eg: polylysine, protamine) are complexed with nucleic acids by electrostatic interactions (Yin et al., 2014). Some of the advantages of non-viral gene delivery systems include production in large scale, non-toxic and non-immunogenic profile and lack of constraint with regard to the size of DNA. However their application is mostly limited by transient gene expression and low efficacy of gene transfer (Zhang et al., 2012).

Viral vectors are considered ideal gene transfer systems because of their inherent ability to transfer genetic material into the host cell upon infection. Recombinant viral vectors are generated using vector constructs containing the transgene of interest and the transcriptional regulatory elements flanked by essential viral genes along with the packaging constructs which deliver the genes for replication and virion production (Verma & Weitzman, 2005). All dispensable genes responsible for the pathogenicity and antigenicity of the virions are deleted to produce replication defective vectors with minimal probability of recombination to create infectious parental virus. RNA viruses such as retrovirus and lentivirus, and DNA viruses like adenovirus, AAV and herpes virus have been tested as viral vectors for gene therapy (O'Connor & Crystal, 2006) (Figure 2). Unlike non-viral gene transfer, viral vectors permit enhanced transduction of target tissues to achieve stable and long term transgene expression. Nevertheless the improved efficacy comes with the associated risks of eliciting immune response, oncogenesis (in case of integrating vectors) by random integration of viral genes into host genome and generation of pathogenic native viruses by inadvertent genetic recombination, in

addition to the limitation of the size of DNA they can carry (Mingozzi & High, 2011).

2.1.3 Human clinical trials and concerns

Since the first reported human trial in 1990 (Cavazzana-Calvo et al., 2000), gene therapy has been extensively tested for a broad range of diseases from cancer to cardiovascular, monogenic and infectious diseases. As of 2012, over 1800 gene therapy trials had been completed, approved or ongoing as reviewed by Ginn *et al*(Ginn et al., 2013). After the initial years of trials and tribulations, the successful immune reconstitution in children suffering from ADA-SCID using retroviral vectors restored faith in gene therapy in 2009 (Aiuti et al., 2002, Aiuti et al., 2009). Objective regression of tumor was achieved in metastatic melanoma after transfer of autologous lymphocytes modified by retrovirus to express T- cell receptor specific to tumor- associated antigens (Morgan et al., 2006). A more recent trial extended this strategy and showed improved clinical outcome in metastatic synovial cell carcinoma (Robbins et al., 2011). Therapeutic benefit was also documented in patients suffering from chronic lymphoid leukemia and acute lymphoid leukemia following infusions of T cells transduced with a lentivirus designed to express chimeric antigen receptors specific for B cell antigen CD19 (Porter et al., 2011, Grupp et al., 2013).

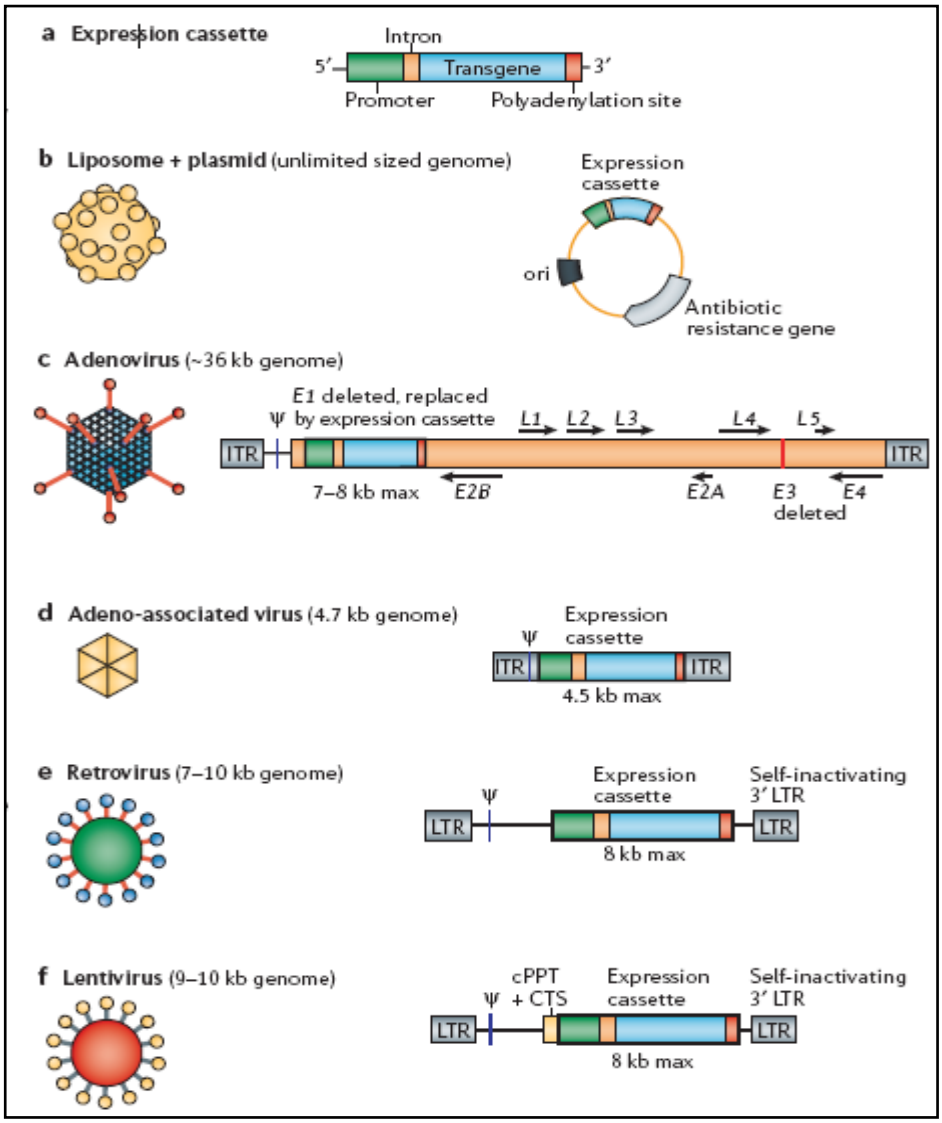

Figure 2: ***Common gene transfer vectors used to treat hereditary diseases.*** *a) Prototypic expression cassette showing the transgene flanked by 5'promoter and 3'poly (A) site. b-f) Various vector systems used to deliver transgene into target cells. The viral vectors have the expression cassettes, with maximum size as indicated, inserted between the terminal repeats, inverted terminal repeats (ITR) for adenovirus and AAV while long terminal repeat (LTR) for retrovirus and lentivirus. Vectors are rendered self—inactivating by deletion of the promoter and enhancer regions in the 3' LTR to prevent LTR-driven transcription. The packaging signal Ψ at 5'end is shown. The central polypurine tract (cPPT) and central termination sequence (CTS) are cis-acting sequences, which are unique to lentiviruses,that improve nuclear importof proviral DNA, with consequent increases in transduction. Ori: origin of replication; E1-E4: early genes; L1-L5: late genes. Adapted(O'Connor & Crystal, 2006).*

In LCA, an autosomal recessive retinal dystrophy, gene transfer using AAV vector expressing RPE65 gene showed promising results with marked improvement in the visual function of patients for upto 2 years of follow- up (Maguire et al., 2008, Cideciyan et al., 2009, Simonelli et al., 2010). Therapeutic response in patients from gene therapy trials has been highly encouraging for many other diseases such as chronic granulomatous disease (CGD), Parkinson disease, β-thalassaemia, hemophilia, Wiscott- Aldrich syndrome and X- linked adrenoleukodystrophy (X-ALD). Among the diseases targeted by gene therapy clinical trials, the most common one is cancer followed by monogenic diseases and cardiovascular diseases (Ginn et al., 2013). Infectious diseases, neurological diseases, ocular pathologies and inflammatory diseases are other indications addressed by gene therapy. The most recent highlight in gene therapy is however the approval of Alipogene tiparvovec, which is AAV1 encoding human LPL enzyme, for marketing as a medicine by European commission (Gaudet et al., 2013).

Nevertheless, some major setbacks have been encountered in the trials which raised speculations regarding the safety of gene therapy application in future, if administered as a standard of care. The first instance of an unfortunate event took place in 1999, following adenoviral mediated gene delivery into 18-year-old Jesse Gelsinger, an ornithine transcarbamylase (OTC) deficiency patient, which resulted in his death due to systemic inflammatory response (Raper et al., 2003). This shocked the public and scientific regulatory bodies forcing research restrictions and halt on several trials. Two years following the initial success of SCID-X1 trial, few of the patients who underwent treatment developed T- cell leukemia on account of insertional mutagenesis of the retroviral vector at the *LMO2* proto- oncogene promoter (Hacein-Bey-Abina et al., 2003). These adverse incidents underscore the

need to thoroughly investigate the safety profile of integrating and immunogenic vectors utilized in gene therapy.

2.2 Adeno-associated virus (AAV)

AAV is a small virus, which is classified under the genus *Dependovirus* and the family *Parvoviridae*. It has a 4.7kb single-stranded DNA as genome encapsulated within a non-enveloped, icosahedral protein capsid of ~22nm in size. Though AAV infects humans, it has not been associated with any known disease (Daya & Berns, 2008). Until now 13 serotypes of AAV and more than 100 variants have been identified, of which AAV1-9 are classified into 6 distinct phylogenetic clades (Gao et al., 2002, Gao et al., 2004, Schmidt et al., 2008).

2.2.1 Discovery

AAV was first described by Atchison *et al* in 1965 (Atchison et al., 1965) Small DNA containing particles were found as contaminants in monkey kidney cells infected with simian adenovirus 15 (SV15) when observed under an electron microscope. These virus-like particles were infectious, immunologically distinct, and replicated in cultures only when co-inoculated with adenovirus. These replication defective particles hence came to be referred to as adeno-associated viruses. Their unique physical and biological characteristics were confirmed with further evidence by Hoggan *et al*(Hoggan et al., 1966). It was initially believed that AAV genome was double-stranded but later it was demonstrated that virions contain single-stranded DNA which forms duplex structures, when released (Rose et al., 1969). The first infectious clone of AAV was derived in 1982 and it was tested as a recombinant viral

vector to transduce mammalian cells with *neomycin resistance* gene, which was cloned into AAV genome in place of capsid genes (Samulski et al., 1982, Hermonat & Muzyczka, 1984). AAV serotypes 1-4, 6, 12 and 13 have been isolated from different adenoviral stock cultures while AAV5 and AAV9 were originally isolated from human tissues. Monkeys have also been sources for isolation of AAV: AAV7 and 8 from rhesus monkeys whereas AAV 10 and 11 from cynomolgus monkeys (Balakrishnan & Jayandharan, 2014).

2.2.2 Genome organization

AAV has a linear single-stranded DNA genome of approximately 4.7Kb which can be of either plus or minus polarity. The DNA ends contain 145bp long sequences termed as inverted terminal repeats (ITR), of which the first 125 bases are palindromic and fold into a T shaped hairpin structure while 20 bases remain unpaired and constitute the D sequence (Koczot et al., 1973). The ITR plays a crucial role in viral DNA replication by serving as the origin of replication. It is also indispensable for transcription, genome packaging, site- specific integration and regulation of gene expression. The ITRs flank two ORFs corresponding to the viral genes *rep* and *cap*, which encode for the proteins involved in replication and capsid formation respectively (Berns, 1990). The *rep* gene produces four regulatory proteins Rep78, Rep68, Rep52 and Rep40 (named based on molecular weight), using two promoters (P5 and P19), and the *cap* gene encodes for three structural proteins VP1 (87KDa), VP2 (72KDa) and VP3 (62KDa) using P40 promoter, with the transcripts processed through alternate splicing for both the genes. Recently an overlapping ORF within the *cap* gene was described which encoded for assembly- activating protein (AAP), involved in capsid formation (Sonntag et al., 2011). The genome of AAV2 is shown in figure 3.

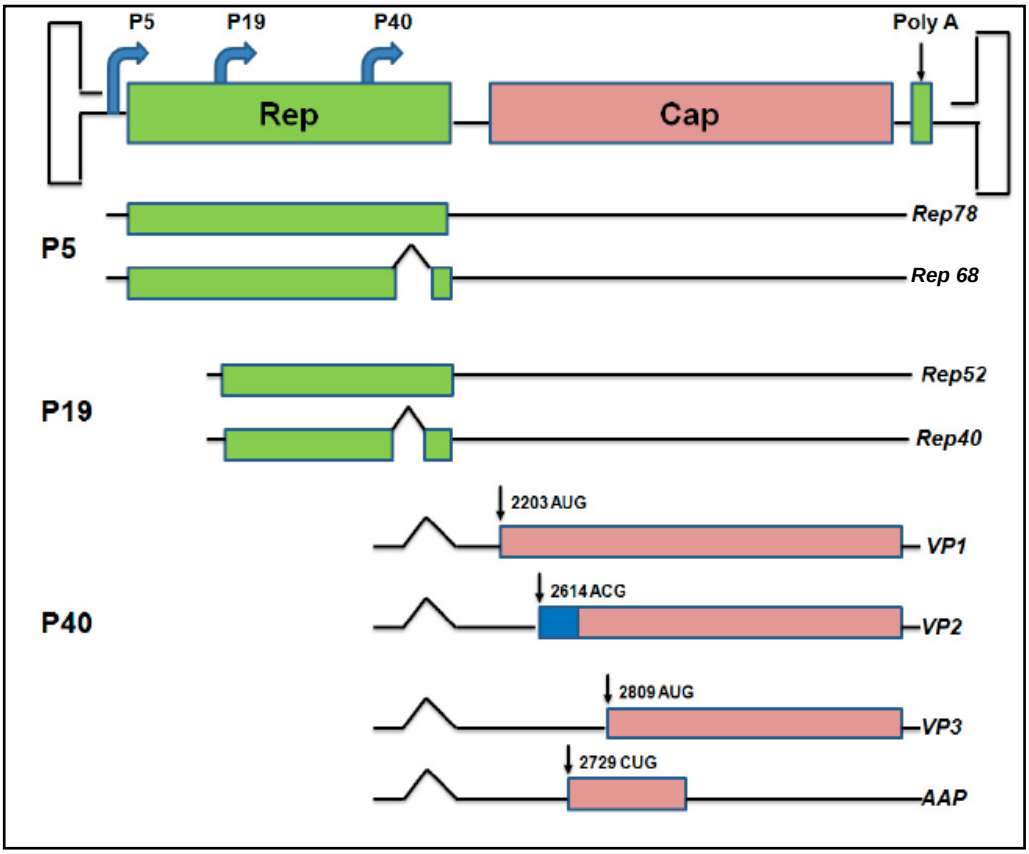

Figure 3: ***Organization of AAV2 genome.*** *The ITRs flanking the two ORFs, Rep and Cap and the genes encoding the respective proteins responsible for viral replication (Rep78, Rep68, Rep52, Rep 40) and capsid structure (VP1, VP2, VP3) are shown. The position of the three promoters P5, P19 and P40 and start codons of cap genes are indicated. AAP- assembly- activating protein. Adapted (Balakrishnan & Jayandharan, 2014).*

Rep78 and Rep68 regulate the AAV replication, transcription, gene expression as well as site specific integration processes (Pereira et al., 1997). These DNA binding proteins have endonuclease activity, and interact with specific sites within the ITR namely Rep binding element, RBE and terminal resolution site, trs. Rep52 and Rep40 are DNA helicases which mediate the generation and packaging of single stranded DNA within the AAV capsid (Chejanovsky & Carter, 1989, Im & Muzyczka, 1990). The virion proteins VP1, VP2 and VP3 are assembled in the molar

ratio of 1:1:10 to form the icosahedral symmetrical capsid of 260A° diameter, consisting of 60 subunits. The VP1 protein contains a conserved phospholipase A2 (PLA2) domain at the N terminus which is essential for the trafficking of AAV from the endosome to the nucleus and hence for the virus infectivity (Girod et al., 2002).

2.2.3 Capsid structure

AAV has a T=1 icosahedral capsid, made of 60 units each containing the VP1, VP2 and VP3 proteins in a stoichiometric ratio of 1:1:10. These three proteins share a common C-terminal region (the ~530 amino acids of VP3) but have different amino termini resulting from alternative start codon usage (Tseng & Agbandje-McKenna, 2014).The VP3 protein assembles the capsid in the presence of assembly activating protein (AAP) encoded by the *aap* ORF by 2-, 3-, and 5-fold symmetry-related interactions (Sonntag et al., 2011). The three dimensional structures of AAV1-9 serotypes and other AAV variants have been determined by either X-ray crystallography or a combination of cryo electron microscopy and pseudoatomic model building. The structure of AAV1 capid is illustrated in figure 4. The VP protein basically consists of a conserved α-helix and a conserved eight-stranded antiparallel β-barrel motif at the core, with large loops inserted between the strands of the β-barrel. These loops comprise of the variable regions, which determine the topological differences in capsid surface and functional differences in receptor binding, transduction potential and immunological profile (by altering antigenic epitopes) between the various AAV serotypes/variants (Lochrie et al., 2006, McCraw et al., 2012, Govindasamy et al., 2013, Gurda et al., 2013). The AAV2 capsid structure, which is very similar to other serotypes is well characterized and consists of depressions at the 2-fold axes (dimple), surrounding a cylindrical channel at the 5-fold axes (canyon), and protruding spikes surrounding the 3-fold axes. Between the

depression at the 2-fold axis and surrounding the 5-fold channel, a wall or plateau is located which is termed as the "2/5-fold wall" (Halder et al., 2013). The 3-fold axis of the AAV2 capsid dictates the capsid/receptor binding. Two arginines at positions 585 and 588, located at this symmetry bind to heparan sulfate proteoglycan (HSPG), the primary receptor of AAV2(Opie et al., 2003).

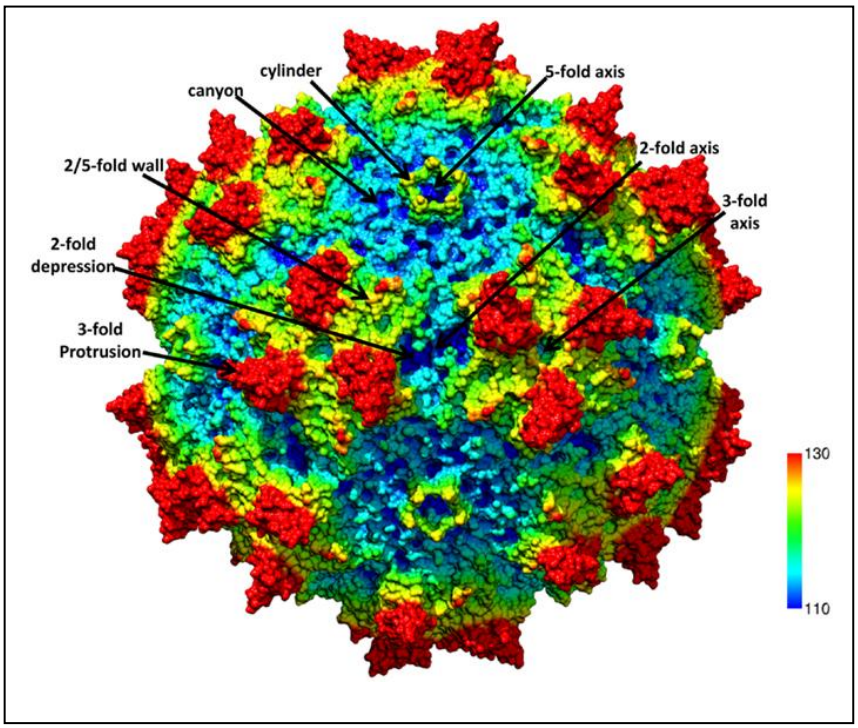

Figure 4: ***AAV capsid structure.*** *Radially color-cued (from capsid center to surface: blue-green-yellow-red; ~110–130 Å) of the AAV1 capsid generated from 60 VP monomers (RCSB PDB # 3NG9). The approximate icosahedral 2-, 3-, and 5-fold symmetry axes are as well as the AAV capsid surface features are indicated by the arrows and labeled. This image was generated using the Chimera program. Adapted (Tseng & Agbandje-McKenna, 2014).*

2.2.4 AAV infection

AAV infection of the target cell is a complex process which involves multiple steps such as receptor attachment and internalization, endosome trafficking

and release, nuclear translocation, capsid uncoating and gene expression(Daya & Berns, 2008). Figure 5 shows the various steps involved in wild-type AAV2 infection. In the first step during infection, AAV binds to specific receptors on the cell surface, unique to different serotypes. Heparin sulphate proteoglycan (HSPG) is the primary receptor utilized by AAV2. The broad tropism of AAV2 found in human, non-human primate, canine, murine and avian cells is explained by the ubiquitous presence of HSPG in several species (Summerford & Samulski, 1998) Certain co-receptors such as $\alpha_v\beta_5$ integrin, fibroblast growth factor receptor type I, hepatocyte growth factor receptor (c-Met), $\alpha_v\beta_1$ integrin and laminin receptor further facilitate the viral internalization (Ling et al., 2010). AAV5 and AAV4 use N- and O-linked sialic acids respectively as their receptors. Further platelet derived growth factor receptor also serves as a receptor for AAV5 transduction (Di Pasquale et al., 2003). AAV1 and AAV6, which are closely related serotypes require α2,3 and α2,6 N- linked sialic acids for cell surface attachment and efficient transduction (Wu et al., 2006). Among the six amino acid residues which differ between AAV1 and AAV6, the presence of lysine at position 531 was found to impart additional HSPG binding properties to AAV6 (Asokan et al., 2006, Wu et al., 2006). Laminin receptor acts a cellular receptor for AAV serotypes 8, 2, 3 while AAV9 utilizes terminal N-linked galactose as receptor for cellular entry (Shen et al., 2011).

Receptor binding is followed by viral internalization through the plasma membrane by receptor mediated endocytosis into clathrin coated vesicles, which requires $\alpha_v\beta_5$ integrin and activation of GTP- binding protein Rac1 (Sanlioglu et al., 2000). Dynamin, a GTPase protein is required for the formation and pinching of the clathrin coated pits from the cell membrane (Duan et al., 1999). Subsequent intracellular trafficking of AAV2 particles through the cytosol to the nucleus is dependent upon the activation of PI3K pathway as well as microtubules and

microfilaments (Sanlioglu et al., 2000). A recent study showed using chlorpromazine, a drug which inhibits the formation of clathrin coated vesicles, that AAV2 endocytosis is independent of clathrin mediated process and requires clathrin-independent carriers (CLIC) and GPI-anchored-protein-enriched endosomal compartment (GEEC) pathways (Nonnenmacher & Weber, 2011). The release of virions from early endosomes takes place upon acidification of the vesicles, following which they accumulate perinuclearly and slowly penetrate into the nucleus. Whether the viral capsid uncoating happens in the nucleus or the cytoplasm is still unclear. Most of the evidence accumulated from studies based on immunofluorescence microscopy and sub cellular trafficking strongly suggest that AAV uncoats in the nucleus (Lux et al., 2005, Johnson & Samulski, 2009). Using fluorophore labeled AAV2 particles, it was shown that within 2 hours of infection, virus translocates into the nucleus possibly through the nuclear pore complex (Bartlett et al., 2000). Endosomal cysteine proteases, cathepsins B and L have been shown to bind and cleave the capsids of AAV2 and AAV8 differently and thus acting as uncoating factors for these serotypes (Akache et al., 2007). The higher rate of transduction for AAV8 compared to AAV2 is postulated to be due to the faster rate of capsid processing by cathepsins for the former. The PLA2 motif within the N termini of VP1 protein protrudes through the fivefold pore of AAV2 capsid as a result of conformational changes during infection, whereby the phospholipase activity is induced and plays a key role in the nuclear trafficking of AAV genome from the endosomes and subsequent viral gene expression (Girod et al., 2002).

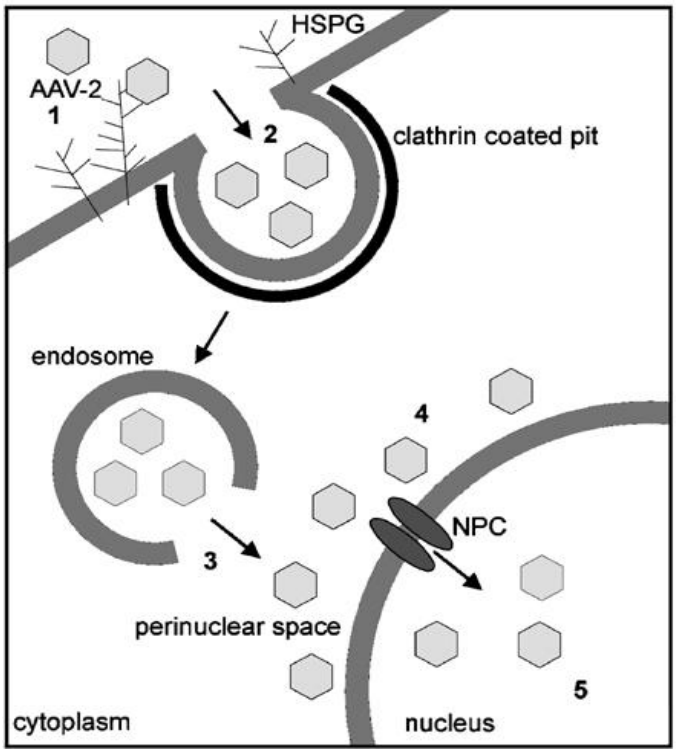

Figure 5: ***Infectious pathway of wild-type AAV-2****. Schematic representation of AAV entry and endocytic trafficking in HeLa cells as seen by fluorescent and confocal laser microscopy, following binding to heparan sulfate proteoglycans (HSPG) on the cell surface (1), AAV is rapidly internalized via clathrin-coated pits (2) through a process involving* $\alpha_v\beta_5$ *integrin, dynamin and Rac1. Following endocytosis, the activation of phosphatidylinositol-3 kinase seems to support the initiation of the intracellular movement.After acidification, AAV is released from the endosome into the cytoplasm (3), where it is found in a perinuclear localization (4). Then AAV slowly enters the nucleus (5) probably via nuclear pore complexes (NPC). Adapted and modified (Buning et al., 2003).*

2.2.5 AAV life cycle: lytic and lysogenic phases

Once inside the nuclear compartment, AAV can follow either the lytic or the lysogenic cycle. In the presence of a helper virus such as adenovirus or herpes virus, AAV adopts the lytic stage, characterized by genome replication, gene expression and virion production. The adenoviral genes which provide the helper

functions for AAV productive infection include E1a, E1b, E2a, E4 and VA RNA while Herpes virus regulate AAV gene expression by providing viral DNA polymerase and helicase, thus creating a permissive intracellular milieu for AAV transduction (Chang et al., 1989, Duan et al., 1999b). The lytic phase also ensues in response to cellular genotoxic stress like UV irradiation and metabolic inhibitors, albeit with low efficiency (Yalkinoglu et al., 1988, Sanlioglu et al., 1999). AAV replication is believed to take place by a rolling hairpin model. The 3'-hydroxyl end of ITR serves as a primer for DNA polymerization leading to the formation of duplex monomeric and dimeric replicative forms. These duplex concatenated replicative intermediates are resolved by strand displacement mechanism to generate single stranded progeny DNA with the aid of Rep proteins. Both 'plus' and 'minus' single stranded AAV genomes produced are encapsidated into virions with equal efficiency (Berns, 1990, Ni et al., 1998). During virus assembly, VP3 capsid protein translocates from the cytosol into the nucleus by associating with VP1 and VP2 which possess nuclear localization signals (Ruffing et al., 1992). AAV capsids get assembled within the nucleoli, enter the nucleoplasm and then package the genome in a Rep dependent manner to produce infectious AAV particles (Wistuba et al., 1997).

In the absence of a helper virus, AAV undergoes latent infection by repressing viral gene expression and integrating its genome into a 4 Kb region on human chromosome 19 (q13.4) termed AAVS1 site, possibly by a non-homologous end joining (NHEJ) pathway (Daya et al., 2009). In 1975, Berns *et al* first demonstrated this phenomenon by latently infecting *Detroit 6* fibroblast like cells with AAV2 and showing the persistence of the viral DNA for nearly 47 passages (Berns et al., 1975). The site directed integration of AAV is directed by a 33bp sequence at AAVS1, that has an RBE – like and trs- like sequence within a gap of 8

nucleotides (Giraud et al., 1994). Rep78/ Rep68 proteins have been shown to bind GCTC repeat elements in the AAVS1 site and mediate the complex formation between AAVS1 site and the ITR (Balague et al., 1997).Targeted integration at AAVS1 site is shown to enhance upon co-transfection with a plasmid encoding Rep78, however its application is limited by the cytotoxicity of host cells induced by this Rep protein (Recchia & Mavilio, 2011). The integration efficiency element (IEE), a 138bp sequence within the P5 promoter is also identified as a viral factor important for AAV integration (Philpott et al., 2002). The frequency of site specific integration at AAVS1 site is estimated to be 0.05% in tissues of humans and rhesus monkeys (McCarty et al., 2004). The switch to lytic phase in the presence of helper virus infection is brought about by the rep- mediated excision of the integrated provirus from the host genome. The life cycle of the wild-type AAV and the recombinant form is shown in figure 6.

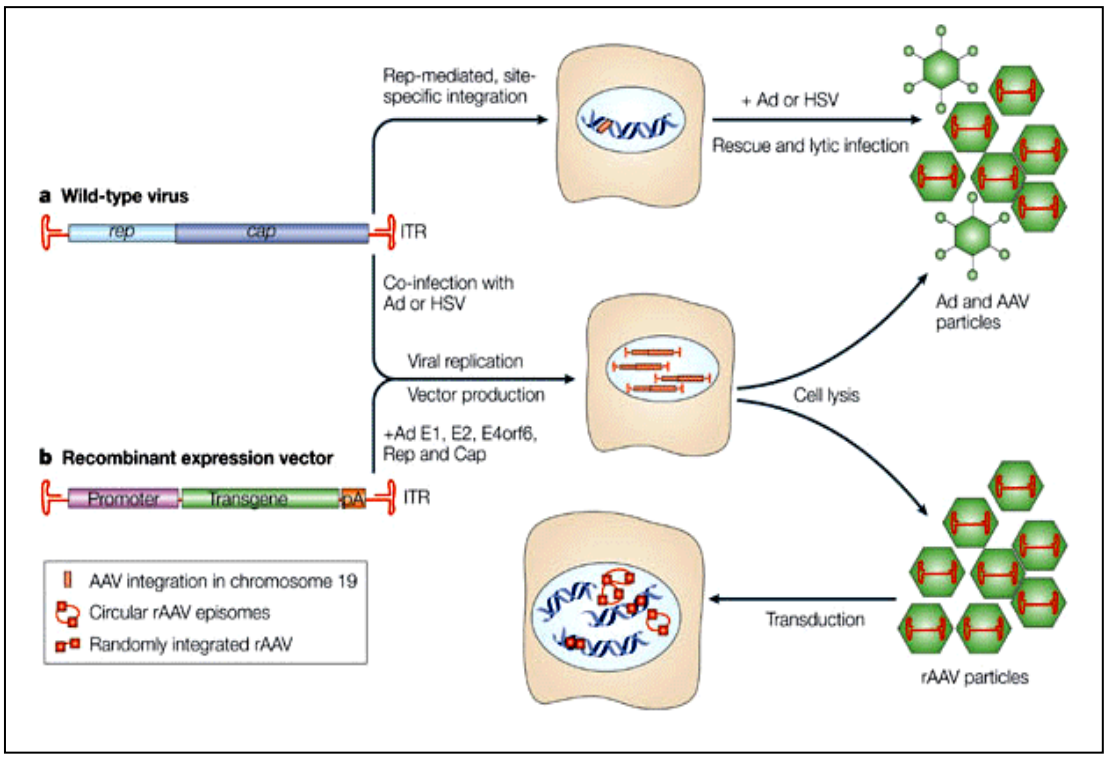

Figure 6: ***Life cycle of AAV****. The wild-type virus in the latent phase of life cycle, undergoes rep- mediated site specific integration at AAVS1on chromosome 19. The integrated provirus can be rescued by co-infection with a helper virus (adenovirus or herpes simplex virus) to switch to the lytic phase. The wild-type AAV in the presence of the helper virus undergoes replication and transcription of the viral genes and subsequent helper virus mediated host cell lysis to produce intact AAV particles. Whereas during rAAV production, the rep-cap and helper genes are supplied in trans facilitating gene expression.rAAV particles are then used to transduce cells, which mostly exists as circular episomes or rarely integrate in random. Adapted (Vasileva & Jessberger, 2005).*

2.3 Recombinant AAV

2.3.1 Design and production

The intact genome of AAV was first cloned into a bacterial plasmid in 1982, and for vector packaging, the viral DNA rescue was achieved by transfecting HEK 293 cells infected with adenovirus 5, thus recapitulating the lytic phase of AAV infection (Samulski et al., 1982). The knowledge that ITRs contain all the *cis* functions required for AAV genome replication and virion assembly paved way for the production of recombinant AAV (rAAV) vectors. The design of rAAV follows the concept of 'gutless' vectors which retain only the ITRs in *cis* while the viral encoding genes meant for replication and capsid structure formation are replaced by the foreign DNA of choice, as shown in figure 2 (Daya & Berns, 2008). The rep- cap functions are provided in *trans* as a separate plasmid during vector packaging. This negates the possibility of generation of wild-type AAV and any undesirable effects associated with it during gene transfer. Unlike the wild-type virus, the lack of rep protein prevents the site specific integration of rAAV vectors which usually exist in episomal form within the target tissues although there are reports which claim that a rep independent integration event can also take place (Figure 6) (Asokan et al., 2012). The classical rAAV vector based on native virus contains the single-stranded genome, which needs to undergo the second strand synthesis during replication and hence produces delayed and low level gene expression (Ferrari et al., 1996). To overcome this limitation, self-complementary (sc) AAV vectors were designed with a mutation in *trs* of right ITR, which facilitated their spontaneous re-annealing, bypassing the second strand synthesis to form transcriptionally active genomes with enhanced transgene expression (Nathwani et al., 2006)Nonetheless the packaging capacity of scAAV was reduced to 2.4Kb compared to 4.7Kb in ssAAV vectors.

Earlier methods of rAAV production involved the transfection of HEK 293 packaging cell line with the two plasmids namely the transgene plasmid with the ITRs and the rep- cap plasmid, and co- infection with adenovirus (Ad) (Pfeifer & Verma, 2001). The helper functions for AAV production are provided by the adenoviral genes such as E1a, E1b, E2a, E4 and VA RNA, as described in the previous section. However, there are some problems associated with Ad co-infection. The most serious of them is the elimination of contaminating Ad particles from the final vector preparation which is done using physical methods like caesium chloride, column chromatography and heat denaturation, none of which can guarantee absolute purity of the AAV vector stock (Vincent et al., 1997). Additionally, there could be potential competition between both the viruses for the essential genes for their life cycle, adversely affecting the AAV vector yield. A triple plasmid transfection method for rAAV production where Ad co- infection is replaced by a plasmid carrying the Ad helper genes was introduced in 1998 (Grimm et al., 1998). Several modifications on this protocol were then reported to further improve the process of vector production using either calcium phosphate or PEI as the transfection reagent (Lock et al., 2010). In addition, baculovirus expression systems based on insect cell lines such as SF9 cells have shown to scale up the production of rAAV vectors (Kotin, 2011).

2.3.2 Gene therapy using recombinant AAV vectors

AAV has been evaluated as a lead candidate vector for a broad spectrum of diseases. The features of AAV which make it attractive as a promising tool for gene therapy include non-pathogenicity, low immunogenicity, long term persistence in the host cell and stable transgene expression (Mingozzi & High, 2011). The availability of multiple serotypes (AAV1-12) with diverse tissue targeting properties

expands the scope for disease correction by gene transfer to any type of tissue such as brain, liver, heart, lung, eye or muscle. Promising results that emerged from pre-clinical studies conducted on small and large animal models paved way for phase I/II clinical trials on human subjects. Valuable insights pertaining to vector tropism and persistence, transduction efficiency, immune profile and toxicity were gathered from the animal studies (Asokan et al., 2012). Nonetheless, the clinical transition of AAV gene transfer furnished some unpredicted events related to immune response in human subjects.

AAV (serotype 2) was first used as a gene therapy vector in human clinical trial in1996, for delivering *CFTR* (cystic fibrosis transmembrane conductance regulator)gene to treat patients with cystic fibrosis, a chloride channel defect which affects the lung airways (Flotte et al., 1996). Subsequently AAV clinical trials were initiated for several diseases, some of which include hemophilia B, AAT deficiency, LPL deficiency, Canavan disease, muscular dystrophy, LCA and Pompe disease among the inherited disorders; and Parkinson disease, severe heart failure and rheumatoid arthritis among the acquired diseases. Table 1 provides information on the recent clinical trials using AAV. The outcome of LCA trials stand out as a testimony for the success of gene replacement using AAV. LCA is a group of congenital degenerative disorders affecting the retina, resulting in blindness. Three independent trials were undertaken for AAV2 based sub- retinal delivery of *RPE65* (retinal pigment epithelium specific 65 Kda protein), the gene that is mutated in 10% of the patients with this disease. In nearly all subjects, restoration of vision was demonstrated following AAV vector intervention as assessed by psychophysical (visual acuity and visual field testing) and objective (pupillometry and electroretinograms) measures. Vector administration into the relatively immunoprivileged site did not elicit any adverse immune response in the patients, as

predicted previously from long term studies on murine and canine models of RPE65 deficiency (Maguire et al., 2008, Cideciyan et al., 2009, Simonelli et al., 2010).

In November 2012, another remarkable event occurred which reinforced the success of AAV. The European Medicines Agency (EMA) granted approved for commercialization of the first gene therapy product, Glybera (alipogene tiparvovec) developed by uniQure for the treatment of familial LPL deficiency (LPLD) (Gaudet et al., 2012). It is a rare inherited disease characterized by severe hypertriglyceridaemia (triglyceride (TG) concentration>20mmol/L), chylomicronaemia and risk of recurrent acute pancreatitis and other complications, caused by the lack of LPL, a key enzyme involved in catabolism of TG rich lipoproteins. Glybera is AAV1 encoding a natural gain-of function human *LPL* gene variant, LPL^{S447X}which is injected intramuscularly into the lower limbs. Results from three open label interventional trials using AAV1- LPL^{S447X} suggested that the local administration of the vector into muscles was well tolerated with improvement of clinical symptoms and reduced incidence of pancreatitis for a follow-up period of 2 years (Gaudet et al., 2012).

Disease	Target tissue	AAV Serotype	Transgene	Clinical Phase	Route of Administration
LPL Deficiency	Skeletal muscle	AAV1	LPL	Phase I/II/III	Intramuscular
Alpha 1 Anti-trypsin Deficiency	Skeletal muscle	AAV2, AAV1	α1-antitrypsin	Phase I/II	Intramuscular
Duchenne Muscular Dystrophy	Skeletal muscle	AAV1/AAV2 chimera	Microdystrophin	Phase I	Intramuscular
Limb-Girdle Muscular Dystrophy	Skeletal muscle	AAV1	α-sarcoglycan	Phase I	Intramuscular
Leber Congential Amaurosis	Eye	AAV2	RPE-65	Phase I/II	Subretinal
Choroderemia	Eye	AAV2	REP1	Phase I/II	Subretinal
Hemophilia B	Liver	AAV2	Factor IX	Phase I/II Phase I	Intramuscular Hepatic
	Liver	AAV8		Phase I/II	Intravenous
Severe Heart Failure	Cardiac muscle	AAV1	SERCA2a	Phase I/II	Coronary Artery Infusion

Table 1: ***Recent clinical trials using AAV vectors.*** *Adapted and modified (Kotterman & Schaffer, 2014)*

2.4 Hemophilia B: a target disease for AAV gene therapy

2.4.1 Summary of the disease

Hemophilia is an X- linked recessive disorder caused due to the deficiency of blood coagulation factors, Factor VIII (hemophilia A) and Factor IX (hemophilia B). The reported incidence of hemophilia A is 1 in 5000 and of hemophilia B is 1 in 25, 000 live male births (Peyvandi et al., 2006). It is categorised into three different forms, severe if factor concentration of <1% of normal level when spontaneous bleeding occurs into joints and muscles, moderate if it is 1-5% where bleeding occurs

upon minor injuries or trauma and mild with 5- 40% factor levels, in which case bleeding happens only post surgery or accidents. In severe hemophilia patients, recurrent bleeding into joints can cause synovial hypertrophy with progressive damage to cartilage and subchondral bone, resulting in hemarthrosis. Other possible complications are intracranial bleeding, hematuria and intramuscular hemorrhage (Bolton-Maggs & Pasi, 2003, Street et al., 2006). The deficiency of either factor VIII or IX disrupts the secondary hemostasis, which generates the fibrin clot that is critical to arrest bleeding. The formation of fibrin from fibrinogen requires adequate amounts of thrombin to be produced, which inturn depends on activation of factor X by a complex of factor VIII and IXa (tenase complex). Hence the absence of either factor VIII or IX can adversely affect the process of blood coagulation (Ahmad et al., 2003)

The genes encoding FVIII and FIX are located on the q arm of chromosome X. *F8* gene is relatively big having 26 exons spanning 186 Kb compared to *F9* gene which is 34 Kb and has 8 exons. These clotting factors are synthesized primarily in the liver. The half life of FVIII is about 12h and that of FIX is 24h in adults. FIX is present at a plasma concentration that is 50 times that of FVIII (Jayandharan & Srivastava, 2012). Hemophilia is reported to be caused by a variety of mutations in *F8* (~2183 in HGMD (Human Gene Mutation Database)) and *F9* (~1101 in HGMD) genes including point mutations (mis-sense or non-sense), deletions, insertions and splice site mutations. In addition, hemophilia A can be caused by two inversions, the common intron 22 inversion and intron 1 inversion which is comparatively rare (Bolton-Maggs & Pasi, 2003). Hemophilia A and hemophilia B are clinically indistinguishable and are diagnosed by specific factor assays. Diagnosis is based on either a known family history or bleeding diathesis. Clinical evaluation is substantiated by genetic diagnosis which is imperative in

understanding the genotype-phenotype correlations, prenatal diagnosis and genetic counseling, and for the advancement of treatment.

In the present clinical scenario, there is no cure for hemophilia. Treatment which is symptomatic encompasses control of spontaneous/ traumatic bleeding by replacement therapy or administration of the deficient factor (Mannucci, 2008). *F9* and *F8* genes were cloned in 1984 and 1982 respectively, and in the 1990s, recombinant FVIII and FIX concentrates were introduced for medical use. Treatment is given either 'on demand' when bleeding occurs or as prophylaxis to prevent bleeding. Frequent dosing of clotting factor concentrates interrupt the daily activities of patients and affect their normal life style (Bolton-Maggs & Pasi, 2003). Long acting recombinant factors (FVIII, FIX or FVIIa) with prolonged half- life and reduced immunogenicity are being actively tested in patients to assess their clinical benefit. These factors are engineered by either covalently coupling them to polyethylene glycol (PEG)/ polysialic acids (PSAs) or by forming a fusion protein with Fc region of an antibody/ albumin(Peyvandi et al., 2013).

2.4.2 AAV-mediated gene therapy for hemophilia

Hemophilia is a monogenic disorder in which intervention by gene therapy has proven to be successful in preventing bleeds even with low levels of transgene expression. A modest increase in factor VIII or IX levels by 3-5%, if achieved can prevent spontaneous bleeding and thus significantly improve the lifestyle of patients. The F9 cDNA is about 1.4 Kb in length and can easily be incorporated into an AAV vector whereas the full length cDNA of F8 is ~8Kb, which exceeds the packaging capacity of AAV (Murphy & High, 2008). For this apparent reason, most of the gene transfer studies using AAV target hemophilia B, as opposed to hemophilia A.

Sustained phenotypic correction of hemophilia B was achieved in canine models by injecting AAV2-FIX vectors into muscles, with no noticeable toxicity associated with it (Herzog et al., 1999). Based on the promising data from this pre-clinical study and others on hemophilic mice and dogs, an open label clinical trial was initiated by intramuscular injection of AAV2 expressing FIX into patients with severe hemophilia B. There was no evidence of any local or systemic toxicity related to vector administration into the skeletal muscles; however, the gene transfer failed to elevate the circulating levels of FIX to more than 1% in the subjects (Manno et al., 2003). One of the patients recruited in this trial died in 2012 due to complications unrelated to gene transfer and his autopsy samples of skeletal muscle were collected for analysis. It was surprisingly found that there was sustained FIX transgene expression and AAV vector persistence in the injected muscle fibres more than a decade after AAV-mediated gene delivery (Buchlis et al., 2012).

Considerable efficacy was demonstrated in the second clinical trial when AAV2 vector carrying human FIX was delivered through the hepatic artery into seven patients (Manno et al., 2006). Three different doses of the AAV vector ranging from 8×10^{10}vgs/kg to 2×10^{12} vgs/kg were tested. Therapeutic levels of FIX (3-11%) were attained in the two patients who received the highest dose but it was maintained only for a limited period of approximately 8 weeks. The FIX levels declined gradually after 4 weeks of vector infusion, and reached the baseline of <1% in both these patients. In one of the patients, it was observed that the loss of FIX expression coincided with the aymptomatic elevation of liver transaminases, ALT and AST, which was attributed to the immune mediated destruction of transduced hepatocytes. The other subject within the high dose group did not manifest transaminitis, although had a high pretreatment anti-AAV2 neutralizing antibody (Nab) titer of 1:17, which effectively blocked transduction.

The recent trial for hemophilia B utilized AAV8 vectors, owing to their better liver tropism and transduction in comparison to AAV2 vectors (Nathwani et al., 2011, Nathwani et al., 2014). Two approaches were taken to enhance the transduction profile of the AAV vector: a self-complementary genome and codon optimization, both of which are known to promote efficient and stable transduction. The scAAV8-FIX vectors were infused intravenously in three dose cohorts ranging from 2×10^{11} vgs/kg to 2×10^{12} vgs/kg, with two patients in each. All patients recruited were negative for Nab against AAV8. It was observed that in patients within the first two cohorts, there was modest improvement in circulating FIX levels which stabilized at 1-3%. In one patient injected with high dose, the FIX levels elevated to 8%-10% of normal, but after 8 weeks the levels dropped with concomitant rise in liver enzymes, ALT and AST. The transaminitis was resolved by a short course of prednisolone (60mg/d) and the FIX levels remained at 2%. The other patient in the high dose cohort also was given steroid therapy, which was tapered after 4 weeks and stable FIX levels at 6% were noted for a year. The long term follow-up report of this study was published in November 2014 furnishing evidence of circulating FIX levels in all patients at 1-6% of normal value over a median period of 3.2 years achieved by single intravenous infusion of AAV8-FIX vectors (Nathwani et al., 2014). In all 6 patients within the high dose group, including four additional patients enrolled in 2012, FIX levels remained consistently high at nearly 5% with about 90% reduction in bleeding episodes and stoppage of the prophylactic infusion of FIX concentrates. The results of this trial encourage in reinstating that AAV gene therapy can become a potential treatment modality for hemophilia B, provided the vector associated immune complications are averted.

On the other hand, AAV gene therapy for hemophilia A has been difficult owing to the large size of FVIII cDNA and low expression levels of the pro-

coagulant protein. In mice, therapeutic levels of FVIII were attained by AAV-based gene transfer of B-domain deleted (BDD) FVIII variant which is about 4.4 Kb in size (Chao H et al, Blood 2000). Later it was reported that partial deletion of B-domain, retaining the N' 226 amino acid portion (N6) highly improves the secretion of FVIII protein (Pipe, 2009). The BDD-FVIII protein is now available as a recombinant product for clinical use under the trade name Refacto marketed by Pfizer. Recently a novel 5.2Kb AAV-hFVIII construct was described, which contains a codon optimized BDD-hFVIII cDNA along with a 17 amino-acid stretch at N terminus. Stable hFVIII levels were demonstrated both in murine and macaque models using the bio-engineered FVIII gene delivered using AAV at vector doses found to be safe in humans (McIntosh et al., 2013). Alternatively, co-administration of two AAV vectors, one expressing the heavy chain of FVIII protein and the other encoding the light chain, if not two halves of the trangene expression cassette to intracellularly form a functional FVIII molecule are other approaches being investigated to make AAV gene transfer for hemophilia A feasible (Chen et al., 2009).

2.5 Immune response to AAV vectors

It is apparently clear from the clinical studies that unless controlled, the immunity to AAV can defeat the ultimate purpose of therapeutic gene transfer. AAV was originally thought to be a safe vector with low immunogenicity, as documented from several pre-clinical studies. The unprecedented occurrence of immune responses against AAV in human subjects has forced scientists to reconsider the safety and utility of this viral vector (Basner-Tschakarjan & Mingozzi, 2014). In this perspective, a thorough understanding of AAV vector immunology is crucial to overcome this obstacle to gene therapy.

2.5.1 Innate immune response

The innate arm of the immune system represents the first line of defense of the body against any invading pathogen. During an anti-viral response, the innate immune cells such as dendritic cells (DCs) and macrophages get activated and secrete inflammatory mediators like cytokines and chemokines. These molecules inturn trigger the processing and presentation of viral peptides on MHC complexes by antigen presenting cells (APC) (Zaiss & Muruve, 2008).C3 component of the complement system, which plays a central role in innate response against viruses, was shown to directly bind to AAV capsid leading to vector opsonisation and activation of macrophages (Zaiss et al., 2008). Immature DCs infected by AAV *ex vivo*, when adoptively transferred to immune-competent mice, directed the T cell mediated destruction of transduced muscle fibres in a CD40 dependent fashion (Zhang et al., 2000).

Pathogens including viruses have certain molecular patterns called PAMP (pathogen associated molecular motifs) which bind to PRR (pattern recognition receptors) on host cell surface upon infection, to activate immune signaling pathways that culminate in the production of pro-inflammatory cytokines and factors. These in turn activate and cause the infiltration of macrophages, DCs and neutrophils to the site of pathogen invasion. This phenomenon also intensifies the immune response to produce a more specific adaptive response, characterized by immunological memory of the antigen (Mogensen, 2009). Toll like receptor (TLR) pathway is known to function in innate immune signaling against AAV. It was reported that TLR2 elicits an innate response to the AAV capsid in liver non-parenchymal cells (kupffer and liver sinusoidal endothelial cells) of humans (Hosel et al., 2012). While TLR2 detects the capsid, TLR9 signaling is implicated to act against AAV genome. In

plasmacytoid DCs, single-stranded genome of AAV2 vector was shown to activate the TLR9/MyD88 signaling pathway to produce type I interferon (IFN). Martino *et al*demonstrated that liver directed gene transfer in mice resulted in a dose-dependent increase in innate response to self-complementary genome of AAV vectors and enhanced transgene immunogenicity, both mediated by TLR9 which is an endosomal receptor that recognizes unmethylated CpG DNA motifs (Martino et al., 2011b). The critical role of this signaling pathway in production of AAV specific Nab response as well as CD8+ T cell response against AAV capsid or transgene was demonstrated using *TLR9* or *MyD88*-deficient mice (Zhu et al., 2009). In addition, the Th1-dependent antibody response to AAV was shown to be regulated by MyD88 signaling in B cells (Sudres et al., 2012).

AAV infection also activates the NF-kB signaling. This transcription factor is a central player which arbitrates the inflammatory responses associated with the innate immune system(Hoffmann & Baltimore, 2006). NF-kB signaling and its association with AAV is described in detail later in this thesis. The unfolded protein response (UPR) pathway genes, specifically IRE1α is known to activate NF-kB leading to the expression of the downstream pro-inflammatory target genes (Hu et al., 2006). During intracellular trafficking, the massive influx of AAV particles into ER (endoplasmic reticulum) is thought to activate the UPR as an ER stress response mechanism. We have recently shown that scAAV activates UPR, particularly the PERK and IRE1 pathways more prominently as opposed to ssAAV. Further UPR inhibition using metformin effectively suppressed NF-kB directed innate immune response against scAAV2 vectors in mice while modestly augmenting the transgene expression in liver (Balakrishnan et al., 2013). Although most of the knowledge pertaining to innate immune recognition of AAV is gained from animal experiments, it is logical to assume to that similar or more complex innate responses could be

expected to take place in human beings, a higher order species in animal kingdom. In short, the encounter of AAV vector with the host innate immune system may either induce an inflammatory response causing its clearance or lead to the activation of a more specific adaptive immune response. As both courses limit its application in humans as a gene therapy vector, repressing this first line of defense against AAV is all the more important.

2.5.2 Adaptive immune response

2.5.2.1 Humoral immunity

Humans act as natural host to AAV and hence on exposure to the wild-type virus at an early age generate anti-AAV antibodies in the sera. The seroprevalence of AAV2 in human population is estimated to be roughly 70% (maximum) and of AAV8 is ~30% (minimum), while for the other serotypes it ranges between 40%- 67% (Calcedo et al., 2009). Based on the degree of homology between the capsid gene sequences, the various AAV serotypes display cross-reactivity of their antibodies. AAV4, the most antigenically divergent serotype is not neutralized by any other anti-AAV sera whereas antibodies to AAV1 and AAV6, which are closely related, are found to cross-react robustly. AAV7 and AAV8, isolated from rhesus monkeys are serologically distinct and show minimal cross-reactivity to other serotypes (Harbison et al., 2012). Subtype analysis of anti- AAV immunoglobulin has shown that IgG1 is most prevalent followed by IgG2, IgG3 and IgG4. The best age for AAV vector infusion was determined to be 7-11 months in a study which compared the Nab titers to AAV2 and AAV8 in human subjects between 0-18 years (Calcedo et al., 2011, Calcedo & Wilson, 2013). Pre-existing antibody titers exceeding 1:10 were shown to significantly reduce the liver

transduction of AAV8 vectors in non-human primates and cause stable sequestration of capsid proteins in the splenic DCs (Wang et al., 2011). The impact of pre-existing antibodies on the treatment outcome of gene therapy is illustrated by the decline in circulating FIX levels in the one of the patients with Nab titer of 1:17 and infused with high vector dose in the AAV2 based clinical trial for hemophilia B (Manno et al., 2006).

2.5.2.1 Cellular immunity

When AAV particles undergo degradation within the host cell, the antigenic peptides derived from the viral capsid can be cross-presented on MHC-I molecule. This in turn induces CTL response against the transduced cell, which is the most common form of adaptive T cell reactivity to AAV vectors. The cross presentation of AAV capsid antigens on MHC-1 has been shown to be dependent on virion escape from the endosomes and capsid degradation by the proteasome system (Li et al., 2013). Apart from antibodies, memory B cells and T cells specific to AAV are also found in humans who are naturally infected with AAV in early life (Li et al., 2011). These memory immune cells can get re-activated upon exposure to AAV vectors and abrogate sustained transgene expression. Screening of healthy donors for the presence of immunity to natural AAV1 infection showed that ~30% of donors presented T cell response, which was largely prompted by effector memory CD8+T cells and moreover there was no correlation between AAV1 specific T cell and humoral responses (Veron et al., 2012).

2.5.3 Factors influencing the immune response to AAV

The immune response against AAV is targeted mostly to the capsid and/or the transgene product. The AAV capsid is detectable within a transduced cell for a

defined period of time, which may vary from weeks to months, depending on the tissue. Intact capsid of AAV was detected in canine retina by electron microscopy for upto 6 years after gene delivery (Stieger et al., 2006). Furthermore, in human muscles, immunostaining showed the presence of capsid particles for about a year after AAV administration (Mueller et al., 2013).

There is ample evidence of T cell responses to viral capsid collated from clinical trials using AAV. The IFNγ ELISPOT analysis of PBMNCs (peripheral blood mononuclear cells) from one of the patients in AAV2-FIX trial, who had transminitis 4 weeks following vector infusion, showed that a T cell response had been activated against the AAV capsid. It was reasoned later that antigenic presentation of AAV capsid on MHC-I in transduced hepatocytes had activated a pool of AAV primed memory CD8+ T cells, which effectively destroyed the transduced cells (Mingozzi et al., 2007). Figure 7 shows the hypothetical model which explains how CTL response was initiated against the AAV transduced liver cells, based on the observations from this clinical trial. Dose-dependent kinetics in capsid specific T cell activation was similarly documented against AAV1 transduced muscle fibres in a gene therapy trial for LPL deficiency. The loss of transgene expression with concomitant elevation of muscle creatinine phosphokinase (CPK) levels was observed at 4 weeks post gene transfer. Subjects in the high dose cohort with detectable capsid driven CD4+ and CD8+ T cell responses also developed high IgG3 Nab titers to AAV1 (Mingozzi et al., 2009).However, in AAV1-AAT trial, the long term expression of transgene was not affected by T cell responses (Brantly et al., 2009).

Adaptive immune response against the vector- encoded transgene occurs only if the body is not tolerant to the transgene protein and considers it as foreign.

The target tissue and route of vector administration are major determinants of transgene immunity in AAV gene transfer. It has been noted that transgene expression in the liver is associated with induction of tolerance to the transgene when compared to other tissues such as muscle (Hareendran et al., 2013). In dogs and non-human primates, it has been shown that the intravenous route of gene delivery to skeletal muscles is relatively safe and does not induce immunotoxicity (Haurigot et al., 2010, Toromanoff et al., 2010). CD8+ T cell response to the transgene was reported in only one clinical trial where AAV-mediated transfer of *dystrophin* gene into patients with DMD (Duchenne muscular dystrophy) resulted in the activation of previously primed pool of dystrophin specific memory T cells (Mendell et al., 2010). A recent study has underscored the fundamental role of AAV genome and underlying genetic mutation in influencing the immunity to the transgene product. In hemophilic mice with *F9* gene deletion, it was shown that single-stranded (ss) and self-complementary (sc) genomes of AAV1 induce similar Nab responses which affect the delivered FIX expression nevertheless scAAV1 vectors generated a more potent CD8+ T cell response to the transgene than the other. However, in mice with truncated hFIX, the AAV genome induced cellular immunity did not affect the tolerance to FIX, suggesting further that the transgene specific responses are a function of underlying disease causing mutation than the vector genome of AAV (Rogers et al., 2014). Destructive CD8+ T cells were found to be activated in the presence of certain cryptic epitopes in the FIX expression cassette in mice expressing human MHC class I molecule B0702, which highlights the importance of carefully designing the vector to evade immunotoxicity (Li et al., 2009).

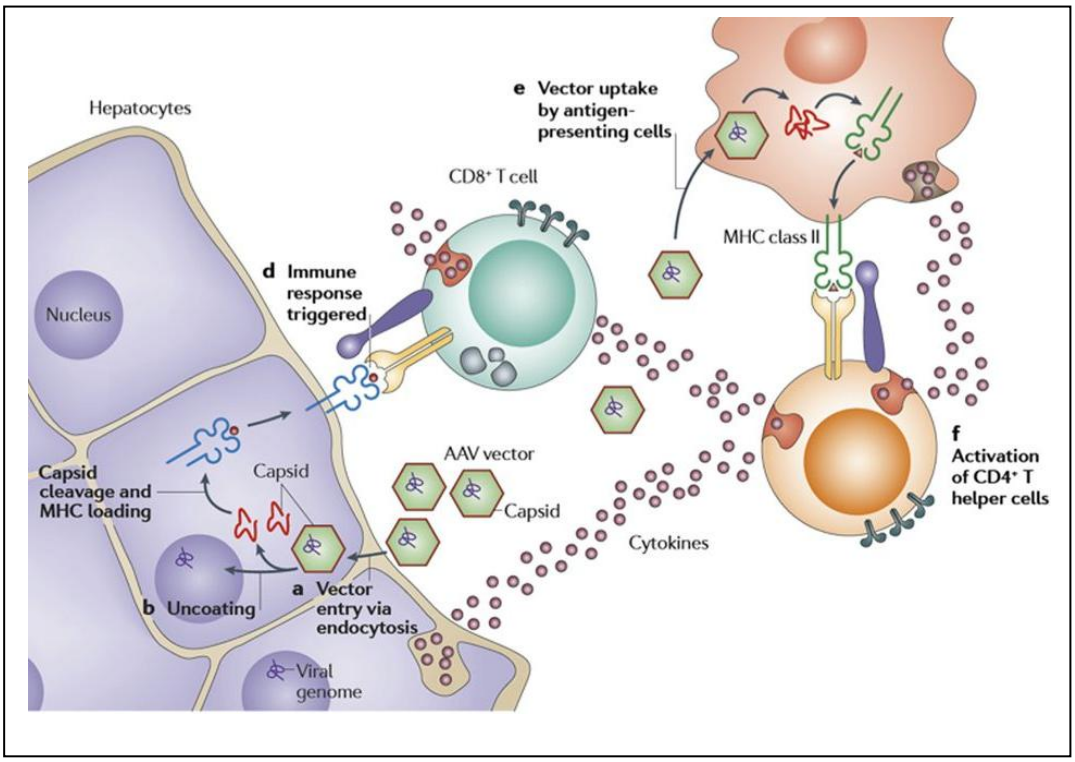

Figure 7: ***Working hypothesis of CD8$^+$T cell–mediated destruction of AAV-transduced hepatocytes***. *On transduction, vector enters hepatocytes, and following escape from the endosome and uncoating, vector DNA directs synthesis of FIX. Some capsid remains behind in the cytosol and undergoes proteasomal processing. Capsid-derived peptides are then transported to the endoplasmic reticulum and loaded onto MHC I molecules, making the transduced hepatocyte a target for circulating capsid-specific CD8$^+$ T cells. Note that activation of CD8$^+$ T cells and presentation of capsid-derived peptides must occur in a similar time course to result in a clinically detectable event.Adapted and modified (Mingozzi & High, 2013)*

2.6 Approaches to overcome the immunogenicity of AAV vectors

AAV gene transfer to immune-privileged sites such as eye and brain has been associated with minimal or no detectable immune response, even though vector doses tested were lower compared to those administered in liver or muscles. AAV vectors have been directly administered into the brain to treat Parkinson disease, Canavan disease and late infantile neuronal ceroid lipofuscinosis, and into the eye for the correction of LCA and Choroderemia, establishing the immunological unresponsiveness of these target tissues (Kotterman & Schaffer, 2014). The possible strategies that have been tested to prevent the immune clearance of AAV vectors during gene transfer to the other tissues are discussed below.

2.6.1 Improve the transduction efficiency of AAV vectors

The immune response to AAV has been found to be dependent on the vector dose, as projected by data from multiple clinical trials (Mingozzi & High, 2013). For example, in the AAV8-FIX trial for hemophilia B, the patients administered with the highest vector dose of 2×10^{12} vgs/kg developed CD8+T cell response to the capsid, which required intervention with steroids. This trial had however excluded patients with Nab against AAV8 (Nathwani et al., 2014). The seroprevalence of AAV8 in human population as discussed earlier is nearly 30% while that of AAV2 is ~70% (Calcedo et al., 2009). Unless the efficacy of AAV gene therapy is extended to the vast majority, it cannot be regarded as a viable treatment option. Reducing the vector dose or otherwise the capsid load would prevent activation of T cell response to a large extent, although compromising on the efficacy of gene therapy. Alternatively, if the capsid doses are low, they are easily subject to antibody neutralization. Hence it is necessary to optimize the vector dose to a critical

threshold wherein therapeutic efficacy using AAV vector is achieved and at the same time the deleterious cellular and humoral responses are averted as shown in figure 8(Mingozzi & High, 2013).

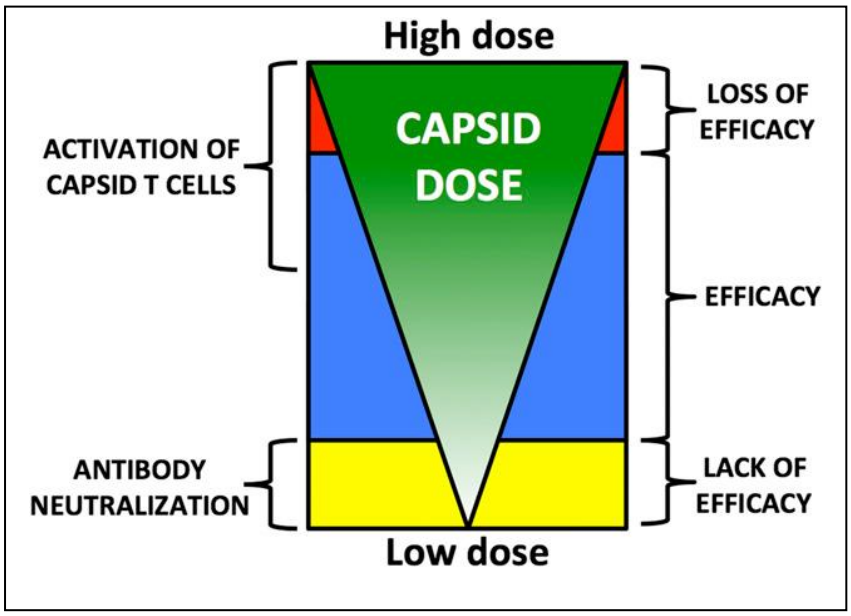

Figure 8: ***Model of the relationship between vector capsid dose and outcome of gene transfer.*** *Low capsid doses are more likely to be neutralized by anti-AAV antibodies, even low-titer Nab. This results in lack of efficacy. Higher capsid doses overcome this limitation, leading to therapeutic efficacy. Capsid-specific T cell activation is detected as the total capsid dose administered increases. This does not affect efficacy until a critical threshold is reached, above which immune-mediated clearance of transduced target cells results in loss of efficacy. Adapted (Mingozzi & High, 2013).*

Developing AAV vectors with superior transduction is a feasible solution to this problem, as these vectors can possibly attain therapeutic transgene expression at relatively low doses. Engineering of AAV capsids to augment the vector transduction efficiency was first reported by Zhong et al in 2008 (Zhong et al., 2008). Introducing tyrosine (Y) to phenylalanine (F) mutations on surface exposed regions of the AAV2 capsid significantly increased the transduction potential of these

vectors. Novel AAV vectors generated using single or multiple combinations of Y to F mutations on the capsid, exhibiting improved transduction profile have been described in the context of gene delivery to liver, retina, mesenchymal stem cells and dentritic cells (Petrs-Silva et al., 2011, Kotterman & Schaffer, 2014). It was postulated that mutating the tyrosine residues on the viral capsid prevented their phosphorylation by EGFP tyrosine kinases and subsequent degradation by ubiquitin-proteasome system. In this study, the same rationale was applied to generate mutant AAV2 vectors with alterations of serine/ threonine/ lysine (S/T/K) residues to alanine (A) residues on the capsid surface and demonstrated their ability for enhanced transduction in both cell lines and during *in vivo*gene transfer to murine liver (Gabriel et al., 2013). *[The data pertaining to S/T mutant AAV2 vectors is included as a chapter in this thesis]*. The increase in vector transduction efficiency achieved by selectively modifying S/T/K residues on the viral capsid was subsequently reported for other AAV serotypes as well (Sen et al., 2013a, Sen et al., 2013b). In a similar study, site directed mutagenesis of S to valine (V) residues augmented the efficacy of AAV2 based gene transfer to human monocyte derived dendritic cells with implications on development of more potent AAV-based antitumor vaccines (Aslanidi et al., 2012).

A recent report described an AAV variant, LK03 which exhibited remarkably higher transduction of human primary hepatocytes in comparison to AAV8 vectors. Using the directed evolution approach, a large library of replication-competent shuffled AAV capsid mutants was screened for selective infectivity of human hepatocytes *in vivo*in a chimeric human- murine liver model (Lisowski et al., 2013). Besides boosting vector performance, some of the capsid modified AAV vectors escape immune-surveillance. Using a mouse model which closely mimicked the capsid specific CTL response seen in humans, it was demonstrated that an

AAV2(Y-F) mutant prevented the loss of vector driven FIX expression by evading the CD8+T cell response to tranduced hepatocytes (Martino et al., 2013). One of the AAV2 (S→A) mutants described in this study has also demonstrated low Nab titers in mice compared to unmodified AAV2 vector (Gabriel et al., 2013). Another study has shown that genome engineering is an alternate way to endow AAV vectors with better transduction properties. The removal of NF-κB repressing factor (NRF) binding site from one of the ITRs of ssAAV vectors and insertion of glucocorticoid receptor binding element (GRE) in its place considerably improved the vector based transgene expression in human cells and murine liver (Ling et al., 2015).

2.6.2 Generate AAV vectors with immune evasion properties

Targeted engineering of the capsid is another effective approach for altering the immunogenic epitopes on the AAV surface. The identification of the antibody binding site on the capsid is the first step in this direction. Peptide scanning based epitope mapping of AAV2 and AAV8 neutralising antibodies have been described (Moskalenko et al., 2000, Gurda et al., 2013). One could also generate AAV capsid variant libraries by rational design or directed evolution, in the presence of Nab or T cell activating peptides to select mutants, which escape immune recognition. Rational design encompasses methods such as site directed mutagenesis or peptide insertions to disrupt the epitopic domains on the AAV capsid while directed evolution randomized the process to generate chimeric capsids through error-prone PCR and DNA shuffling (Bartel et al., 2011). Maersch *et al* combined both these approaches to generate a randomized capsid library containing 6 x 10^6 clones, which was screened for infectivity of HEK293 cells in the presence of human Nab. Five amino acid positions corresponding to immunogenic epitopes were identified and two vectors showed significant reduction in neutralization with human

sera or pooled IVIG (intravenous immunoglobulin) in the range of 2-5 fold (Maersch et al., 2009). Chimeric AAV libraries generated by DNA shuffling of the *cap* genes of various serotypes have been used to identify stealth AAV vectors with resistance to IVIG neutralization. One of these studies reportedly identified a mutant cB4, which showed 400-fold decreased neutralization in the presence of pooled anti-sera (Koerber et al., 2009). Besides genetic alterations, shielding of immunogenic epitopes on the AAV capsid by chemical conjugation with polymers such as PEG have also yielded vectors which evade Nab response (Selot et al., 2014).

2.6.3 Transient Immunosuppression

Another approach taken to avert immune challenge to AAV gene therapy is transient immunosuppression (IS). Pharmacological drugs which either attenuate the immune responses or more specifically target the B cell/ T cell populations are tested for this purpose. Mycophenolate mofetil, which prevents the expansion of T and B lymphocytes, and tacrolimus, a calcineurin inhibitor when co-administered along with AAV8-FIX vector was found to effectively block anti-AAV antibody response without affecting liver transduction in a NHP model (Jiang et al., 2006). The non specific anti-inflammatory effect of glucorticoids has been exploited to attenuate AAV immunotoxicity in AAV8-FIX trial for hemophilia B and AAV1-LPL trial for LPL deficiency (Gaudet et al., 2012, Nathwani et al., 2014). It has been demonstrated that bortezomib, by virtue of being a proteasome inhibitor can mitigate CTL response in mice having Nab to AAV8 and reduce antigenic presentation of AAV2 on MHC-I molecules (Finn et al., 2010, Karman et al., 2012).

Several antibody based IS regimens have been tested to moderate T cell responses to AAV vectors. Combination of CTLA-4Ig and PD-1 ligands has shown

to suppress T cell reactivity in muscle fibres transduced with AAV (Adriouch et al., 2011). A 20-fold reduction in Nab titers to AAV8 was reported in immune-competent mice treated with non-depleting anti-CD4 antibody and cyclosporine (McIntosh et al., 2012). Combined targeting of CD40L and CTLA prevented humoral response to AAV and enabled disease correction in dystrophic *mdx* mouse injected with AAV1 vectors (Lorain et al., 2008). Figure 9 shows some of these immunosuppressive drugs which target different stages of T cell-APC interactions and thereby inhibit T cell reactivity.

2.6.4 Tolerance induction

Induction of immune tolerance to the transgene following AAV gene transfer into liver was found to be mediated by regulatory T cells (Tregs). Using adoptive T cell transfer studies in mice, it was shown that Tregs (CD4+CD25+FoxP3+) effectively suppress antibody and CD8+ T cell responses to the AAV encoded transgene (Martino et al., 2009). Cytokines such as IL-10 and TGFβ have been implicated in the induction of peripheral tolerance by Tregs (Hoffman et al., 2011). De Groot *et al* first described the presence of MHC-II T cell epitopes (Tregitopes) on Fc region of IgG, which specifically triggered the expansion of Tregs. They also demonstrated that the co-incubation of these epitopes and other immunogens with PBMNCs resulted in activation of Tregs, reduction of effector T cell proliferation and suppression of CD4+ T cell responses against the antigen (De Groot et al., 2008).

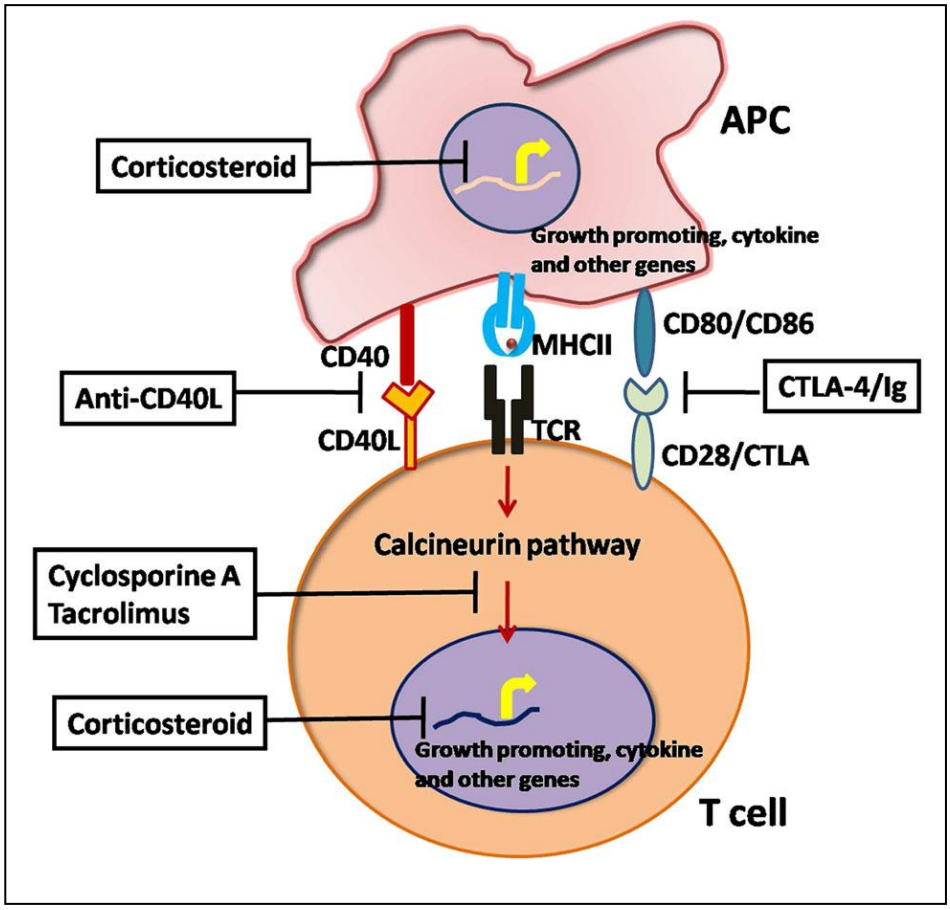

Figure 9: ***Immunosuppressive agents to target antigen presenting cell and T cell interactions.*** *The interactions between various ligand and receptors of APC and T cells apart from the effect of different immuno-suppressant drugs acting at distinct steps are shown. The engagement of T cell receptor (TCR) with peptide-MHC complex presented by APC activates calcineurin, a calcium dependent phosphatase that activates nuclear factor of activated T cells (NFAT). This leads to increased expression of interleukin (IL)-2 cytokine. Cyclosporin A and tacrolimus are known to block this pathway. Corticosteroids block the expression of cytokines like IL-2 and TNF-γ at the nuclear level in T cellsand also prevent APC differentiation and maturation. T cell activation also requires the interaction of co- stimulatory molecules on T cells and their respective ligands on APC. The interaction between CD40L and CD40 is inhibited by anti - CD40L antibody. Similarly, the interaction between CD28/ CTLA and CD80/CD86 is inhibited by CTLA-4/Ig. Adapted(Hareendran et al., 2013)*

A recent study exploited this strategy in modulating immune response to AAV vectors. Co-expression of AAV2 VP1 capsid protein and Tregitopes in an AAV1 vector significantly suppressed the CD8+T cell responses to AAV2 capsid when injected intramuscularly into a murine immunization model, which exhibits strong immunotoxicity (Hui et al., 2013).

Mingozzi *et al* demonstrated the utility of capsid decoys to facilitate AAV transduction in presence of high Nab (1:100) titers. Inclusion of empty capsids in the vector formulation resulted in the effective adsorption of pre-existing anti-AAV antibodies in a dose-dependent manner as shown in mice and NHP models. It was observed that Nab neutralization of AAV8-FIX vector was rescued by addition of excess (9-fold) of AAV8 empty capsids, thereby overcoming the inhibitory effect of humoral immunity on AAV gene transfer (Mingozzi et al., 2013). However there is a concern with this approach that it might not prevent or on the contrary might induce CD8+ T cell responses by virtue of increasing the capsid load of AAV, although further studies are needed to clarify this (Basner-Tschakarjan & Mingozzi, 2014).

2.7 Targeted inhibition of the immune response

2.7.1 NF-κB signaling pathway

2.7.1.1 Basic overview

NF-κB (Nuclear Factor- κB) transcription factor was first described in 1986 by David Baltimore in B cells as a DNA binding protein with affinity for transcriptional enhancer of immunoglobulin κ light chain gene and its activation was

implicated in antibody production (Sen & Baltimore, 1986). But soon it was found that NF-κB is expressed in almost all cell types and is associated with diverse functions such as cell survival, differentiation and apoptosis; and in host defense against pathogens. Many distinct intracellular and extracellular stimuli can induce the NF-κB activity through receptor mediated signal transduction pathways. NF-κB signaling plays a fundamental role in regulating several genes responsible for evoking inflammatory and immune responses against bacterial and viral infections (Hoffmann & Baltimore, 2006).

The mammalian NF-κB protein family comprises five Rel proteins which contain the characteristic Rel homology domain (300 amino acids) at their N terminus. Among these, RelA (p65), RelB and c-Rel have a transactivation domain at the C terminus to bring about the non-homologous activation of target genes while the other two proteins, NF-κB1 (p50 and its precursor p105) and NF-κB2 (p52 and its precursor p100), which are transcriptionally inactive have ankyrin repeats at C termini. These proteins can form homo or hetero- dimers in the cytoplasm using their conserved Rel homology domain. These dimers then translocate into the nucleus, bind to certain sequences called κB sites (8-10bp) on their target genes to activate their transcription (Hayden & Ghosh, 2004). The activation of NF-κB is tightly regulated as its aberrant and constitutive activity can lead to malignancy and inflammatory diseases (Ruland, 2011). At resting state, the NF-κB proteins remain inactive by binding to inhibitor of κB (IκB) proteins in the cytoplasm. These inhibitory proteins (IκBα, IκBβ, IκBε, IκBγ and BCL-3) are characterized by the ankyrin repeats (as in the p100 and p105 NF-κB proteins) which can bind to NF-κB

dimers and mask their nuclear localization signal (NLS). In response to appropriate stimuli, the IκB proteins get phosphorylated by IκB kinases (IKK) to activate NF-κB mediated signal transduction. The IKK complex contains two kinase subunits IKKα and IKKβ; and a regulatory subunit NEMO (NF-κB essential modifier) (Rahman & McFadden, 2011). The various components of the NF-κB signaling module are shown in figure 10.

Two NF-κB activation pathways have been described, the classical (canonical) pathway and the alternative (non-canonical) pathway based on which IKK molecule mediates the upstream phosphorylation process (Figure 11). The classical NF-κB pathway which is important for innate immunity is activated by diverse stimuli such as Tumor necrosis factor receptor (TNFR1/2), T cell and B-cell receptors (TCR and BCR), Toll-like receptor family (TLR), Interleukin-1β (IL-1R) and genotoxic stress (UV) leading to IKKβ mediated phosphorylation of IκBα(Hayden et al., 2006). The alternate NF-κB pathway is stimulated by ligands belong to TNF family such as lymphotoxin β (LTβR), B cell-activating factor (BAFF), CD40R and receptor activator of NF-κB ligand (RANKL). It is initiated by NIK (NF-κB inducing kinase) mediated activation of IKKα, which inturn phosphorylates p100 resulting in its processing to form p52. This pathway is mainly involved in lymphoid organ development, cellular differentiation and survival, and implicated in adaptive immunity(Zheng et al., 2011).

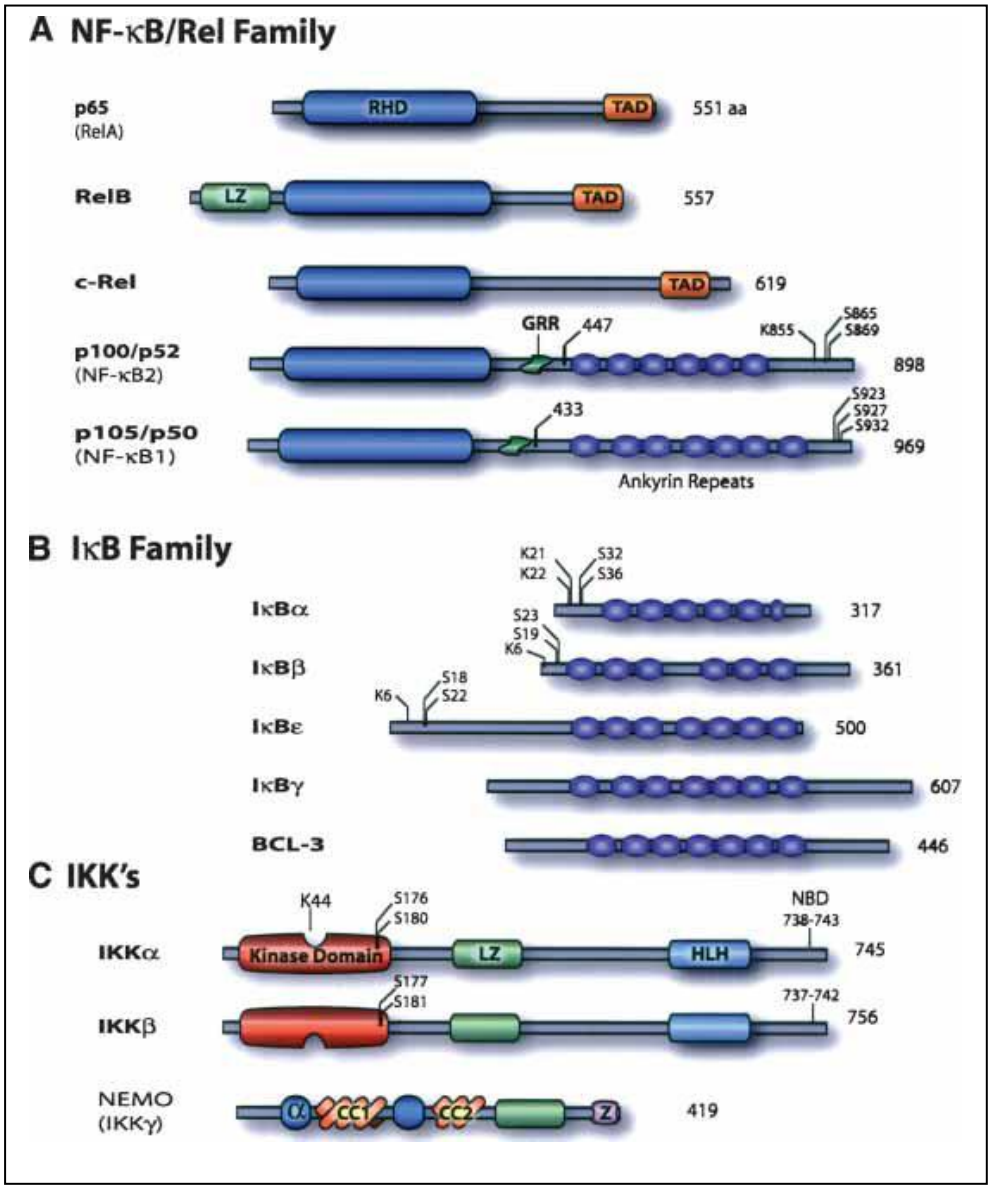

Figure 10: The NF-κB signaling module*. Members of the NF-κB, IκB and IKK proteins families are shown. The number of amino acids in each protein is indicated on the right. Presumed sites of cleavage for p100 (amino acid 447) and p105 (amino acid 433) are shown. Phosphorylation and ubiquitination sites on p100, p105, and IκB proteins are indicated. (RHD) Rel homology domain; (TAD) transactivation domain; (LZ) leucine zipper domain on IKKα/β and Rel-B; (GRR) glycine-rich region; (HLH) helix–loop–helix domain; (Z) zinc finger domain; (CC1/2) coiled-coil domains; (NBD) NEMO-binding domain; (α)-αhelical domain. Adapted (Hayden & Ghosh, 2004).*

The SCF- βTRCF family of ubiquitin ligases induces the proteasome-mediated degradation of phosphorylated IκBα and the processing of NF-κB subunits (p105 and p100) during activation of NF-κB pathways (Ruland, 2011). The activation of NF-κB pathways occurs in the presence of certain adapters proteins which possess domains involved in protein-protein interactions. Some of the key adapter molecules which function in NF-κB signal transduction include TIR (Toll IL-1R) domain containing proteins like MyD88 (Myeloid differentiation primary response gene 88), TRIF (TIR domain containing adapter inducing interferon β), TIRAP (TIR domain containing adapter protein) or TRAM (Toll like receptor adapter molecule); TRAF proteins which contain TRAF (TNF receptor associated factor) domain; RIP-1 (Receptor interacting proteins); CARD (caspase activation and recruitment domains) proteins and Death Domain (DD) containing proteins such as TRADD (TNFR associated protein with DD) and FADD (Fas associated protein with DD). Certain kinases such as IRAK (interleukin -1 receptor associated kinase), TAK (TGFβ associated kinase)and TBK (TANK binding kinase) also act as mediators in the signaling cascades which culminate in NF-κB activation (Hayden & Ghosh, 2012).

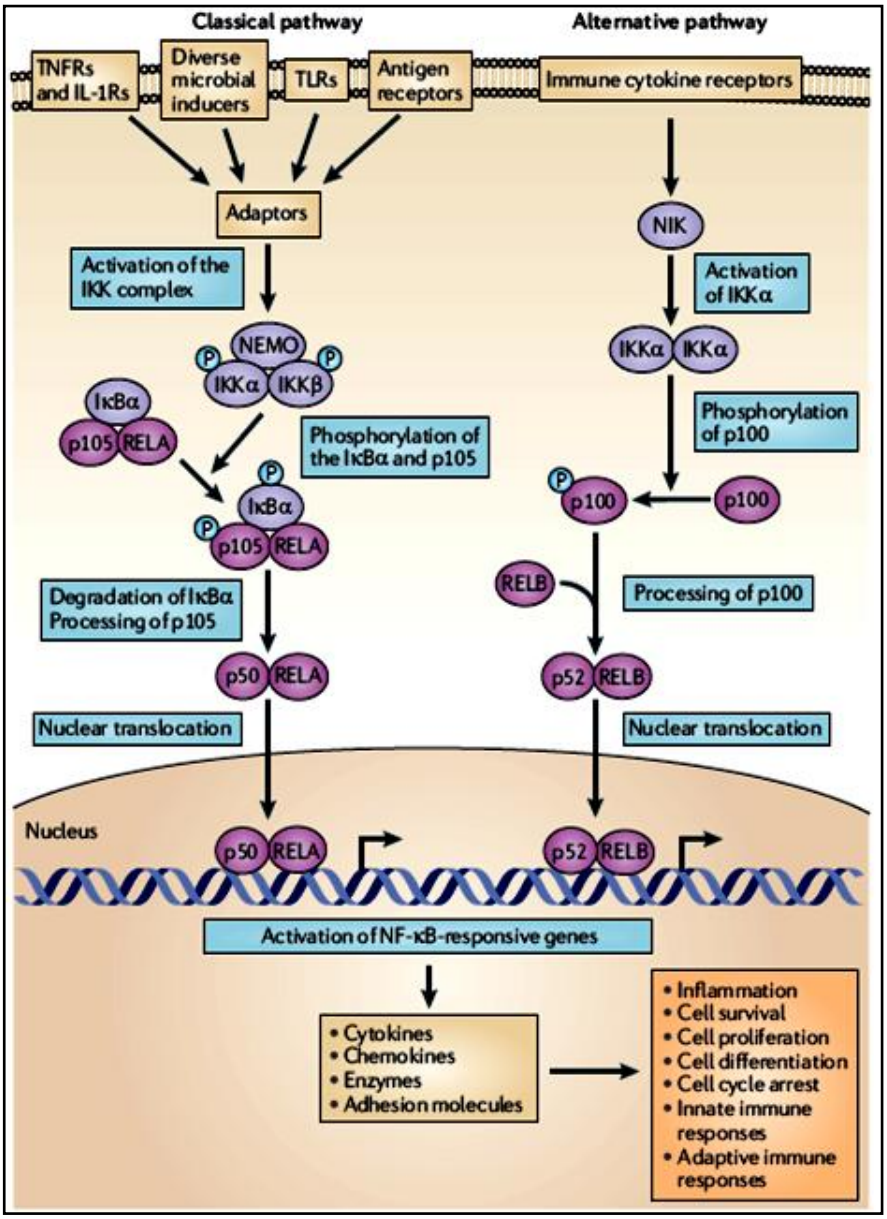

Figure 11: The classical and alternative NF-κB signaling pathways. *These two NF-κB pathways use a wide variety of signals to control a diverse set of cellular responses. Protein levels and activity of signaling molecules can be regulated through post-translational modifications such as phosphorylation, ubiquitylation and acetylation. The activation of nuclear factor-κB (NF-κB) ultimately results in the transcription of genes that encode pro-inflammatory factors and factors that influence cell proliferation. IκBα, NF-κB inhibitor-α (also known as NF-κBIα); IKK, IκB kinase; IL-1R, interleukin-1 receptor; NEMO, NF-κB essential modulator (also known as IKKγ); NIK, NF-κB-inducing kinase (also known as MAP3K14); TLR, Toll-like receptor; TNFR, TNF receptor. Adapted (Rahman & McFadden, 2011).*

2.7.1.2 NF-κB in the context of AAV-based gene transfer

Viruses are known to activate NF-κB mostly by the engagement of TLRs (Toll- like receptor), which recognize the viral nucleic acids as an inducing stimuli or PAMPs. TLR3, TLR7 and TLR8 located in the nuclear membrane bind to dsRNA or ssRNA molecules of viruses such as reovirus, HIV-1 and Influenza virus while TLR9 binds to viral CpG sequences or dsDNA of HSV (Herpes simplex virus) to activate NF-κB and produce Type I Interferons (IFNα/β). In addition RNA helicases (eg: RIG-1, MDA) are involved in recognition of dsRNA genomes of viruses like Sendai virus or Newcastle disease virus (Hayden et al., 2006). Some viruses like HIV-1 and RSV (Rous sarcoma virus) activate and exploit the NF-κB transcription factor to trigger the viral gene replication and expression during their infectious cycle. Oncogenic viruses such as HTLV (Human T lymphotropic virus) and EBV bring about cellular transformation by the constitutively activating NF-κB pathways. There are also certain viruses which are known to inhibit NF-κB such as Epstein Barr virus (EBV), Hepatitis C virus, Adenovirus and Human cytomegalovirus (Rahman & McFadden, 2011).

AAV is shown to activate NF-κB pathway both *in vitro* in HeLa cells and *in vivo* during hepatic gene delivery into mice (Jayandharan et al., 2011). It was demonstrated that VP16, an NF-κB activator increased the *in vitro* transduction of AAV2 vectors by 25-fold while an NF-κB activator, Bay11 abrogated it. The western blot analysis of nuclear extracts showed that the alternative pathway component, p52 was enriched upon NF-κB activation in AAV infected cells. AAV gene transfer into murine liver resulted in the activation of the classical NF-κB pathway within 2 hours of vector administration which was followed by the induction of alternative NF-κB pathway at 9 hours. Treatment of mice with Bay 11 before vector infusion effectively

reduced the expression of various pro-inflammatory cytokines and factors, associated with NF-κB pathway and also lowered the anti-AAV2 humoral response without affecting the long term expression of transgene in the liver (Jayandharan et al., 2011).

Bortezomib (PS-341) is a proteasome inhibitor which is clinically approved for the treatment of multiple myeloma. It inhibits the core of the 26S proteasome unit by covalently binding to the threonine residue on the active site. The inhibition of NF-κB pathway is one of the known mechanisms by which Bortezomib targets the proliferation and survival of cancer cells, processes in which the aberrant NF-κB activity is highly implicated (Hideshima et al., 2002). Few studies have used this proteasome inhibitor in improving the efficacy of AAV gene transfer. In canine models of hemophilia A, it was shown that Bortezomib augmented the intrahepatic delivery of AAV2 or AAV8 vectors expressing *FVIII*, a relatively large transgene to establish sustained disease correction (Monahan et al., 2010). Bortezomib also effectively reduced the CD8+T cell responses against AAV2 vectors by blocking the MHC class I presentation of the capsid specific epitopes (Finn et al., 2010). It was shown to efficiently lower the pre-existing anti-AAV antibody levels and mitigate the CD8+ T cell responses in mice, however not to the extent of allowing the subsequent re-administration of the vectors, without evoking an immune response (Karman et al., 2012). This suggested that Bortezomib as a single agent was not able to completely abrogate the pre-existing humoral response to AAV and therefore the study recommended the use of it in combination with other immune suppressive agents (Karman et al., 2012).

2.7.2 Poly(ADP-ribose) polymerase (PARP)

Members of the Poly(ADP- ribose) polymerase (PARP) family of proteins are chromatin associated enzymes which primarily function in DNA damaging sensing and repair. Of the 18 members described so far, PARP-1 is the most abundant and well characterized. It is a 116-Kda zinc finger protein which was first described by Chambon and colleagues in 1963 (Chambon et al., 1963). PARP is known to play fundamental roles in diverse cellular processes such as DNA damage response and maintenance of genome integrity, transcriptional regulation, chromatin modification, cell- cycle arrest and apoptosis. It is associated with multiple DNA repair pathways such as SSB (single strand break), DSB (double-strand break) and BER (Base excision repair).

DNA breaks trigger the activation of PARP-1 nuclear enzyme, which then cleaves nicotinamide adenine dinucleotide (NAD) to nicotinamide and ADP ribose. These ADP-ribose units are covalently attached to the glutamic or aspartic acid residues of the PARP substrates in the form of long and branched chains of poly (ADP-ribose) or PAR linked by glycosidic bonds. Nuclear proteins such as DNA polymerase I and II, Ca2+- Mg2+ endonuclease, histones, several chromatin binding proteins like transcriptional factors, topoisomerases, DNA protein kinase and PARP-1 itself (automodification) serve as targets of this enzyme (D'Amours et al., 1999). Addition of negatively charged PAR chains adjacent to the DNA nicks relaxes the chromatin to recruit scaffold proteins like XRCC1and other chromatin remodelling proteins to facilitate the DNA repair. Once the repair of DNA damage is complete, the PAR chains get degraded by poly(ADP-ribose) glycohydrolase (PARG) (Javle &

Curtin, 2011). PARP-1 has three highly conserved domains: N terminal DNA binding domain containing zinc finger motifs, a central automodification domain and a C terminal catalytic domain (Figure 12A). The fate of a cell upon PARP-1 activation depends on the intracellular levels of NAD+ and ATP, which are used up in the process of poly (ADP) ribosylation of its target proteins. The increase in activated PARP-1 levels in a cell is coupled to simultaneous decrease in NAD+/ATP or otherwise the source of cellular energy. At normal NAD+/ATP levels, PARP-1 activation induces DNA repair and cell survival. At low levels of NAD+/ATP, PARP-1 gets inactivated through cleavage by caspase-3 and the cell undergoes apoptosis. Conversely, at critically low levels of NAD+/ATP resulting in acute energy depletion, the cell dies rapidly of necrosis (Figure 12B) (Strom & Helleday, 2012).

Increasing the susceptibility of malignant cells to apoptosis is one of the approaches targeted in cancer therapy. The reversal of genetic lesions by DNA damage repair pathways operating in the cell is counterproductive in targeting cancer. Hence the inhibition of DNA repair using PARP-1 inhibitors induces specific killing of cancer cells by causing synthetic lethality. In 2005, it was shown that BRCA1 or BRCA2 (tumor suppressor proteins) deficient cells which have inherent defect in homologous recombination mediated DSB repair, were effectively destroyed in the presence of PARP-1 inhibitors (Bryant et al., 2005).

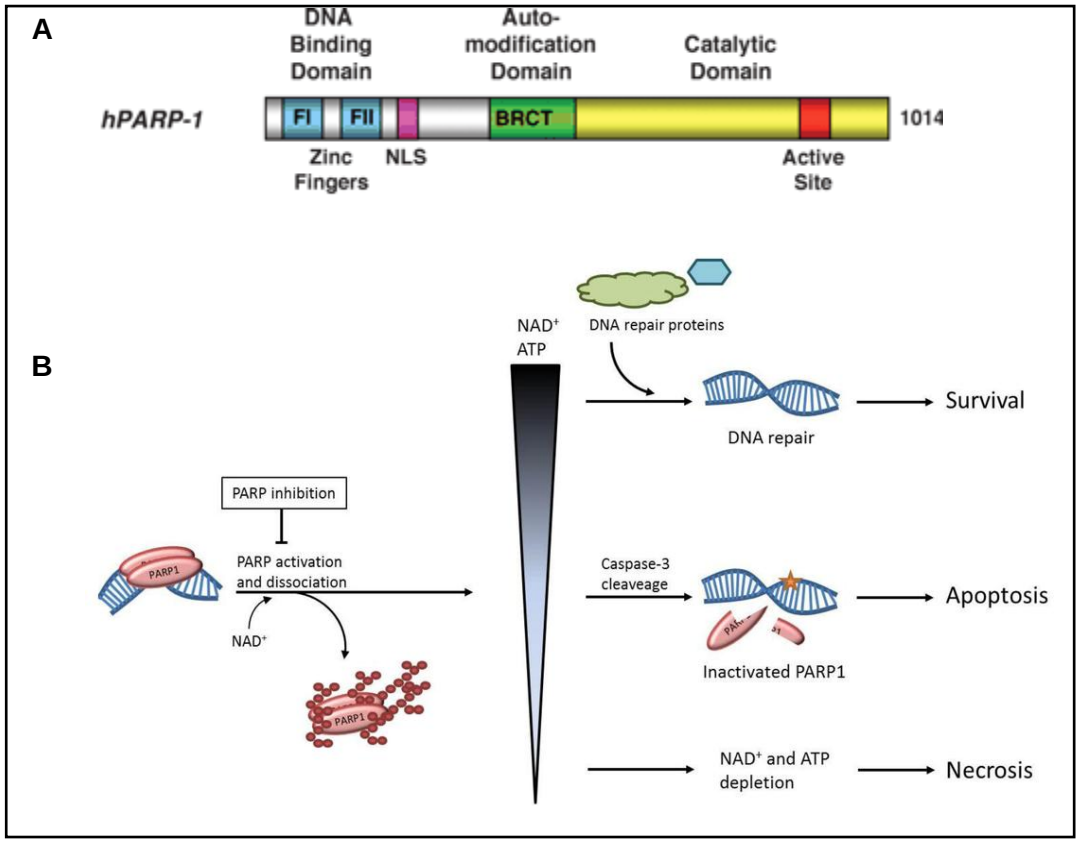

Figure 12: ***Structure and biology of PARP-1.*** *(A) Structural and functional organizations of PARP-1. PARP-1 has a highly conserved structural and functional organization including (1) an N-terminal DNA-binding domain with two Cys-Cys-His-Cys zinc finger motifs (FI and FII), (2) a nuclear localization signal, (3) a central automodification domain containing a BRCT protein-protein interaction motif, and (4) a C-terminal catalytic domain with a contiguous 50-amino-acid sequence, the "PARP signature" motif, that forms the active site. Adapted (Kim et al., 2005). (B) Possible outcomes of PARP activation. PARP-1 binds a DNA lesion and the resulting activation of the enzyme causes poly(ADP-ribose)ylation (PARylation) of PARP1 itself and other proteins. PARP1 utilizes NAD+ as a substrate for this modification and as the levels of activated PARP1 increase in a cell, the corresponding levels of NAD+ and ATP decrease. The fate of the cell after PARP1 activation depends on these intracellular levels of NAD+/ATP. At normal levels, cell survival is promoted, as the post-translational modification of PARP1 induces DNA repair. At lower levels of NAD+/ATP, PARP1 is inactivated through cleavage by caspase-3 to conserve energy for the controlled induction of apoptosis. At extremely low levels of NAD+/ATP, the cell rapidly dies through necrosis as a result of acute energy depletion. Adapted (Strom & Helleday, 2012).*

Currently several PARP-1 inhibitors are being tested in clinical trials for targeting of cancers such as ovarian cancer, breast cancer, solid tumors, lung cancer, melanomas, pancreatic cancer, lymphoma and others, either as a monotherapy or in combination with chemotherapy/ radiation. Some of the potential PARP-1 inhibitors tested in phase II/III trials include veliparib (ABT-888), Olaparib (AZD2281), Rucaparib (AG-014699), and Iniparib (BSI-201) (Lupo & Trusolino, 2014).

The activation of PARP-1 is associated with the pathogenesis of certain inflammatory diseases such as arthritis, type-1 diabetes, colitis, ischaemia and septic shock (Szabo & Dawson, 1998, Hassa et al., 2001). The contributing factors for this could either be the overactivation of PARP-1 leading into energy depletion and necrotic tissue damage or the activation of NF-κB mediated transcription of pro-inflammatory genes. Cellular stress is known to activate NF-κB pathway through PARP-1 and/or ataxia telangiectasia mutated (ATM) kinase, which arbitrate signaling cascades that converge on IKK (Hinz et al., 2010). PARP-1 was found to act as a co-activator of NF-κB driving the expression of its target genes in response to pro-inflammatory stimuli and genotoxic stress (Ullrich et al., 2001). Studies in PARP-1 knockout mice showed down-regulation of the expression of several NF-κB dependent inflammatory response genes (Hassa et al., 2003). The protective effect of PARP-1 inhibitors against tissue injury in various inflammatory conditions has been demonstrated in animal models (Giansanti et al., 2010).

PARP-1 has also been implicated in regulating viral DNA replication and gene expression by virtue of its binding to DNA terminal repeat sequences in several viruses including Epstein Barr virus and Kaposi's sarcoma-associated herpesvirus (Tempera et al., 2010). HIV-1 has been shown to inhibit NF-κB by forming a complex with PARP-1 using its Vpr protein in association with glucocorticoid

receptor (Muthumani et al., 2006). This suggests that virus interactions with PARP-1 can regulate diverse functions related its infection and gene expression. Until now there is only one report which links PARP-1 with AAV. Romanova *et al* have shown that PARP-1 directly interacts with AAV Rep and that depletion of PARP-1 using small hairpin RNA enhances the integration of the AAV genome in HeLa cells (Romanova et al., 2011). In this doctoral study efforts have been made to define the role of PARP-1 in regulating AAV-based transgene expression and examine the effect of its modulation on host immune response to the vector.

3. MATERIALS AND METHODS

3.1 Study design

3.1.1 Role of NF-κB in AAV-mediated gene transfer

To examine the effect of inhibiting NF-κB pathway on the AAV2 based transgene expression*in vitro,* HeLa cells were pretreated with NF-κB inhibitors prior to virus infection and analysed 48 hours later. Three NF-κB inhibitors were further screened for their ability to down-regulate the expression of various cytokine/ chemokine and other inflammatory marker genes associated with NF-κB pathway in AAV2 infected cells.

3.1.2 Role of PARP-1 in AAV-mediated gene transfer

To determine the effect of PARP-1 inhibition on AAV2 transduction, the vector based transgene expression was analysed either *in vitro* in human cervical carcinoma (HeLa) cell line treated with PARP-1 specific siRNA or *in vivo* in liver lobes of mice treated with PJ34, a pharmacological inhibitor of PARP-1 (Figure 13). The effect of PJ34 treatment on the pro-inflammatory response in mice wasascertained by measuring the relative fold change in the expression of NF-κB associated cytokine and pro-inflammatory genes in the liver tissue.

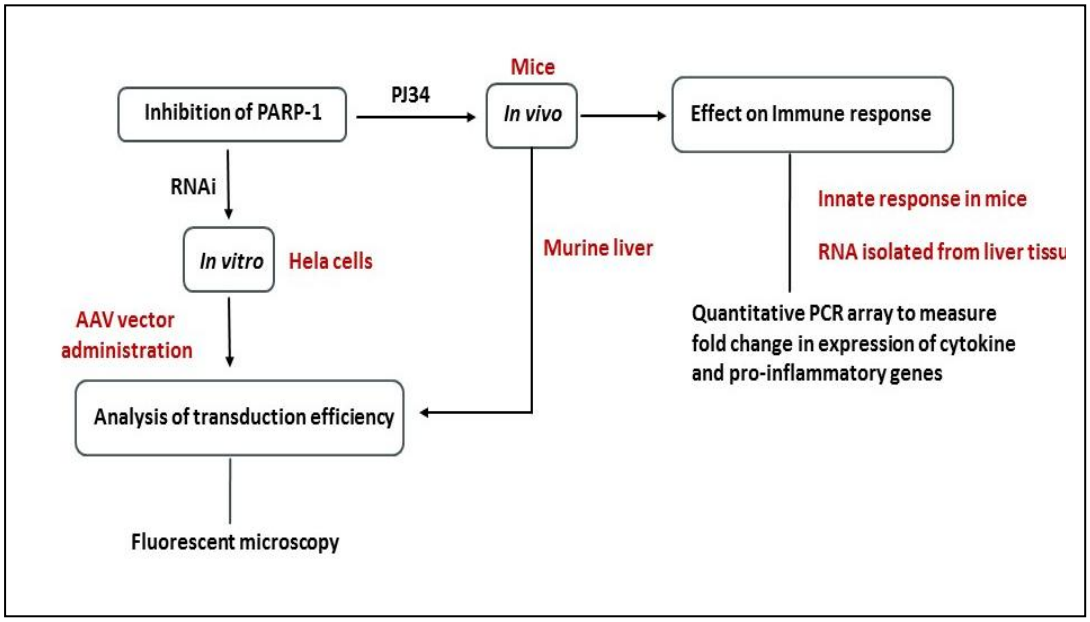

Figure 13: ***Flowchart of the experimental design to study the role of PARP-1 in AAV-based gene transfer***

3.1.3 Study of bio-engineered AAV2 capsid mutants

AAV2 mutant vectors were generated by selective modification of serine/ threonine (S/T) amino acids on the capsid surface to alanine (A) residues. The transduction efficiency of these AAV2 S/T mutant vectors were first analysed in HeLa cells, at 48 hours post-transduction and in liver sections of mice 4 weeks after vector administration. The packaging efficiency of these vectors was determined as shown in the study design (Figure 14).

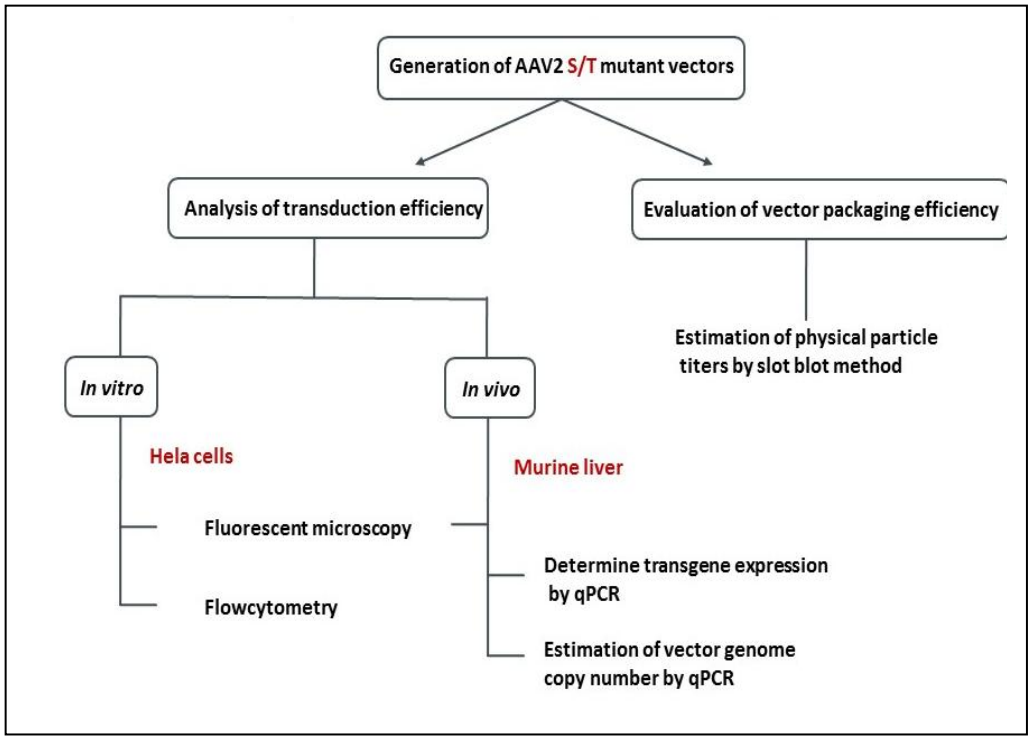

Figure 14: Experimental workflow to study the capsid modified AAV2 mutant vectors

3.1.4 The effect of synergistic inhibition of PARP-1 and NF-κB on AAV-mediated gene transfer

Mice pretreated with inhibitors of PARP-1 and NF-κB were injected with either AAV2 or AAV8 vectors carrying reporter genes like luciferase (Luc) or EGFP (enhanced green fluorescence protein). The effect of the combined inhibition of PARP-1 and NF-κB on the transgene expression and the host immune response against AAV2 vectors was assessed. In addition, the AAV2 based transgene expression in HeLa cells subjected to PARP-1 and NF-κB combined inhibition was also analysed. The data obtained with AAV2 vectors was further evaluated during hepatic delivery of *FIX* gene into hemophilia B mice. The design of the study is shown in figure 15.

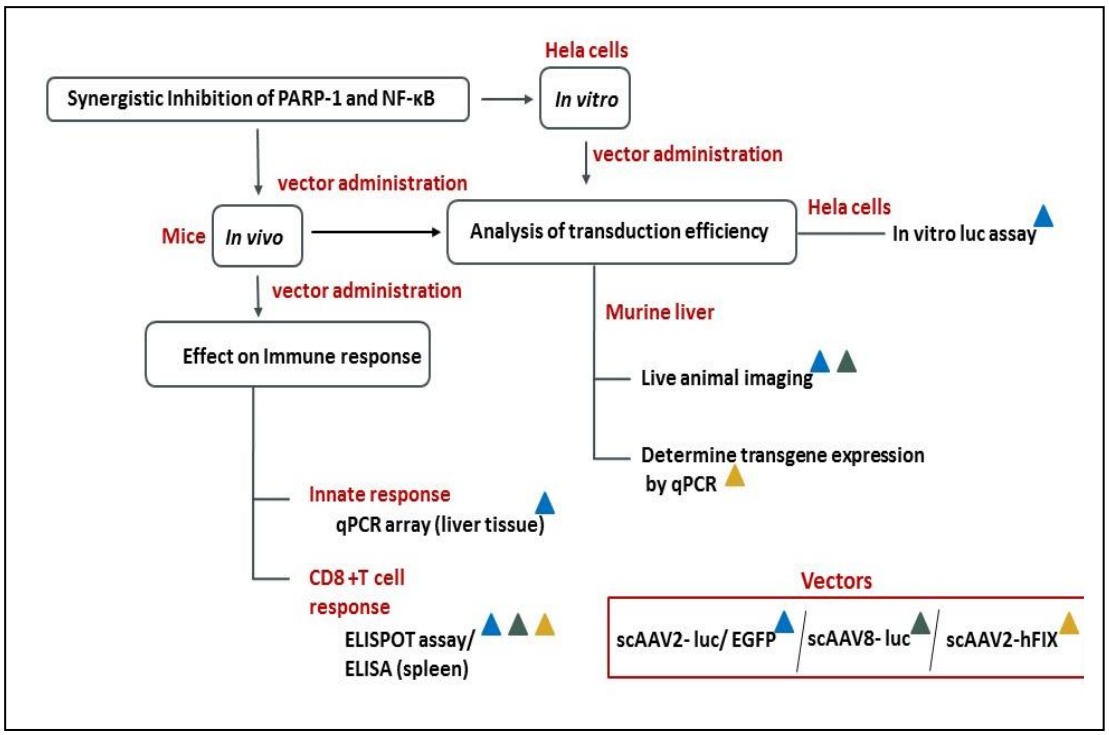

Figure 15: ***Experimental flowchart of the study to evaluate the combined inhibition of PARP-1 and NF-κB on AAV-mediated gene transfer.*** *Each type of vector is represented by a different colored triangle to indicate the experiments conducted with it.*

3.2 Animal procedures

All the experiments involving animals were performed according to the institutional guidelines for animal care specified at Christian Medical College (Vellore, India). BALB/c and C57BL/6 mice strains and hemophilia B mice were purchased from Jackson Laboratory (Bar Harbour, ME, USA). Experimental mice were housed at 22-24°C in individually ventilated cages with free access to water and food. Small molecule inhibitors and viral vectors were injected either intraperitoneally or intravenously. At the end of the studies, mice were euthanized by carbon dioxide (CO_2) inhalation.

3.3 Chemicals and reagents

Lyzozyme, Benzonase, Lithium chloride, Tris- Cl, EDTA, polyethylene glycol (PEG), LB-broth, LB-agar, Agarose, Sodium hydroxide (NaOH), Sodium dodecyl sulphate (SDS), Sodium acetate and PJ34 were obtained from Sigma-Aldrich (Sigma-Aldrich, St Louis, MO, USA). ABT-888 was from Enzo Life Sciences (Enzo Life Sciences, Farmingdale, NY, USA). Bay11-7085, Ro106 and Isohelenin were sourced from Calbiochem (Calbiochem, Darmstadt, Germany). PARP-1 siRNA and western blot antibodies were from Cell Signaling Technology (Cell Signaling Technology, Boston, MA, USA). D- Luciferin substrate was purchased from BioVision Inc (BioVision Inc, Milpitas, CA). Bortezomib was a kind gift from Natco Pharma (Natco Pharma Ltd, Hyderabad, India).

3.4 Cell lines

HeLa cell line was sourced from American Type Culture Collection (ATCC, Rockville, MD, USA) and used for *in vitro* infection studies. AAV-293 packaging cell line was procured from Stratagene- Agilent Technologies. It is an HEK-293 derivative, expressing Adenovirus genes *E1a* and *E1b*. Both these cell lines were maintained at 37°C with 5% CO_2 in a humidified incubator and grown in Iscove's Modified Dulbecco's Medium (IMDM, GIBCO-Life Technologies, Carlsbad, CA, USA) supplemented with 10% fetal bovine serum (FBS, GIBCO-Life Technologies), 1.2g/L of sodium bicarbonate and 1% (by volume) of 100X stock solution of antibiotics (10,000 U penicillin+10,000 mg streptomycin; GIBCO-Life Technologies). During passaging, the cells were dissociated at about 60-70% confluency using 0.05% Trypsin – EDTA (GIBCO-Life Technologies), thereafter

resuspended in media and counted in a hemocytometer. The cells were cryopreserved in media containing 10% DMSO (Sigma-Aldrich) and 20% FBS.

3.5 Site directed mutagenesis

Point mutations corresponding to specific amino acid changes (S/T →A) were introduced on AAV *rep- cap* plasmid using Quik Change II XL Site Directed Mutagenesis Kit (Stratagene- Agilent Technologies) in accordance with manufacturer's protocol. This method involves primer directed PCR amplification of dsDNA using PfuUltra High Fidelity DNA polymerase. The oligonucleotide primers containing the desired mutation (S/T→A) along with a silent mutation (to change restriction pattern for selection) were designed in vector NTI software (Life Technologies). Approximately, 125ng of each primer (forward and reverse) was added to a reaction mixture of 50 µl containing about 10ng of template ds plasmid, dNTPs and 1µl of Pfu polymerase. The primer sequences used for site directed mutagenesis are shown in table 2. The thermal cycling parameters of PCR reaction were: 95°C for 1min; 18 cycles of 95°C for 50sec, 60°C for 50sec and 68°C for 8min; 68°C for 7 min.

Extension of the oligonucleotide primers generates a mutated plasmid containing staggered nicks. Following temperature cycling, the product was treated with *DpnI* endonuclease, which specifically digests the methylated parental DNA template and helps in selection of mutationcontaining synthesized DNA. 1µl of *DpnI* restriction enzyme was added to the amplication reaction and incubated at 37°C for 1 hour. Finally 2µl of *DpnI* treated DNA was transformed into XL10-Gold ultracompetent *E.coli* cells. For the transformation reaction, 45µl of the competent

cells and 2µl of DNA was gently mixed and incubated on ice for 30 minutes. Immediately the reaction tubes were heat pulsed at 42°C for 30 seconds followed by cooling on ice for 2 minutes. 500µl of pre-warmed NZY+ broth was added to the tube and incubated for 1 hour at 37°C with shaking at 220rpm. These cells were then spread on ampicillin (100mg/ ml) containing LB agar plates. Mini prep plasmid DNA was isolated from starter cultures of ampicillin resistant colonies. The presence of desired mutation was verified by change in restriction digestion patterns corresponding to the additional identifying mutations. Further confirmation of the generated mutations was done by DNA sequencing.

RESIDUE	MUTATION PRIMER SEQUENCE (5' TO 3')
S276A	CACTACTTTGGCTACGCCACCCCTTGGGGGTATTTTGACTTC
S489A	TACCGCCAGCAGCGAGTAGCTAAGACATCTGCGG
S498A	AAGACATCTGCAGATAACAACAACGCTGAATACTCGTGGACT
S525A	CCGGGCCCGGCGATGGCAGCCCACAAGGACG
S537A	AGAAAAGTTTTTTCCTCAGGCCGGGGTTCTCATCTTTGGG
S547A	CATCTTTGGGAAGCAAGGCGCCGAGAAAACAAATGTGGACA
S662A	AATCCTTCGACCACCTTCGCTGCGGCAAAGTTTGCTTC
S668A	GCGAATCCGTCGACCACCTTCAGTGCGGCAAAGTTTGCTGCCTTCATCACA
T251A	ACCCGAACCTGGGCCCTGCCGGCCTACAACAACCACCTCTAC
T454A	TATTACTTAAGCAGAACAAACACTCCAAGTGGAGCCACCACGCAGTCAAGG
T503A	ACATCTGCAGATAACAACAACAGTGAATACTCGTGGGCTGGAGCTACCAAG
T671A	TTCAGTGCGGCCAAGTTTGCTTCCTTCATCGCACAGTACTCCACGGGA
T701A	CGCTGGAATCCCGAAATTCAGTACGCTTCCAACTACAACAAGTCTGTT
T713A	GTTAATGTGGACTTTGCTGTCGACACTAATGGCGTGTATTCAGAG
T716A	AAGTCTGTTAATGTAGACTTTACTGTGGACGCTAATGGCGTGTATTCA

Table 2: ***Sequences of the primers used for site directed mutagenesis****. Amino acid residues mutated at specific positions along with the change in nucleotide (red) and restriction pattern of silent mutations (green) incorporated within the primers.*

3.6 Large scale preparation of plasmids

Alkaline lysis method followed by caesium chloride (CsCl) based density gradient centrifugation was used for large scale preparation of plasmids. Transformed *E.coli* cells were grown in 1L LB broth by overnight incubation at 37° C and continuous shaking at 220rpm. For plasmid isolation, bacterial cells were first lysed by treatment with lysozyme and subsequently by alkaline lysis (0.2N NaOH-1% SDS). Following cell lysis step, 3M sodium acetate and chloroform were added to separate the plasmid DNA from cell debris and denatured genomic DNA. Next Plasmid DNA was precipitated by addition of 40% PEG. This solution was spun down and the pellet was dissolved in distilled water. Addition of 5.5M lithium chloride then facilitated the precipitation of RNA. Further isopropanol was added to the supernatant to separate out DNA, which was then dissolved in TE buffer (10mM Tris, 1mMEDTA, pH8)

To this solution, about 10grams of CsCl was added along with 10µl of ethidium bromide (EtBr). The tubes were sealed and subjected to centrifugation at 45,000rpm for nearly 15 hours in an ultracentrifuge using a 90Ti rotor (Beckman Coulter, Optima L-100K Ultra Centrifuge, USA). Under high centrifugal force, CsCl molecules dissociate and form a stable linear density gradient, with increasing density towards the bottom of the tube. DNA molecules placed in this gradient migrate to the point of equilibrium where they have the same density as the gradient (the neutral buoyancy or isopycnic point). TheCsCl gradient can resolve DNAmolecules with slight differences in density due to differing [G+C] content, or physical form (*e.g.*, linear *Vs* circular molecules).The DNA band thus obtained was visualized in the presence of a UV lamp, which detects the fluorescence of intercalated EtBr. Later it was aspirated using a 21gauge needle syringe and

subjected to hydrated-butanol wash to remove EtBr contamination. DNA was further dialyzed in TE buffer overnight with continuous stirring, so as to remove butanol and residual salts. Finally, the purified supercoiled plasmid DNA was dissolved in TE buffer and its concentration was determined using a spectrophotometer.

3.7 Recombinant AAV vector production

Highly purified stocks of rAAV vectors were generated and used in this study. For vector preparation, three types of reporter genes were used: AAV-CB-EGFP (enhanced green fluorescent protein gene driven by chicken β- actin promoter), AAV-CB-Luc (Luciferase gene driven by chicken β- actin promoter) and AAV-LP1-hFIX (Human FIX gene driven by LP1 promoter). The AAV-CB-EGFP vectors generated were either single stranded (ss) or self-complementary (sc) while the other two transgene based vectors were scAAV. The rep-cap plasmids were constructed using *rep* genes of AAV2 and *cap* genes from either AAV2 or AAV8 serotype. The maps of the plasmids used for packaging of scAAV2- EGFP vectors are shown in appendix A1.

As shown in the flowchart (Figure 16), the production of rAAV vector involves the following five steps.

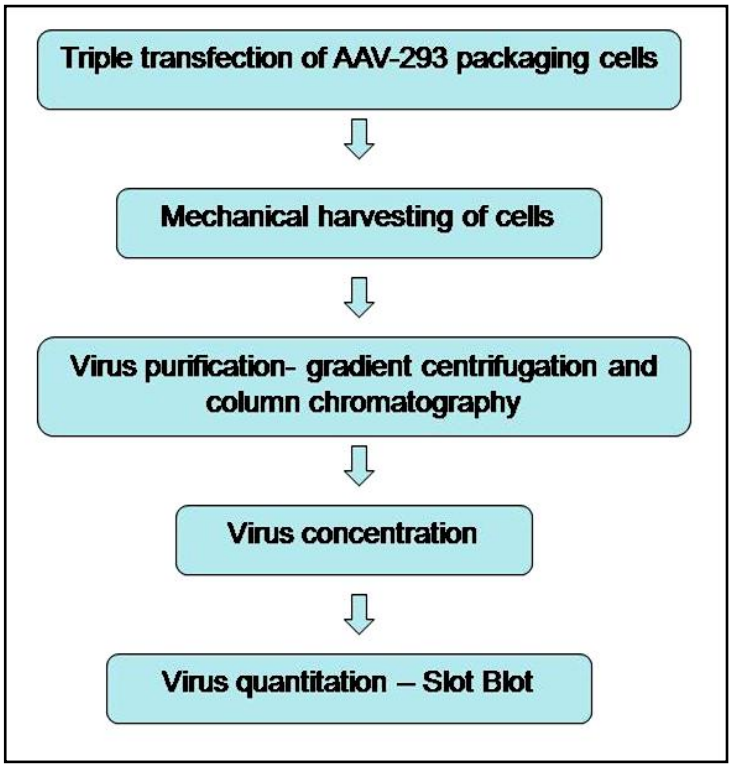

Figure 16: Flowchart showing the steps involved in recombinant AAV vector production

3.7.1 Plasmid transfection of packaging cell line

Production of rAAV was done using a triple plasmid transfection and helper-virus free method described previously (Xiao et al., 1998). AAV vector packaging basically required three different plasmids: pHelper (provides the helper virus functions), *rep-cap* plasmid (provides the genes for replication and capsid structure) and transgene plasmid (comprises of the desired transgene flanked by the AAV ITRs). To produce mutant AAV vectors, instead of wild-type*rep-cap* plasmid, the mutated plasmid generated by site directed mutagenesis was used. Initially AAV-293 cells were seeded in 150 mm^2 culture dishes at a density of $4x10^6$ cells/ plate and allowed to reach 60-70 % confluency. Forty 150 mm^2 culture dishes were used at a time to prepare one AAV2 vector stock, which required about 1200µg of each of the three plasmids.

Two different transfection protocols have been followed in this study, both of which were equally competent. *Calcium phosphate method*- For 10 plates, a 50ml solution of HEPES buffer (50mM HEPES, 1.5mM Na_2HPO_4, 140mM NaCl, pH 7.05) and 0.3M Calcium chloride was prepared, to which 300µg of each plasmid was added. The solution was mixed and set aside for 5 minutes, and later 5 ml of it was gently dispensed/ 150 mm^2 culture dish. This method is based on the formation of calcium phosphate which serves as the transfection reagent. *PEI method*- 1.25ml of polyethyleneimine (0.1% in deionized water) was added to a plasmid mixture containing 300µg of each packaging plasmidin IMDM medium and made upto a final volume of 10ml (recipe for 10 plates) (Ling et al., 2011). After 10 minutes of incubation, 1ml of this solution was added/ 150 mm^2 culture dish. The media was changed 4 hours after transfection and plates were kept back in the CO_2 incubator for about 48- 72 hours.

3.7.2 Harvesting of cells

Transfected cells were mechanically dislodged from the culture dishes using cell scrapers and the resulting cell suspension was collected into 250ml tubes. The cells were then collected by centrifugation at 3500rpm for 20minutes in a refrigerated centrifuge. The cell pellet was resuspended in a buffer (50mM Tris, 150mM NaCl, pH 8.0) and stored at -80^o C until purification.

3.7.3 Virus purification

Virus containing cells were lysed by subjecting them to repeated cycles (thrice) of freeze- thaw by placing the sample tube in a dry ice- ethanol bath and 37°C water bath alternatively. Post cell lysis, benzonase nuclease (25 units/ ml, Sigma Aldrich) was added to remove any unpackaged plasmids remaining in the cell

suspension. The crude cell lysate was then added on top of an iodixanol gradient (Optiprep, Sigma-Aldrich), prepared by layering different concentrations (15%, 25%, 40% and 60% from top to bottom) of iodixanol in a quick seal tube (Beckman Coulter). Centrifugation of the sample containing gradient was done at 75,000rpm for 1hour in an ultra centrifuge (Optima L-100K Ultra Centrifuge, Beckman Coulter). Fully packaged viruses were retrieved by injecting out the iodixanol fraction at the 40% - 60% boundary and then resuspended in low salt buffer (0.3X PBS). Next level of purification was performed using ion exchange column chromatography. For this, a peristaltic pump apparatus (GE Healthcare, Pittsburg, USA) was assembled along with HiTrap SP sepharose columns (GE Healthcare). Before adding the sample, the column was charged by running low salt and high salt (0.3X PBS+1M NaCl) buffers through it. Finally, the purified virus was collected in 20ml of elution buffer (0.3X PBS+350mM NaCl).

3.7.4 Virus concentration

The purified virus was concentrated in Amicon Ultra filter units (EMD Millipore, Bedford, MA) by centrifugation at 3500rpm for 20 minutes. Repeated washing of the filter unit membrane was done to retrieve all the virus particles from its surface. The concentrated virus was resuspended in 600µl to 1ml volume of sterile PBS. The virus stocks were immediately made into smaller aliquots and stored at -80°C. The frozen virus stocks were thawed on ice before use.

3.7.5 Virus quantitation by slot blot method

Purified AAV vectors were further quantitated by slot blot method. 1ng and 10 ng of the transgene plasmid were used as standards for virus titration. The virus aliquots (1µl and 10µl) and the plasmid standards were denatured by adding

100mM NaOH and incubating at 65°C for 30 minutes. The slot blot apparatus (Biodot SF cell, Bio-Rad, CA, USA) was setup with the nucleic acid blotting membrane (Immobilon NY+, EMD-Millipore) on top. The samples were serially diluted (total of 6 dilutions) by adding 10X SSC buffer (87.5g NaCl and 44.1g sodium citrate made upto 1L in distilled water) and dispensed on the membrane. The denatured DNA was crosslinked to the membrane using a UV crosslinker (UVP, Upland, CA). Membrane was suspended in pre-hybridisation solution and incubated overnight at 65°C in a rotating hybridization oven (GE Healthcare). The pre-hybridisation solution was prepared by mixing 15ml of 20X SSC, 5ml of 50X Denhardt's solution (1g Ficoll+1g Polyvinyl Pyrrilidone+1g BSA in 100ml distilled water) and 2.5ml 20% SDS and made upto 50ml with distilled water. 1ml of denatured salmon sperm DNA (10mg/ ml, Sigma-Aldrich) was also added to it.

Radiolabeled probe was synthesized by a klenow DNA polymerase I based reaction using α-P^{32} labeled dCTP (BRIT, Hyderabad, India), other unlabeled dNTPs, hexanucleotide mix and 100ng of transgene fragment at 37^0C for 2hours. Probe was then purified using a Probe quant G50 column (GE Healthcare) and its radioactivity was quantified in a liquid scintillation counter (Perkin Elmer, Waltham, MA, USA). About $6x10^5$ cpm (counts per minute unit) of probe was added to the membrane in the pre-hybridisation solution and incubated at 65^0C overnight. The membrane was then washed with wash buffers I, II and III (2X SSC+0.1%SDS, 0.1X SSC+0.1%SDS and 0.1X SSC respectively), and finally air-dried. Finally it was placed in the radioactive cassette with the blanked phosphor screen over it and exposed for 24-48 hours at room temperature. The phosphor screen was then scanned using Phosphoimager (GE Healthcare) and the image was developed in Storm Scanner software. Band intensities of the virus samples were compared with that of the plasmid standards across the dilutions. The physical particle titer of the virus was

calculated as described previously (Kube & Srivastava, 1997) and expressed as viral genomes per millitre.

3.8 DNA Sequencing

The presence of the desired nucleotide changes in the mutated *rep-cap* plasmid was confirmed by DNA sequencing using primers flanking the region of mutation on the *cap* gene. Big dye terminator v3.1 cycle sequencing kit (Life Technologies, Carlsbad, CA, USA) was used for DNA sequencing in ABI 3130 Genetic analyzer (Life Technologies, Carlsbad, CA, USA). Sequencing was done by capillary electrophoresis using Sanger's dideoxy nucleotide method. Cycling conditions of the DNA sequencing reaction were set to 25 cyles of 96°C for 15sec; 50°C for 20sec and 60°C for 40min. The primers used for sequencing of AAV2 *cap* gene are shown in appendix A2.

3.9 Estimation of vector genome copies

Genomic DNA was isolated from murine liver tissue using QIAamp DNA mini kit (Qiagen) as per the protocol described in the product manual. Vector genome copy numbers per diploid genome were quantified with TaqMan probes andprimers designed against the AAV2 inverted terminal repeat (ITR) sequence and estimated as described previously, using a low-ROX quantitative PCR MasterMix (Eurogentec). The sequences of the AAV2 ITR primers/ probe are forward: *GGAACCCCTAGTGATGGAGTT;* Reverse: *CGGCCTCAGTGAGCGA*and probe: *FAM-CACTCCCTCTCTGCGCGCTCG-TAMRA* (Aurnhammer et al., 2011). Data

was captured and analyzed in the ABI Prism 7500 Sequence Detection System (Life Technologies). Gene expression was measured by the comparative threshold cycle (ΔΔCt) method.

3.10 Quantitative RT-PCR profiler array to assess the pro-inflammatoryresponse

For assessing the modulation of the pro-inflammatory response to AAV vectors, mice pretreated with appropriate compounds (Bay11-7085, PJ34, Bo or ABT) as single agents or in combination (n=4-5) were either mock-injected or injected with ~5 x 10^{10} vgs of scAAV2 vectors and euthanized 2 hours post-PBS or AAV administration. The dosage and timing of drug intervention are described in the results section.At the end of the experiment, the mice were sacrificed and the RNA from the liver tissue was extracted using the RNeasy mini kit (QIAGEN, Valencia, CA) as per the kit protocol. The purity of the isolated RNA was verified in a Nanodrop Spectrophotometer (ND-1000) by assessing the absorbance ratios at 260nm/ 280nm. 1µg of RNA was reverse transcribed to cDNA using RT^2 First Strand kit (Qiagen) according to the manufacturer's instructions. The cDNA was profiled by the mouse NF-κB RT Profiler PCR array system (Qiagen, SABiosciences) to determine the relative gene expression of 84 key genes related to NF-κB-mediated signal transduction and inflammatory response. A human NFκB Signaling Pathway PCR Array (Qiagen, SABiosciences) was used to comparatively assess the ability of three NF-κB inhibitors in down-regulating the various NF-κB pathway related genes in cells transduced with AAV vectors. The Real-Time PCR reaction involved a 2 step cycling program done at 95°C for 10min followed by 40

cycles of 95°C for 15sec and 60°C for 1min. The data was analysed using an ABI Prism 7500 Sequence Detection System version 1.1 (Life Technologies, Applied Biosystems). Gene expression was measured by the comparative threshold cycle (ΔΔCt) method and analysed by the SABiosciences web based software [a]. The genes analysed using the array are listed in table 3.

Activation of the NFκB Pathway:
Ligands and Receptors: Card10, Irak1, Myd88, Tlr1, Tlr2, Tlr3, Tlr4, Tlr6, Tnf, Tnfsf14.
Kinases: Chuk, Ikbkb, Ikbke, Ikbkg, Irak1.
IκB kinase and the NFκB Cascade: Bcl10, Chuk (IKK-1), Ikbkb (IKK-2), Ikbke (IKK-I), Myd88, Tlr4.
Transcription Factors: Ikbkg, Irak1, Nfkb1.
Inflammatory Response: Myd88, Tlr1, Tlr2, Tlr3, Tlr4, Tlr6.
NFkB Responsive Genes:
Acute Phase Response Proteins: C3 (PLP).
Cytokines: Csf2, Csf3, Ifng, Il6, Irf1, Lta, Tnf.
Ligands and Receptors: Csf2, Ifng, Il6, Lta.
Other Extracellular and Membrane Molecules: C3, Csf3, Icam1.
Transcription Factors: Ifng, Irf1.
Other Factors Involved in the NFκB Pathway:
Ligands and Receptors: Ccl2, Csf2, Lpar1, F2r, Fasl (Tnfsf6), Htr2b, Ifng, Il10, Il1a, Il1b, Il1r1, Il6, Irak2, Lta, Ltbr, Map3k1, Eif2ak2 (Prkr), Raf1, Slc20a1, Tgfbr1, Tgfbr2, Tlr7, Tlr8, Tlr9, Tnfrsf10b (DR5), Tnfrsf1a, Tnfrsf1b, Cd40 (Tnfrsf5), Cd27 (Tnfrsf7), Tnfsf10, Tollip, Traf2.
Other Extracellular and Membrane Molecules: C3, Csf3, Gja1, Icam1, Smad3.
Kinases: Akt1, Irak2, Map3k1, Mapk3, Eif2ak2 (Prkr), Raf1, Ripk1, Ripk2, Tbk1, Tgfbr1, Tgfbr2, Zap70.
Transcription Factors: Atf1, Atf2, Crebbp, Egr1, Elk1, Fos, Ifng, Irf1, Jun, Nfkb2, Kat2b, Rel, Rela, Relb, Smad3, Stat1.
Inflammatory Response: C3, Ccl2, Il10, Il1a, Il1b, Tlr7, Tlr8, Tlr9, Tnfrsf1a, Tnfrsf1b, Tollip.
Others: Bcl3, Nod1 (Card4), Casp1, Casp8, Cflar, Fadd, Nlrp12 (Nalp12), Nfkbia, Tnfaip3, Tradd, Traf3.

Table 3: ***Functional gene grouping of mouse NFκB signaling pathway PCR array.*** *Adapted [b].*

3.11 AAV transduction studies in vitro

HeLa cells seeded into multi-well plates were either mock infected or infected with appropriate AAV vectors (mutant or wild-type) at a specific multiplicity of infection (MOI) and forty-eight hours later the transgene expression was measured by fluorescence microscopy or flow cytometry. To study the effect of inhibiting PARP-1 and NF-κB pathway on AAV transduction *in vitro*, the specific inhibitors were added to the cells 24 hours prior to the wild-type AAV2 infection.

3.11.1 Fluorescence microscopy for EGFP imaging

The EGFP expression in AAV infected HeLa cells was visualized using fluorescent microscopy (Leica DM 16000B, Leica Microsystems, Wetzlar, Germany) at laser excitation wavelength of 495nm. Images from five visual fields/ well of mock and vector infected cells were captured and then analyzed by Adobe Photoshop CS2 software. The transgene expression was quantitated as mean of total area of green fluorescence ($Pixels^2$) per visual field.

3.11.2 Flow Cytometric analysis of EGFP expression

EGFP fluorescence in AAV infected HeLa cells was also quantitated by measuring mean fluorescence intensity (MFI) by flow cytometry (FACS caliber, Becton Dickinson, USA). After microscopic imaging of EGFP fluorescence, the cells were dissociated using trypsin-EDTA and made into single cell suspension in 350µl PBS. About 10,000 cells were acquired for each condition and the percentage of the EGFP positive cells within the appropriately gated population of homogenous cells was calculated using the Cell Quest Pro software. The percentage of EGFP positivity

was plotted against each condition to analyse the EGFP transgene expression with respect to the wild-type vector.

3.11.3 Confocal microscopy

Capsids of AAV2 viral particles were labeled with carbocyanine (Cy3) fluorescent dye (GE Healthcare) as described previously (Bartlett et al., 2000). HeLa cells seeded in coverglass-bottom confocal dish (35mm X 10mm) were treated with various inhibitors for 24 hours and then infected with Cy3 labeled AAV2 particles at an MOI of $3x10^4$ in 800µl of IMDM media. After allowing the Cy3 labeled AAV particles to bind to the cell surface for 30 minutes at 37°C, 100 µl of FBS and 10 µl of Penicillin/Streptomycin (100X) were added and the total volume was made upto 1 ml with IMDM media. To localize the Cy3 labeled AAV signal within the infected cell, images were obtained by confocal laser scanning microscopy at an excitation wavelength of 552nm (Olympus Fluoview1200 Confocal Microscope, Japan). Images were then processed by Olympus Fluoview FV1000 confocal software. After 15 hrs of live cell imaging, HeLa cells infected with Cy3 labeled AAV were fixed at 17 hours post-infection, using 10% buffered formalin and the nuclei were stained with Hoechst (33258) (Sigma-Aldrich). The EGFP transgene expression and Cy3 labeled AAV particles, if any, localized within the cell at that time point were visualized and compared across the different treatment conditions.

3.12 AAV transduction studies in vivo

For *in vivo*studies, 8-12 weeks old mice (C57BL/6 or BALB/c) were mock-injected (PBS) or injected with AAV vectors in 200µl sterile PBS

intravenously through the tail vein. In the PARP-1/NF-κB inhibition studies, specific pharmacological inhibitors to these factors were administered into mice prior to the vector injection. PARP inhibitors, PJ34 and ABT-888 were administered at doses of 10mg/ kg (i.p) and 12.5mg/ kg (i.p) respectively while NF-κB inhibitors, Bay11-7085 and Bortezomib were injected at doses 20mg/ kg (i.p) and 1mg/ kg (i.v) respectively. To study the CD8+ T cell response, an equal booster dose of the inhibitors and the vectors was administered two weeks after the first set of injections. Mice were euthanized 4 weeks after vector administration and the transgene (EGFP or Luc) expression in the liver was analyzed by fluorescence microscopy or live animal imaging.

3.12.1 Fluorescence microscopy for EGFP imaging

Liver was dissected out and washed gently with sterile PBS. Each of the three liver lobes of the mock- injected and vector- injected mice were assessed for EGFP expression by fluorescence microscopy. Images from five visual fields were analyzed and quantitated by Adobe Photoshop CS2 software. Transgene expression was quantitated as mean of total area of green fluorescence ($Pixels^2$) per visual field.

3.12.2 Live animal imaging

Mice were anaesthetized and injected with D-Luciferin (BioVision Inc, Milpitas, CA, USA) at a dosage of 2.5mg/ 100µl/ 20gm mouse body weight into the intraperitonial cavity. Five minutes later, the luciferase gene expression was measured by serial imaging of the mice in an IVIS Spect-CT small animal imaging system (Perkin Elmer- Caliper Life Sciences). The bioluminescence was captured in the large or medium binning based on the signal intensity and quantitatively expressed as photons per second.

3.12.3 Quantitative Real time PCR for measuring transgene expression

Total RNA was isolated from homogenized mouse liver tissue using RNeasy Mini Kit (Qiagen, Valencia, CA, USA) as per manufacturer's instructions. Concentration and purity of the RNA was determined in a Nanodrop spectrophotomer (ND-1000, Thermo Scientific, Surrey, UK). Good quality RNA should ideally have absorbance ratio 260nm/ 280nm equal to1.8-2.0. Approximately 1µg of RNA was reverse transcribed to prepare cDNA using Verso cDNA synthesis kit (Thermo Scientific) according to the manufacturer's protocol. EGFP transcript levels were measured using TaqMan PCR (Mastermix obtained from Eurogentec, Seraing, Belgium) and specific primers/ probe designed for amplication of *EGFP* gene (Forward primer: *CTTCAAGATCCGCCACAACATC*; Reverse primer:*ACCATGTGATCGCGCTTCTC*; probe: *FAM-CGCCGACCACTACCAGCAGAACACC-TAMRA*). *FIX* gene expression was quantitated using SYBR Real time PCR (MESA GREEN Mastermix, Eurogentec) using specific primers designed against human *FIX* gene (Forward primer:*TTCGATCTACAAAGTTCACCATCTATAAC*; Reverse primer: *AAACTGGTCCCTTCCACTTCAG*). Glyceraldehyde-3-phosphate dehydrogenase (GAPDH) was used as the housekeeping control gene. Data was captured and analyzed with ABI Prism 7500 sequence detection system version 1.1 software (Life Technologies). Gene expression was measured by the comparative threshold cycle (ΔΔCt) method.

3.13 MTT cell viability assay

To determine the effective and least toxic concentration of the various inhibitors used in the study, MTT (3-(4,5-dimethylthiazol-2-yl)-2,5-diphenyltetrazolium bromide) assay was done. It is a calorimetric assay for assessing cell viability and cytotoxicity of drugs. Cellular NAD(P)H dependent-oxidoreductase enzymes reduce the tetrazolium dye, MTT to insoluble formazan, which is purple in colour. Intensity of the colour developed is directly proportional to the number of viable cells. HeLa cells seeded in a 96 well plate were treated with appropriate inhibitors at different concentrations, ranging around the IC50 value. After 24 hours, 15µl of 10X MTT reagent (5mg/ ml) was added to 150µl of media in each well and incubated for 4 hours in dark. Further added 100µl of 10% SDS in 0.01N HCl (per well) and incubated for 3 hours at 37°C to dissolve the purple formazan formed. The absorbance at 550nm with reference at 620nm was measured using an ELISA plate reader.

3.14 Western blot

To perform western blot, HeLa cells were seeded in a 6 well plate at a density of $0.4x10^6$ cells/ well. Cells in the test condition were transfected with 100nM of PARP-1 siRNA or scrambled siRNA using Lipofectamine (Life Technologies). Twenty-four hours post siRNA or mock transfection, cells were transduced with scAAV2-EGFP or ssAAV2-EGFP vectors at MOI of 2000 viral genomes (vgs) per cell. Forty-eight hours post-infection, nuclear fractions were isolated from HeLa cells using the NE-PER kit (Thermo Scientific –Pierce Biotechnology) as per the manufacturer's protocol, denatured by boiling for 5 min

and mixed with Blue gel loading buffer (Cell Signaling Technologies) containing DTT. Normalized amounts of the nuclear protein extracted from different conditions were resolved by SDS-PAGE using 4-20% Tris-HCl gradient gels (Biorad Laboratories, Hercules, CA, USA) and Tris/ glycine/ SDS running buffer and further transferred to Immobilon- P membrane (Millipore) using Tris/glycine/methanol transfer buffer. The membrane was then probed with the following antibodies: polyclonal rabbit anti- PARP-1 or monoclonal mouse anti- Lamin A/C. The immuno-reactive bands were detected by anti-idiotype, HRP linked anti- rabbit IgG or anti-mouse IgG antibodies, visualized using chemiluminescence detection kit (ECL-Plus, GE healthcare) and documented in ImageQuant 400 imager (GE healthcare).

3.15 ELISPOT assay and ELISA to study the T cell response

Initially mouse splenocytes were isolated by mashing the dissected-out spleen in RPMI media (Life Technologies, Carlsbad, CA) and straining the cell suspension through a 100µm cell strainer. These cells were spun down and subjected to RBC lysis using 1ml of RBS lysis buffer. The splenocytes were then counted and seeded in RPMI media containing 10% FBS, to which 2µg/ ml of appropriate T- cell epitope containing peptide (specific to AAV2/AAV8 serotype and C57BL/6 mice strain) was added (JPT Peptide Technologies GmbH, Berlin) (Martino et al., 2011a). 96 well plates pre-coated with anti- IFNγ antibodies (MABTECH, Ohio, USA) were used for the ELISPOT assay. The assay was done as per the manufacturer's protocol. Concanavalin A (ConA) at a concentration of 2µg/ ml was added as a positive control to stimulate T cells to secrete IFNγ. After about 30 hours of incubation, the plates were developed by BCIP/NBT ALP reaction and spots formed were

enumerated in an ELISPOT reader system (AID GmbH, Germany). The spots obtained correspond to the IFNγ secretion by activated CD8+T cells.

To perform IFN-γ ELISA, the processed splenocytes were seeded in normal 96 well plates with seeding densities and other conditions similar to ELISPOT assay. After the incubation period of about 30 hours, the cell culture supernatant was collected from each well, diluted and analysed using ELISA kit for mouse IFNγ (MABTECH), as per the kit protocol. Briefly, the samples were added to ELISA plates pre-coated with anti- mouse IFNγ monoclonal antibody. After incubation, biotinylated detection antibody followed by Streptavidin-HRP was added. Addition of a chromogen enzyme substrate (TMB enzyme) resulted in a colored product whose intensity was directly proportional to the IFNγ concentration in the sample. The absorbance was read in a microplate reader at 450nm wavelength. All samples were diluted two-fold in the kit diluent. Only the positive control (ConA) was diluted three-fold.A standard curve ranging from 1-1000 pg/ml was prepared by serially diluting the reconstituted IFNγ cytokine standard stock solution (1µg/ml) and plotting the concentrations against the 450nm absorbance values. A sigmoidal standard curve was generated and the sample values were extrapolated from it using the Graph PAD Prism 6 software [c]. The final IFNγ protein concentrations of the samples (dilution factor multiplied) were determined and compared across the treatment groups.

3.16 Histological analysis

Liver tissues were fixed in 10% buffered formalin and processed for microscopy. Three micron thick liver sections were cut and stained with hematoxylin

and eosin. The degree of lobular and portal inflammation was scored (inflammation score, IS) by a hepato-pathologist, who was blinded to the experimental conditions. Inflammation scores were based on degree of lobular and portal inflammation and calculated based on the criteria, 0- No inflammation, 1- Mild inflammation, 2- Moderate inflammation, 3- Severe inflammation**.**

3.17 Statistical analysis

Data is represented as mean of values ± SD (standard deviation) or SEM (standard error of mean) as indicated in the figure legends of results section. Two-tailed student's t-test was used to statistically compare the data sets. Multiple groups of data were analysed by one way- ANOVA (Analysis of variance). p value < 0.05 was considered statistically significant.

4. RESULTS

4.1 Role of NF-κB in AAV-mediated gene transfer

4.1.1 In vitro dose standardization of NF-κB inhibitors by MTT assay

Three commercially available small molecule inhibitors, which selectively and irreversible inhibited NF-κB pathway and showed potent anti- inflammatory properties were used to examine the effect of targeting NF-κB pathway on AAV-based gene delivery. These compounds namely Bay11-7085, Ro106 and Isohelenin blocked NF-κB signaling primarily at the cytoplasmic level by interfering with the phosphorylation or degradation of IκBα and thereby the activation of the precursor NF-κB molecules. To determine the optimal *in vitro* concentration of these inhibitors, MTT cell viability assay was performed. HeLa cells, seeded in 96 well plates were treated with these drugs at three different concentrations starting with the IC50 value and subsequently with 1:2 and 1:10 dilutions, in triplicate wells. The IC50 values of the compounds were obtained from the respective product datasheets (Calbiochem, Darmstadt, Germany) and are shown in the table 4. After 48 hours, MTT assay was done and absorbance reading was taken at 550nm wavelength with reference reading at 620nm. By comparing with the viability of mock infected cells, the least toxic concentration of the compounds with comparable viability were inferred to be same as the IC50 value for Bay11-7085 and Isohelenin, and 1:2 dilution of IC50 for Ro106 (Figure 17).

NF-κB Inhibitor	IC50 value
Bay11-7085	10μM
Ro106	5μM
Isohelenin	1μM

Table 4: IC50 values of the NF-κB inhibitors tested in the study

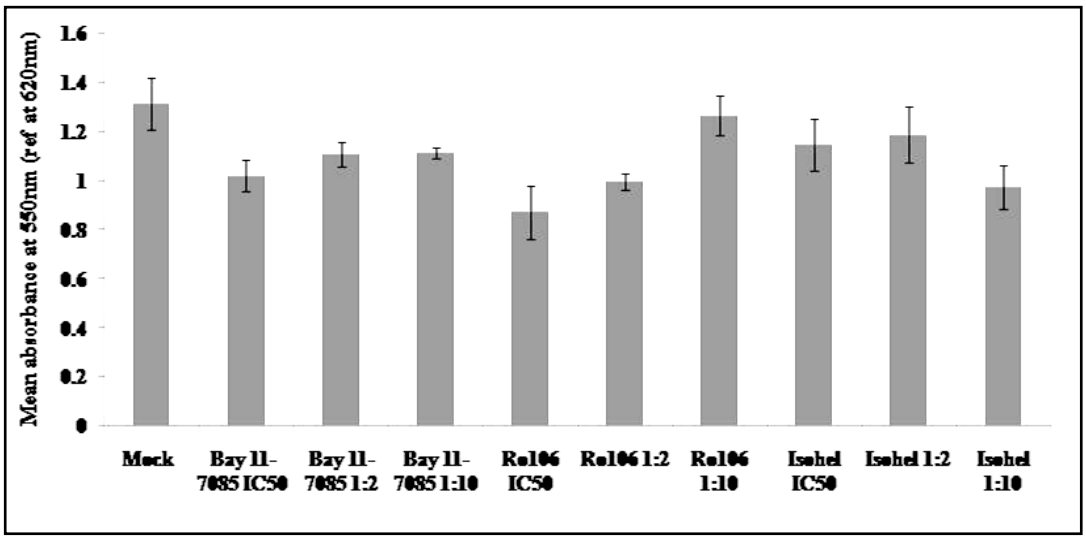

Figure 17: ***MTT assay to determine the optimal concentration of NF-κB inhibitors.*** *HeLa cells were treated with different concentrations of NF-κB inhibitors such as 10μM (IC50) of Bay11-7085, 5μM (IC50) of Ro106, 1μM (IC50) of Isohelenin (Isohel) and two further dilutions from the IC50 value (1:2 and 1:10) of each compound for 48 hours following which MTT assay was done. Absorbance values at 550nm are plotted in the graph (mean±SD). Reference absorbance reading was taken at 620nm.*

4.1.2 Inhibition of NF-κB pathway does not affect the AAV2-mediated transgene expression *in vitro*

To evaluate the effect of inhibiting NF-κB pathway on AAV2 transduction *in vitro*, HeLa cells were pretreated with the selected NF-κB inhibitors (Bay11-7085, Ro106 and Isohelenin) for nearly 24 hours, at the concentration determined by MTT assay. The cells were then infected with recombinant self-complementary (sc) AAV2 vectors encoding EGFP transgene (scAAV2-EGFP) at a vector dose of 10,000 viral particles per cell (MOI). Forty-eight hours post-transduction, the EGFP signal across the different conditions was imaged using fluorescence microscopy and the expression was quantitated by measuring the mean fluorescence intensity (MFI) in a flow cytometer (FACS Caliber, BD). As shown in the figure 18, the effect on the vector directed transgene expression was found to be minimal with the NF-κB inhibitors tested, at the specific concentrations used. However, it has been reported earlier that the *in vitro* transduction of AAV2 at a lower MOI of 2000 vgs/ cell can be totally ablated by 12 hours of treatment with NF-κB inhibitor, Bay11 while the *in vivo* transduction in murine liver remains unaltered in the presence of Bay 11 (Jayandharan et al., 2011). The rescue of the *in vitro*transgene expression in this study could be explained by the delivery of high amounts of AAV2 vector particles into HeLa cells, which bypassed the inhibitory effect of Bay11 on vector transduction, in concordance with the*in vivo* data of the previous report (Jayandharan et al., 2011).

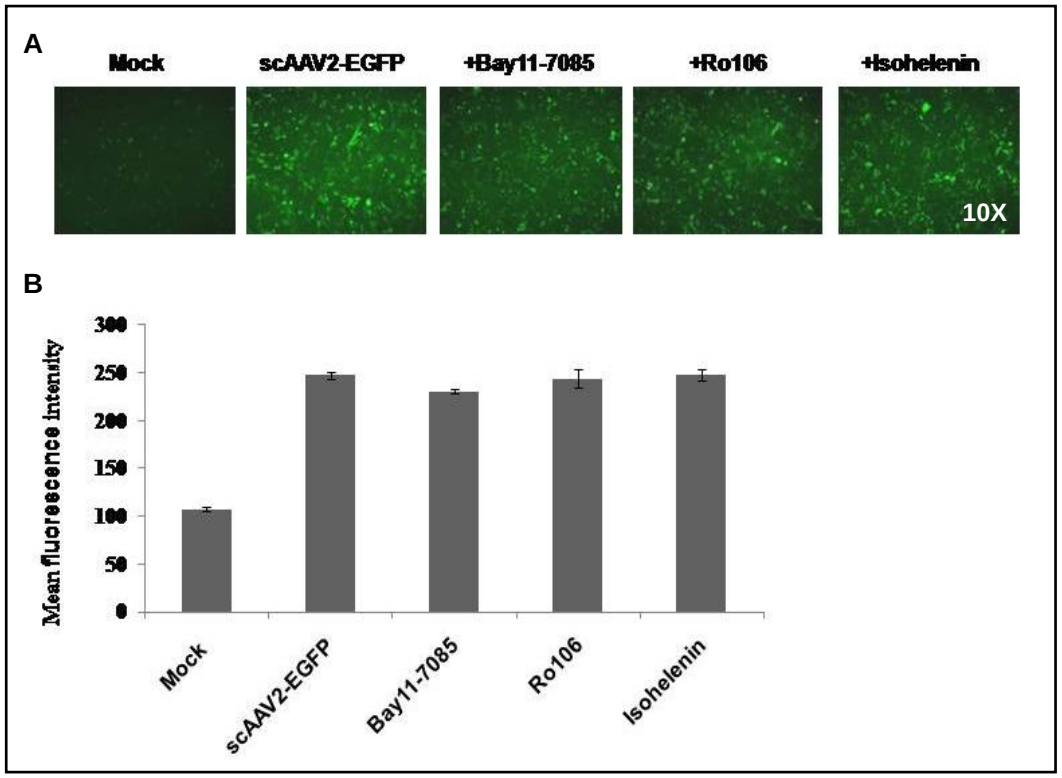

Figure 18: ***Inhibition of NF-κB pathway does not alter the in vitro transduction of AAV2 vectors at high vector dose.*** *(A) HeLa cells were infected with scAAV2-EGFP vectors at 10,000 MOI. Forty-eight hours later, the EGFP signal from the transduced cells was captured using a fluorescent microscope. Representative images are shown. (B) EGFP expression was measured in a flowcytometer and MFI values were plotted for different conditions (mean ± SD). All images were captured at uniform setting of exposure time 500msec, gain 1.7 and intensity 5.*

4.1.3 Screening for the optimal NF-κB inhibitor by comparative analysis of the down-regulation of NF-κB associated genes in AAV2 transduced cell line

The next step was to identify the most potent NF-κB inhibitor among Bay11-7085, Ro106 and Isohelenin, which could effectively suppress the expression of pro-inflammatory and other NF-κB target genes induced upon AAV infection. HeLa cells pretreated with the three NF-κB inhibitors for 24 hours were infected with

scAAV2- EGFP vectors at an MOI of 10,000 viral particles per cell. Vector treated cells without any inhibitors served as the control. At 6 hours post-infection, RNA was isolated from the cellsand the expression level of a focused panel of 84 genes related to NF-κB mediated signal transduction was determined using the SABioscience RT Profiler PCR array. Gene expression was measured by the comparative threshold cycle (ΔΔCt) method and analyzed as outlined in methods section. Of the three compounds tested, Bay11-7085 was found to be most effective in significantly repressing the expression of various NF-κB associated genes induced by AAV2 transduction in HeLa cells (Figure 19).

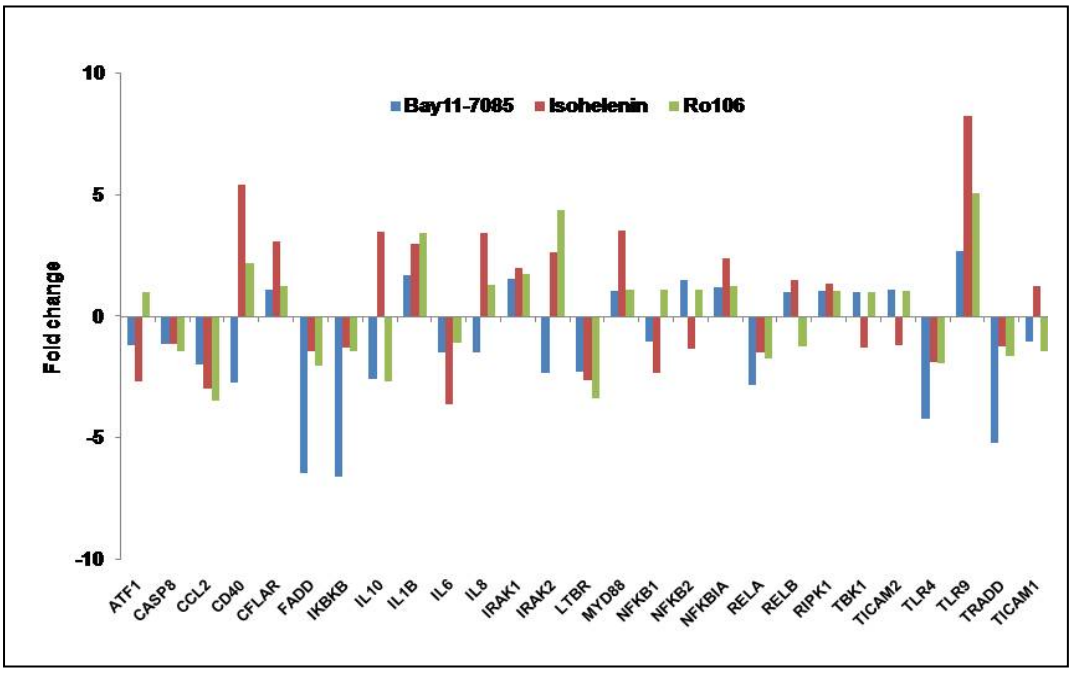

Figure 19: ***Comparative analysis of the down-regulation of NF-κB associated genes in AAV2 transduced cell line.*** *HeLa cells pretreated with NF-κB inhibitors for 24 hours. were infected with scAAV2 vectors and 6 hours later, mRNA levels of NF-κB response and target genes was measured using RT profiler qPCR array. Fold change in the expression of various cytokine and pro-inflammatory genes associated with NF-κB pathway in the presence of specific inhibitors relative to the vector transduced cells, without inhibitors. Genes showing significant difference (≥2 fold, p ≤0.05) between groups are only shown in the graph.*

4.2 Role of PARP-1 protein in AAV-mediated gene transfer

4.2.1 RNAi mediated knockdown of PARP-1 improves the transduction efficiency of AAV2 vectors

To determine the role of PARP-1 on AAV-based gene transfer, HeLa cells were transfected with 100μM of PARP-1 specific siRNA or scrambled oligo control using Lipofectamine (Life Technologies) and 24 hours later transduced with scAAV2-EGFP or ssAAV2-EGFP vectors at MOI of 2000vgs/cell. The EGFP expression relative to mock-transfected cells was thereafter measured by fluorescence microscopy at 48 hours post-transduction.As shown in figure 20A-B, the transduction efficiencies of scAAV2 and ssAAV2 vectors increased significantly upon RNAi mediated knockdown of PARP-1.The level of transgene expression in PARP-1 depleted cells was significantly higher for both vectors, but more prominent for ssAAV2 vectors than with scAAV2 vectors (~174% and ~85% respectively, $p<0.05$). Western blot analysis of nuclear extracts from cells transduced with ssAAV2 vectors was performed to validate the specificity of PARP-1 siRNA versus the scrambled siRNA control in down-regulating the PARP-1 protein levels (Figure 20C). This data implies that PARP-1 repression in human cells could enhance the transgene expression from AAV vectors.

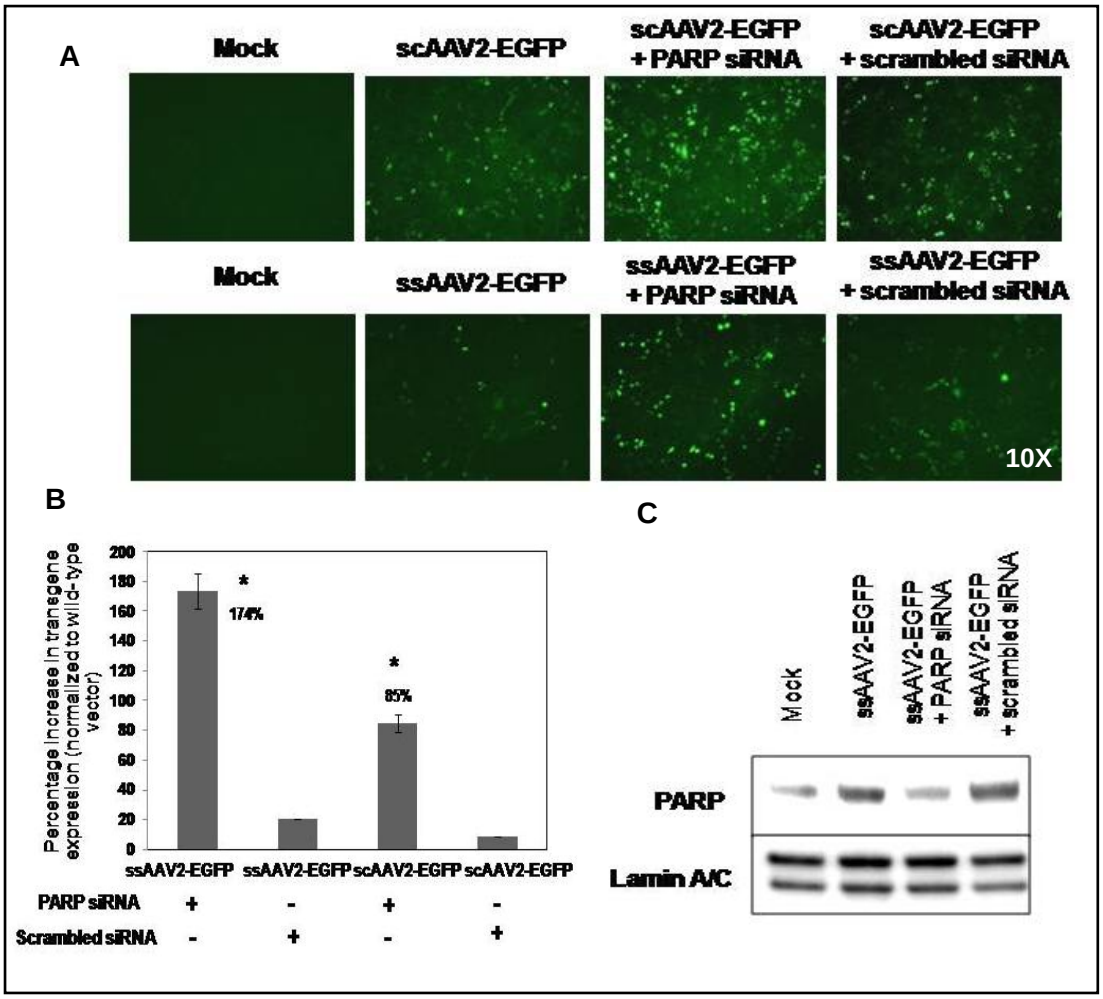

Figure 20: ***RNAi mediated PARP-1 inhibition enhances the AAV2 transduction in vitro*** *(A) transgene expression observed in HeLa cells, 48 hours post-infection with ssAAV2-EFGP/scAAV2- EGFP vectors either in the presence or absence of PARP-1 siRNA/ scrambled siRNA control. (B) Quantitative analysis of the fluorescence microscopy data from (A) showing the percentage increase in EGFP expression levels, normalized to that of the wild-type vector. The data presented here is representative of six independent experiments. Mean±SEM *p<0.05. All images were captured at uniform exposure settings(500msec, gain 1.7 and intensity 5). (C) Western blot analysis of HeLa cell nuclear extracts following mock (PBS)-infection or infection with ssAAV2 vector, either in the presence or absence of PARP-1 siRNA or scrambled siRNA control. Anti-Lamin A/C antibody was used as a loading control.*

4.2.2 Pharmacological inhibition of PARP-1 improves the AAV-mediated hepatic gene transfer

Further on the basis of *in vitro* results, it was investigated if inhibition of PARP-1 can improve the transgene expression from AAV vectors *in vivo.* Groups of 8-12 weeks-old BALB/c mice (n=4) were administered with PARP-1 inhibitor, PJ-34 (10mg/ kg body weight) intraperitoneally in a 100µl volume, diluted in sterile water at 24 hours (Day0) and 30 minutes (Day1) prior to vector injection and subsequently once a week till the animals were euthanized. PJ-34 is a selective PARP-1 inhibitor used extensively in pre-clinical animal models (Abdelkarim et al., 2001, Scott et al., 2004, Haddad et al., 2006).It is a water soluble phenanthridinone derivature, which competitively inhibits the PARP-1 enzyme activity by blocking the NAD+ binding site within its catalytic domain(Jagtap & Szabo, 2005, Phulwani & Kielian, 2008). On day 1, these animals were mock-injected (PBS) or injected with ~5 x 10^{10} vgs of scAAV2- EGFP vectors or ~1 x 10^{10} vgs of ssAAV2-EGFP vectors or ~5 x 10^{10} vgs of ssAAV8-EGFP vectors per animal in a 200µl suspension *via* the tail vein.

Four weeks after vector administration, the mice were euthanized andthe EGFP expression in the liver lobes was assessed by fluorescence microscopy. As expected, at four weeks time point, the AAV vector induced transgene levels in the liver were found to be significantly increased in groups of mice administered with PJ34 (Figure 21). The increase in *in vivo* transduction upon PARP-1 inhibition was strikingly evident in single stranded AAV vectors, ssAAV8 vectors (~3.4-fold) and ssAAV2 vectors (~2-fold), while there was only modest increase with scAAV2 vectors (~50%) (Figure 21 B-D). It can thus be inferred that blocking of PARP-1 enzyme activity improves the AAV gene transfer into murine liver.

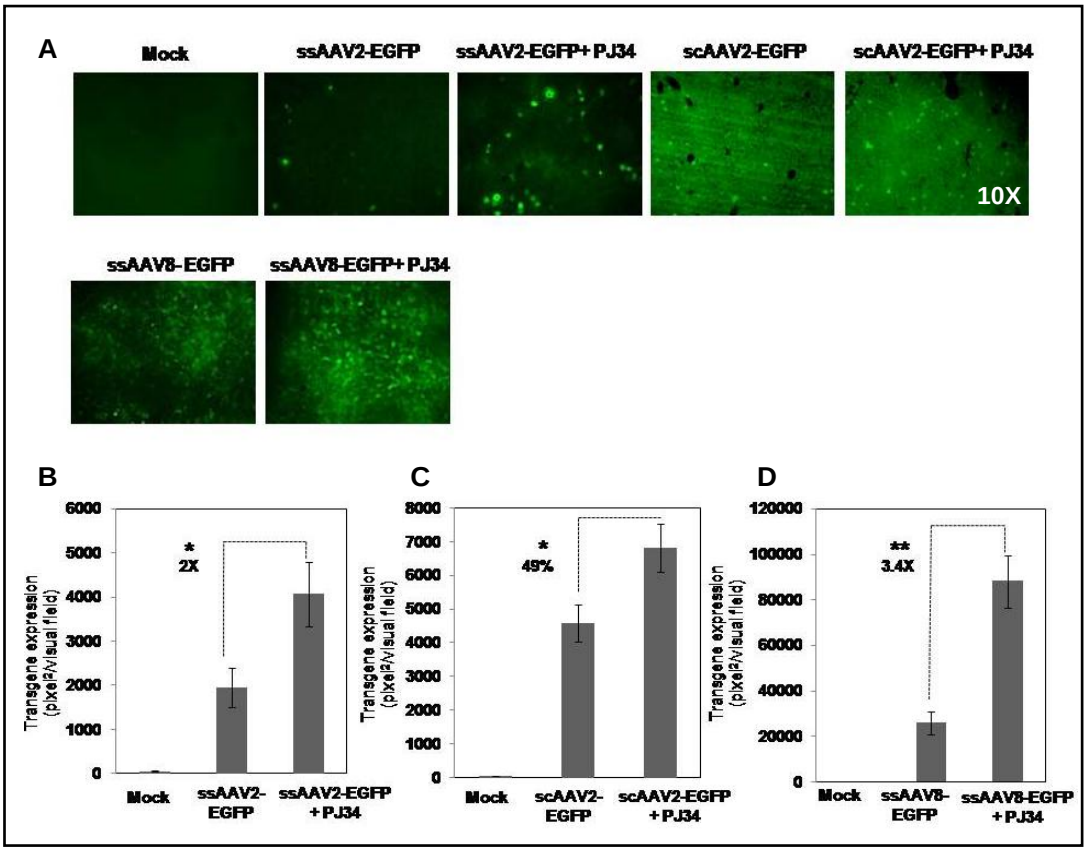

Figure 21: ***Pharmacological inhibition of PARP-1 augments the AAV-mediated hepatic gene transfer in vivo****. Transgene expression was measured in liver sections of BALB/c mice 4 weeks after mock (PBS)-injection or administration of ssAAV2-EGFP/ scAAV2-EGFP/ ssAAV8-EGFP vectors alone or in the presence of PARP-1 inhibitor, PJ-34. (B-D) Quantitative analyses of the data from (A) Mean±SD; *p<0.05;**p<0.05. Representative images are shown. All images were captured at uniform settings of exposure time 2 sec, gain 2 and intensity 5.*

4.2.3 PARP-1 inhibition in mice modulates the pro-inflammatory response against AAV2 vectors

As PARP-1 blockade did not improve the transduction efficiency of scAAV2 vectors considerably, its effect on regulation of host immune response against these vectors was investigated. This was supported by the fact that PARP-1 is

involved in the transcriptional activation of NF-κB in response to pro-inflammatory stimuli (Hassa et al., 2003). It is shown to directly interact with NF-κB subunits p65 and p50 using different domains (Hassa et al., 2001). PARP-1 forms a stable complex with p300 *in vivo,* allowing stable interactions to take place between NF-κB subunits and p300, which are crucial for the activation of NF-κB in a stimuli dependent manner (Hassa et al., 2003, Hassa et al., 2005).

Hence it was assessed if inhibition of PARP-1 activity could moderate the expression of pro-inflammatory cytokineand other NF-κB pathway genes induced upon infection with scAAV2 vectors, which are known to be more immunogenic than ssAAV2 vectors (Wu et al., 2012, Balakrishnan et al., 2013, Martino et al., 2013). Previous reports have demonstrated that cytokine secretion can take place in the liver in response to agonist stimulation or pathogen invasion, and this process is mediated by kupffer cells (Rowell et al., 1997, Dong et al., 1998). In this study, therefore thechange in the expression levels of various pro-inflammatory marker genes in the vector transduced liver tissue was measured upon PARP-1 inhibition. Groups of PJ-34 (10mg/kg body weight) pretreated BALB/c mice (n=4) were either mock-injected (PBS) or injected with ~5 x 10^{10} vgs of scAAV2- EGFP vector and euthanized 2 hours later (Jayandharan et al., 2011). RNA was isolated from liver tissue and reverse transcribed to cDNA. Relative expression of key genes associated with NF-κB-mediated signal transduction and innate immune response was measured using the NF-κB RT-PCR Profiler array (Qiagen, SABiosciences). As shown in Figure 22, a variety of genes involved in activation of NF-κB signaling (such as CD40, TNF, TLR4, RelA), inflammatory response (IL1b, TLR1, TLR4, TLR9) as well as other molecules involved in propagation of the cytokine/ chemokine response to AAV (TRAF2, TRAF3, BCL3, LTBR) were suppressed by PARP-1 inhibition.

Some of genes which had more than 40- fold down- regulation have not been represented in the graph (Figure 22) and these include TLR2, CASP1, ELK1, CD40, MAP3K1 and RelA. This data supports the speculation that ablation of PARP-1 suppresses the inflammatory response targeted against AAV.

4.2.4 PARP-1 inhibition does not cause any hepatotoxicity in mice

Liver tissue sections of AAV vector infused BALB/c mice with or without PJ-34 treatment, were fixed and stained with hematoxylin and eosin. As documented by a pathologist, the *in vivo* administration of PJ-34, did not lead to any significant histological abnormalities in the murine liver 4 weeks post-AAV2/ AAV8 vector administration. The liver tissues from any of the PBS- or PJ-34 and/or AAV injected animals did not demonstrate significant toxicity, as revealed by the average inflammation scores (IS) of portal and lobular inflammation (Figure 23). A set of representative images are shown which corroborate that PJ-34 administration was non-toxic to murine liver.

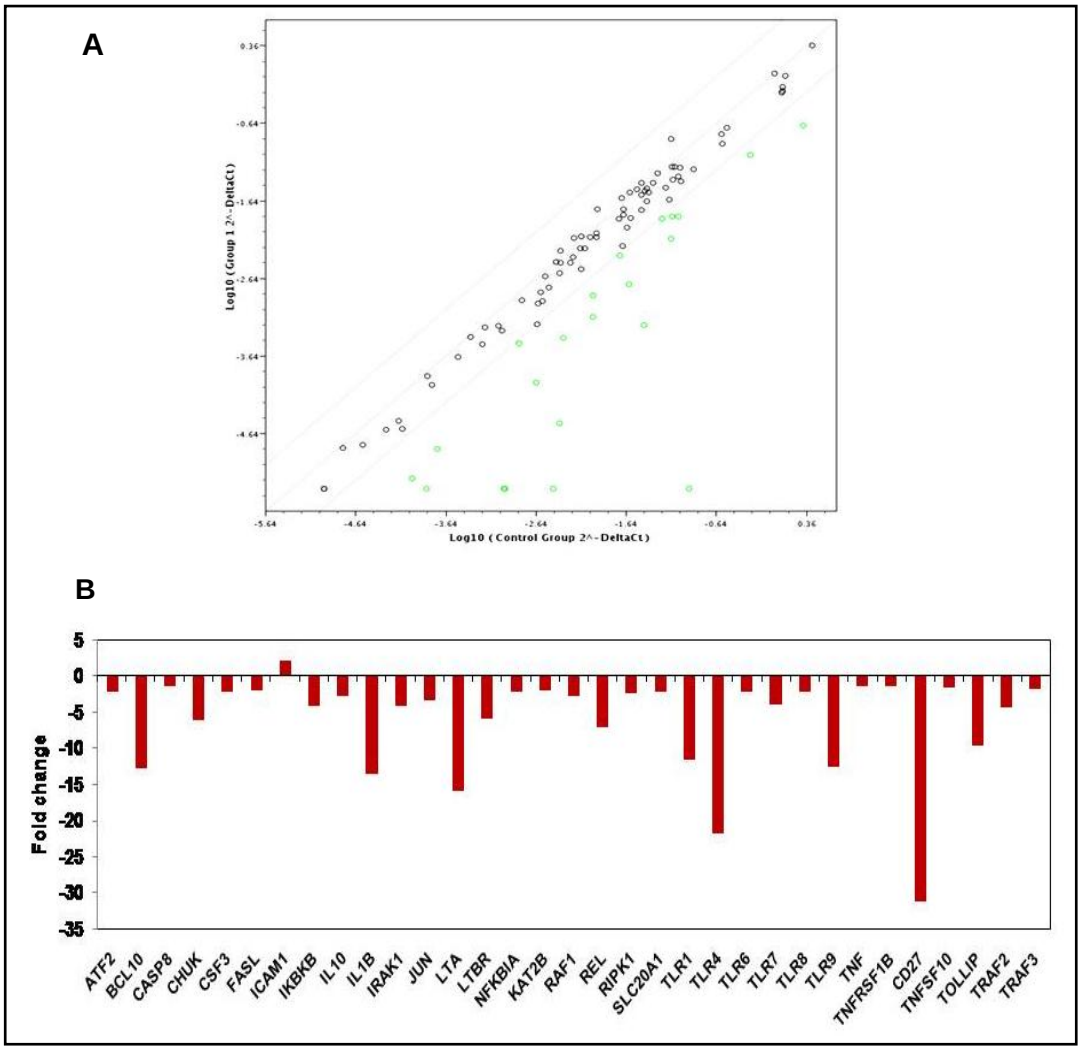

Figure 22: ***Suppression of AAV vectorinduced expression of pro-inflammatory marker genes in murine liver upon PARP-1 inhibition*** *(A) Scatter plot of hepatic gene expression of NF-κB responsive factors in the scAAV2 vector injected BALB/c mice in the presence or absence of PJ-34 and measured 2 hours post-vector administration. Green spots indicate the genes which are down-regulated in PJ-34 injected group compared to the vector alone group. Genes showing significant down regulation (≥2 fold, $p<0.05$) between these groups are shown in B.*

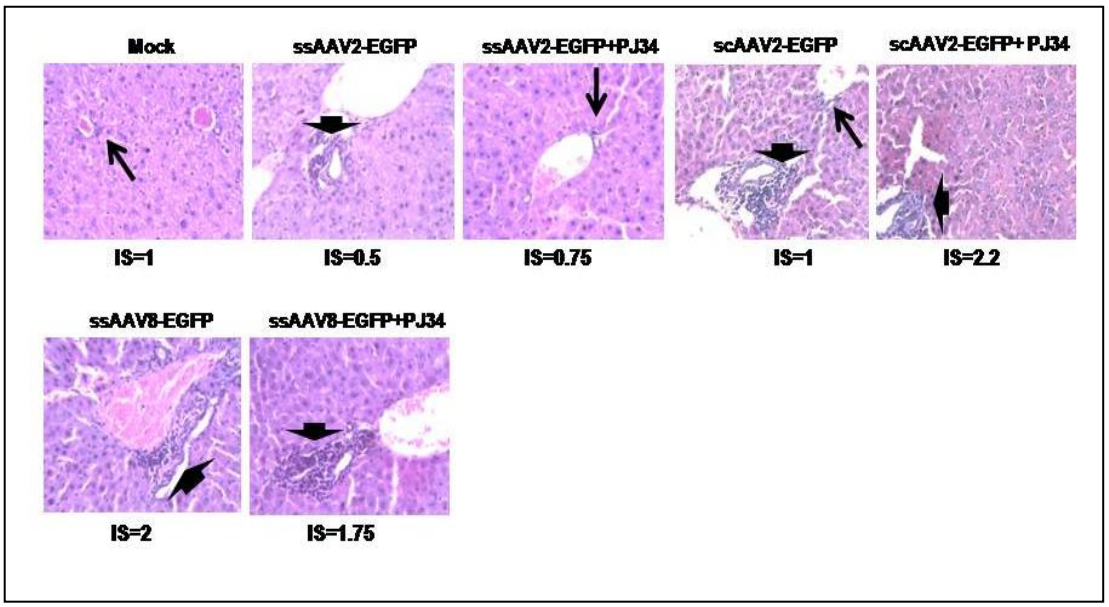

Figure 23: PARP-1 inhibition in mice does not cause liver toxicity. *Histological examination of murine liver samples 4 weeks post-injection of PBS/ ssAAV2-EGFP/ scAAV2-EGFP/ ssAAV8-EGFP vectors alone, or with co-administration of the PARP-1 inhibitor. Liver sections were stained with hematoxylin-eosin. Inflammation scores were based on degree of lobular and portal inflammation and calculated based on the criteria, 0- No inflammation, 1- Mild inflammation, 2- Moderate inflammation, 3- Severe inflammation. For all groups, the individual scores for portal and lobular inflammation ranged between 0-1. The average inflammation score (IS) for each group is indicated below the images (Magnification – 40X). Arrowhead and thin arrow denote portal and focal lobular inflammation, respectively.*

4.3 Modification of AAV2 capsid at specific serine/threonine residues enhances the transduction efficiency of AAV2 vectors

4.3.1 Pharmacological inhibition of cellular serine/ threonine kinases improves the *in vitro* transduction of AAV2 vectors

According to the hypothesis of the study, AAV2 capsid could be phosphorylated by host cellular kinases at specific serine/ threonine residues, which could signal its degradation by ubiquitin- proteasome system. To test if serine/ threonine kinases PKA (Protein kinase A), PKC (Protein kinase B) and CKII (Casein kinase II) play a rate-limiting role in AAV2 transduction, HeLa cells were treated with specific inhibitors of these kinases before virus infection. HeLa cells pretreated with optimal concentrations of PKA inhibitor (25nM), PKC inhibitor (70nM) and CKII inhibitor (1μM) or with combination of each of these inhibitors for 24 hours were transduced with scAAV2-EGFP vectors at 2000MOI. The safe and effective concentration of kinase inhibitors used for the *in vitro* study was determined by MTT assay. Twenty-four hours post- transduction, the transgene expression was measured by flow cytometry. A total of 1 x 10^4 events were analyzed for each sample. Mean of percentage EGFP positivity from three replicate samples were used for comparison between treatment groups. As shown in Figure 24, the transduction efficiency of the wild-type AAV2 vector was significantly up-regulated when HeLa cells were pretreated with these kinase inhibitors, with maximal increase seen in cells treated with the CKII inhibitor (70% *Vs* 37%). Combination of inhibitors containing CKII inhibitor improved the EGFP expression much better than the other combinations. This demonstrates that one or more surface-exposed serine and/or threonine amino acid in the AAV2 capsid is phosphorylated within the host cell by PKA, PKC and CKII serine/threonine kinases and specific inhibition of this process improves the gene expression from AAV vectors. Since systemic administration of serine/ threonine kinase inhibitors in an *in vivo* setting is likely to be toxic (Force & Kolaja,

2011), alternatively the kinase targets on AAV capsid were modified to further improve the transduction efficiency of AAV vectors.

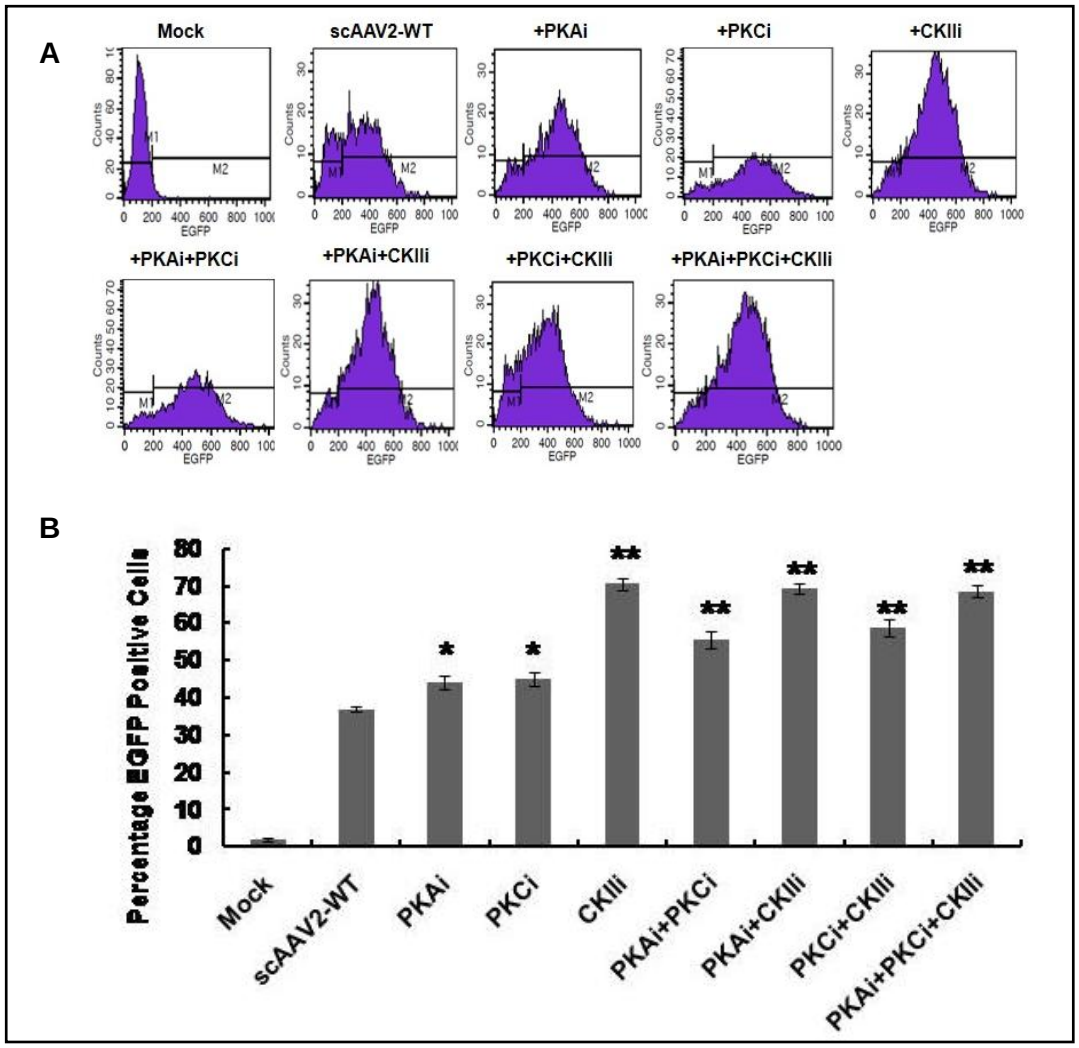

Figure 24: Inhibition of host cellular serine/ threonine kinases augments the AAV2-mediated gene expression in vitro. *HeLa cells were pretreated with protein kinase A (PKA), protein kinase C (PKC), casein kinase (CK)-II inhibitors as single agents or in combination, 24hrs prior to transduction with scAAV2-EGFP vectors. Twenty-four hours post-transduction, cell suspensions were analyzed for EGFP expression by flow cytometry and the FACS histograms obtained are shown in A. (B) Quantitative representation of the data from (A).*p<0.05; **p<0.01Vs AAV2-WT infected cells.*

4.3.2 Generation of AAV2 mutant vectors by modification of specific serine/ threonine residues on the capsid surface

Fifteen AAV2 capsid mutant vectors were generated by altering serine/ threonine (S/T) amino acids at specific positions to alanine (A) residue by site directed mutagenesis. These residues were chosen based on their conservation across the various serotypes (AAV1-10) or their location within or in close proximity to any of the three phosphodegrons identified by *insilico* structural analysis of the AAV2 capsid (Gabriel et al., 2013). Figure 25 shows the conservation status of the various residues selected for mutation in AAV2 capsid sequence. A vast majority of these S/T capsid mutations did not affect the vector packaging efficiency (Table 5) suggesting that modification of these specific amino acids had negligible effect on the capsid structure.

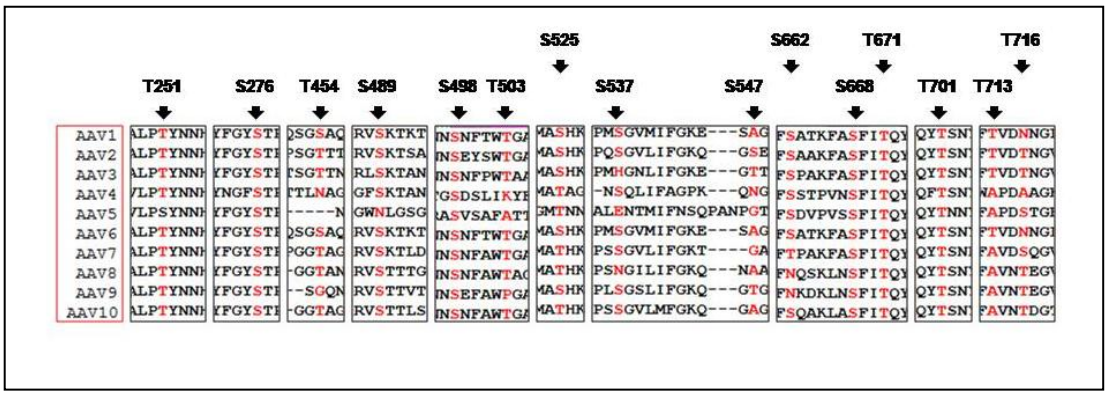

Figure 25: Schematic representation and conservation status of the various S/T residues mutated in AAV2 capsid. *VP1 protein sequences from AAV serotypes 1 through 10 were aligned by ClustalW and the conservation status of the each of the mutated site is given. The specific residue indicated is shown in red font.*

Serine (S)>Alanine (A)	Threonine (T)>Alanine (A)
S276A (1.65x 10^{10})	T251A (1.8 x 10^{12})
S489A (3.2x10^{12})	T454A (2.5 x 10^{10})
S498A (1 x 10^{12})	T503A (5.25x10^{10})
S525A (3.2x10^{12})	T671A (1.6 x 10^{12})
S537A (8x10^{11})	T701A (3.2 x 10^{12})
S547A (1.6x10^{12})	T713A (3.2 x 10^{12})
S662A (3.2x10^{12})	T716A (5.25x10^{10})
S668A (4 x 10^{11})	

Table 5. ***Physical particle packaging titers of AAV2 serine/threonine mutant vectors.*** *Purified vectors resuspended in a final volume of 0.5ml PBS, were quantitated by slot blot method. The physical particle titers are represented in viral genomes/ ml. The titers of wild-type scAAV2 vectors range between 4x10^{11}-1x10^{12} viral genomes/ ml in the laboratory. Average packaging titers from at least two packaging experiments are shown.*

4.3.3 Selective AAV2 serine/ threonine mutant vectors demonstrate significantly improved transduction efficiency *in vitro*

To assess the efficacy of the novel mutant vectors generated, HeLa cells were mock infected or infected with 2 x 10^3 MOI of either AAV2-WT or AAV2 S/T mutant vectors, encoding EGFP reporter gene. Forty-eight hours post-transduction, the transgene expression was quantitated by flow cytometry and EGFP imaging was done using fluorescence microscopy. For flow cytometric analysis, total of 1 x 10^4 events were analyzed for each sample. Totally, three independent experiments (n=3) were performed including three intra-assay replicates in each of the experiment. Mean of percentage GFP positivity from these nine replicate samples were used for comparison between AAV2-WT or AAV2 S/T/K infected cells. Among the 15 S/T→A mutant AAV2 vectors tested for their transduction efficiency at a MOI of 2000 in HeLa cells, 11 had significantly higher percentage of EGFP positive cells (63 to 97%) compared to AAV2-WT vector infected cells (41%) by FACS analysis (Figure 26), suggesting that mutations at serine or threonine residues in the capsid consistently generate superior AAV2 vectors. Fluorescence imaging of AAV vector infected cells demonstrates the higher EGFP expression obtained with most of the AAV S/T mutant vectors (Figure 27).Nevertheless, it was found that four (T454A, T671A, T701A, T713A) threonine capsid mutants had reduced or complete absence of transgene expression compared to their wild-type counterparts. This could be probably because these mutations on the viral capsid adversely affected any of the steps in the rAAV life cycle and consequently their infectivity, *in vitro*.

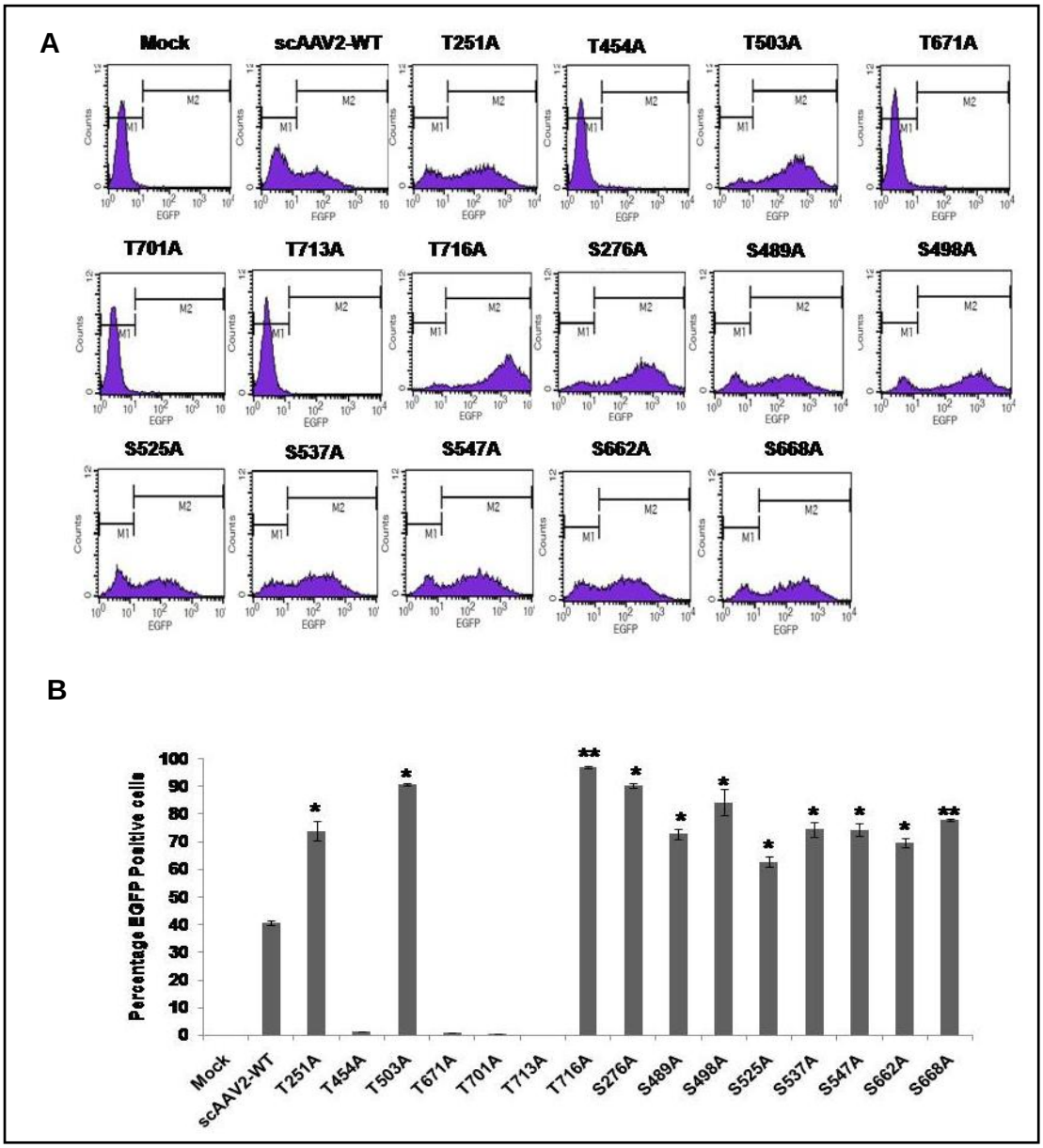

Figure 26: ***Selective AAV2 serine/threonine mutant vectors demonstrate increased transduction efficiency in vitro.*** *Flow cytometric analysis of HeLa cells either mock-infected or infected with 2000 MOI of AAV2-WT or AAV2-S/T→A mutant vectors forty-eight hours post-virus infection. (A) Representative FACS histograms generated upon acquiring 10,000 events for each condition. (B) Quantitative analysis of the data showing the percentage EGFP positive cells. For the conditions where vertical bars are missing, the values are less than 1%. Mean ±SD. *p<0.05, **p<0.01Vs AAV2-WT infected cells.*

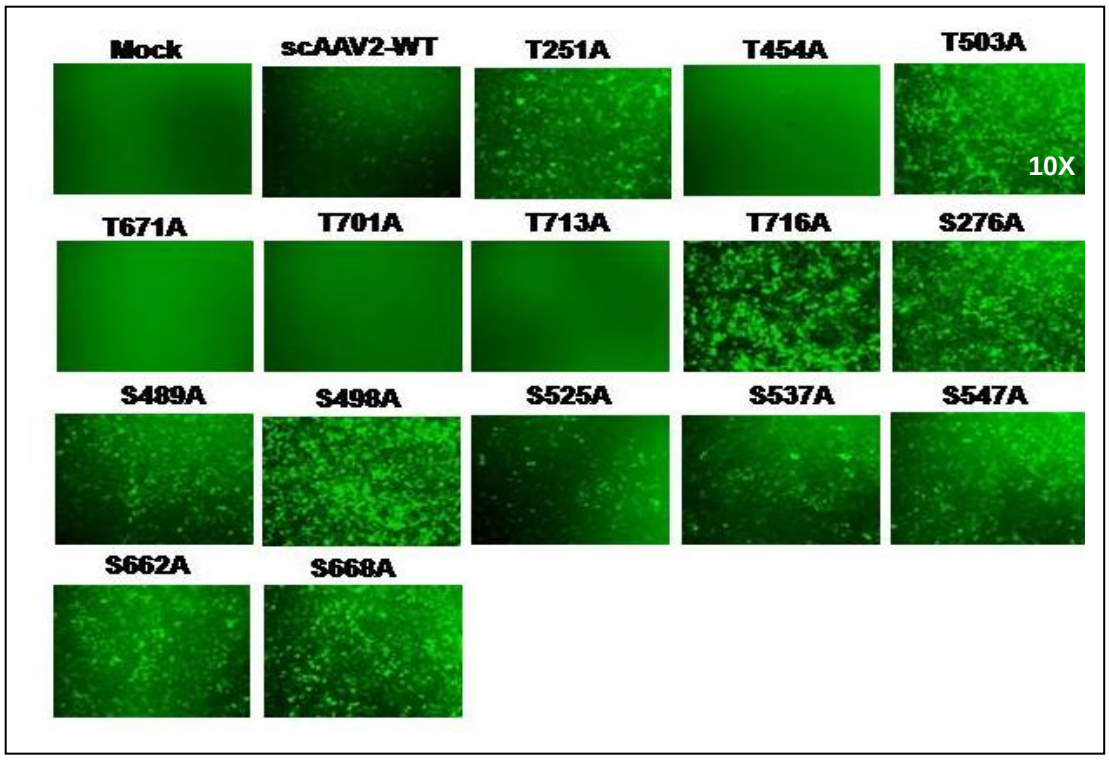

Figure 27: ***Selective AAV2 serine/threonine mutant vectors exhibit enhanced EGFP fluorescence in vitro.*** *HeLa cells were either mock-infected or infected with 2000 vgs/cell of AAV2-WT or AAV2-S/T→A mutant vectors and forty-eight hours later, the EGFP expression was captured by fluorescence microscopy. Representative images are shown. All images were captured at uniform setting of exposure time 633msec, gain 1.7 and intensity 5.*

4.3.4 Selective AAV2 S/T mutant vectors exhibit improved hepatic gene transfer in C57BL/6 mice

The relative transgene levels in the target tissue were analysed following the liver directed delivery of the various AAV2 mutant vectors into mice.Groups (n=4 per group) of 8-12 weeks-old C57BL/6 mice were mock-injected or injected with 5 x 10^{10} vgs each of scAAV2-WT or scAAV2-S/T mutant vectors containing EGFP transgene, *via* the tail vein. For *in vivo* study, AAV2 S/T mutant vectors that

package as efficiently as the AAV2-WT vector and those that showed enhanced transgene expression *in vitro* were administered. Mice were euthanized 4 weeks after vector administration. The hepatic lobes of the mice under the mock- injected and vector- injected groups were assessed for EGFP expression by fluorescence microscopy. Consistent with the *in vitro* data, liver tissues of mice administered with the four S → A mutants (S489A, S498A, S662A, S668A) and the T251A mutant showed higher levels of transgene expression when compared to animals injected with AAV2-WT as evident from the EGFP images (Figure 28A). To corroborate this data, the EGFP transcript levels in hepatic RNA isolated from these mice were measured. Higher levels of EGFP mRNA expression (up to 14-fold) were found in AAV2 S/T mutant administered mice in comparison to AAV2-WT vector injected animals following hepatic gene transfer (Figure 28C). Further AAV vector genome copy numbers in the liver tissue of vector or mock- injected mice were also measured. As shown in Figure 28B, a significant increase in the vector copies per diploid genome (up to 4.5-fold) was observed in animals injected with S/T mutant vectors in comparison to animals that were administered AAV2-WT vector. In all these studies, AAV8 injected animals was used as a control group for hepatic gene transfer. Collectively these results show that selective S/T→A mutations on the viral capsid can augment the transduction efficiency of AAV2 vectors *in vivo.*

4.3.5 AAV2 S/T mutant vectors do not cause any adverse event in C57BL/6 mice

The *in vivo* administration of AAV2 S/T mutant vectors did not lead to any significant histological abnormalities in the livers of C57BL/6 mice 4 weeks post-vector administration. Livers of mice injected with either AAV2-WT or AAV2 S/T/K mutant vectors were grossly normal with comparable inflammation scores. A

set of representative data, shown in figure 29, corroborate that AAV2-S/T/K mutant vectors were generally non-toxic and no adverse events appear to be evident at the 4 weeks post-injection time point.

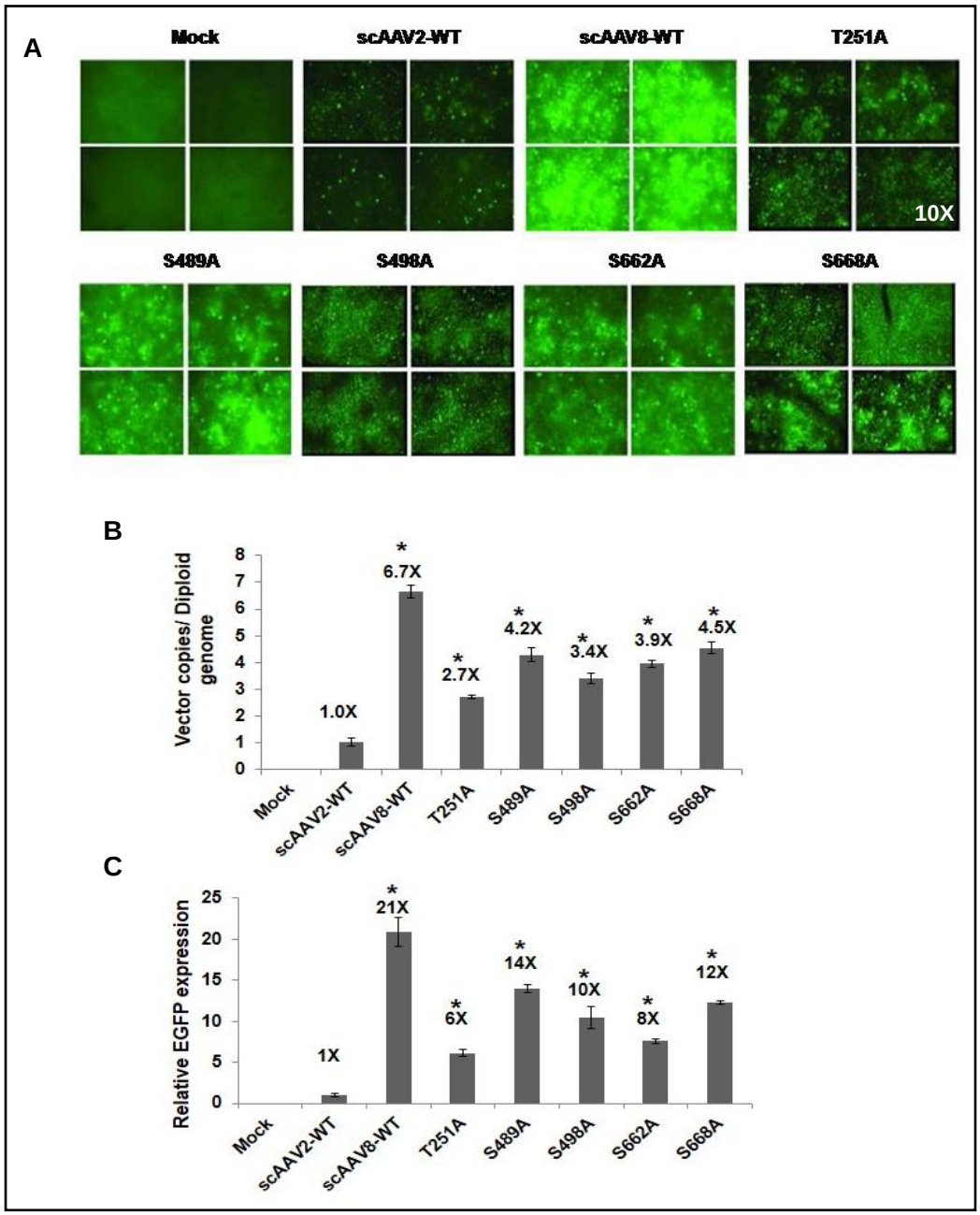

Figure 28: ***SelectiveAAV2 serine/threonine mutant vectors exhibit enhanced transduction upon hepatic gene transfer in vivo.*** *(A) Transgene expression in the liver was detected by fluorescence microscopy 4-weeks post-injection*

*with 5 x 10^{10} vector particles/animal of scAAV2-EGFP, scAAV8-EGFP or AAV2 mutant S/T vectors. Representative images of hepatic tissues from four different animals in each group are shown. All images were captured at uniform setting of exposure time 2 sec, gain 2 and intensity 5. (B) Estimation of vector genome copies in the liver after AAV-mediated gene transfer. Genomic DNA was isolated from liver tissue of C57BL/6 mice 4-weeks post vector administration and the viral copy numbers estimated by a quantitative PCR as described in Materials and methods. (C) Analysis of EGFP transcript levels by real-time quantitative PCR. Hepatic RNA isolated from animals injected with AAV2-WT, AAV8-WT or AAV2 S/T vectors were analyzed for EGFP expression and the data normalized to the GAPDH reference gene. *p<0.05 Vs AAV2-WT injected animals.*

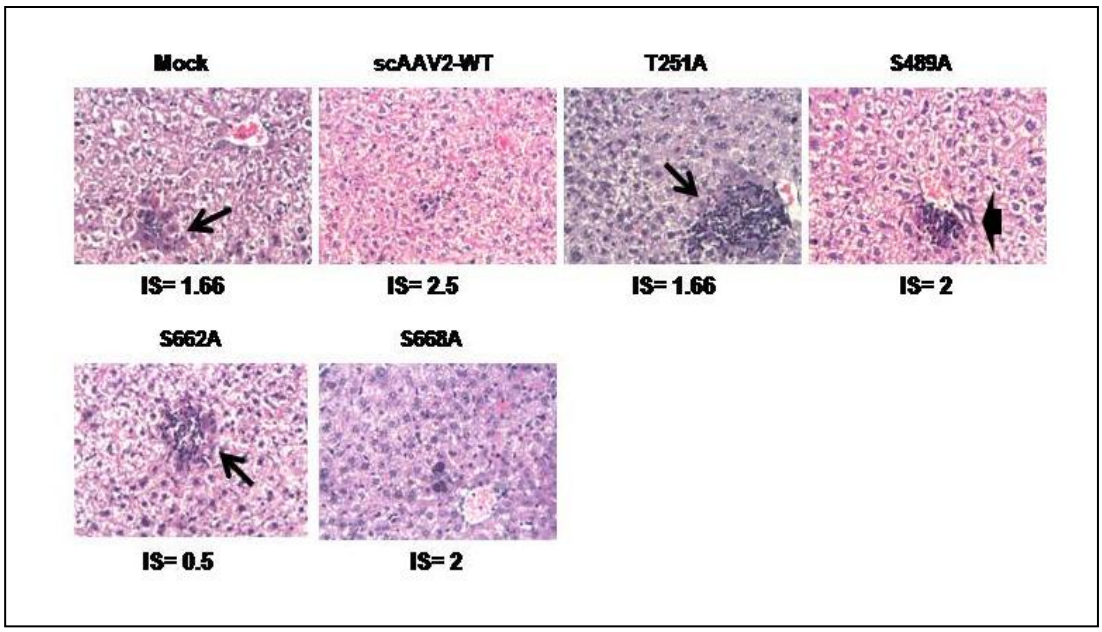

Figure 29: ***AAV2 S/T mutant vectors do not cause any hepatotoxicity in mice****. Histological examination of mice liver samples 4-weeks post-injection of AAV2-WT or mutant vectors. Hepatic sections were fixed in 10% buffered formalin and stained with hematoxylin-eosin. The median inflammation score (IS) for each group is indicated below the images (Magnification–40X) with the range of values given within brackets. Arrowhead and thin arrow denote portal and focal lobular inflammation, respectively. Representative images of the liver section of one animal from each group (n=3) is shown.*

4.4 Synergistic inhibition of PARP-1 and NF-κB pathway modulates immune response against AAV vectors in C57BL/6 mice

4.4.1 Inhibition of PARP-1 and NF- κB modulates the pro-inflammatory response against AAV2 vectors

In the initial part of the study, it was found that inhibition of PARP-1 was instrumental in down regulating the expression of several pro- inflammatory genes related to NF-κB signaling, induced upon AAV vector administration in mice. Nonetheless, not all the NF-κB target genes depend on PARP-1 for their expression, as inferred from the fact that $PARP^{-/-}$ mice does not exhibit the same phenotype as $p65^{-/-}$ mice (Beg et al., 1995). Likewise, PARP-1 is known to activate other transcription factors such as HIF-1 and AP-1 besides NF-κB (Martin-Oliva et al., 2006). It was thus speculated that combined inhibition of PARP-1 and NF-κB signaling might further moderate the expression of inflammatory markergenes in liver during AAV gene delivery, in comparison to PARP-1 inhibition alone. Pharmacological inhibitors of PARP-1 (PJ34) and NF-κB (Bay11-7085) were tested both individually and in combination. In addition, clinically approved/ tested inhibitors of NF-κB and PARP-1 such as Bortezomib and ABT-888 respectively, were also tested as single agents and in combination. Bortezomib is a proteasome inhibitor approved for the treatment of patients with advanced relapsed and/or refractory multiple myeloma and is a potent NF-κB inhibitor(Ludwig et al., 2005, Berenson et al., 2006, Juvekar et al., 2011), though an opposing effect has also been reported (Dolcet et al., 2006, Li et al., 2010). ABT-888 (Veliparib) is a PARP-1 inhibitor tested for its chemo-sensitisation potential in the treatment of several types of solid tumors such as lung, ovarian, fallopian, pancreatic, breast, liver, prostate, head and neck, and brain (Lupo & Trusolino, 2014).

Groups of C57BL/6 mice (n=5) pretreated with appropriate compounds as single agents (Bay11-7085, PJ34, ABT-888 or Bortezomib) or in combination were either mock-injected (PBS) or injected with scAAV2 and euthanized 2 hours later. Drugs dosages used for *in vivo* administration are given in table 6. RNA isolated from the liver tissue was reverse transcribed to synthesize cDNA. Expression profile of the various innate immune response markers in murine liver was then evaluated using the NF-κB RT-PCR Profiler array. As shown in figure 30, the relative expression of AAV-vector induced NF-κB pathway components and responsive factors was down-regulated to a greater extent in mice subjected to synergistic inhibition of both PARP- 1 and NF-κB, in comparison to inhibition of either NF-κB pathway or PARP-1 alone. Particularly pro-inflammatory genes within the Toll- like receptor family such as TLR1, TLR2, TLR3, TLR6 and TLR9, Tumor necrosis factor receptors (Tnfrsf1a, Tnfrsf1b), components of NF-κB pathway (RelA, NF-κB1, NF-κB2) and mediator of cytokine response like TRAF, TRADD, LTBR, BCL3, IL1B were mainly suppressed. Down-regulation of RelA, Lta, IL-10, TLR4 and RelB was more than 20-fold and hence has not been represented in the graph (Figure 30). The suppressive effect on AAV induced NF-κB responsive genes was remarkably pronounced in the group of animals which were administered combination of clinically tested drugs targeting PARP-1 and NF-κB. This data supports the notion that synergistic inhibition of PARP-1 and NF-κB signaling is more effective in attenuating the pro-inflammatory cytokine response against AAV vectors than independently targeting PARP-1 or NF-κB pathway.

Inhibitor	Stock	Dosage in mice	Route of administration
Bay11-7085	10mg/ml	20mg/kg (Yang et al., 2004)	i.p
PJ34	5mg/ml	10mg/kg (Stone et al., 2005)	i.p
ABT-888	5mg/ml	12.5mg/kg (Kinders et al., 2008)	i.p
Bortezomib	1mg/ml	1mg/kg (Nathwani et al., 2009)	i.v

Table 6: ***Dosage and route of administration of the inhibitor drugs****. These compounds were used to evaluate the effect of synergistic inhibition of PARP-1 and NF-κB signaling on the host innate immune response against AAV2 vectors in C57BL/6 mice. The drug dosage was selected based on data gathered from the literature as indicated. i.p- intraperitoneal; i.v- intravenous.*

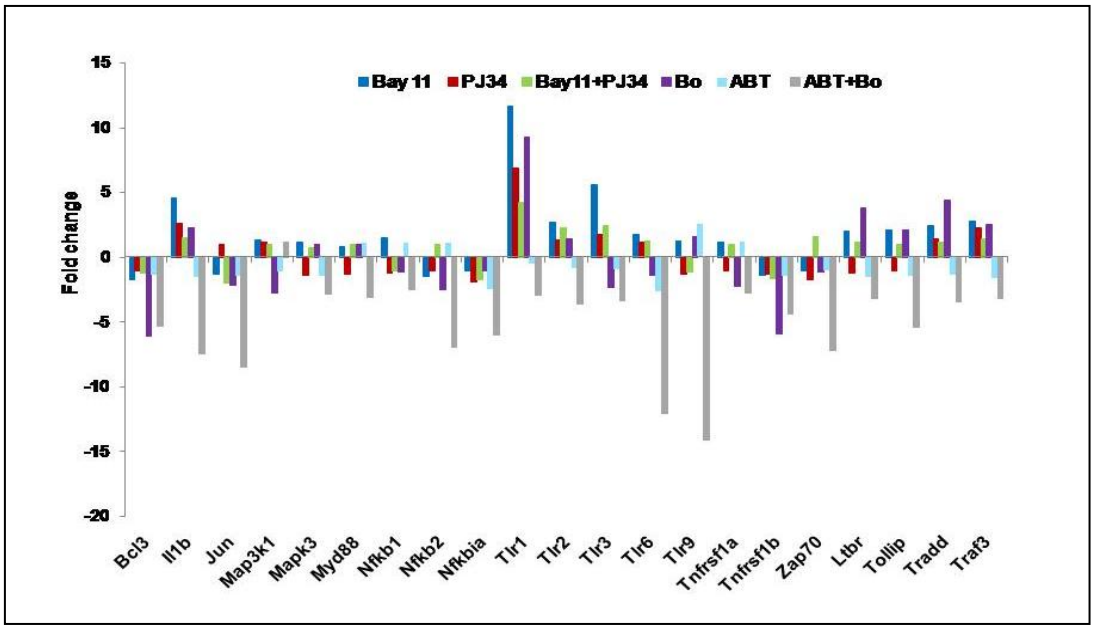

Figure 30: ***Synergistic inhibition of PARP-1 and NF- κB modulates the expression of AAV2 vector induced pro-inflammatory marker genes.*** *Relative expression of NF-kB responsive genes and markers ofpro-inflammatory response, measured in the hepatic tissue of C57BL/6 mice from various treatment*

groups (as indicated), at two hours post-AAV gene transfer. Fold change in gene expression compared to the AAV2 vector alone injected mice is shown in the graph. Genes which were significantly regulated (≥2 fold, p value <0.05) in any of the treatment groups with respect to the vector administered group alone, are selectively represented in the figure.

4.4.2 Synergistic inhibition of PARP-1 and NF- κB enhances the AAV2 transduction *in vitro*

To test if the synergistic inhibition of PARP-1 and NF- κB would augment the AAV2 transduction *in vitro*, HeLa cells were treated with combination of bortezomib and ABT-888 for 24 hours. The dosage of these drugs to be used in *in vitro* experiments was verified to be non-toxic to cells by MTT cell viability assay with different dilutions (Figure 31A). Final concentration used for testing in HeLa cells was 5μM for ABT-888 and 15nM for Bortezomib as determined from MTT assay. After treatment with the inhibitors, the cells were mock infected or infected with scAAV2-Lucvectors expressing luciferase gene at MOI of 2000vgs/cell. Forty-eight hours post-transduction, the luciferin substrate was added to the cells and after 5minutes of incubation the bioluminescence corresponding to luciferase expression was captured in an IVIS Spect-CT small animal imaging system. As shown in the figure 31B, the bioluminescence of the transgene expressed in photons/second was 1.62-fold higher in the cells treated with bortezomib plus ABT-888. This data suggests that synergistic inhibition of PARP-1 and NF- κB enhances the *in vitro* transduction efficiency of AAV2 vectors.

This phenomenon was validated by infecting HeLa cells using Cy3 labeled scAAV2-EGFP vectors. HeLa cells seeded in 35 mm^2 coverglass bottom dishes were

treated with the inhibitors for 24 hours and transduced with fluorescent labeled AAV2- EGFP vectors at 30, 000 MOI to enable visualization of virus particles. About an hour after virus infection, live imaging of the cells was done using confocal microscopy (Olympus FV1000). Vector infected HeLa cells without any drug treatment was used as the control. In both conditions, DIC images showed Cy3 labeled virus particles localized within individual cells, inside the cytoplasm and in the nuclear periphery (Figure 32A). Further at 17 hours post-infection, the cells were fixed in 10% buffered formalin and hoechst fluorescent dye was added to stain the nucleus. Fluorescent signals from Cy3 labeled virus, Hoechst stained nucleus and EGFP transgene expressing cells were captured in the confocal microscope. As shown in figure 32B, the EGFP levels were visually higher with more number of HeLa cells expressing the vector encoded transgene, upon targeted and combined inhibition of PARP-1 and NF- κB signaling. Cy3 labeled vectors particles were not seen within the fixed cells at 17 hours post- transduction. Apparently at this time point, stages of life cycle such as virus entry, intracellular trafficking and nuclear translocation are known to be completed with regard to AAV2 vectors (Xiao et al., 2012). This reasonably explains why Cy3 signal was not visible in HeLa cells at 17 hours after infection. The merged images clearly help to distinguish the EGFP expression within the nucleus and cytoplasm of individual cells. Taken together these results imply that synergistic inhibition of PARP-1 and NF- κB augments the AAV2 mediated transgene expression *in vitro*.

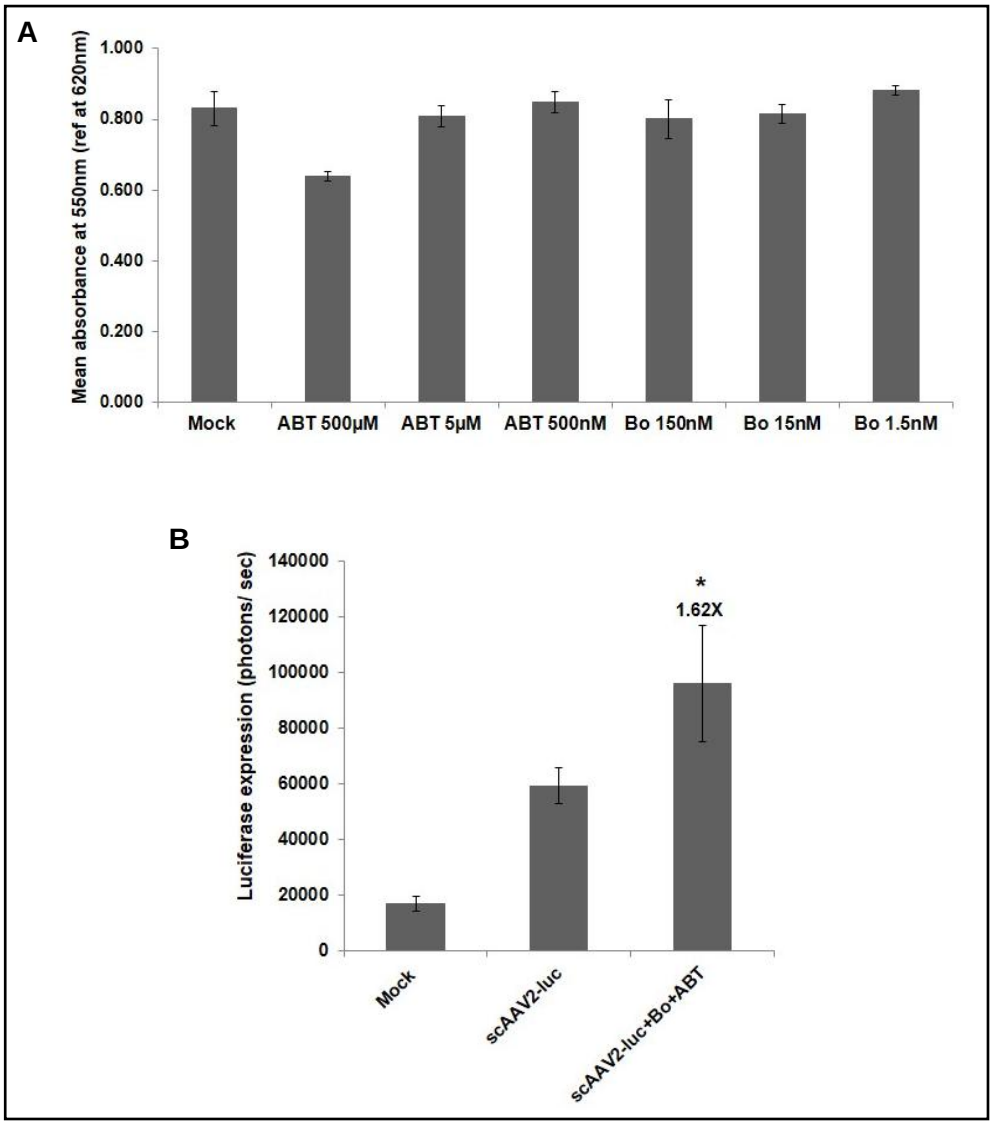

Figure 31: ***Synergistic inhibition of PARP-1 and NF- κB enhances the AAV2 transduction in vitro****. (A) HeLa cells were treated with different concentrations of Bortezomib (Bo) and ABT-888 (ABT) as indicatedfor 24 hours following which MTT assay was done. Absorbance values at 550nm are plotted in the graph (mean±SD). Reference absorbance reading was taken at 620nm. (B) HeLa cells in the presence or absence of Bo plus ABT, were mock infected or infected with scAAV2-Luc vectors at MOI of 2000vgs/cell. Forty-eight hours post-transduction, the luciferin substrate was added and the bioluminescence was captured. Quantitative analysis of the in vitro luciferase expression obtained is shown. Mean ±SD; *p<0.05.*

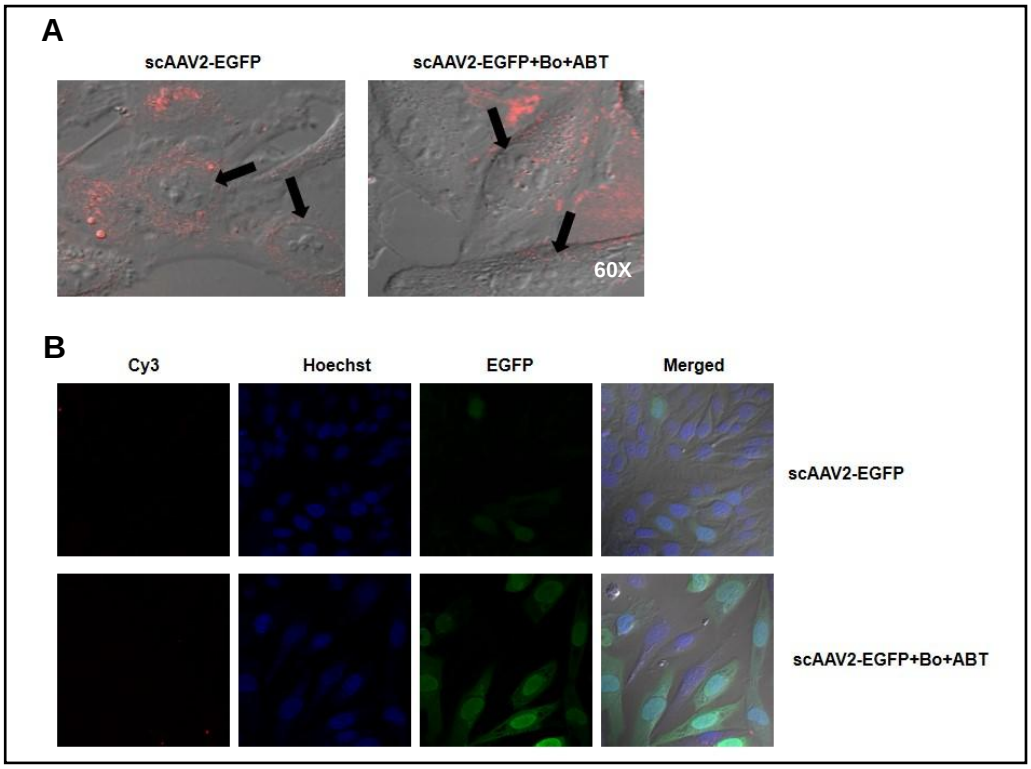

Figure 32: Confocal imaging of AAV2 infection and transgene expression in HeLa cells upon synergistic inhibition of PARP-1 and NF- κB. *HeLa cells pretreated with inhibitors for 24 hours, were infected with Cy3 labeled AAV2- EGFP vectors at 30, 000 MOI.(A) One hour after virus infection, live images of the cells were taken using confocal microscope (Olympus FV1000). Zoomed in DIC images showing Cy3 labeled virus particles (as red dots) localized within individual cells. Arrows indicate nuclear periphery. (B) At 17 hours post-infection, the cells were fixed in 10% buffered formalin and hoechst fluorescent dye was added to stain the nucleus. Fluorescent signals from Cy3 labeled virus, Hoechst stained nucleus and EGFP transgene expressing cells were captured in the confocal microscope.*

4.4.3 Synergistic inhibition of PARP-1 and NF- κB does not alter the AAV2-mediated transgene expression in C57BL/6 mice

Next it was examined if the synergistic inhibition of PARP-1 and NF-κB pathway might enhance the liver directed gene transfer efficacy of scAAV2 vectors.

Groups of C57BL/6 mice (n=4) pretreated with combination of Bortezomib (1mg/kg) and ABT-888 (12.5mg/kg) were injected with 1 x 10^{11} vgs of scAAV2 vector carrying luciferase reporter gene. Booster dosing of the drug followed by the vector was done at two weeks time point. At the end of 4 weeks after the initial administration, the mice were imaged in an IVIS Spect-CT small animal imaging system to document the bioluminescence corresponding to the expression of luciferase gene. Scheme of the experiment is shown in figure 33. Unlike the *in vitro* data, there was no significant change in the *in vivo*AAV2 mediated transgene expression between the treated and untreated groups as shown by the quantitative analysis of bioluminescence in mice liver (Figure 34). This shows that combined inhibition of PARP-1 and NF-κB does not alter the luciferase transgene expression from scAAV2 vectors in normal C57BL/6 mice.

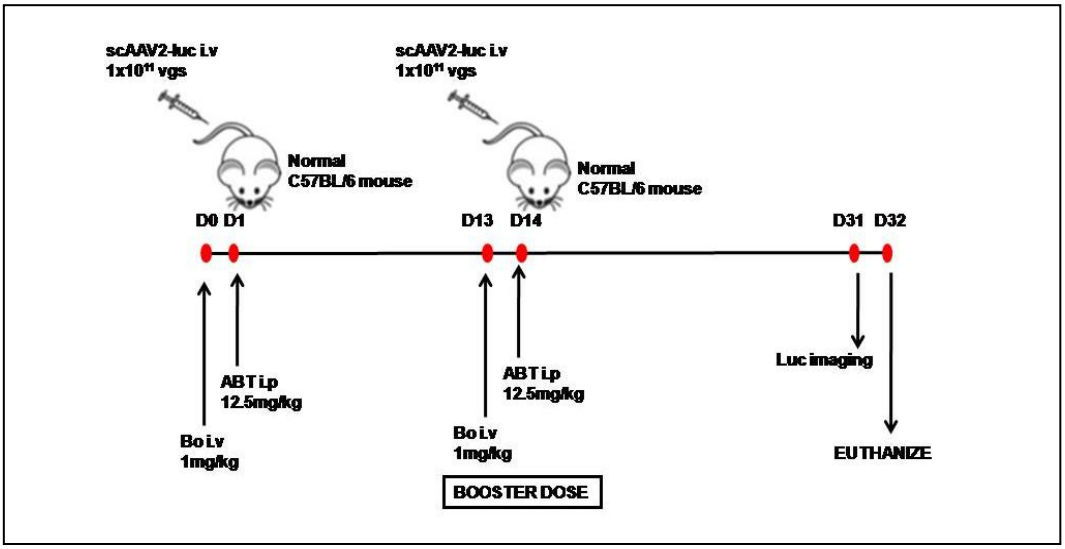

Figure 33: ***Schema of the experiment to study the effect of synergistic inhibition of PARP-1 and NF- κB on in vivo transduction and adaptive immune response against AAV2 vectors in C57BL/6 mice***

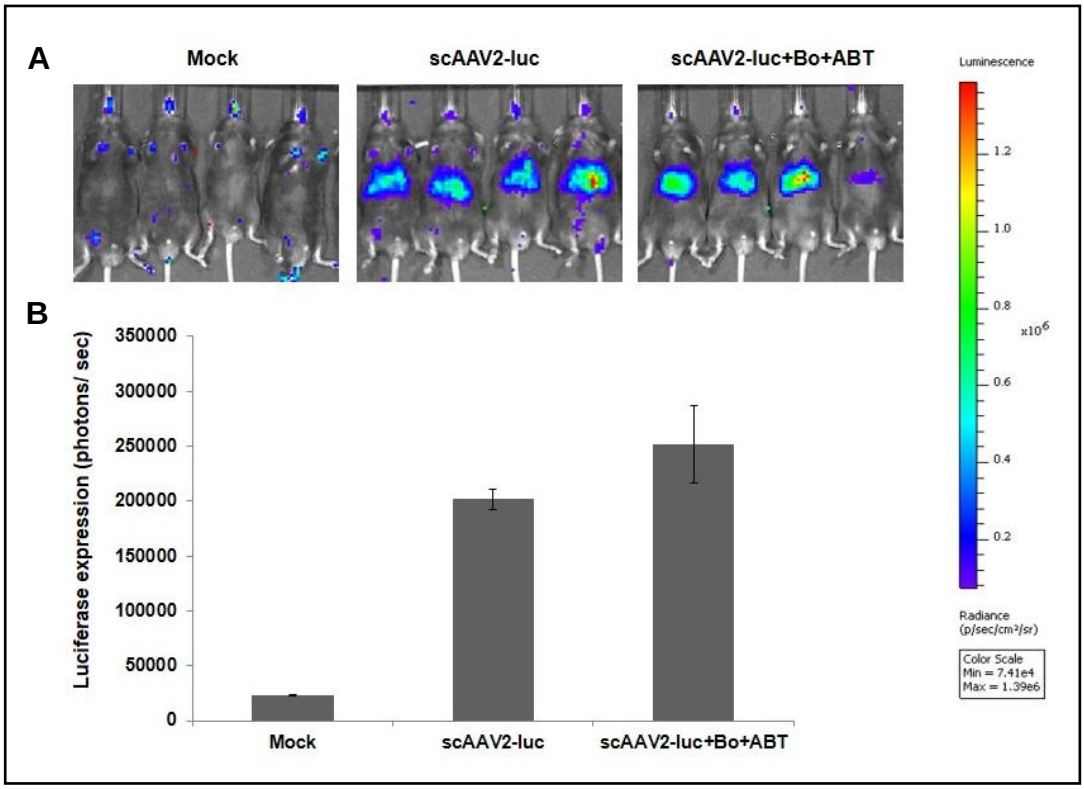

Figure 34: Combined inhibition of PARP-1 and NF-κB does not alter the transgene expression from scAAV2 vectors in normal C57BL/6 mice. *(A) Mice pretreated with combination of Bortezomib (1mg/kg) and ABT-888 (12.5mg/kg) were injected with 1 x10^{11} vgs of scAAV2 –Luc vector. Booster dose of the inhibitors and vectors was given after 2 weeks. Four weeks after the initial administration, the mice were imaged in an IVIS Spect-CT small animal imaging system to capture the luciferase based bioluminescence. The radiance corresponding to the colour intensity of luminescence is shown on the right. (B) Quantitation of the luciferase expression data obtained in (A). Mean±SEM.*

4.4.4 Synergistic inhibition of PARP-1 and NF-κB signaling modulates the cytotoxic T cell response against AAV2 vectors in C57BL/6 mice

The adaptive T cell response against AAV vector remains as a major confounding factor impeding the translational application of AAV in humans. Hence it was evaluated whether combined inhibition of PARP-1 and NF-κB signaling would down regulate the AAV2 specific CD8+ T cell based immune response. As shown in the scheme (figure 33), C57BL/6 mice (n=4) were administered with Bortezomib and ABT-888 followed by intravenous administration of scAAV2-Luc at a vector dose of 1 x 10^{11} vgs/mouse. Two weeks later, the drugs were re- injected along with a booster dose of vector. At the end of 4 weeks time point, the mice were euthanized. The splenocytes were isolated and the capsid specific IFNγ response was evaluated by ELISPOT assay. As shown in figure 35, the number of spots produced per million splenocytes stimulated with AAV2 capsid specific peptide was significantly reduced (1.57-fold) in the mice treated with the bortezomib and ABT-888 as compared to the untreated group. This data implies that synergistic inhibition of PARP-1 and NF-κB signaling is effective in minimizing the host T cell response against AAV vectors.

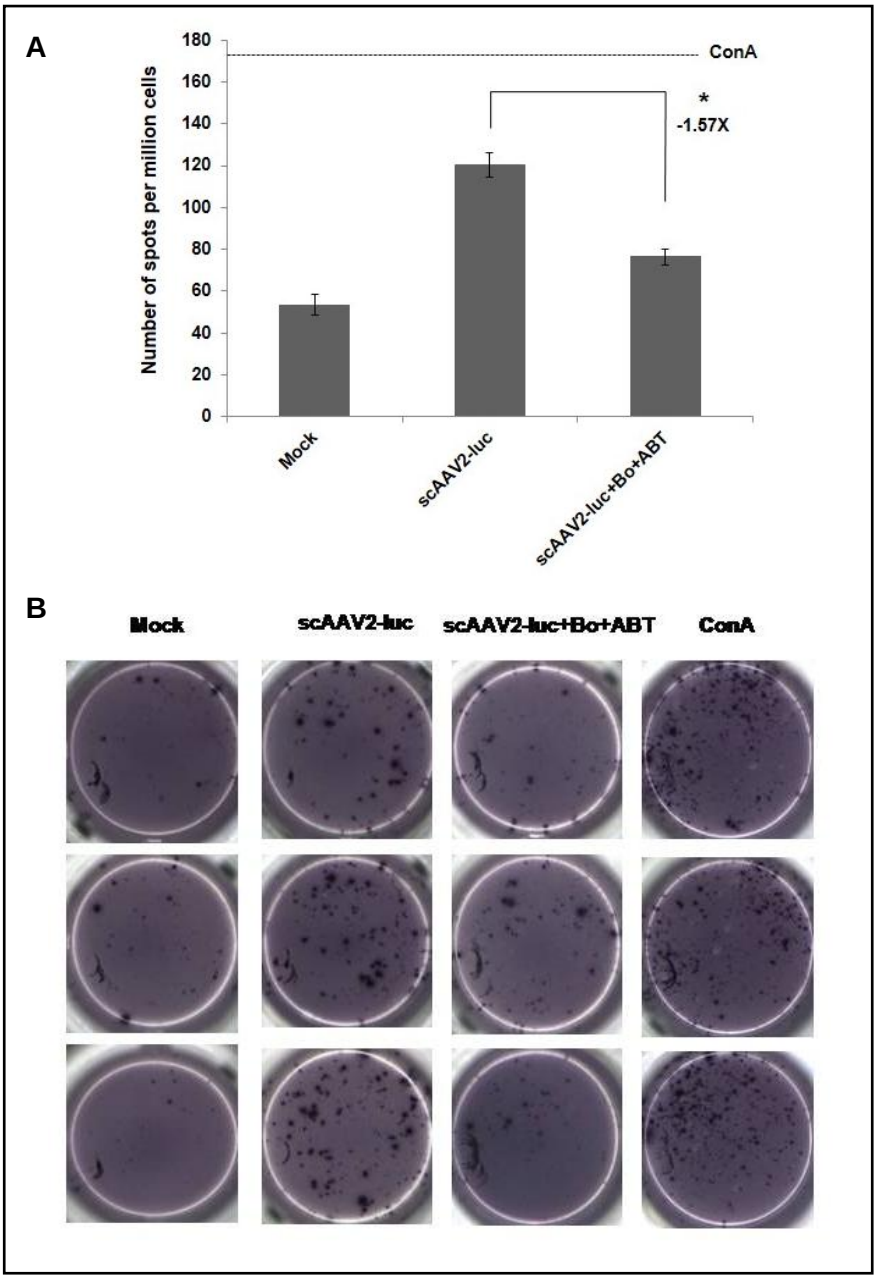

Figure 35: ***Combined inhibition of PARP1 and NF-κB modulates the cytotoxic T cell response against AAV2 vectors.*** *(A) AAV2 capsid specific T cell response was quantitated by IFNγ based ELISPOT assay. The graph shows the number of spots generated per million splenocytes stimulated with AAV2 capsid specific peptide. Concanavalin A (ConA) at a concentration of 2µg/ ml was used as the positive control (dotted line). (B) Representative wells from the ELISPOT plate, for the various treatment groups as shown. Mean±SEM. *p<0.05.*

4.4.5 Synergistic inhibition of PARP-1 and NF-κB signaling shows a trend towards reducing the CD8+ T cell immune response against AAV8 vectors without altering the transgene expression in mice

Subsequently a study was designed to examine if the immune-modulation approach tested on AAV2 vectors could be extended to AAV8 vectors as well. Normal C57BL/6 mice (n=5) were administered Bortezomib, i.v and ABT-888, i.p at doses similar to AAV2 study. Two additional doses of ABT-888 were included prior to vector injection, to check if conditioning of mice with PARP-1 inhibition for some time before vector exposure could have any added advantage. Schema of the experiment is shown in figure 36A. The scAAV8 vectors carrying luciferase transgene were injected through the tail vein at a dose of 1×10^{11} vgs/ mouse. Booster dose of the drugs and vector was given at two weeks time point and the mice were sacrificed at the end of four weeks. AAV8 capsid driven CD8+ T cell based IFNγ response was measured by ELISPOT assay. The number of spots produced per million splenocytes stimulated with T cell epitope containing AAV8 capsid peptide was decreased (1.2-fold) upto the mock levels in mice treated with the bortezomib and ABT-888 (figure 36B). This data demonstrates that synergistic inhibition of PARP-1 and NF-κB signaling does not have a major effect ($p= 0.178$) on the regulation of host cytotoxic T cell response against AAV8 vectors, possibly due to the variable innate/ adaptive immune profile noted against AAV8 vectors in comparison to AAV2 (Chen et al., 2006, Wu et al., 2014).

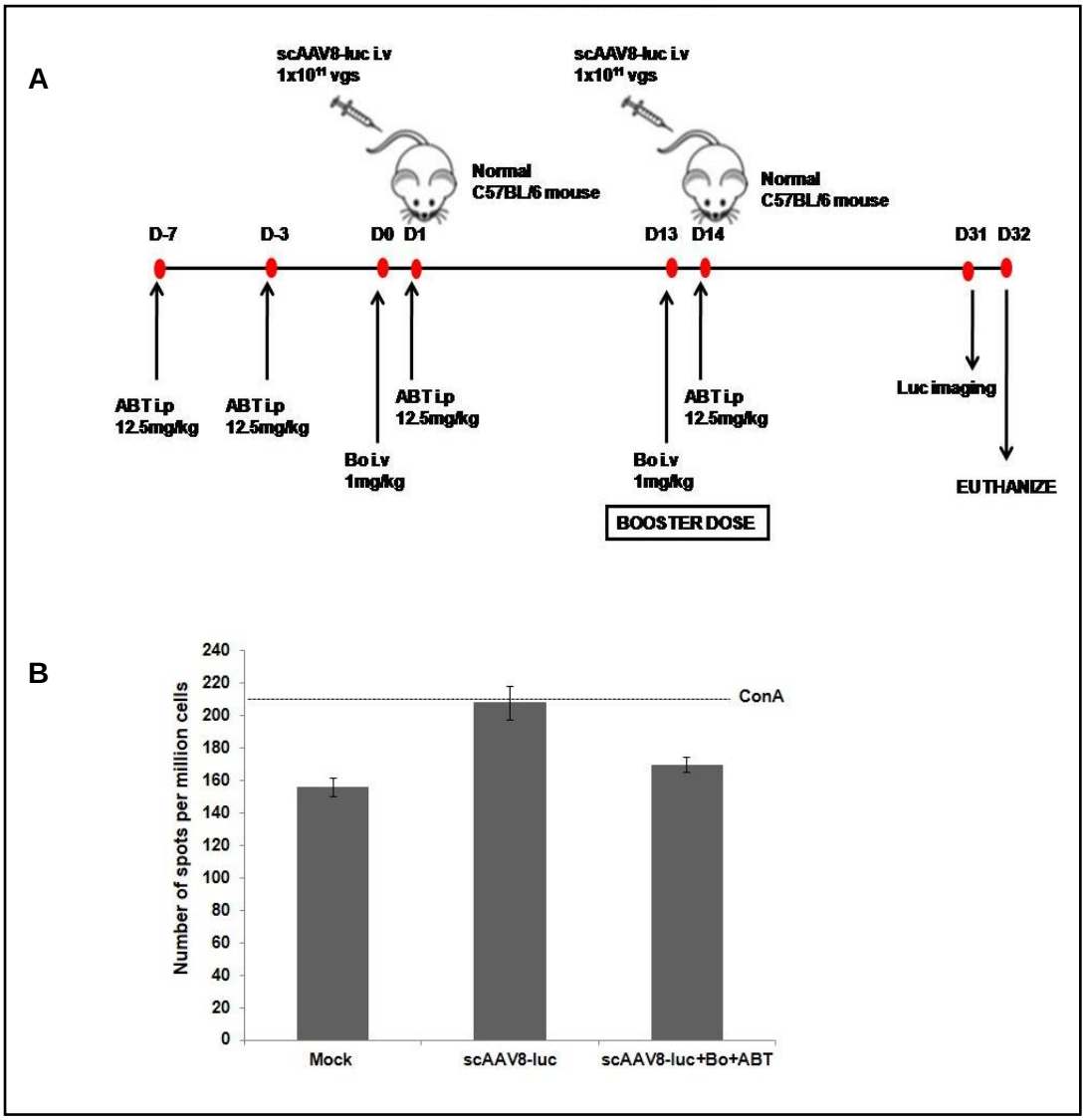

Figure 36: ***Effect of synergistic inhibition of PARP-1 and NF- κB on AAV8 vectors.*** *(A) Schema of the experiment to study the effect of synergistic inhibition of PARP-1 and NF- κB on in vivo transduction and adaptive immune response against AAV8 vectors in C57BL/6 mice (B) AAV8 capsid specific CD8+ T cell response in the mice injected with scAAV8- Luc vectors as shown in (A), was measured by IFNγ based ELISPOT assay. The number of spots generated per million splenocytes stimulated with AAV8 capsid specific peptide is plotted in the graph. Concanavalin A (ConA) at a concentration of 2µg/ ml was used as the positive control (dotted line). Mean± SEM.*

Analysis of the luciferase levels in different groups of mice after 4 weeks further showed that combined inhibition of PARP-1 and NF-κB does not alter the transgene expression from scAAV8 vectors in normal C57BL/6 mice (Figure 37).

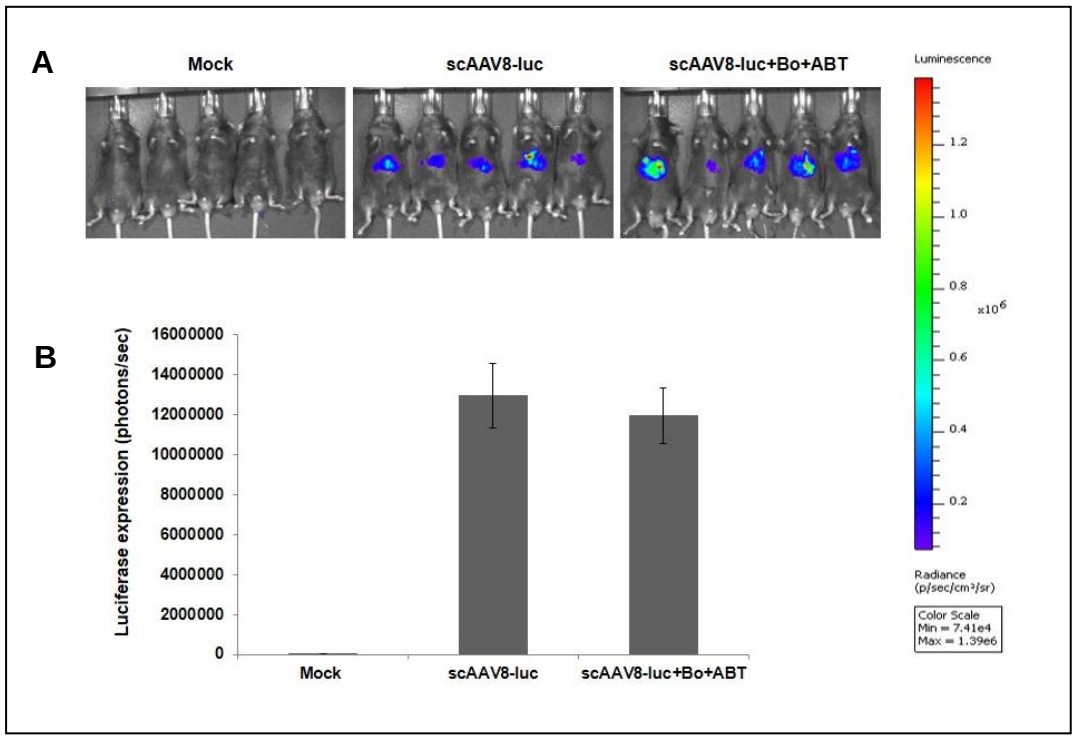

Figure 37: ***Combined inhibition of PARP-1 and NF-κB does not alter the AAV8 based transgene expression in mice.*** *(A) Mice pretreated with combination of Bortezomib plus ABT-888 and injected with 1 x10^{11} vgs of scAAV8 –Luc vector as shown in schema (figure 37A) were imaged after 4 weeks in an IVIS Spect-CT small animal imaging system to capture the luciferase based bioluminescence. The radiance corresponding to the colour intensity of luminescence is shown on the right. (B) Quantitation of the luciferase expression data obtained in (A). Mean±SEM.*

4.4.6 Synergistic inhibition of PARP-1 and NF-κB signaling does not lead to hepatotoxicity in mice

Since bortezomib and ABT-888 were administered systemically into the mice, it was important to examine if there is any toxic effect of it in mice. Blood samples were collected from AAV8 vector administered mice at the end of the study (schema shown in figure 36A). Liver toxicity was assessed by measuring the levels of ALT and AST transaminases in the serum. As shown in figure 38, the liver transaminases' levels of the vector injected mice with/ without PARP-1 and NF-κB combined inhibition are comparable, and not significantly different. This indicates that the transient inhibition of PARP-1 and NF-κB signaling does not cause liver toxicity in mice.

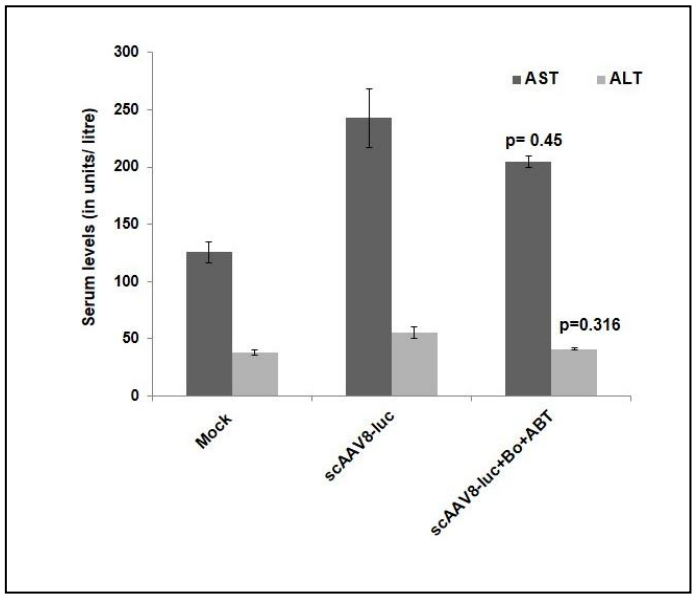

Figure 38: ***Synergistic inhibition of PARP-1 and NF-κB signaling does not cause toxicity in recipient animals.*** *Blood samples were collected from AAV8 vector administered mice with/without subjecting to PARP-1 and NF-κB combined inhibition. Levels (units/litre) of liver transaminases, AST and ALT in sera of different groups of mice are shown. Mean±SEM. pvalue: scAAV8-Luc Vs scAAV8-Luc+Bo+ABT.*

4.5 Evaluation of PARP-1 and NF-κB combined inhibition as an immunomodulation strategy against AAV2 vectors in hemophilia B mice model

4.5.1 Synergistic inhibition of PARP-1 and NF-κB modulates the CD8+ T cell response against AAV2 vectors in hemophilia B mice

Finally, the proposed immune-modulation strategywas evaluated in a murine model of hemophilia B, subjected to FIX gene correction using AAV2 vectors. hemophilia B mice (n=3) pretreated with 1mg/ kg Bortezomib and 12.5 mg/ kg ABT-888 were injected with 5 x 10^{10} viral dose of scAAV2-LP1-hFIX vector intravenously *via* the tailvein. After 10 days, booster injection of the drugs followed by the vectors was given and the mice were sacrificed a week later. Control group were administered only the vectors and not the inhibitor drugs. This was undertaken as a proof of concept study to evaluate the novel immune suppression regimen in a disease model administered with relatively lower vector dose (5 x 10^{10} vgs/ animal) and maintained for a minimum of one-week time period after booster injections to attenuate the cytotoxic T cell response. The schema of the experiment is shown in figure 39A. The splenocytes were isolated and seeded in 96 well plate in appropriate media conditions. After about 30 hours of incubation, the cell culture supernatant was collected and ELISA was done to measure the IFNγ cytokine secretion from activated T cells. The IFN-γ standard curve from which the cytokine concentration of the test conditions was deduced is depicted in figure 39B. It was found that the vector targeted IFNγ T cell response reduced significantly by 2.78-fold in hemophilia B mice subjected to combined inhibition of PARP-1 and NF-κB signaling(Figure 40). This strategy is thus effective in mitigating innate as well as adaptive immune

responses targeting AAV vectors, which might have clinical implications in gene therapy.

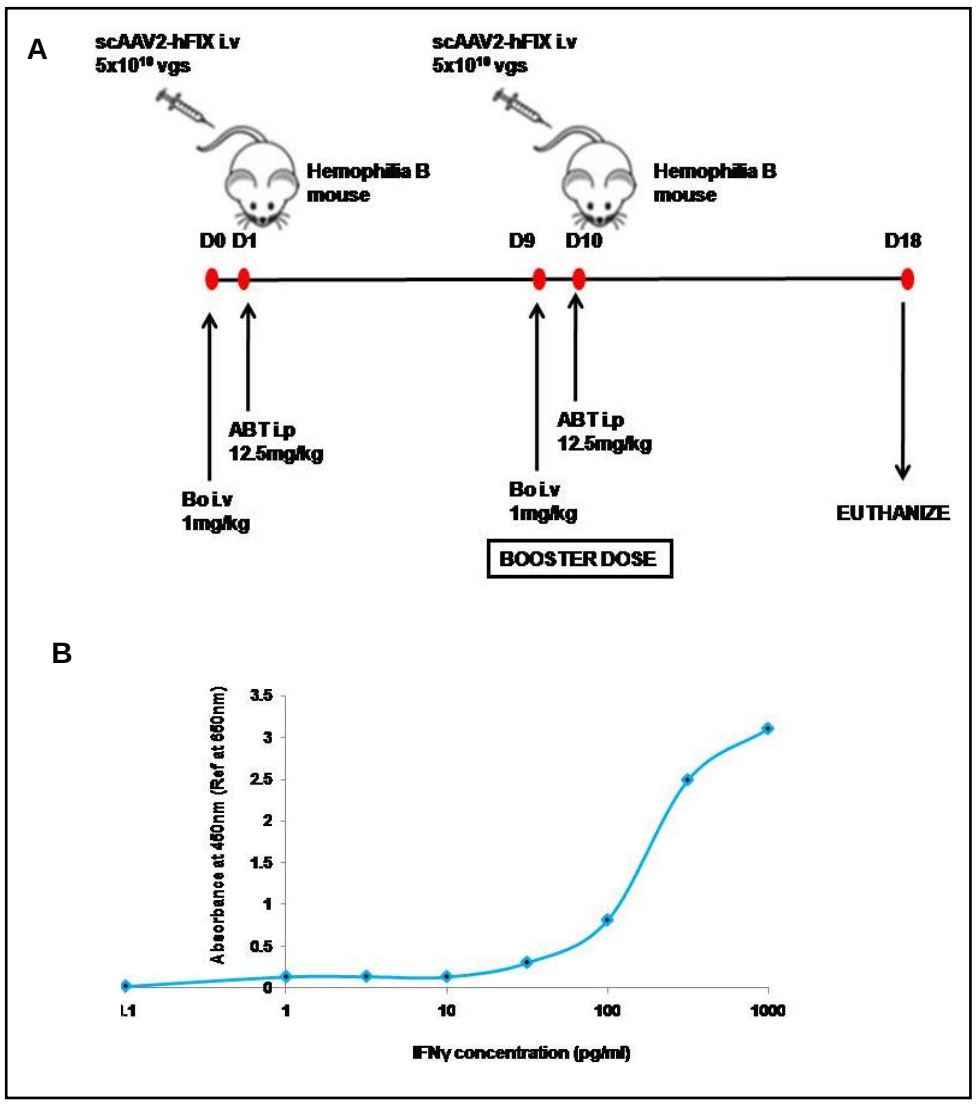

Figure 39: ***Schema of the hemophilia B mice study and ELISA based IFNγ standard curve.*** *(A) Schema of the experiment to validate the effect of synergistic inhibition of PARP-1 and NF- κB on in vivo transduction and adaptive immune response against AAV2-hFIX vectors in hemophilia B mice.(B) The sigmoidal standard curve generated by diluting 1µg/ ml of recombinant mouse IFNγ to get concentrations ranging from 1-1000pg/ml, using the Graph PAD Prism 6 software. Graph showing the IFNγ concentrations (pg/ml) in X axis and mean absorbance at 450nm with reference at 650nm*

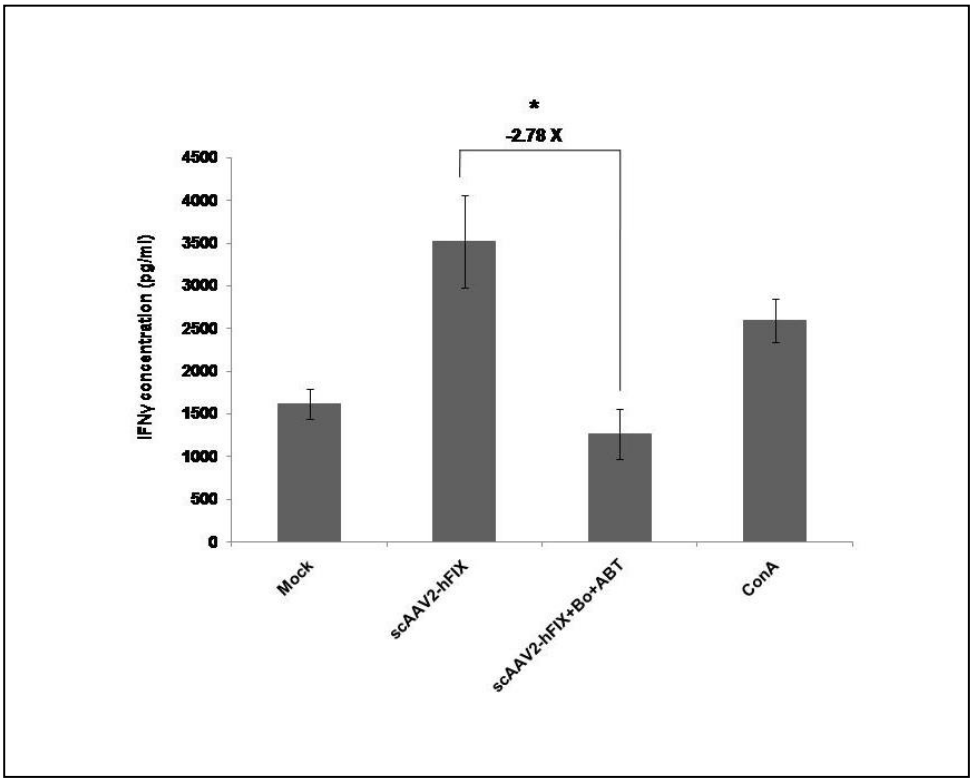

Figure 40: ***Synergistic inhibition of PARP1 and NF-κB attenuates the AAV2-hFIX vector induced cytotoxic T cell response in hemophilia B mice.*** *Splenocytes isolated from different groups of mice were seeded in a 96 well plate in appropriate media conditions. After about 30 hours of incubation, the cell culture supernatant was collected and ELISA was done to measure the IFNγ cytokine secretion from activated T cells. Concentration of IFNγ in the samples was determined by extrapolating the absorbance values from the standard curve using the GraphPAD Prism 6 software. Mean±SEM; *p<0.05.*

4.5.2 Synergistic inhibition of PARP-1 and NF- κB modestly enhances the AAV2-mediated FIX gene expression in hemophilia B mice model

To ascertain that combined inhibition of PARP-1 and NF- κB pathway does not affect the vector driven transgene expression, FIX mRNA levels in the liver tissue of hemophilia B mice were measured. Schema of the experiment was as described in figure 39A. It was observed that the FIX gene levels were modestly enhanced (1.59-fold) in the hepatocytes of AAV2 vector injected mice, treated with bortezomib and ABT-888 in comparison to the untreated group (Figure 41). Unlike the data obtained with normal C57BL/6 mice wherein the AAV2 vector driven EGFP transgene levels did not change upon PARP-1/NF- κB combined inhibition (figure 34), in hemophilia B mice it was instrumental in marginally elevating the vector based FIX levels as well as downplaying the immune response. This disparity on the effect of AAV2- mediated transgene expression could probably be attributed to the difference in the transgene (*EGFP Vs FIX*).

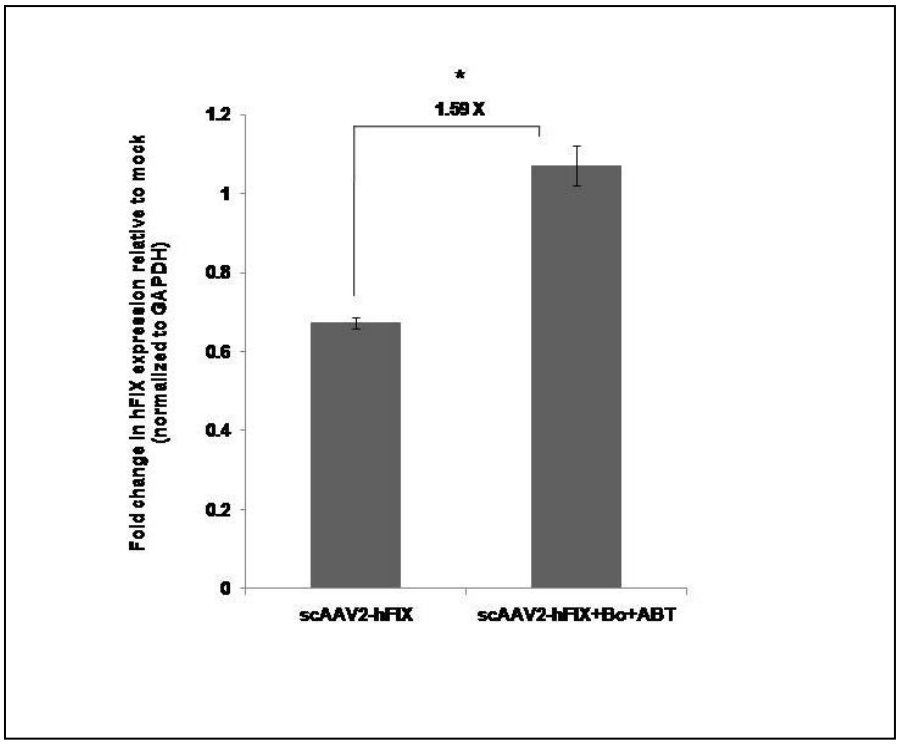

Figure 41: ***Synergistic inhibition of PARP-1 and NF- κB modestly enhances the AAV2 based FIX expression in hemophilia B mice model.*** *Analysis of human FIX transcript levels by real-time quantitative PCR. Hepatic RNA isolated from animals injected with scAAV2-hFIX vectors with/ without treatment with Bortezomib and ABT-888, were analyzed for hFIX expression and the data normalized to the GAPDH reference gene. The fold change in hFIX expression relative to the mock group is shown. Mean ± SEM; *p<0.05.*

5. DISCUSSION

AAV has now established itself as a safe and effective vector for gene therapy. Alipogene tiparvovec (Trade name: Glybera) is the first AAV (serotype 1) based gene therapy product which recently received approval for clinical use, in the treatment of lipoprotein lipase deficiency by European commission (Gaudet et al., 2012). The success in clinical trials using AAV for some of the other diseases was weighed down because of the immune challenge encountered in the patients, which adversely impacted the clinical outcome. Multiple lines of evidence suggest a direct correlation between the vector dosage and the immune response, as in most studies the patients within the high vector dose cohort developed immune-related complications. Maximum efficacy of AAV gene transfer has to be thus achieved, preferably by maintaining the dosage of vector particles within theimmune-tolerance limit of the body (Mingozzi & High, 2013).

To attain this goal, two approaches can be envisaged. First would be to employ ways to augment the transduction efficiency of AAV vectors. Vectors modified by introducing specific tyrosine to phenylalanine mutations on the viral capsid have shown to exhibit superior transduction (Zhong et al., 2008). Such mutant vectors may be delivered at comparatively lower doses without compromising the expression level of therapeutic transgene. Secondly, alleviation of the immune response against AAV vectors will be needed to realize the full potential of gene therapy. A better understanding of the mediators and signal transduction pathways associated with immune response is imperative to evading the immune clearance of AAV vectors during gene therapy (Hareendran et al., 2013).

5.1 Role of NF-κB in AAV gene therapy

Most viruses are known to activate NF-κBusing a variety of stimuli which act through distinct signal transduction pathways. However the outcome of the activation of this transcription factor could either benefit the host in case of eliciting an anti-viral response or in some other cases the pathogen wherein the virus exploits this pathway to bring about its replication and survival(Santoro et al., 2003). Viruses such as HIV-1, HTLV-1, hepatitis B and C viruses and HSV hijack the NF-κB pathway to facilitate their productive infection, or manipulate the host cell survival and proliferation while some other viruses like vaccinia virus and cowpox inhibit NF-κB activation to escape the immune response(Bowie et al., 2000, Hiscott et al., 2001, Oie & Pickup, 2001). HSV-1 is shown to constitutively activate NF-κB pathway inducing the expression of several pro-inflammatory cytokines and chemokines such as IL-1β, IL-6, IL-8, MIP-1α, MCP-1, RANTES and TNF-α, resulting in viral pathogenesis. Nonetheless HSV infection can also trigger production of type I and II interferon and NOS, which arbitrate the host anti-viral response(Mogensen & Paludan, 2001, Boivin et al., 2002).

Activation of NF-κB pathway has been previously described in relation to AAV infection (Jayandharan et al., 2011). Liver targeted delivery of AAV showed the sequential activation of canonical NF-κB pathways by 2 hours and alternative NF-κB pathway by 9 hours in hepatocytes. The transient inflammatory cytokine response and anti- AAV antibody production mediated by NF-κB up-regulation was effectively blocked with Bay 11, a pharmacological NF-κB inhibitor, distinctly highlighting the role of NF-κB in modulating immune response to AAV.

With this background knowledge, in the present study three commercially available NF-κB inhibitors were screened for their ability to modulate the levels of various inflammatory and cytokine molecules, kinases, receptors/ ligands and other factors associated with NF-κB pathway *in vitro* after infecting with AAV2 vector (Figure 19). Moreover, it was found that inhibition of NF-κB pathway with these compounds does not affect the AAV2 mediated transgene expression in HeLa cells when infected at a higher MOI of 10,000 (Figure 18). The *in vitro*AAV2 transduction has been shown to be abrogated on Bay11 treatment of cells at a low vector doses while the long term transgene expression in murine liver remained unaltered (Jayandharan et al., 2011). Unless the transgene expression is retained, the targeting of NF-κB pathway will not be a beneficial approach, even if it modulates pro-inflammatory response. The current study shows that delivering these vectors at relatively high doses into cell lines can circumvent the inhibitory impact of Bay11 on AAV2 transduction while effectively attenuating expression of pro-inflammatory genes. NF-κB pathway is the central regulator of cytokine and inflammatory responses, hence it was important to verify its role in the context of immune response to AAV vectors.

5.2 Role of PARP-1 in AAV gene transfer: implication on transgene expression and immune response

The inhibitory activity of DNA repair proteins on the process of AAV integration is well documented. DNA-dependent PK, a DNA repair enzyme was reported to inhibit AAV integration both in an*in vitro* cell-free integration system as well as in murine liver (Song et al., 2004). Persistence of AAV vector genomes was considerably higher when AAV2 was injected into the portal vein of severe

combined immune-deficient mice (DNA-PKc$^{-/-}$) mice compared to that of normal C57BL/6 (DNA-PKc$^{+/+}$) mice, indicating that absence of DNA-PK facilitates better integration of AAV genome. It is further interesting to note that cellular DNA-damage-response proteins such as MRE11-RAD50-NBS1 (MRN complex) restrict vector transduction by negatively regulating the processing of AAV genomes. AAV DNA accumulates within the nucleus in discrete foci which are in close proximity to the proteins of the MRN complex (Cervelli et al., 2008). Romanova *et al* have shown that PARP-1 directly interacts with AAV Rep and that depletion of PARP-1 using small hairpin RNA enhances integration of the AAV genome in HeLa cells (Romanova et al., 2011). However, the role of PARP-1 in regulating AAV transduction and the immune response against these vectors has not been elucidated.

Towards this, experiments were designed to elucidate the effect of PARP-1 inhibition on the AAV-mediated gene expression. The inhibition of PARP-1 by RNAi enhanced the transgene expression from ssAAV vectors (Figure 20). These vectors also exhibited enhanced gene transfer efficacy when targeted to murine liver in the presence of a pharmacological inhibitor of PARP-1, PJ34. The increase in liver directed transgene expression was more predominant with ssAAV8 vectors (~3.4-fold) than ssAAV2 vectors (~2-fold) upon PARP-1 ablation (Figure 21A, B, D). On the other hand, only modest improvement was noted in self-complementary AAV2 transduction when PARP-1 was inhibited (Figure 21A, C). This might be probably due to the fact that scAAV are considerably more immunogenic than ssAAV2 vectors (Martino et al., 2011b, Wu et al., 2012, Balakrishnan et al., 2013). Histological analysis of liver sections was also done to confirm that administration of PJ34 did not cause any hepato -toxicity to mice (Figure 23). From this data, it could be deduced that PARP-1 inhibition can augment the transduction potential of AAV

vectors. This augurs well for delivering genes such as coagulation factor VIII in ssAAV8, which are too large to be encapsidated by scAAV genomes.

PARP-1 is associated with various acute and chronic inflammatory conditions. It is known to be a co-activator of NF-κB transcription factor, a central player in the development of inflammatory and immune responses (Hassa et al., 2003). Several reports suggest that inflammation could be controlled when PARP-1 activity is blocked, probably because it is known to induce the activation of transcription factors like NF-κB, AP-1 or HIF-1 (Roebuck et al., 1995, Oliver et al., 1999, Martinez-Romero et al., 2008). PARP-1 inhibition has also been shown to be therapeutic in inflammatory animal models such as chronic colitis, hemorrhagic shock, cerebral ischemia, autoimmune nephritis and LPS induced septic shock (Cohen, 2002, Roesner et al., 2006, Jog et al., 2009). T cell activation requires transcriptional regulation by PARP-1 which also modulates the Th1/Th2 balance (Oumouna et al., 2006, Saenz et al., 2008) and regulates NFAT (Olabisi et al., 2008).

So next it was evaluated if inhibition of PARP-1 might be effective in regulating host immune response against scAAV2 vectors. Indeed, it was found that PARP-1 blockade results in marked attenuation of the expression of various NF-κB responsive pro-inflammatory factors (Figure 22). A direct impact on NF-κB pathway was evident by suppression of the RelA, a key molecule in canonical pathway. Most of the Toll- like receptor (TLR) proteins was also down-regulated by PARP-1 inhibition. PJ-34, the PARP-1 inhibitor significantly down-regulated TLRs, including TLR9 which has been shown to be a major endosomal sensing molecule of scAAV genomes during hepatic gene transfer (Martino et al., 2011b). Briefly the role of PARP-1 in AAV-mediated gene transfer was demonstrated for the first time, in this study, with reference to transduction and the vector induced inflammatory response.

5.3 Modification of specific serine/ threonine residues on viral capsid improves the transduction efficiency of AAV2 vectors

AAV2 is the prototype AAV vector largely tested in gene therapy applications as it is best characterized in terms of vector biology, transduction profile and toxicology in pre-clinical and clinical studies (Kotterman & Schaffer, 2014). On the other hand, the alternate serotypes of AAV (AAV1- AAV10) are being explored for different diseases owing to their unique features such as tissue tropism, level of transgene expression and seroprevalence in humans (Asokan et al., 2012). Recent data from AAV gene therapy trial for hemophilia B strongly advocate the potential of AAV8 as a promising vector (Nathwani et al., 2014). In comparison to AAV2, serotype 8 vector is known to exhibit 10-50 fold higher transduction in animal models and importantly, has a seroprevalence of ~30% vs ~70% for AAV2 in humans (Gao et al., 2002, Calcedo et al., 2009). However dose-dependent immune responses occurred even in the case of AAV8- hemophilia B trial, wherein patients falling under the high dose group showed elevation in serum levels of ALT and AST transaminases, indicating destruction of transduced hepatocytes (Nathwani et al., 2011). The optimal use of AAV as a tool for gene transfer is contingent upon a thorough understanding of fundamental steps in virus–host cell interactions, and as previously noted, the viral intra-cellular trafficking is an important rate-limiting step that directly influences the efficiency of transgene expression (Sanlioglu et al., 2001).

The concept of mutagenesis of AAV capsid sequence has been previously employed to generate novel AAV vectors either by targeted evolution or by targeted design. Directed evolution of AAV vectors to generate chimeric AAV with enhanced gene transfer to the airway epithelia, CNS tissue or retina has been reported.

Similarly rationally designed AAV strains with robust gene transfer abilities into the muscle such as AAV2.5, which has been tested in Phase I trial for DMD (Bowles et al., 2012) or AAVrh32.22 variant with enhanced immunogenic profileto act as vaccine candidates (Lin et al., 2009) are also available. When AAV traverses through the cytoplasm, it is likely to interact with various molecules and processes within the cell. The protein capsid of AAV is known to get phosphorylated by cellular tyrosine kinases and modification of these kinase targets, tyrosines (Y) to phenylalanine (F) has been shown to substantially improve gene expression by up to several folds in a variety of tissues such as the liver, retina, and musculo-skeletal target (Zhong et al., 2008, Petrs-Silva et al., 2009, Petrs-Silva et al., 2011). It is believed that phosphorylation of viral capsid might signal the ubiquitination and subsequent proteasome degradation of vector particles. As this defeats the overall purpose of gene therapy, efforts to prevent the destruction of vector particles within the cell is essential to enable high transgene expression. It was noted that the transduction efficiency of the tyrosine mutant vectors varies according to the target cell type. For example, the AAV2 Y730F mutant shows enhanced gene transfer into hepatocytes but when directed to stem cells or the retina, it is not very efficacious (Kauss et al., 2010, Ryals et al., 2011).

Besides tyrosine amino acids, modifying other kinase targets such as S/T residues on AAV capsid could be an alternate strategy to improve vector efficacy. It is important to consider that capsid phosphorylation also serves as a trigger for uncoating and release of viral genome inside the host cell. Therefore, phosphorylation sites have to be mutated logically. It has been recently demonstrated that the AAV2 capsid mutants generated with different amino acid substitutions can have varied transduction efficiencies (Aslanidi et al., 2012). Amino acid chosen for mutagenesis can thus impact AAV2 vector packaging and transduction efficiency. In

this study, S/T residues on AAV2 capsid surface were modified mostly based on their evolutionary conservation across the serotypes (Figure 26) (Gabriel et al., 2013).

Consistent with the hypothesis of the study, it was observed that specific inhibition of CKII serine/ threonine kinase increased the AAV2-WT mediated transgene expression *in vitro* (Figure 24). Subsequently, 15 single S/T residues on the capsid were modified by site directed mutagenesis and mutant vectors were generated (Figure 25). Transduction studies with these mutant vectors showed that selective targeting of S/T kinase phophorylation sites on AAV2 capsid substantially improves the gene expression from AAV2 vectors both *in vitro* (up to 97 %) (Figure 26), and *in vivo* during hepatic gene transfer into mice (up to 14-fold), as shown in figure 28.A similar study had shown that a differentthreonine capsid mutation (T→V) when combined with tyrosine mutations (Y→F) resulted in a AAV2 quadruple mutant vector which exhibited enhanced transduction in H2.35 hepatocyte cell line and murine liver (Aslanidi et al., 2013).These novel AAV2 vectors with superior transduction have immense potential considering the current scenario in gene therapy, as it may be possible to deliver them at lower doses to attain therapeutic index without eliciting dose-dependent immune responses. Introducing a specific serine to valine mutation (S662V) on the capsid has been reportedto considerably improvethe AAV2 transduction of DCs. The serine mutant vector was then used to modify DCs *ex vivo* by delivering *hTERT* gene and further shown to causetargeted lysis of K562 cells by stimulating cytotoxic T cells. This underscores the potential application of such capsid modified AAV vectors in tumor immunotherapy as well (Aslanidi et al., 2012).

5.4 Combined inhibition of PARP-1 and NF-κB signaling effectively modulates the host immune response against AAV vectors

In the recent clinical trial for hemophilia B using scAAV8 vectors, two patients were given a short course of glucocorticoid therapy to suppress the immune response causing inflammation in liver, as evidenced by the elevated levels of serum amino transferaseThis rescued the hepatocytes from being destroyed by the cytotoxic T cells and allowed persistent expression of the transgene (Nathwani et al., 2014).Combination of a non-depleting CD4 antibody and cyclosporine was shown to abrogate humoral responses to the AAV8 capsid and the transgeneprotein in mice (McIntosh JH et al., 2012). However, transient and intensive immunosuppression aimed at blocking the B cell and T cell adaptive responses failed to improve AAV5-based liver gene transfer in non-human primates (Unzu et al., 2012).An alternate approach would be to specifically target molecules or pathways that trigger immune activation as opposed to general immunosuppression upon AAV delivery.

As demonstrated in this work, PARP-1 inhibition suppresses the immune response against AAV2 vectors, by way of repressing the vector induced expression of various inflammatory cytokine and other genes related to NF-κB signaling in murine liver. This implies that PARP-1 interacts with NF-κB pathway, supporting the fact that it is a co-activator of this transcription factor (Hassa et al., 2003). However, it is known to modulate the activation of other transcription factors such as AP-1 and HIF-1 as well (Oliver et al., 1999, Martinez-Romero et al., 2008). The phenotype of PARP knockout mice is different from that of mice lacking NF-κB subunit ($p65^{-/-}$ mice), which is embryonically lethal (Beg et al., 1995). Thus it can be inferred that though PARP-1 and NF-κB interact, in the context of immune response they can still have mutually exclusive effects. Moreover, NF-κB is a widely

expressed inducible transcription factor and the activation of its downstream target genes requires multiple co-activators and co-factors (Sheppard et al., 1999). In addition other transcription factors such as AP1, ETS, C/EBP, STAT-1 and p53 might also influence the expression of NF-κB dependent genes (Hassa & Hottiger, 2002), suggesting that only a subset of NF-κB target genes would be affected by PARP-1. Along these lines, it would be reasonable to investigate the effect of a combined inhibition of PARP-1 and NF-κB signaling on the host immune response against AAV.

As hypothesized, the data showed that several pro-inflammatory and cytokine genes induced by AAV infection were significantly down-regulated in mice subjected to synergistic inhibition of PARP-1 and NF-κB (Figure 30). Relative expressions of pro-inflammatory markers belonging to Toll- like receptor family, Tumor necrosis factor receptors, NF-κB subunits and other mediators of inflammation were particularly suppressed upon the combined inhibition, in comparison to inhibition of either NF-κB pathway or PARP-1 alone. The suppressive effect on inflammatory response was more profound when combination of clinically tested drugs, Bortezomib and ABT-888 was used as shown in figure 30. Bortezomib (PS-314) is an FDA approved drug for clinical use in the treatment of Multiple myeloma (Richardson et al., 2003). It is a proteasome inhibitor which targets the catalytic 20S core of proteasome and induces apoptosis in cancer cells (Shah & Orlowski, 2009). The anti-tumor activity of bortezomib is attributed to its inhibitory effect on NF-κB, which has been implicated in pathogenesis of cancers, by regulating genes involved in cancer cell proliferation, survival, and drug resistance (Hideshima et al., 2002). Previous studies have demonstrated that Bortezomib improves the transduction AAV vectors encoding large factor VIII transgene,

resulting in long term phenotypic correction of hemophilia A canine model(Monahan et al., 2010). Bortezomib is shown to be partially effective in abrogating the pre-existing immunity to AAV in mice (Karman et al., 2012). ABT-888 (Veliparib), a PARP-1 inhibitor has been successfully tested in numerous Phase II/III clinical trials for the treatment of different cancers such as ovarian cancer, Breast cancer, solid tumors, lung cancer, pancreatic cancer, lymphoma and so on either as a monotherapy or in conjugation with other chemotherapeutic drugs (Lupo & Trusolino, 2014). Nevertheless, in the context of AAV gene therapy, it was tested for the first time in this study.

Further it was evaluated if the combination of Bortezomib and ABT-888 would be effective in moderating the cytotoxic T cell response against AAV vectors. Interestingly, PARP-1/NF-κB combined inhibition significantly attenuated the AAV capsid driven IFNγ response in mice, as determined by ELISPOT assay. The alleviation of cytotoxic response on treatment with combination of the inhibitors was more prominent using AAV2 than AAV8 during gene delivery into normal C57BL/6 mice (Figure 35*Vs* figure 36) whereas the transgene expression was not altered using both vectors (Figures 34 and 37). In contrast, the *in vitro* AAV2 tranduction in HeLa cells was enhanced upon treatment with these drugs (Figure 31), thus highlighting the discrepancy noted in the *in vitro* testing systems.

Finally, this immune suppression strategy was validated in a hemophilia B murine model. Consistent to the results observed in C57BL6 mice, it was observed that the IFNγ secretion from activated T cells was significantly decreased in AAV2 vector injected hemophilia B mice, upon treatment with inhibitors targeting PARP-1 and NF-κB (Figure 40). In these mice, a modest increase in FIX transgene expression was also found in the drug treated group, which indicates that the

transgene might influence the AAV-mediated expression (Figure 41). Taken together, these results strongly suggest that the immune suppression model of synergistic inhibition of NF-κB signaling and PARP-1 in AAV gene delivery, put forth in this doctoral study might have clinical relevance.However, its efficacy needs to be assessed in comparison to other approaches such as steroid therapy which have demonstrated effective attenuation of immune responses in AAV clinical trials (Nathwani et al., 2011).

5.5 Limitations of the study

The goal of this study was to define strategies to overcome the immune barrier in AAV gene therapy by focussing primarily on enhancing the transduction profile of AAV vectors and transiently suppressing the immune response against them. With respect to immune response, the effect of specific drug combinations that target cellular barriers to AAV transduction was analysed. However, it is also important to consider the effect of the pre-existing immunity to AAV, which is yet to be surmounted. While it was found that effective inhibition of immune responses to AAV vector could be achieved by blocking NF-κB/ PARP-1 pathway using Bo and ABT-888 respectively, we willneed to find other suitable drugs also, with more acceptable toxicity profiles for use in this clinical setting. It will also be important to compare and assess the performance of this drug combination with steroids alone to determine its clinical utility. As reported earlier, the data from small animal models like mice do not fully recapitulate the immunological outcome in humans (Somanathan et al., 2010). Hence it would be ideal to study the immune effect in humanized mice (Li et al., 2009), which might more closely mimic the immune response seen in humans.

5.6 Future directions

The promising data obtained with novel AAV2 S/T mutant vectors in this study offers several possibilities. Multiple combinations of these AAV S/T mutations could be designed on the capsid to have incremental effects on the vector based transgene expression. Similar modifications could also be introduced in other AAV serotypes, with the aim of improving transduction and tissue tropism. It is interesting to note that AAV3, which is known to poorly transduce mouse liver,has been recently reported to exhibit selective tropism and efficienttransduction of human liver tumors in a mouse xenograft model (Ling et al., 2014). Tyrosine mutants of AAV3 were shown to further improve the transduction of human liver cancer cells *in vitro* and xenograft liver tumor cells in mice(Cheng et al., 2012). Besides altering the capsid residues, the manipulation of the viral genome has now emerged as an attractive approach to generate superior AAV-based vectors. Bio-engineering of ssAAV genome by replacing the NRF binding site on one of the ITRs with glucocorticoid receptor binding element (GRE) significantly augmented the transduction efficiency of these vectors (Ling et al., 2015).

Regulatory T cells (Tregs) are known to play an important role in induction of tolerance to immune responses (Hoffman et al., 2011). It would be interesting to examine if the synergistic inhibition of PARP-1 and NF-κB signaling affects the Treg population, to bring about immunomodulation during gene transfer with AAV vectors. In a broader perspective, Bortezomib plus ABT-888, each independently known for its antitumor activity, if concomitantly assessed with AAV-mediated delivery of cytotoxic genes such as thymidine kinase and cytosine deaminase could unlock avenues of research in cancer gene therapy.

6. SUMMARY AND CONCLUSIONS

1. AAV has emerged as a promising gene therapy vector owing to its properties includingnon-pathogenicity, broad tissue tropism, generally low immunogenicity, stable and long-term transgene expression in target cells (Mingozzi & High, 2011).

2. However one of the major obstacles in employing AAV vectors for the treatment of diseases is the pre-existing immunity to AAV seen in humans with a sero-prevalence of nearly 70% for AAV2 while 30% for AAV8, and rangingbetween 40% to 67% for other AAV serotypes (Calcedo et al., 2009).

3. Due to the relatively low efficiency of transduction in certain tissues with specific serotypes, AAV vectors often need to be delivered at high doses to attain the therapeutic index of transgene expression. Thishas subsequently shown to cause dose-dependent cytotoxic T cell responses, as evidenced from clinical trials (Manno et al., 2006, Mingozzi et al., 2009). Immune response is thus currently the prominent factor impeding the gene therapy application of AAV vectors.

4. In this study, two approaches were designed and tested to circumvent the immune barrier, particularly the cellular responsesseen in AAV gene therapy:

a) First of the two strategies was to test if the transduction potential of AAV vectors could be augmented by altering specific serine/ threonine residues on AAV2 capsid by site directed mutagenesis. Vectors with superior transduction make it possible to attain therapeutic index at relatively lower doses, without causing immune activation.

b) Secondly, target the signaling pathways and molecules which are involved in evoking the immune response to AAV vectors. Combined targeting of PARP-1 protein and NF-κB pathway was tested as a strategy to suppress the vector induced pro-inflammatory and cytotoxic responses.

5. Targeted modification of serine/ threonine residues [S/T→A] on AAV2 capsid resulted in the generation of mutant AAV vectors which demonstrated enhanced transduction efficiency, both *in vitro* (in HeLa cells) and *in vivo* during gene delivery to murine liver. During liver targeted gene transfer into mice, selective AAV2 S/T mutant vectors exhibited 6 to 14-fold increase in transgene expression compared to the wildtype vector, with the maximal transduction obtained with scAAV2 S489A vector. These specific mutant vectors thus offer the possibility of achieving therapeutic levels of transgene encoded protein at much lower vector doses, which might inturn avert dose-dependent immune responses.

6. In the other part of the study, it was observed that pharmacological inhibition of NF-κB pathway does not alter the AAV2-mediated transgene expression in HeLa cells, infected at high MOI.Further the comparative analysis of the

down-regulation of the various NF-κB responsive genes in AAV2 transduced cells,pretreated with compounds targeting NF-κB pathway lead to the identification of a more potent NF-κB inhibitor.

7. Repression of PARP-1 was demonstrated to considerably improve the transduction efficiency of single-stranded AAV vectors both *in vitro* and *in vivo*, during liver targeted gene transfer.

8. The inhibition of PARP-1 significantly down-regulated the expression of several cytokine and other pro-inflammatory marker genes induced upon AAV2 vector infection. This study thus describes for the first time the role of PARP-1 in AAV-mediated transgene expression and modulation of pro-inflammatorycytokine response against the vector.

9. Suppression of the pro-inflammatory and T cell response against AAV2 vector was more effective upon combined inhibition of PARP-1 and NF-κB signaling using clinically tested drugs, ABT-888 and Bortezomib respectively.

10. The immune-suppression achieved by simultaneously targeting PARP-1 and NF-κB was further validated in a therapeutic mice model of hemophilia B. Corroborating the data in normal mice, it was observed that the IFNγ response of AAV2 capsid peptide stimulated T cells was substantially reduced when the hemophilia B mice were treated with combination of ABT-888 plus Bortezomib.

11. The synergistic inhibition of PARP-1 and NF-κB signaling pathway is a novel strategy that is proposed in this study for evading the immune challenges to AAV vectors. This opens up new possibilities for immunomodulation after gene transfer using AAV vectors.

12. Further, based on the two major deductions from this doctoral study, it would be interesting to employ the specific AAV2 S/T capsid mutants, which exhibited about two-fold increase in vector transduction *in vitro*along with ABT-888 and Bortezomib in combination, to achieve a cumulative five-fold increase in transduction of human cells. In addition, the significantly enhancedliver transduction documented in mice with these capsid mutant vectors could enable therapeutic transgene levels to be attained at much lower vector doses in comparison to the wild-type AAV2 vector.

7. BIBLIOGRAPHY

Abdelkarim GE, Gertz K, Harms C, Katchanov J, Dirnagl U, Szabo C Endres M (2001) Protective effects of PJ34, a novel, potent inhibitor of poly(ADP-ribose) polymerase (PARP) in vitro and in vivo models of stroke. *Int J Mol Med* 7: 255-260.

Adriouch S, Franck E, Drouot L, Bonneau C, Jolinon N, Salvetti A Boyer O (2011) Improved Immunological Tolerance Following Combination Therapy with CTLA-4/Ig and AAV-Mediated PD-L1/2 Muscle Gene Transfer. *Front Microbiol* 2: 199.

Ahmad SS, London FS Walsh PN (2003) The assembly of the factor X-activating complex on activated human platelets. *J Thromb Haemost* 1: 48-59.

Aslanidi GV, Rivers AE, Ortiz L, Govindasamy L, Ling C, Jayandharan GR, Zolotukhin S, Agbandje-McKenna M Srivastava A (2012) High-efficiency transduction of human monocyte-derived dendritic cells by capsid-modified recombinant AAV2 vectors. *Vaccine* 30: 3908-3917.

Aslanidi GV, Rivers AE, Ortiz L, Song L, Ling C, Govindasamy L, Van Vliet K, Tan M, Agbandje-McKenna M Srivastava A (2013) Optimization of the capsid of recombinant adeno-associated virus 2 (AAV2) vectors: the final threshold? *PLoS One* 8: e59142.

Asokan A, Schaffer DV Samulski RJ (2012) The AAV vector toolkit: poised at the clinical crossroads. *Mol Ther* 20: 699-708.

Atchison RW, Casto BC Hammon WM (1965) Adenovirus-Associated Defective Virus Particles. *Science* 149: 754-756.

Aurnhammer C, Haase M, Muether N, Hausl M, Rauschhuber C, Huber I, Nitschko H, Busch U, Sing A, Ehrhardt A Baiker A (2011) Universal Real-Time PCR for the Detection and Quantification of Adeno-Associated Virus Serotype 2-Derived Inverted Terminal Repeat Sequences. *Hum Gene Ther*.

Balague C, Kalla M Zhang WW (1997) Adeno-associated virus Rep78 protein and terminal repeats enhance integration of DNA sequences into the cellular genome. *J Virol* 71: 3299-3306.

Balakrishnan B Jayandharan GR (2014) Basic biology of adeno-associated virus (AAV) vectors used in gene therapy. *Curr Gene Ther* 14: 86-100.

Balakrishnan B, Sen D, Hareendran S, Roshini V, David S, Srivastava A Jayandharan GR (2013) Activation of the cellular unfolded protein response by recombinant adeno-associated virus vectors. *PLoS One* 8: e53845.

Bartel M, Schaffer D Buning H (2011) Enhancing the Clinical Potential of AAV Vectors by Capsid Engineering to Evade Pre-Existing Immunity. *Front Microbiol* 2: 204.

Bartlett JS, Wilcher R Samulski RJ (2000) Infectious entry pathway of adeno-associated virus and adeno-associated virus vectors. *J Virol* 74: 2777-2785.

Basner-Tschakarjan E Mingozzi F (2014) Cell-Mediated Immunity to AAV Vectors, Evolving Concepts and Potential Solutions. *Front Immunol* 5: 350.

Beg AA, Sha WC, Bronson RT, Ghosh S Baltimore D (1995) Embryonic lethality and liver degeneration in mice lacking the RelA component of NF-kappa B. *Nature* 376: 167-170.

Berenson JR, Yang HH, Sadler K, Jarutirasarn SG, Vescio RA, Mapes R, Purner M, Lee SP, Wilson J, Morrison B, Adams J, Schenkein D Swift R (2006) Phase I/II trial assessing bortezomib and melphalan combination therapy for the treatment of patients with relapsed or refractory multiple myeloma. *J Clin Oncol* 24: 937-944.

Berns KI (1990) Parvovirus replication. *Microbiol Rev* 54: 316-329.

Berns KI, Pinkerton TC, Thomas GF Hoggan MD (1975) Detection of adeno-associated virus (AAV)-specific nucleotide sequences in DNA isolated from latently infected Detroit 6 cells. *Virology* 68: 556-560.

Boivin G, Coulombe Z Rivest S (2002) Intranasal herpes simplex virus type 2 inoculation causes a profound thymidine kinase dependent cerebral inflammatory response in the mouse hindbrain. *Eur J Neurosci* 16: 29-43.

Bolton-Maggs PH Pasi KJ (2003) Haemophilias A and B. *Lancet* 361: 1801-1809.

Bowie A, Kiss-Toth E, Symons JA, Smith GL, Dower SK O'Neill LA (2000) A46R and A52R from vaccinia virus are antagonists of host IL-1 and toll-like receptor signaling. *Proc Natl Acad Sci U S A* 97: 10162-10167.

Bowles DE, McPhee SW, Li C, Gray SJ, Samulski JJ, Camp AS, Li J, Wang B, Monahan PE, Rabinowitz JE, Grieger JC, Govindasamy L, Agbandje-McKenna M, Xiao X Samulski RJ (2012) Phase 1 gene therapy for Duchenne muscular dystrophy using a translational optimized AAV vector. *Mol Ther* 20: 443-455.

Brantly ML, Chulay JD, Wang L, Mueller C, Humphries M, Spencer LT, Rouhani F, Conlon TJ, Calcedo R, Betts MR, Spencer C, Byrne BJ, Wilson JM Flotte TR (2009) Sustained transgene expression despite T lymphocyte responses in a clinical trial of rAAV1-AAT gene therapy. *Proc Natl Acad Sci U S A* 106: 16363-16368.

Bryant HE, Schultz N, Thomas HD, Parker KM, Flower D, Lopez E, Kyle S, Meuth M, Curtin NJ Helleday T (2005) Specific killing of BRCA2-deficient tumours with inhibitors of poly(ADP-ribose) polymerase. *Nature* 434: 913-917.

Buchlis G, Podsakoff GM, Radu A, Hawk SM, Flake AW, Mingozzi F High KA (2012) Factor IX expression in skeletal muscle of a severe hemophilia B patient 10 years after AAV-mediated gene transfer. *Blood* 119: 3038-3041.

Buning H, Ried MU, Perabo L, Gerner FM, Huttner NA, Enssle J Hallek M (2003) Receptor targeting of adeno-associated virus vectors. *Gene Ther* 10: 1142-1151.

Calcedo R, Morizono H, Wang L, McCarter R, He J, Jones D, Batshaw ML Wilson JM (2011) Adeno-associated virus antibody profiles in newborns, children, and adolescents. *Clin Vaccine Immunol* 18: 1586-1588.

Calcedo R, Vandenberghe LH, Gao G, Lin J Wilson JM (2009) Worldwide epidemiology of neutralizing antibodies to adeno-associated viruses. *J Infect Dis* 199: 381-390.

Calcedo R Wilson JM (2013) Humoral Immune Response to AAV. *Front Immunol* 4: 341.

Cervelli T, Palacios JA, Zentilin L, Mano M, Schwartz RA, Weitzman MD Giacca M (2008) Processing of recombinant AAV genomes occurs in specific nuclear structures that overlap with foci of DNA-damage-response proteins. *J Cell Sci* 121: 349-357.

Chambon P, Weill JD Mandel P (1963) Nicotinamide mononucleotide activation of new DNA-dependent polyadenylic acid synthesizing nuclear enzyme. *Biochem Biophys Res Commun* 11: 39-43.

Chen J, Wu Q, Yang P, Hsu HC Mountz JD (2006) Determination of specific CD4 and CD8 T cell epitopes after AAV2- and AAV8-hF.IX gene therapy. *Mol Ther* 13: 260-269.

Chen L, Lu H, Wang J, Sarkar R, Yang X, Wang H, High KA Xiao W (2009) Enhanced factor VIII heavy chain for gene therapy of hemophilia A. *Mol Ther* 17: 417-424.

Cheng B, Ling C, Dai Y, Lu Y, Glushakova LG, Gee SW, McGoogan KE, Aslanidi GV, Park M, Stacpoole PW, Siemann D, Liu C Srivastava A (2012) Development of optimized AAV3 serotype vectors: mechanism of high-efficiency transduction of human liver cancer cells. *Gene Ther* 19: 375-384.

Cohen J (2002) The immunopathogenesis of sepsis. *Nature* 420: 885-891.

D'Amours D, Desnoyers S, D'Silva I Poirier GG (1999) Poly(ADP-ribosyl)ation reactions in the regulation of nuclear functions. *Biochem J* 342 (Pt 2): 249-268.

Daya S Berns KI (2008) Gene therapy using adeno-associated virus vectors. *Clin Microbiol Rev* 21: 583-593.

Daya S, Cortez N Berns KI (2009) Adeno-associated virus site-specific integration is mediated by proteins of the nonhomologous end-joining pathway. *J Virol* 83: 11655-11664.

De Groot AS, Moise L, McMurry JA, Wambre E, Van Overtvelt L, Moingeon P, Scott DW Martin W (2008) Activation of natural regulatory T cells by IgG Fc-derived peptide "Tregitopes". *Blood* 112: 3303-3311.

Dolcet X, Llobet D, Encinas M, Pallares J, Cabero A, Schoenenberger JA, Comella JX Matias-Guiu X (2006) Proteasome inhibitors induce death but activate NF-kappaB on endometrial carcinoma cell lines and primary culture explants. *J Biol Chem* 281: 22118-22130.

Dong W, Simeonova PP, Gallucci R, Matheson J, Fannin R, Montuschi P, Flood L Luster MI (1998) Cytokine expression in hepatocytes: role of oxidant stress. *J Interferon Cytokine Res* 18: 629-638.

Duan D, Li Q, Kao AW, Yue Y, Pessin JE Engelhardt JF (1999) Dynamin is required for recombinant adeno-associated virus type 2 infection. *J Virol* 73: 10371-10376.

Ferrari FK, Samulski T, Shenk T Samulski RJ (1996) Second-strand synthesis is a rate-limiting step for efficient transduction by recombinant adeno-associated virus vectors. *J Virol* 70: 3227-3234.

Finn JD, Hui D, Downey HD, Dunn D, Pien GC, Mingozzi F, Zhou S High KA (2010) Proteasome inhibitors decrease AAV2 capsid derived peptide epitope presentation on MHC class I following transduction. *Mol Ther* 18: 135-142.

Flotte T, Carter B, Conrad C, Guggino W, Reynolds T, Rosenstein B, Taylor G, Walden S Wetzel R (1996) A phase I study of an adeno-associated virus-CFTR gene vector in adult CF patients with mild lung disease. *Hum Gene Ther* 7: 1145-1159.

Force T Kolaja KL (2011) Cardiotoxicity of kinase inhibitors: the prediction and translation of preclinical models to clinical outcomes. *Nat Rev Drug Discov* 10: 111-126.

Friedmann T (1992) A brief history of gene therapy. *Nat Genet* 2: 93-98.

Friedmann T (1999) The Origins, Evolution, and Directions of Human Gene Therapy In: Friedmann T (ed) *The Development of Human Gene Therapy*, Cold Spring Harbor Laboratory Press, New York, pp. 1-20.

Gabriel N, Hareendran S, Sen D, Gadkari RA, Sudha G, Selot R, Hussain M, Dhaksnamoorthy R, Samuel R, Srinivasan N, Srivastava A Jayandharan GR (2013) Bioengineering of AAV2 Capsid at Specific Serine, Threonine, or Lysine Residues Improves Its Transduction Efficiency in Vitro and in Vivo. *Hum Gene Ther Methods*.

Gao GP, Alvira MR, Wang L, Calcedo R, Johnston J Wilson JM (2002) Novel adeno-associated viruses from rhesus monkeys as vectors for human gene therapy. *Proc Natl Acad Sci U S A* 99: 11854-11859.

Gaudet D, Methot J Kastelein J (2012) Gene therapy for lipoprotein lipase deficiency. *Curr Opin Lipidol* 23: 310-320.

Giansanti V, Dona F, Tillhon M Scovassi AI (2010) PARP inhibitors: new tools to protect from inflammation. *Biochem Pharmacol* 80: 1869-1877.

Ginn SL, Alexander IE, Edelstein ML, Abedi MR Wixon J (2013) Gene therapy clinical trials worldwide to 2012 - an update. *J Gene Med* 15: 65-77.

Giraud C, Winocour E Berns KI (1994) Site-specific integration by adeno-associated virus is directed by a cellular DNA sequence. *Proc Natl Acad Sci U S A* 91: 10039-10043.

Girod A, Wobus CE, Zadori Z, Ried M, Leike K, Tijssen P, Kleinschmidt JA Hallek M (2002) The VP1 capsid protein of adeno-associated virus type 2 is carrying a phospholipase A2 domain required for virus infectivity. *J Gen Virol* 83: 973-978.

Graham FL van der Eb AJ (1973) Transformation of rat cells by DNA of human adenovirus 5. *Virology* 54: 536-539.

Grimm D, Kern A, Rittner K Kleinschmidt JA (1998) Novel tools for production and purification of recombinant adenoassociated virus vectors. *Hum Gene Ther* 9: 2745-2760.

Gurda BL, DiMattia MA, Miller EB, Bennett A, McKenna R, Weichert WS, Nelson CD, Chen WJ, Muzyczka N, Olson NH, Sinkovits RS, Chiorini JA, Zolotutkhin S, Kozyreva OG, Samulski RJ, Baker TS, Parrish CR Agbandje-McKenna M (2013) Capsid antibodies to different adeno-associated virus serotypes bind common regions. *J Virol* 87: 9111-9124.

Haddad M, Rhinn H, Bloquel C, Coqueran B, Szabo C, Plotkine M, Scherman D Margaill I (2006) Anti-inflammatory effects of PJ34, a poly(ADP-ribose) polymerase inhibitor, in transient focal cerebral ischemia in mice. *Br J Pharmacol* 149: 23-30.

Halder S, Nam HJ, Govindasamy L, Vogel M, Dinsart C, Salome N, McKenna R Agbandje-McKenna M (2013) Structural characterization of H-1 parvovirus: comparison of infectious virions to empty capsids. *J Virol* 87: 5128-5140.

Harbison CE, Weichert WS, Gurda BL, Chiorini JA, Agbandje-McKenna M Parrish CR (2012) Examining the cross-reactivity and neutralization mechanisms of a panel of mAbs against adeno-associated virus serotypes 1 and 5. *J Gen Virol* 93: 347-355.

Hareendran S, Balakrishnan B, Sen D, Kumar S, Srivastava A Jayandharan GR (2013) Adeno-associated virus (AAV) vectors in gene therapy: immune challenges and strategies to circumvent them. *Rev Med Virol* 23: 399-413.

Hassa PO, Buerki C, Lombardi C, Imhof R Hottiger MO (2003) Transcriptional coactivation of nuclear factor-kappaB-dependent gene expression by p300 is regulated by poly(ADP)-ribose polymerase-1. *J Biol Chem* 278: 45145-45153.

Hassa PO, Covic M, Hasan S, Imhof R Hottiger MO (2001) The enzymatic and DNA binding activity of PARP-1 are not required for NF-kappa B coactivator function. *J Biol Chem* 276: 45588-45597.

Hassa PO, Haenni SS, Buerki C, Meier NI, Lane WS, Owen H, Gersbach M, Imhof R Hottiger MO (2005) Acetylation of poly(ADP-ribose) polymerase-1 by p300/CREB-binding protein regulates coactivation of NF-kappaB-dependent transcription. *J Biol Chem* 280: 40450-40464.

Hassa PO Hottiger MO (2002) The functional role of poly(ADP-ribose)polymerase 1 as novel coactivator of NF-kappaB in inflammatory disorders. *Cell Mol Life Sci* 59: 1534-1553.

Haurigot V, Mingozzi F, Buchlis G, Hui DJ, Chen Y, Basner-Tschakarjan E, Arruda VR, Radu A, Franck HG, Wright JF, Zhou S, Stedman HH, Bellinger DA, Nichols TC High KA (2010) Safety of AAV factor IX peripheral transvenular gene delivery to muscle in hemophilia B dogs. *Mol Ther* 18: 1318-1329.

Hayden MS Ghosh S (2004) Signaling to NF-kappaB. *Genes Dev* 18: 2195-2224.

Hayden MS Ghosh S (2012) NF-kappaB, the first quarter-century: remarkable progress and outstanding questions. *Genes Dev* 26: 203-234.

Hayden MS, West AP Ghosh S (2006) NF-kappaB and the immune response. *Oncogene* 25: 6758-6780.

Herzog RW, Yang EY, Couto LB, Hagstrom JN, Elwell D, Fields PA, Burton M, Bellinger DA, Read MS, Brinkhous KM, Podsakoff GM, Nichols TC, Kurtzman GJ High KA (1999) Long-term correction of canine hemophilia B by gene transfer of blood coagulation factor IX mediated by adeno-associated viral vector. *Nat Med* 5: 56-63.

Hideshima T, Chauhan D, Richardson P, Mitsiades C, Mitsiades N, Hayashi T, Munshi N, Dang L, Castro A, Palombella V, Adams J Anderson KC (2002) NF-kappa B as a therapeutic target in multiple myeloma. *J Biol Chem* 277: 16639-16647.

Hinz M, Stilmann M, Arslan SC, Khanna KK, Dittmar G Scheidereit C (2010) A cytoplasmic ATM-TRAF6-cIAP1 module links nuclear DNA damage signaling to ubiquitin-mediated NF-kappaB activation. *Mol Cell* 40: 63-74.

Hiscott J, Kwon H Genin P (2001) Hostile takeovers: viral appropriation of the NF-kappaB pathway. *J Clin Invest* 107: 143-151.

Hoffman BE, Martino AT, Sack BK, Cao O, Liao G, Terhorst C Herzog RW (2011) Nonredundant roles of IL-10 and TGF-beta in suppression of immune responses to hepatic AAV-factor IX gene transfer. *Mol Ther* 19: 1263-1272.

Hoffmann A Baltimore D (2006) Circuitry of nuclear factor kappaB signaling. *Immunol Rev* 210: 171-186.

Hoggan MD, Blacklow NR Rowe WP (1966) Studies of small DNA viruses found in various adenovirus preparations: physical, biological, and immunological characteristics. *Proc Natl Acad Sci U S A* 55: 1467-1474.

Hosel M, Broxtermann M, Janicki H, Esser K, Arzberger S, Hartmann P, Gillen S, Kleeff J, Stabenow D, Odenthal M, Knolle P, Hallek M, Protzer U Buning H (2012) Toll-like receptor 2-mediated innate immune response in human nonparenchymal liver cells toward adeno-associated viral vectors. *Hepatology* 55: 287-297.

Hu P, Han Z, Couvillon AD, Kaufman RJ Exton JH (2006) Autocrine tumor necrosis factor alpha links endoplasmic reticulum stress to the membrane death receptor pathway through IRE1alpha-mediated NF-kappaB activation and down-regulation of TRAF2 expression. *Mol Cell Biol* 26: 3071-3084.

Hui DJ, Basner-Tschakarjan E, Chen Y, Davidson RJ, Buchlis G, Yazicioglu M, Pien GC, Finn JD, Haurigot V, Tai A, Scott DW, Cousens LP, Zhou S, De Groot AS Mingozzi F (2013) Modulation of CD8+ T cell responses to AAV vectors with IgG-derived MHC class II epitopes. *Mol Ther* 21: 1727-1737.

Jagtap P, Szabo C (2005) Poly(ADP-ribose) polymerase and the therapeutic effects of its inhibitors. *Nat Rev Drug Discov* 4: 421-440.

Javle M Curtin NJ (2011) The role of PARP in DNA repair and its therapeutic exploitation. *Br J Cancer* 105: 1114-1122.

Jayandharan GR, Aslanidi G, Martino AT, Jahn SC, Perrin GQ, Herzog RW Srivastava A (2011) Activation of the NF-kappaB pathway by adeno-associated virus (AAV) vectors and its implications in immune response and gene therapy. *Proc Natl Acad Sci U S A* 108: 3743-3748.

Jayandharan GR Srivastava A (2012) Role of molecular genetics in hemophilia: from diagnosis to therapy. *Semin Thromb Hemost* 38: 64-78.

Jiang H, Couto LB, Patarroyo-White S, Liu T, Nagy D, Vargas JA, Zhou S, Scallan CD, Sommer J, Vijay S, Mingozzi F, High KA Pierce GF (2006) Effects of transient immunosuppression on adenoassociated, virus-mediated, liver-directed gene transfer in rhesus macaques and implications for human gene therapy. *Blood* 108: 3321-3328.

Jog NR, Dinnall JA, Gallucci S, Madaio MP Caricchio R (2009) Poly(ADP-ribose) polymerase-1 regulates the progression of autoimmune nephritis in males by inducing necrotic cell death and modulating inflammation. *J Immunol* 182: 7297-7306.

Juvekar A, Manna S, Ramaswami S, Chang TP, Vu HY, Ghosh CC, Celiker MY Vancurova I (2011) Bortezomib induces nuclear translocation of IkappaBalpha resulting in gene-specific suppression of NF-kappaB--dependent transcription and induction of apoptosis in CTCL. *Mol Cancer Res* 9: 183-194.

Karman J, Gumlaw NK, Zhang J, Jiang JL, Cheng SH Zhu Y (2012) Proteasome inhibition is partially effective in attenuating pre-existing immunity against recombinant adeno-associated viral vectors. *PLoS One* 7: e34684.

Kauss MA, Smith LJ, Zhong L, Srivastava A, Wong KK, Jr. Chatterjee S (2010) Enhanced long-term transduction and multilineage engraftment of human hematopoietic stem cells transduced with tyrosine-modified recombinant adeno-associated virus serotype 2. *Hum Gene Ther* 21: 1129-1136.

Kim MY, Zhang T Kraus WL (2005) Poly(ADP-ribosyl)ation by PARP-1: 'PAR-laying' NAD+ into a nuclear signal. *Genes Dev* 19: 1951-1967.

Kinders RJ, Hollingshead M, Khin S, Rubinstein L, Tomaszewski JE, Doroshow JH Parchment RE (2008) Preclinical modeling of a phase 0 clinical trial: qualification of a pharmacodynamic assay of poly (ADP-ribose) polymerase in tumor biopsies of mouse xenografts. *Clin Cancer Res* 14: 6877-6885.

Koczot FJ, Carter BJ, Garon CF Rose JA (1973) Self-complementarity of terminal sequences within plus or minus strands of adenovirus-associated virus DNA. *Proc Natl Acad Sci U S A* 70: 215-219.

Koerber JT, Klimczak R, Jang JH, Dalkara D, Flannery JG Schaffer DV (2009) Molecular evolution of adeno-associated virus for enhanced glial gene delivery. *Mol Ther* 17: 2088-2095.

Kotin RM (2011) Large-scale recombinant adeno-associated virus production. *Hum Mol Genet* 20: R2-6.

Kotterman MA Schaffer DV (2014) Engineering adeno-associated viruses for clinical gene therapy. *Nat Rev Genet* 15: 445-451.

Kube DM Srivastava A (1997) Quantitative DNA slot blot analysis: inhibition of DNA binding to membranes by magnesium ions. *Nucleic Acids Res* 25: 3375-3376.

Li C, Chen S, Yue P, Deng X, Lonial S, Khuri FR Sun SY (2010) Proteasome inhibitor PS-341 (bortezomib) induces calpain-dependent IkappaB(alpha) degradation. *J Biol Chem* 285: 16096-16104.

Li C, Goudy K, Hirsch M, Asokan A, Fan Y, Alexander J, Sun J, Monahan P, Seiber D, Sidney J, Sette A, Tisch R, Frelinger J Samulski RJ (2009) Cellular immune response to cryptic epitopes during therapeutic gene transfer. *Proc Natl Acad Sci U S A* 106: 10770-10774.

Li C, He Y, Nicolson S, Hirsch M, Weinberg MS, Zhang P, Kafri T Samulski RJ (2013) Adeno-associated virus capsid antigen presentation is dependent on endosomal escape. *J Clin Invest* 123: 1390-1401.

Li H, Lasaro MO, Jia B, Lin SW, Haut LH, High KA Ertl HC (2011) Capsid-specific T-cell responses to natural infections with adeno-associated viruses in humans differ from those of nonhuman primates. *Mol Ther* 19: 2021-2030.

Lin J, Calcedo R, Vandenberghe LH, Bell P, Somanathan S Wilson JM (2009) A new genetic vaccine platform based on an adeno-associated virus isolated from a rhesus macaque. *J Virol* 83: 12738-12750.

Ling C, Lu Y, Cheng B, McGoogan KE, Gee SW, Ma W, Li B, Aslanidi GV Srivastava A (2011) High-efficiency transduction of liver cancer cells by recombinant adeno-associated virus serotype 3 vectors. *J Vis Exp*.

Ling C, Wang Y, Lu Y, Wang L, Jayandharan GR, Aslanidi GV, Li B, Cheng B, Ma W, Lentz T, Xiao X, Samulski RJ, Muzyczka N Srivastava A (2015) Enhanced transgene expression from recombinant single-stranded D-sequence-substituted adeno-associated virus vectors in human cell lines in vitro and in murine hepatocytes in vivo. *J Virol* 89: 952-961.

Ling C, Wang Y, Zhang Y, Ejjigani A, Yin Z, Lu Y, Wang L, Wang M, Li J, Hu Z, Aslanidi GV, Zhong L, Gao G Srivastava A (2014) Selective in vivo targeting of human liver tumors by optimized AAV3 vectors in a murine xenograft model. *Hum Gene Ther* 25: 1023-1034.

Lisowski L, Dane AP, Chu K, Zhang Y, Cunningham SC, Wilson EM, Nygaard S, Grompe M, Alexander IE Kay MA (2013) Selection and evaluation of clinically relevant AAV variants in a xenograft liver model. *Nature* 506: 382-386.

Lorain S, Gross DA, Goyenvalle A, Danos O, Davoust J Garcia L (2008) Transient immunomodulation allows repeated injections of AAV1 and correction of muscular dystrophy in multiple muscles. *Mol Ther* 16: 541-547.

Ludwig H, Khayat D, Giaccone G Facon T (2005) Proteasome inhibition and its clinical prospects in the treatment of hematologic and solid malignancies. *Cancer* 104: 1794-1807.

Lupo B Trusolino L (2014) Inhibition of poly(ADP-ribosyl)ation in cancer: old and new paradigms revisited. *Biochim Biophys Acta* 1846: 201-215.

Lyon AR, Sato M, Hajjar RJ, Samulski RJ Harding SE (2008) Gene therapy: targeting the myocardium. *Heart* 94: 89-99.

Maersch S, Huber A, Buning H, Hallek M Perabo L (2009) Optimization of stealth adeno-associated virus vectors by randomization of immunogenic epitopes. *Virology* 397: 167-175.

Manno CS, Chew AJ, Hutchison S, Larson PJ, Herzog RW, Arruda VR, Tai SJ, Ragni MV, Thompson A, Ozelo M, Couto LB, Leonard DG, Johnson FA, McClelland A, Scallan C, Skarsgard E, Flake AW, Kay MA, High KA Glader B (2003) AAV-mediated factor IX gene transfer to skeletal muscle in patients with severe hemophilia B. *Blood* 101: 2963-2972.

Manno CS, Pierce GF, Arruda VR, Glader B, Ragni M, Rasko JJ, Ozelo MC, Hoots K, Blatt P, Konkle B, Dake M, Kaye R, Razavi M, Zajko A, Zehnder J, Rustagi PK, Nakai H, Chew A, Leonard D, Wright JF, Lessard RR, Sommer JM, Tigges M, Sabatino D, Luk A, Jiang H, Mingozzi F, Couto L, Ertl HC, High KA Kay MA (2006) Successful transduction of liver in hemophilia by AAV-Factor IX and limitations imposed by the host immune response. *Nat Med* 12: 342-347.

Mannucci PM (2008) Back to the future: a recent history of haemophilia treatment. *Haemophilia* 14 Suppl 3: 10-18.

Martin-Oliva D, Aguilar-Quesada R, O'Valle F, Munoz-Gamez JA, Martinez-Romero R, Garcia Del Moral R, Ruiz de Almodovar JM, Villuendas R, Piris MA Oliver FJ (2006) Inhibition of poly(ADP-ribose) polymerase modulates tumor-related gene expression, including hypoxia-inducible factor-1 activation, during skin carcinogenesis. *Cancer Res* 66: 5744-5756.

Martinez-Romero R, Martinez-Lara E, Aguilar-Quesada R, Peralta A, Oliver FJ Siles E (2008) PARP-1 modulates deferoxamine-induced HIF-1alpha accumulation through the regulation of nitric oxide and oxidative stress. *J Cell Biochem* 104: 2248-2260.

Martino AT, Basner-Tschakarjan E, Markusic DM, Finn JD, Hinderer C, Zhou S, Ostrov DA, Srivastava A, Ertl HC, Terhorst C, High KA, Mingozzi F Herzog RW (2013) Engineered AAV vector minimizes in vivo targeting of transduced hepatocytes by capsid-specific CD8+ T cells. *Blood*.

Martino AT, Herzog RW, Anegon I Adjali O (2011a) Measuring immune responses to recombinant AAV gene transfer. *Methods Mol Biol* 807: 259-272.

Martino AT, Nayak S, Hoffman BE, Cooper M, Liao G, Markusic DM, Byrne BJ, Terhorst C Herzog RW (2009) Tolerance induction to cytoplasmic beta-galactosidase by hepatic AAV gene transfer: implications for antigen presentation and immunotoxicity. *PLoS One* 4: e6376.

Martino AT, Suzuki M, Markusic DM, Zolotukhin I, Ryals RC, Moghimi B, Ertl HC, Muruve DA, Lee B Herzog RW (2011b) The genome of self-complementary adeno-associated viral vectors increases Toll-like receptor 9-dependent innate immune responses in the liver. *Blood* 117: 6459-6468.

McCarty DM, Young SM, Jr. Samulski RJ (2004) Integration of adeno-associated virus (AAV) and recombinant AAV vectors. *Annu Rev Genet* 38: 819-845.

McIntosh J, Lenting PJ, Rosales C, Lee D, Rabbanian S, Raj D, Patel N, Tuddenham EG, Christophe OD, McVey JH, Waddington S, Nienhuis AW, Gray JT, Fagone P, Mingozzi F, Zhou SZ, High KA, Cancio M, Ng CY, Zhou J, Morton CL, Davidoff AM Nathwani AC (2013) Therapeutic levels of FVIII following a single peripheral vein administration of rAAV vector encoding a novel human factor VIII variant. *Blood* 121: 3335-3344.

McIntosh JH, Cochrane M, Cobbold S, Waldmann H, Nathwani SA, Davidoff AM Nathwani AC (2012) Successful attenuation of humoral immunity to viral capsid and transgenic protein following AAV-mediated gene transfer with a non-depleting CD4 antibody and cyclosporine. *Gene Ther* 19: 78-85.

Mendell JR, Campbell K, Rodino-Klapac L, Sahenk Z, Shilling C, Lewis S, Bowles D, Gray S, Li C, Galloway G, Malik V, Coley B, Clark KR, Li J, Xiao X, Samulski J, McPhee SW, Samulski RJ Walker CM (2010) Dystrophin immunity in Duchenne's muscular dystrophy. *N Engl J Med* 363: 1429-1437.

Mingozzi F, Anguela XM, Pavani G, Chen Y, Davidson RJ, Hui DJ, Yazicioglu M, Elkouby L, Hinderer CJ, Faella A, Howard C, Tai A, Podsakoff GM, Zhou S, Basner-Tschakarjan E, Wright JF High KA (2013) Overcoming preexisting humoral immunity to AAV using capsid decoys. *Sci Transl Med* 5: 194ra192.

Mingozzi F High KA (2011) Therapeutic in vivo gene transfer for genetic disease using AAV: progress and challenges. *Nat Rev Genet* 12: 341-355.

Mingozzi F High KA (2013) Immune responses to AAV vectors: overcoming barriers to successful gene therapy. *Blood* 122: 23-36.

Mingozzi F, Maus MV, Hui DJ, Sabatino DE, Murphy SL, Rasko JE, Ragni MV, Manno CS, Sommer J, Jiang H, Pierce GF, Ertl HC High KA (2007) CD8(+) T-cell responses to adeno-associated virus capsid in humans. *Nat Med* 13: 419-422.

Mingozzi F, Meulenberg JJ, Hui DJ, Basner-Tschakarjan E, Hasbrouck NC, Edmonson SA, Hutnick NA, Betts MR, Kastelein JJ, Stroes ES High KA (2009) AAV-1-mediated gene transfer to skeletal muscle in humans results in dose-dependent activation of capsid-specific T cells. *Blood* 114: 2077-2086.

Mogensen TH (2009) Pathogen recognition and inflammatory signaling in innate immune defenses. *Clin Microbiol Rev* 22: 240-273, Table of Contents.

Mogensen TH Paludan SR (2001) Molecular pathways in virus-induced cytokine production. *Microbiol Mol Biol Rev* 65: 131-150.

Monahan PE, Lothrop CD, Sun J, Hirsch ML, Kafri T, Kantor B, Sarkar R, Tillson DM, Elia JR Samulski RJ (2010) Proteasome inhibitors enhance gene delivery by AAV virus vectors expressing large genomes in hemophilia mouse and dog models: a strategy for broad clinical application. *Mol Ther* 18: 1907-1916.

Moskalenko M, Chen L, van Roey M, Donahue BA, Snyder RO, McArthur JG Patel SD (2000) Epitope mapping of human anti-adeno-associated virus type 2 neutralizing antibodies: implications for gene therapy and virus structure. *J Virol* 74: 1761-1766.

Mueller C, Chulay JD, Trapnell BC, Humphries M, Carey B, Sandhaus RA, McElvaney NG, Messina L, Tang Q, Rouhani FN, Campbell-Thompson M, Fu AD, Yachnis A, Knop DR, Ye GJ, Brantly M, Calcedo R, Somanathan S, Richman LP, Vonderheide RH, Hulme MA, Brusko TM, Wilson JM Flotte TR (2013) Human Treg responses allow sustained recombinant adeno-associated virus-mediated transgene expression. *J Clin Invest* 123: 5310-5318.

Murphy SL High KA (2008) Gene therapy for haemophilia. *Br J Haematol* 140: 479-487.

Muthumani K, Choo AY, Zong WX, Madesh M, Hwang DS, Premkumar A, Thieu KP, Emmanuel J, Kumar S, Thompson CB Weiner DB (2006) The HIV-1 Vpr and glucocorticoid receptor complex is a gain-of-function interaction that prevents the nuclear localization of PARP-1. *Nat Cell Biol* 8: 170-179.

Nathwani AC, Cochrane M, McIntosh J, Ng CY, Zhou J, Gray JT Davidoff AM (2009) Enhancing transduction of the liver by adeno-associated viral vectors. *Gene Ther* 16: 60-69.

Nathwani AC, Reiss UM, Tuddenham EG, Rosales C, Chowdary P, McIntosh J, Della Peruta M, Lheriteau E, Patel N, Raj D, Riddell A, Pie J, Rangarajan S, Bevan D, Recht M, Shen YM, Halka KG, Basner-Tschakarjan E, Mingozzi F, High KA, Allay J, Kay MA, Ng CY, Zhou J, Cancio M, Morton CL, Gray JT, Srivastava D, Nienhuis AW Davidoff AM (2014) Long-term safety and efficacy of factor IX gene therapy in hemophilia B. *N Engl J Med* 371: 1994-2004.

Nathwani AC, Tuddenham EG, Rangarajan S, Rosales C, McIntosh J, Linch DC, Chowdary P, Riddell A, Pie AJ, Harrington C, O'Beirne J, Smith K, Pasi J, Glader B, Rustagi P, Ng CY, Kay MA, Zhou J, Spence Y, Morton CL, Allay J, Coleman J, Sleep S, Cunningham JM, Srivastava D, Basner-Tschakarjan E, Mingozzi F, High KA, Gray JT, Reiss UM, Nienhuis AW Davidoff AM (2011) Adenovirus-associated virus vector-mediated gene transfer in hemophilia B. *N Engl J Med* 365: 2357-2365.

Nonnenmacher M Weber T (2011) Adeno-associated virus 2 infection requires endocytosis through the CLIC/GEEC pathway. *Cell Host Microbe* 10: 563-576.

O'Connor TP Crystal RG (2006) Genetic medicines: treatment strategies for hereditary disorders. *Nat Rev Genet* 7: 261-276.

Oie KL Pickup DJ (2001) Cowpox virus and other members of the orthopoxvirus genus interfere with the regulation of NF-kappaB activation. *Virology* 288: 175-187.

Olabisi OA, Soto-Nieves N, Nieves E, Yang TT, Yang X, Yu RY, Suk HY, Macian F Chow CW (2008) Regulation of transcription factor NFAT by ADP-ribosylation. *Mol Cell Biol* 28: 2860-2871.

Oliver FJ, Menissier-de Murcia J de Murcia G (1999) Poly(ADP-ribose) polymerase in the cellular response to DNA damage, apoptosis, and disease. *Am J Hum Genet* 64: 1282-1288.

Opie SR, Warrington KH, Jr., Agbandje-McKenna M, Zolotukhin S Muzyczka N (2003) Identification of amino acid residues in the capsid proteins of adeno-associated virus type 2 that contribute to heparan sulfate proteoglycan binding. *J Virol* 77: 6995-7006.

Oumouna M, Datta R, Oumouna-Benachour K, Suzuki Y, Hans C, Matthews K, Fallon K Boulares H (2006) Poly(ADP-ribose) polymerase-1 inhibition prevents eosinophil recruitment by modulating Th2 cytokines in a murine model of allergic airway inflammation: a potential specific effect on IL-5. *J Immunol* 177: 6489-6496.

Pereira DJ, McCarty DM Muzyczka N (1997) The adeno-associated virus (AAV) Rep protein acts as both a repressor and an activator to regulate AAV transcription during a productive infection. *J Virol* 71: 1079-1088.

Petrs-Silva H, Dinculescu A, Li Q, Deng WT, Pang JJ, Min SH, Chiodo V, Neeley AW, Govindasamy L, Bennett A, Agbandje-McKenna M, Zhong L, Li B, Jayandharan GR, Srivastava A, Lewin AS Hauswirth WW (2011) Novel properties of tyrosine-mutant AAV2 vectors in the mouse retina. *Mol Ther* 19: 293-301.

Petrs-Silva H, Dinculescu A, Li Q, Min SH, Chiodo V, Pang JJ, Zhong L, Zolotukhin S, Srivastava A, Lewin AS Hauswirth WW (2009) High-efficiency transduction of the mouse retina by tyrosine-mutant AAV serotype vectors. *Mol Ther* 17: 463-471.

Peyvandi F, Garagiola I Seregni S (2013) Future of coagulation factor replacement therapy. *J Thromb Haemost* 11 Suppl 1: 84-98.

Pfeifer A Verma IM (2001) Gene therapy: promises and problems. *Annu Rev Genomics Hum Genet* 2: 177-211.

Philpott NJ, Gomos J, Berns KI Falck-Pedersen E (2002) A p5 integration efficiency element mediates Rep-dependent integration into AAVS1 at chromosome 19. *Proc Natl Acad Sci U S A* 99: 12381-12385.

Phulwani NK Kielian T (2008) Poly (ADP-ribose) polymerases (PARPs) 1-3 regulate astrocyte activation. *J Neurochem* 106: 578-590.

Pipe SW (2009) Functional roles of the factor VIII B domain. *Haemophilia* 15: 1187-1196.

Rahman MM McFadden G (2011) Modulation of NF-kappaB signalling by microbial pathogens. *Nat Rev Microbiol* 9: 291-306.

Recchia A Mavilio F (2011) Site-specific integration by the adeno-associated virus rep protein. *Curr Gene Ther* 11: 399-405.

Richardson PG, Barlogie B, Berenson J, Singhal S, Jagannath S, Irwin D, Rajkumar SV, Srkalovic G, Alsina M, Alexanian R, Siegel D, Orlowski RZ, Kuter D, Limentani SA, Lee S, Hideshima T, Esseltine DL, Kauffman M, Adams J, Schenkein DP Anderson KC (2003) A phase 2 study of bortezomib in relapsed, refractory myeloma. *N Engl J Med* 348: 2609-2617.

Roebuck KA, Rahman A, Lakshminarayanan V, Janakidevi K Malik AB (1995) H2O2 and tumor necrosis factor-alpha activate intercellular adhesion molecule 1 (ICAM-1) gene transcription through distinct cis-regulatory elements within the ICAM-1 promoter. *J Biol Chem* 270: 18966-18974.

Roesner JP, Vagts DA, Iber T, Eipel C, Vollmar B Noldge-Schomburg GF (2006) Protective effects of PARP inhibition on liver microcirculation and function after haemorrhagic shock and resuscitation in male rats. *Intensive Care Med* 32: 1649-1657.

Rogers GL, Martino AT, Zolotukhin I, Ertl HC Herzog RW (2014) Role of the vector genome and underlying factor IX mutation in immune responses to AAV gene therapy for hemophilia B. *J Transl Med* 12: 25.

Rogers S, Lowenthal A, Terheggen HG Columbo JP (1973) Induction of arginase activity with the Shope papilloma virus in tissue culture cells from an argininemic patient. *J Exp Med* 137: 1091-1096.

Rogers S Pfuderer P (1968) Use of viruses as carriers of added genetic information. *Nature* 219: 749-751.

Romanova LG, Zacharias J, Cannon ML Philpott NJ (2011) Effect of poly(ADP-ribose) polymerase 1 on integration of the adeno-associated viral vector genome. *J Gene Med* 13: 342-352.

Rose JA, Berns KI, Hoggan MD Koczot FJ (1969) Evidence for a single-stranded adenovirus-associated virus genome: formation of a DNA density hybrid on release of viral DNA. *Proc Natl Acad Sci U S A* 64: 863-869.

Rowell DL, Eckmann L, Dwinell MB, Carpenter SP, Raucy JL, Yang SK Kagnoff MF (1997) Human hepatocytes express an array of proinflammatory cytokines after agonist stimulation or bacterial invasion. *Am J Physiol* 273: G322-332.

Ruffing M, Zentgraf H Kleinschmidt JA (1992) Assembly of viruslike particles by recombinant structural proteins of adeno-associated virus type 2 in insect cells. *J Virol* 66: 6922-6930.

Ruland J (2011) Return to homeostasis: downregulation of NF-kappaB responses. *Nat Immunol* 12: 709-714.

Ryals RC, Boye SL, Dinculescu A, Hauswirth WW Boye SE (2011) Quantifying transduction efficiencies of unmodified and tyrosine capsid mutant AAV vectors in vitro using two ocular cell lines. *Mol Vis* 17: 1090-1102.

Saenz L, Lozano JJ, Valdor R, Baroja-Mazo A, Ramirez P, Parrilla P, Aparicio P, Sumoy L Yelamos J (2008) Transcriptional regulation by poly(ADP-ribose) polymerase-1 during T cell activation. *BMC Genomics* 9: 171.

Samulski RJ, Berns KI, Tan M Muzyczka N (1982) Cloning of adeno-associated virus into pBR322: rescue of intact virus from the recombinant plasmid in human cells. *Proc Natl Acad Sci U S A* 79: 2077-2081.

Sanlioglu S, Benson PK, Yang J, Atkinson EM, Reynolds T Engelhardt JF (2000) Endocytosis and nuclear trafficking of adeno-associated virus type 2 are controlled by rac1 and phosphatidylinositol-3 kinase activation. *J Virol* 74: 9184-9196.

Sanlioglu S, Monick MM, Luleci G, Hunninghake GW Engelhardt JF (2001) Rate limiting steps of AAV transduction and implications for human gene therapy. *Curr Gene Ther* 1: 137-147.

Santoro MG, Rossi A Amici C (2003) NF-kappaB and virus infection: who controls whom. *EMBO J* 22: 2552-2560.

Scott GS, Kean RB, Mikheeva T, Fabis MJ, Mabley JG, Szabo C Hooper DC (2004) The therapeutic effects of PJ34 [N-(6-oxo-5,6-dihydrophenanthridin-2-yl)-N,N-dimethylacetamide.HCl], a selective inhibitor of poly(ADP-ribose) polymerase, in experimental allergic encephalomyelitis are associated with immunomodulation. *J Pharmacol Exp Ther* 310: 1053-1061.

Selot RS, Hareendran S Jayandharan GR (2014) Developing immunologically inert adeno-associated virus (AAV) vectors for gene therapy: possibilities and limitations. *Curr Pharm Biotechnol* 14: 1072-1082.

Sen D, Balakrishnan B, Gabriel N, Agrawal P, Roshini V, Samuel R, Srivastava A Jayandharan GR (2013a) Improved adeno-associated virus (AAV) serotype 1 and 5 vectors for gene therapy. *Sci Rep* 3: 1832.

Sen D, Gadkari RA, Sudha G, Gabriel N, Sathish Kumar Y, Selot R, Samuel R, Rajalingam S, Ramya V, Nair SC, Srinivasan N, Srivastava A Jayandharan GR (2013b) Targeted modifications in adeno-associated virus (AAV) serotype -8 capsid improves its hepatic gene transfer efficiency in vivo. *Hum Gene Ther Methods*.

Sen R Baltimore D (1986) Multiple nuclear factors interact with the immunoglobulin enhancer sequences. *Cell* 46: 705-716.

Shah JJ Orlowski RZ (2009) Proteasome inhibitors in the treatment of multiple myeloma. *Leukemia* 23: 1964-1979.

Sheppard KA, Rose DW, Haque ZK, Kurokawa R, McInerney E, Westin S, Thanos D, Rosenfeld MG, Glass CK Collins T (1999) Transcriptional activation by NF-kappaB requires multiple coactivators. *Mol Cell Biol* 19: 6367-6378.

Shimotohno K Temin HM (1981) Formation of infectious progeny virus after insertion of herpes simplex thymidine kinase gene into DNA of an avian retrovirus. *Cell* 26: 67-77.

Somanathan S, Breous E, Bell P Wilson JM (2010) AAV vectors avoid inflammatory signals necessary to render transduced hepatocyte targets for destructive T cells. *Mol Ther* 18: 977-982.

Song S, Lu Y, Choi YK, Han Y, Tang Q, Zhao G, Berns KI Flotte TR (2004) DNA-dependent PK inhibits adeno-associated virus DNA integration. *Proc Natl Acad Sci U S A* 101: 2112-2116.

Srivastava A (2008) Adeno-associated virus-mediated gene transfer. *J Cell Biochem* 105: 17-24.

Stieger K, Le Meur G, Lasne F, Weber M, Deschamps JY, Nivard D, Mendes-Madeira A, Provost N, Martin L, Moullier P Rolling F (2006) Long-term doxycycline-regulated transgene expression in the retina of nonhuman primates following subretinal injection of recombinant AAV vectors. *Mol Ther* 13: 967-975.

Stone DH, Al-Badawi H, Conrad MF, Stoner MC, Entabi F, Cambria RP Watkins MT (2005) PJ34, a poly-ADP-ribose polymerase inhibitor, modulates renal injury after thoracic aortic ischemia/reperfusion. *Surgery* 138: 368-374.

Street A, Hill K, Sussex B, Warner M Scully MF (2006) Haemophilia and ageing. *Haemophilia* 12 Suppl 3: 8-12.

Strom CE Helleday T (2012) Strategies for the Use of Poly(adenosine diphosphate ribose) Polymerase (PARP) Inhibitors in Cancer Therapy. *Biomolecules* 2: 635-649.

Sudres M, Cire S, Vasseur V, Brault L, Da Rocha S, Boisgerault F, Le Bec C, Gross DA, Blouin V, Ryffel B Galy A (2012) MyD88 signaling in B cells regulates the production of Th1-dependent antibodies to AAV. *Mol Ther* 20: 1571-1581.

Summerford C Samulski RJ (1998) Membrane-associated heparan sulfate proteoglycan is a receptor for adeno-associated virus type 2 virions. *J Virol* 72: 1438-1445.

Szabo C Dawson VL (1998) Role of poly(ADP-ribose) synthetase in inflammation and ischaemia-reperfusion. *Trends Pharmacol Sci* 19: 287-298.

Tempera I, Deng Z, Atanasiu C, Chen CJ, D'Erme M Lieberman PM (2010) Regulation of Epstein-Barr virus OriP replication by poly(ADP-ribose) polymerase 1. *J Virol* 84: 4988-4997.

Toromanoff A, Adjali O, Larcher T, Hill M, Guigand L, Chenuaud P, Deschamps JY, Gauthier O, Blancho G, Vanhove B, Rolling F, Cherel Y, Moullier P, Anegon I Le Guiner C (2010) Lack of immunotoxicity after regional intravenous (RI) delivery of rAAV to nonhuman primate skeletal muscle. *Mol Ther* 18: 151-160.

Tseng YS Agbandje-McKenna M (2014) Mapping the AAV Capsid Host Antibody Response toward the Development of Second Generation Gene Delivery Vectors. *Front Immunol* 5: 9.

Ullrich O, Diestel A, Eyupoglu IY Nitsch R (2001) Regulation of microglial expression of integrins by poly(ADP-ribose) polymerase-1. *Nat Cell Biol* 3: 1035-1042.

Unzu C, Hervas-Stubbs S, Sampedro A, Mauleon I, Mancheno U, Alfaro C, de Salamanca RE, Benito A, Beattie SG, Petry H, Prieto J, Melero I Fontanellas A (2012) Transient and intensive pharmacological immunosuppression fails to improve AAV-based liver gene transfer in non-human primates. *J Transl Med* 10: 122.

Vasileva A Jessberger R (2005) Precise hit: adeno-associated virus in gene targeting. *Nat Rev Microbiol* 3: 837-847.

Verma IM Weitzman MD (2005) Gene therapy: twenty-first century medicine. *Annu Rev Biochem* 74: 711-738.

Veron P, Leborgne C, Monteilhet V, Boutin S, Martin S, Moullier P Masurier C (2012) Humoral and cellular capsid-specific immune responses to adeno-associated virus type 1 in randomized healthy donors. *J Immunol* 188: 6418-6424.

Vincent KA, Piraino ST Wadsworth SC (1997) Analysis of recombinant adeno-associated virus packaging and requirements for rep and cap gene products. *J Virol* 71: 1897-1905.

Wagner JA, Reynolds T, Moran ML, Moss RB, Wine JJ, Flotte TR Gardner P (1998) Efficient and persistent gene transfer of AAV-CFTR in maxillary sinus. *Lancet* 351: 1702-1703.

Wang L, Calcedo R, Bell P, Lin J, Grant RL, Siegel DL Wilson JM (2011) Impact of pre-existing immunity on gene transfer to nonhuman primate liver with adeno-associated virus 8 vectors. *Hum Gene Ther* 22: 1389-1401.

Wang W, Li W, Ma N Steinhoff G (2013) Non-viral gene delivery methods. *Curr Pharm Biotechnol* 14: 46-60.

Wistuba A, Kern A, Weger S, Grimm D Kleinschmidt JA (1997) Subcellular compartmentalization of adeno-associated virus type 2 assembly. *J Virol* 71: 1341-1352.

Wu T, Topfer K, Lin SW, Li H, Bian A, Zhou XY, High KA Ertl HC (2012) Self-complementary AAVs induce more potent transgene product-specific immune responses compared to a single-stranded genome. *Mol Ther* 20: 572-579.

Wu TL, Li H, Faust SM, Chi E, Zhou S, Wright F, High KA Ertl HC (2014) CD8+ T cell recognition of epitopes within the capsid of adeno-associated virus 8-based gene transfer vectors depends on vectors' genome. *Mol Ther* 22: 42-51.

Wu Z, Miller E, Agbandje-McKenna M Samulski RJ (2006) Alpha2,3 and alpha2,6 N-linked sialic acids facilitate efficient binding and transduction by adeno-associated virus types 1 and 6. *J Virol* 80: 9093-9103.

Xiao PJ, Li C, Neumann A Samulski RJ (2012) Quantitative 3D tracing of gene-delivery viral vectors in human cells and animal tissues. *Mol Ther* 20: 317-328.

Xiao X, Li J Samulski RJ (1998) Production of high-titer recombinant adeno-associated virus vectors in the absence of helper adenovirus. *J Virol* 72: 2224-2232.

Yang G, Abate A, George AG, Weng YH Dennery PA (2004) Maturational differences in lung NF-kappaB activation and their role in tolerance to hyperoxia. *J Clin Invest* 114: 669-678.

Zaiss AK, Cotter MJ, White LR, Clark SA, Wong NC, Holers VM, Bartlett JS Muruve DA (2008) Complement is an essential component of the immune response to adeno-associated virus vectors. *J Virol* 82: 2727-2740.

Zaiss AK Muruve DA (2008) Immunity to adeno-associated virus vectors in animals and humans: a continued challenge. *Gene Ther* 15: 808-816.

Zhang Y, Chirmule N, Gao G Wilson J (2000) CD40 ligand-dependent activation of cytotoxic T lymphocytes by adeno-associated virus vectors in vivo: role of immature dendritic cells. *J Virol* 74: 8003-8010.

Zhang Y, Satterlee A Huang L (2012) In vivo gene delivery by nonviral vectors: overcoming hurdles? *Mol Ther* 20: 1298-1304.

Zheng C, Yin Q Wu H (2011) Structural studies of NF-kappaB signaling. *Cell Res* 21: 183-195.

Zhong L, Li B, Mah CS, Govindasamy L, Agbandje-McKenna M, Cooper M, Herzog RW, Zolotukhin I, Warrington KH, Jr., Weigel-Van Aken KA, Hobbs JA, Zolotukhin S, Muzyczka N Srivastava A (2008) Next generation of adeno-associated virus 2 vectors: point mutations in tyrosines lead to high-efficiency transduction at lower doses. *Proc Natl Acad Sci U S A* 105: 7827-7832.

Zhu J, Huang X Yang Y (2009) The TLR9-MyD88 pathway is critical for adaptive immune responses to adeno-associated virus gene therapy vectors in mice. *J Clin Invest* 119: 2388-2398.

Internet based references/ softwares

[a] www.sabiosciences.com/pcr/arrayanalysis.php.

[b] Mouse NF-κB Signaling Pathway PCR Array. [Online]. Available: http://www.sabiosciences.com/rt_pcr_product/HTML/PAMM-025A.html[Accessed 11 October 2014].

[c] http://www.graphpad.com/scientific-software/prism/

8. LIST OF PUBLICATIONS

1. **Hareendran S**, Ramakrishna B, Jayandharan GR. Synergistic inhibition of PARP-1 and NF-κB signaling downregulates immune response against recombinant AAV2 vectors during hepatic gene therapy. *Eur J Immunol*. 2016 Jan;46(1):154-66.doi:10.1002/eji. 201545867. Epub 2015 Nov 5

2. Selot RS, **Hareendran S**, Jayandharan GR. Developing Immunologically Inert Adeno-Associated Virus (AAV) Vectors for Gene Therapy: Possibilities and Limitations. Curr Pharm Biotechnol. 2014;14(12):1072-82.

3. **Hareendran S**, Balakrishnan B, Sen D, Kumar S, Srivastava A, Jayandharan GR. Adeno-associated virus (AAV) vectors in gene therapy: immune challenges and strategies to circumvent them. Rev Med Virol. 2013 Nov;23(6):399-413.

4. Gabriel N[*], **Hareendran S[*]**, Sen D[*], Gadkari RA, Sudha G, Selot R, Hussai M, Dhaksnamoorthy R, Samuel R, Srinivasan N, Srivastava A, Jayandharan GR. Bioengineering of AAV2 capsid at specific serine, threonine, or lysine residues improves its transduction efficiency in vitro and in vivo. Hum Gene Ther Methods. 2013 Apr;24 (2):80-93.
   [* Equal contribution]

5. Balakrishnan B, Sen D, **Hareendran S**, Roshini V, David S, Srivastava A, Jayandharan GR. Activation of the cellular unfolded protein response by recombinant adeno-associated virus vectors. PLoS One. 2013;8(1) e53845.doi:10.1371/ journal.pone.0053845

European Journal of Immunology

Synergistic inhibition of PARP-1 and NF-κB signaling downregulates immune response against recombinant AAV2 vectors during hepatic gene therapy

Sangeetha Hareendran[1], Banumathi Ramakrishna[2] and Giridhara R. Jayandharan[1,3,4]

[1] Centre for Stem Cell Research, Christian Medical College, Vellore, Tamil Nadu, India
[2] Department of General Pathology, Christian Medical College, Vellore, Tamil Nadu, India
[3] Department of Hematology, Christian Medical College, Vellore, Tamil Nadu, India
[4] Department of Biological Sciences and Bioengineering, Indian Institute of Technology, Kanpur, Uttar Pradesh, India

Host immune response remains a key obstacle to widespread application of adeno-associated virus (AAV) based gene therapy. Thus, targeted inhibition of the signaling pathways that trigger such immune responses will be beneficial. Previous studies have reported that DNA damage response proteins such as poly(ADP-ribose) polymerase-1 (PARP-1) negatively affect the integration of AAV in the host genome. However, the role of PARP-1 in regulating AAV transduction and the immune response against these vectors has not been elucidated. In this study, we demonstrate that repression of PARP-1 improves the transduction of single-stranded AAV vectors both in vitro (~174%) and in vivo (two- to 3.4-fold). Inhibition of PARP-1, also significantly downregulated the expression of several proinflammatory and cytokine markers such as TLRs, ILs, NF-κB subunit proteins associated with the host innate response against self-complementary AAV2 vectors. The suppression of the inflammatory response targeted against these vectors was more effective upon combined inhibition of PARP-1 and NF-κB signaling. This strategy also effectively attenuated the AAV capsid-specific cytotoxic T-cell response, with minimal effect on vector transduction, as demonstrated in normal C57BL/6 and hemophilia B mice. These data suggest that targeting specific host cellular proteins could be useful to attenuate the immune barriers to AAV-mediated gene therapy.

Keywords: AAV · Gene therapy · Hemophilia · Immune response · PARP-1

Additional supporting information may be found in the online version of this article at the publisher's web-site

Introduction

Recombinant adeno-associated virus (AAV) vectors are widely acclaimed as versatile tools for gene transfer and gene therapy [1]. AAV has not been associated with any disease to date and is believed to be a potentially safe vector [2]. The prototype AAV vectors based on serotype 2 (AAV2) have shown multiyear clinical benefit when targeted to immune-privileged sites such as eye for Leber congenital amaurosis [3, 4]. However, their therapeutic efficiency when targeted to other organs, such as during hepatic gene transfer in patients with hemophilia B was suboptimal due to a dose-dependent $CD8^+$ T-cell response directed against the vector

Correspondence: Dr. Giridhara R. Jayandharan
e-mail: jayrao@iitk.ac.in

[5, 6]. Recombinant AAV8, which is a more robust vector [7] has been successfully tested in a recent clinical trial for patients with hemophilia B [8]. Nonetheless two of the patients in this study also developed capsid-specific T-cell response, which required a short course of immunosuppression by glucocorticoid therapy. Thus, for this vector system to be widely applicable, a better understanding of the biological interactions between the host cells and the AAV vectors triggering the immune response is crucial.

Throughout its life cycle, AAV continuously interacts with several factors within the host cell, which might have implications on its intracellular trafficking, nuclear entry, transgene expression, as well as the cellular immune response. AAV has been shown to bind to dynein, a microtubule motor protein to facilitate the retrograde transport of its genome to the nucleus [9], although microtubule-independent mechanism of AAV trafficking is also described [10]. The activation of unfolded protein response (UPR) signaling particularly the PERK and IRE1 pathways, as a stress response in ER against the influx of AAV particles into the cell has been documented [11]. Certain surface-exposed residues on the AAV capsid are known to be phosphorylated by cellular kinases, thereby providing cues for ubiquitin-proteasome based degradation of the viral particles. Site-directed mutation of such residues has led to the generation of capsid-modified AAV vectors with superior transduction [12–15]. The immune response documented in clinical trials using AAV vectors shows a direct correlation to the vector dose administered [6, 8, 16]. Hence strategies to enhance the vector transduction could help in achieving therapeutic index by delivering vectors at lower doses, without causing immune activation. To attenuate the humoral and cellular responses to AAV vectors and/or transgene product, transient immunosuppression has been achieved using cyclosporine A, tacrolimus, nondepleting CD4 Ab, anti-CD40L, CTLA-Ig, rituximab, mycophenolate mofetil, or steroids with varying degrees of success [17]. Similarly, specific targeting of molecules and pathways that arbitrate the immune response against AAV could also be beneficial.

In the present study, we hypothesized that inhibition of poly(ADP-ribose) polymerase-1 (PARP-1), a DNA damage response protein might augment the transduction efficiency of AAV vectors and/ or modulate the immune response against them. PARP-1 is a highly abundant chromatin-associated enzyme that catalyzes the covalent attachment of ADP-ribose units on protein acceptors to generate poly(ADP-ribose) (PAR) chains [18]. PARPs perform crucial cellular functions such as DNA damage surveillance and transcriptional regulation [19]. Studies in various model systems have implicated PARPs in multiple DNA repair pathways including single-strand break repair, double-strand break repair, and base excision repair [20]. Not surprisingly, PARP-1 has also been implicated in regulating viral DNA replication and gene expression [21, 22] as well as in antiviral response by virtue of its binding to DNA terminal repeat sequences in several viruses including EBV, Kaposi's sarcoma-associated herpesvirus, and HIV [23].

Our earlier studies have shown that NF-κB specifically interacts with the D-sequence within the inverted terminal repeat of the AAV genome and plays a pivotal role in flagging the innate and adaptive immune response to AAV vectors [24]. It was observed that during hepatic gene transfer with AAV in vivo, the canonical NF-κB pathway was activated by 2 h, while the alternate NF-κB pathway was primed within 9 h in the hepatocytes. Pharmacological inhibition of NF-κB using a small molecule inhibitor, Bay11, effectively attenuated the inflammatory cytokines and anti-AAV Ab response, confirming the central role of NF-κB in mediating immune response against AAV vectors [24]. PARP-1 is known to act as a coactivator of NF-κB driving the expression of its target genes in response to proinflammatory stimuli and genotoxic stress [25]. Studies in PARP-1 KO mice showed downregulation of the expression of several NF-κB-dependent inflammatory response genes [26]. The protective effect of PARP-1 inhibitors against tissue injury in various inflammatory conditions has been demonstrated in animal models [27]. Based on these data, we have attempted to understand the role of PARP-1 in regulation of AAV-based transgene expression and modulation of host immune response to the vector alone or in combination with NF-κB signaling pathway.

Results

Inhibition of cellular PARP-1 enhances transduction efficiency of AAV vectors

Initially we wished to examine the effect of PARP-1 inhibition on the transgene expression mediated by ss AAV vectors. For this, HeLa cells were transfected with 100 μM of PARP-1-specific siRNA or scrambled oligo control and 24 h later were infected with ssAAV2-EGFP (where EGFP is enhanced green fluorescent protein) vectors at an multiplicity of infection of 2000. Forty-eight hours later, the vector-based EGFP expression relative to mock-transfected cells was measured. As shown in Fig. 1A or B, the levels of transgene expression were significantly higher upon RNAi-mediated depletion of PARP-1 (~174%, $p < 0.05$). Western blot analysis of nuclear extracts from cells transduced with ssAAV2 vectors was performed to validate the specificity of PARP-1 siRNA versus the scrambled siRNA control in downregulating the PARP-1 protein levels (Fig. 1C). Further to test if the inhibition of PARP-1 can improve the transduction of ssAAV vectors in vivo, we used PJ-34, a selective PARP-1 inhibitor used extensively in preclinical animal models [28–30]. PJ-34 is a water soluble phenanthridinone derivative, which competitively inhibits the PARP-1 enzyme activity by blocking the NAD^+ binding site within its catalytic domain [31, 32]. We administered PJ34 (10 mg/kg body weight) into groups of BALB/c mice ($n = 4$) i.p. at 24 h (Day 0) and 30 min (Day 1) prior to vector injection and subsequently once a week till the end of the study. On Day 1, these animals were mock injected or injected with $\sim 1 \times 10^{11}$ viral genomes (vgs) of ssAAV2-EGFP vectors or $\sim 5 \times 10^{10}$ vgs of ssAAV8-EGFP vectors via the tail vein. The mice were euthanized 4 weeks later and the EGFP expression in the liver lobes was assessed by fluorescence microscopy. The ssAAV vector induced EGFP levels in the liver were found to be significantly increased in groups of BALB/c mice administered with PJ34 (Fig. 1 D or E or F). The increase in transgene

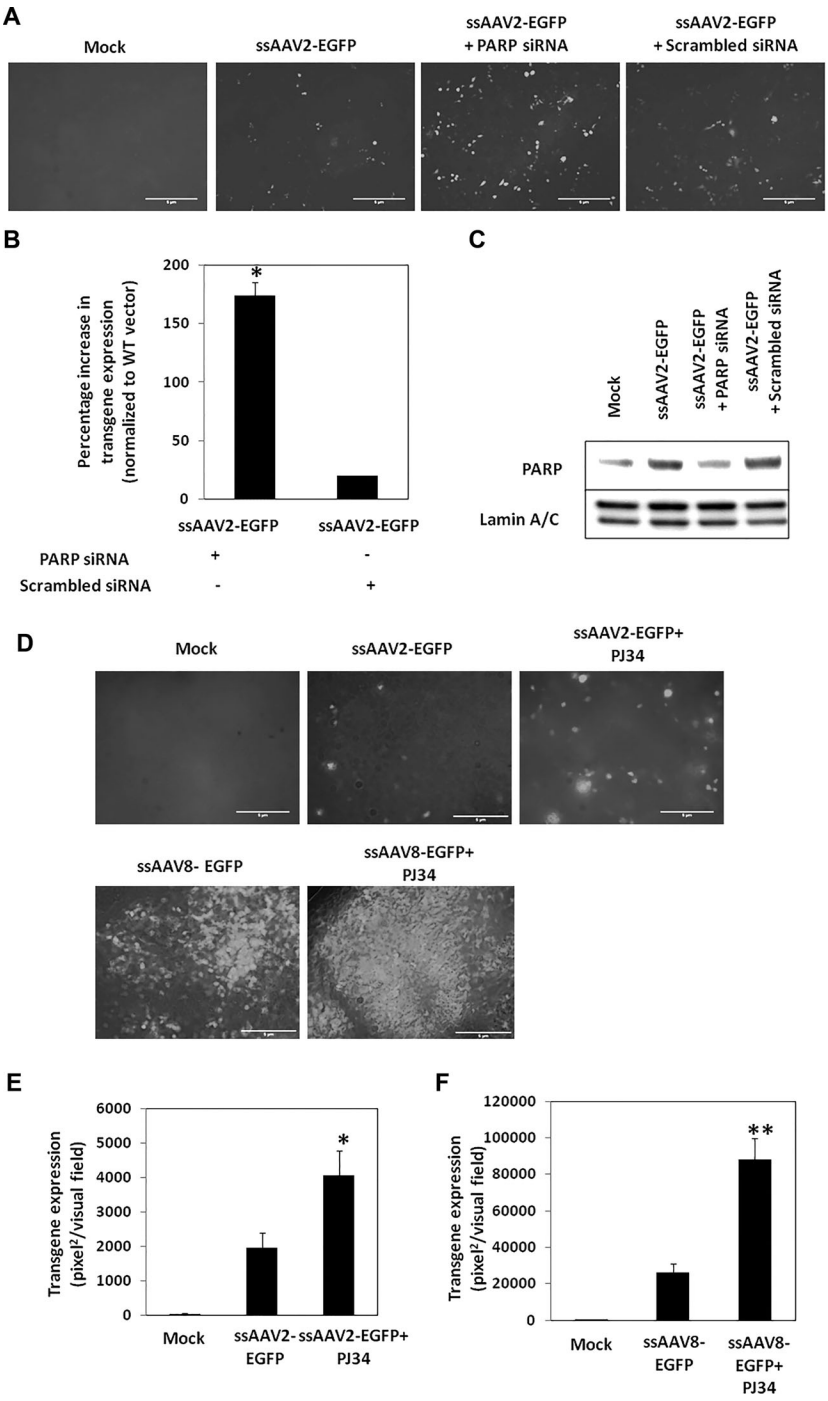

Figure 1. Effect of PARP-1 inhibition on transduction of recombinant ssAAV vectors. (A) RNAi-mediated inhibition of PARP-1 in vitro. HeLa cells were infected with ssAAV2-EFGP vectors either in the presence or absence of PARP-1 siRNA/scrambled siRNA control. The transgene expression in these cells was then measured at 48 h postinfection by fluorescence microscopy (uniform exposure settings: 500 ms, gain 1.7, and intensity 5). Scale bar = 5 μm. (B) Quantitative analysis of the fluorescence microscopy data from (A) showing the percentage increase in EGFP expression levels in comparison to cells treated with WT vector. Data are shown as mean ± SEM ($n = 12$) and are representative of six independent experiments, each done in duplicate conditions. $^{*}p < 0.05$; two-tailed unpaired Student's *t*-test. (C) Western blot analysis of HeLa cell nuclear extracts following mock (PBS) infection or infection with ssAAV2 vector, either in the presence or absence of PARP-1 siRNA or scrambled siRNA control. Anti-Lamin A/C Ab was used as a loading control. (D) Pharmacological inhibition of PARP-1 during AAV-mediated hepatic gene transfer in vivo. BALB/c mice were injected with mock (PBS) or ssAAV2-EGFP/ssAAV8-EGFP vectors alone or in the presence of PARP-1 inhibitor, PJ-34. Transgene expression was measured in liver sections 4 weeks postinjection by fluorescence microscopy (uniform settings of exposure time 2 s, gain 2, and intensity 5). Representative images of the liver sections are shown from one experiment ($n = 4$ mice/group). Scale bar = 5 μm (E, F) Quantitative analyses of the EGFP expression. Data are shown as mean ± SD ($n = 4$ mice/group) and is from one experiment; $^{*}p < 0.05$;$^{**}p < 0.05$; PJ34 treated versus control group; two-tailed unpaired Student's *t*-test.

expression was more prominent in mice injected with ssAAV8 vectors (~3.4-fold) than ssAAV2 vectors (~twofold). These data underscore that PARP-1 repression enhances the transgene expression from ss AAV vectors.

To test if the inhibition of PARP-1 has a similar effect on scAAV2 vector transduction, we performed in vitro infection studies in HeLa after knockdown of PARP-1 using specific siRNA, as was done with ssAAV2 vectors. At 48 h postinfection, we found only modest increase (~84%) in EGFP levels with scAAV2 vectors in the PARP-1 depleted cells (Fig. 2A or B). To further evaluate the effect of PARP-1 inhibition on scAAV2-mediated gene transfer in vivo, PJ34 (10 mg/ kg) was administered into groups of BALB/c mice followed by the i.v. injection of ~5×10^{10} vgs of scAAV2-EGFP vectors. Four weeks post vector administration, the hepatic transgene expression in PARP-1 inhibitor administered mice was marginal (~49%) as shown in Fig. 2C. These results demonstrate that PARP-1 inhibition is effective in improving hepatic gene transfer only with ssAAV vectors. The in vivo administration of PJ-34 did not lead to any significant histological abnormalities in the liver in BALB/c mice 4 weeks post vector administration. Both

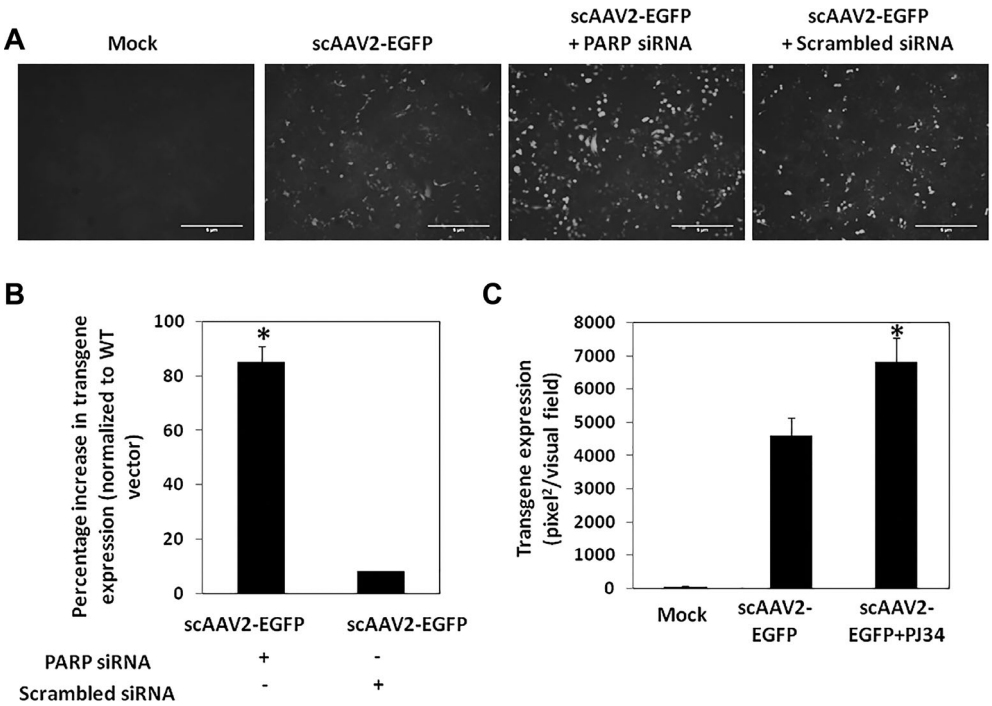

Figure 2. Effect of PARP-1 inhibition on transduction of recombinant self-complementary AAV2 vectors. (A) RNAi-mediated PARP-1 inhibition in vitro: HeLa cells were infected with scAAV2-EGFP vectors either in the presence or absence of PARP-1 siRNA/scrambled siRNA control. EGFP expression was measured 48 h postinfection by fluorescence microscopy (500 ms, gain 1.7, and intensity 5). Representative images of six independent experiments are shown. Scale bar = 5 μm. (B) Quantitative analysis of data from (A) showing the percentage increase in EGFP expression levels, compared to that of the WT vector. Data are shown as mean ± SEM ($n = 12$) and are representative of six independent experiments, each done in duplicates. *$p < 0.05$; two-tailed unpaired Student's *t*-test. (C) Pharmacological inhibition of PARP-1 during AAV-mediated gene delivery into murine liver: quantitative analysis of the transgene expression documented in liver lobes of BALB/c mice at 4 weeks time point, post mock (PBS) injection or administration of scAAV2-EGFP vectors alone or in the presence of PARP-1 inhibitor, PJ-34. Data are shown as mean ± SD of four mice per group from one experiment; *$p < 0.05$;**$p < 0.05$; PJ34 treated versus control group; two-tailed unpaired Student's *t*-test.

PBS and PJ-34 vector injected mice were grossly normal. The liver tissues from any of the PBS- or PJ-34 and/or AAV injected animals did not demonstrate significant toxicity, as revealed by the average inflammation scores of portal and lobular inflammation. A set of representative images, shown in Supporting Information Fig. 1, corroborate that PJ-34 administration was nontoxic to murine liver.

PARP-1 inhibition modulates proinflammatory response against AAV2 vectors in vivo

PARP-1 is known to be involved in transcriptional activation of NF-κB in response to proinflammatory stimuli [33]. PARP-1 is also shown to directly interact with NF-κB subunits p65 and p50 [34]. It forms a stable complex with p300 in vivo, allowing stable interactions to take place between NF-κB subunits and p300, which are crucial for the activation of NF-κB in a stimuli-dependent manner [26, 35].

Hence we assessed if inhibition of PARP-1 could moderate the expression of proinflammatory cytokine/chemokine and other NF-κB pathway associated genes induced upon infection with scAAV2 vectors, which are known to be considerably immunogenic than ssAAV2 vectors [11, 36, 37]. In addition, scAAV vectors alone were further evaluated in anticipation of using them to deliver a therapeutic transgene such as FIX, which is under the packaging capacity of these vectors. Groups of PJ-34 pretreated BALB/c mice ($n = 4$) were either mock injected (PBS) or injected with ~5×10^{10} vgs of scAAV2-EGFP vector and euthanized 2 h later to collect hepatocyte RNA [24]. The relative expression of key genes associated with NF-κB-mediated signal transduction and innate immune response was measured using the NF-κB RT-PCR Profiler array (Qiagen, SABiosciences). As shown in Fig. 3 and Supporting Information Fig. 2, a variety of genes involved in activation of NF-κB signaling (such as CD40, TNF, TLR4, RelA), inflammatory response (IL1b, TLR1, TLR4, TLR9), as well as other molecules involved in propagation of the cytokine/ chemokine response to AAV (TRAF2, TRAF3, BCL3, LTBR (where TRAF is TNF receptor associated factor, BCL is B-cell CLL/lymphoma, and LTBR is lymphotoxin beta receptor)) were suppressed by PARP-1 inhibition. Some of genes such as TLR2, CASP1 (where CASP1 is caspase1), ELK1 (where ELK1 is ELK1, member of ETS oncogene family), CD40, MAP3K1, and RelA that had more than 40-fold downregulation in comparison to mock-treated animals are not represented in the graph (Fig. 3). These data demonstrate that ablation of PARP-1 suppresses the innate immune response targeted against AAV vectors.

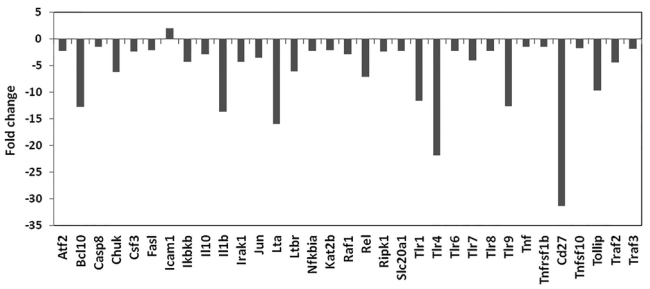

Figure 3. Suppression of AAV vector-induced expression of proinflammatory marker genes in murine liver upon administration of PARP-1 inhibitor. Groups of BALB/c mice, either untreated or treated with PJ-34, were injected with scAAV2 vectors. Expression of NF-κB responsive factors was then measured in the liver tissue 2 h post vector administration. Equal amounts of RNA were pooled from four mice within a group to synthesize the cDNA, which was profiled using the NF-κB RT-PCR Profiler array. β-actin was used as the housekeeping gene for normalization of quantitative PCR data. Genes showing ≥twofold downregulation between PJ-34 and vector administered group versus vector alone injected group from a single experiment are shown.

Synergistic inhibition of PARP-1 and NF-κB effectively suppresses innate response to AAV2 vectors

Even though PARP-1 was instrumental in downregulating the expression of several proinflammatory genes related to NF-κB signaling against AAV vectors, not all the NF-κB target genes depend on PARP-1 for their expression, as inferred from the fact that $PARP^{-/-}$ mice does not exhibit the same phenotype as NF-κB $p65^{-/-}$ mice [38]. Likewise PARP-1 is known to activate other transcription factors such as HIF-1 and AP-1 besides NF-κB [39]. We thus reasoned that combined inhibition of PARP-1 and NF-κB signaling might further impact the inflammatory process during hepatic AAV gene delivery, in comparison to inhibition of PARP-1 alone. Pharmacological inhibitors of NF-κB (Bay11-7085) and PARP-1 (PJ34) were tested both individually and in combination. In addition, clinically approved/tested inhibitors of NF-κB and PARP-1 such as bortezomib (Bo) and ABT-888 (ABT), respectively, were also tested as single agents and in combination. Bo is a proteasome inhibitor approved for the treatment of patients with advanced relapsed and/or refractory multiple myeloma and is a potent NF-κB inhibitor [40–42]. Several PARP-1 inhibitors are currently under Phase I/II clinical trials to evaluate their chemosensitization potential and antitumor activity as single agents or in combination with chemotherapy/radiotherapy toward the potential treatment of various types of cancer. ABT (Veliparib) is one such PARP-1 inhibitor tested for the treatment of several types of solid tumors such as lung, ovarian, fallopian, pancreatic, breast, liver, prostate, head and neck, and brain [43].

Groups of C57BL/6 mice ($n = 5$) pretreated with appropriate compounds as single agents or in combination with these drugs (Fig. 4) were then mock injected (PBS) or injected with scAAV2 vectors. The doses of the drugs used are summarized in Supporting Information Table 1. The expression profile of the various innate immune response markers in murine liver was then evaluated using the NF-κB RT-PCR Profiler array. As shown in Fig. 4, the relative expression of AAV vector induced NF-κB pathway components and responsive factors was downregulated to a greater extent in mice subjected to synergistic inhibition of both PARP-1 and NF-κB, in comparison to inhibition of either NF-κB pathway or PARP-1 alone. In particular, proinflammatory genes within the Toll-like receptor family such as TLR1, TLR2, TLR3, TLR6, and TLR9; TNF receptor (TNFRSF1A, TNFRSF1B); components of NF-κB pathway (RELA, NF-κB1, NF-κB2); and effectors of innate response like TRAF, TRADD, LTBR, BCL3, IL1B were downregulated substantially. Downregulation of RELA, LTA, IL-10, TLR4, and RELB was more than 20-fold and hence has not been represented in the graph (Fig. 4). These data suggest that synergistic inhibition of PARP-1 and NF-κB signaling is more effective in attenuating the proinflammatory response against AAV vectors than independently targeting the PARP-1 or NF-κB pathway.

Combined inhibition of PARP-1 and NF-κB does not alter AAV2-mediated transgene expression in vivo

We next examined if the synergistic inhibition of PARP-1 and NF-κB pathway has any effect on liver-directed gene transfer efficacy of AAV2 vectors. Groups of C57BL/6 mice ($n = 4$) pretreated with combination of Bo and ABT were injected with 1×10^{11} vgs of a scAAV2 vector carrying LUC reporter gene at Day 0 and Day 14. Four weeks after gene transfer, all the treated mice were imaged in an IVIS Spect-CT small animal imaging system to document the bioluminescence corresponding to the expression of LUC gene. As shown in Fig. 5, the difference in AAV2-mediated transgene expression between the treated and untreated groups was insignificant, with (p-value = 0.63). These data show that the combined inhibition of PARP-1 and NF-κB signaling does not alter the transgene expression from scAAV2 vectors in normal mice.

Synergistic inhibition of PARP-1 and NF-κB modulates cytotoxic T-cell response against AAV2 vectors

To evaluate whether combined inhibition of PARP-1 and NF-κB signaling alters the AAV-specific $CD8^+$ T cell based immune response, C57BL/6 mice ($n = 4$) were administered with 1 mg/kg Bo and 12.5 mg/kg ABT followed by i.v. administration of AAV2 at a vector dose of 1×10^{11} vgs/mouse (Fig. 5A). Two weeks later, the drugs were reinjected along with a booster dose of vector. At the end of 4 weeks mice were euthanized. The splenocytes were harvested and the capsid-specific $CD8^+$ T cell based IFN-γ response was evaluated by ELISPOT assay as described in methods. As shown in Fig. 6, the number of spots produced per million splenocytes stimulated with AAV2 capsid-specific peptide was significantly reduced (1.57-fold, $p < 0.05$) in the mice treated with the Bo and ABT as compared to the animals that received AAV2 vectors alone. These data imply that synergistic inhibition of PARP-1 and NF-κB signaling is effective in minimizing the host T-cell response against AAV vectors.

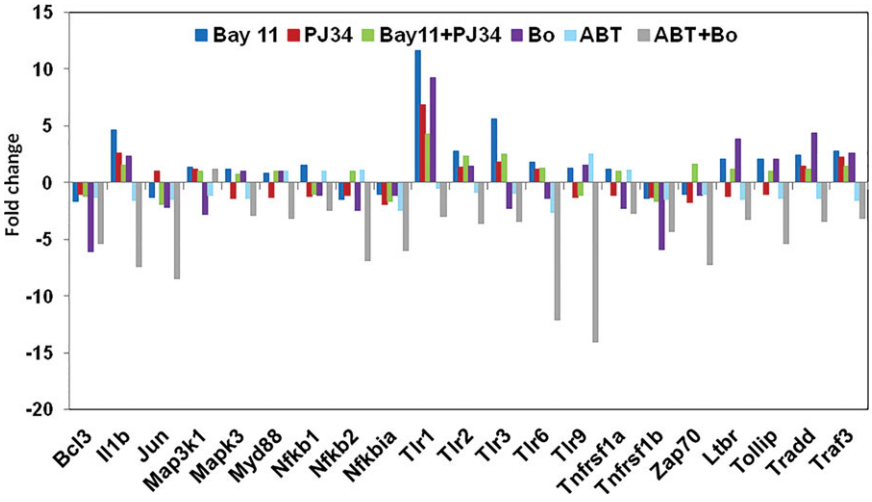

Figure 4. Synergistic inhibition of PARP-1 and NF-κB modulates the levels of AAV2 vector induced proinflammatory marker genes. Relative expression of NF-κB responsive genes and markers of proinflammatory response, measured in the liver tissue of C57BL/6 mice from various treatment groups (as indicated), 2 h after gene transfer with scAAV2 vectors. Equal amounts of RNA were pooled from five mice within a group to make the cDNA, which was profiled using the NF-κB RT-PCR Profiler array. β-actin was used as the housekeeping gene for normalization of quantitative PCR data. Genes showing ≥twofold difference in expression in any of the treatment groups with respect to the vector alone administered group from a single experiment are represented in the graph.

PARP-1/NF-κB combined inhibition suppresses T-cell response to AAV2 vectors in hemophilia B mice

The immune-modulation strategy was further evaluated in a murine model of hemophilia B. Groups of hemophilia B mice ($n = 3$) were pretreated with 1 mg/kg Bo and 12.5 mg/kg ABT and subsequently administered with 5×10^{10} viral dose of scAAV2-LP1-hFIX vector i.v. via the tail vein. After 10 days, booster injection of the drugs followed by the vectors was administered. Control group was administered with only the vectors and not the inhibitor drugs. Subsequently, on Day 18, the splenocytes were isolated and seeded in a 96-well plate in appropriate media conditions. After about 30 h of incubation, the cell culture supernatant was collected and ELISA was done to measure the IFN-γ cytokine secretion from activated T cells. The cytokine concentration of the test conditions was deduced from an IFN-γ standard curve generated as described in methods. As shown in Fig. 7, the vector-targeted IFN-γ T-cell response reduced significantly by 2.78-fold in hemophilia B mice subjected to combined inhibition of PARP-1 and NF-κB signaling. The quantitative PCR analysis of mRNA isolated from liver tissue showed similar levels of FIX expression (1.59-fold) in the AAV2-FIX-administered mice treated with Bo and ABT, in comparison to the untreated animals infused with the vector alone (data not shown). Taken together, these data suggest that the combined inhibition of PARP-1/NF-κB is an effective strategy in mitigating adaptive T-cell responses targeting AAV vectors, which might have implications during gene therapy.

Discussion

In the recent clinical trial for hemophilia B using scAAV8 vectors, two patients were given a short course of glucocorticoid therapy to suppress the immune response causing liver inflammation,

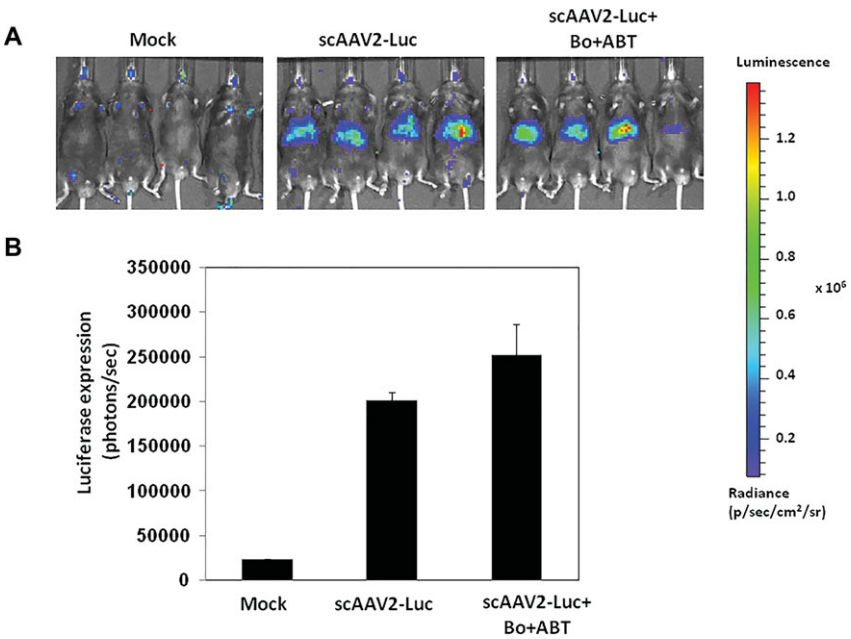

Figure 5. Synergistic inhibition of PARP-1 and NF-κB pathway does not alter the scAAV2-based transgene expression in murine liver. (A) Mice pretreated with combination of Bo and ABT were injected with 1×10^{11} vgs of scAAV2-LUC vector. Booster dose of the inhibitors and vectors was given after 2 weeks. Four weeks after the initial administration, the mice were imaged in an IVIS Spect-CT small animal imaging system to capture the bioluminescence. (B) Quantitation data of the LUC expression from one experiment is shown as mean ± SEM of four mice per group; p-value = 0.63; drug treated versus control group; two-tailed unpaired Student's t-test.

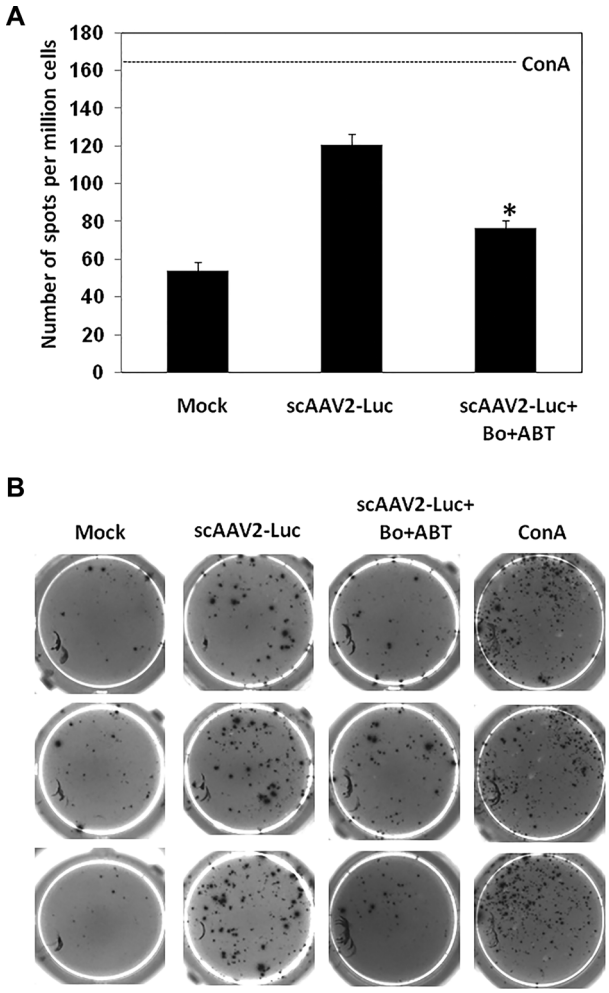

Figure 6. Combined inhibition of PARP-1 and NF-κB modulates the cytotoxic T-cell response against scAAV2 vectors. (A) AAV2 capsid-specific T-cell response was quantitated by IFN-γ-based ELISPOT assay. The graph shows the number of spots generated per million splenocytes stimulated with AAV2 capsid-specific peptide. ConA was used as the positive control (dotted line). Data are shown as mean ± SEM of the number of spots obtained from splenocytes seeded in duplicate wells for each of the four mice per group from one experiment. $^{*}p < 0.05$; drug treated versus control group; two-tailed unpaired Student's *t*-test. (B) Representative images of the wells in the ELISPOT plate of a single experiment, captured using an ELISPOT reader are shown.

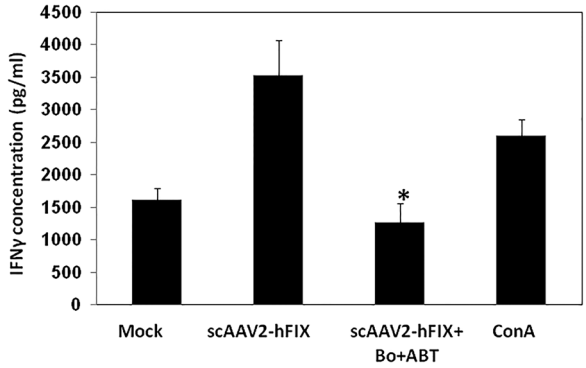

Figure 7. Synergistic inhibition of PARP1 and NF-κB attenuates the AAV2-hFIX vector induced cytotoxic T-cell response in hemophilia B mice. Synergistic inhibition of PARP-1 and NF-κB modulates the $CD8^{+}$ T-cell response against AAV2 vectors in hemophilia B mice. Splenocytes isolated from different groups of mice were seeded in a 96-well plate in appropriate media conditions. The supernatant was collected 30 h after incubation, and IFN-γ secretion from activated T cells was measured by ELISA. IFN-γ concentration in the different samples was determined by extrapolating the absorbance values from the standard curve using the GraphPad Prism 6 software. Data are shown as mean ± SEM of the IFN-γ concentration obtained from splenocytes seeded in duplicate wells for each of the three mice per group from a single experiment. $^{*}p < 0.05$; drug treated versus control group; two-tailed unpaired Student's *t*-test.

as evidenced by the elevated levels of serum amino transferases. The glucocorticoid therapy rescued the hepatocytes from being destroyed by the cytotoxic T cells and allowed persistent expression of the transgene [44]. Combination of a nondepleting CD4 Ab and cyclosporine was shown to abrogate humoral responses to the AAV8 capsid and the transgene protein in mice [45]. However, transient and intensive immunosuppression aimed at blocking the B-cell and T-cell adaptive responses failed to improve AAV5-based liver gene transfer in nonhuman primates [46]. An alternate approach to these strategies would be to specifically target molecules or pathways that trigger immune activation upon AAV delivery.

The inhibitory role of DNA repair proteins in the *Rep*-mediated integration of AAV at AAVS1 site on chromosome 19 has been described. DNA-dependent PK, a DNA repair enzyme, was reported to inhibit AAV integration both in an in vitro cell-free integration system as well as in murine liver [47]. Persistence of AAV vector genomes was considerably higher when AAV2 was injected into the portal vein of severe combined immune-deficient mice (DNA-$PKc^{-/-}$) compared to that of normal C57BL/6 mice (DNA-$PKc^{+/+}$), indicating that absence of DNA-PK facilitates better integration of AAV genome. It is further interesting to note that cellular DNA damage response proteins, such as MRE11-RAD50-NBS1 (MRN complex) restrict the vector transduction. AAV DNA accumulates within the nucleus in discrete foci that are in close proximity to the proteins of the MRN complex [48]. Romanova et al. have shown that PARP-1 directly interacts with AAV Rep and that depletion of PARP-1 using small hairpin RNA enhances integration of the AAV genome in HeLa cells [49]. However, the role of PARP-1 in regulating AAV-based transgene expression and the host immune response to the vector remains unexplored.

In the present study, we first designed experiments to elucidate the effect of PARP-1 inhibition on the AAV vector mediated transgene expression. We found that PARP-1 repression enhances the transgene expression from ssAAV vectors in vitro (Fig. 1A or B). These vectors also exhibited enhanced gene transfer efficacy when targeted to murine liver in the presence of a pharmacological inhibitor of PARP-1, PJ34. On one hand, the increase in liver-directed transgene expression was more predominant with ssAAV8 vectors (~3.4-fold) than ssAAV2 vectors (~twofold) upon PARP-1 ablation (Fig. 1D or E or F). On the other hand, we observed only a modest increase in scAAV2 transduction when PARP-1 was inhibited in vitro (Fig. 2) or in vivo (Fig. 5). This might be possibly

due to the fact that they are more immunogenic than ssAAV2 vectors [11, 36, 37] and/or due to the absence of binding motifs for these cellular proteins in closed scAAV genomes. Taken together, our data show that this strategy of PARP-1 inhibition is likely to be beneficial with ssAAV vectors. This augurs well for delivering large genes such as coagulation factor VIII in ssAAV, which are too large to be encapsidated by scAAV genomes. Nonetheless, for the purpose of gene transfer for hemophilia B, we further evaluated the effect of inhibition of PARP-1/NF-κB using scAAV vectors in vivo. Moreover it has been shown that scAAV vectors are more immunogenic compared to ssAAV vectors [38] and hence this vector system was used to study the effect of synergistic inhibition of PARP/NF-κB on vector-directed immune responses.

Multiple lines of evidence have established the role of PARP-1 in various acute and chronic inflammatory conditions. PARP-1 is a coactivator of NF-κB transcription factor, a central player in the development of inflammation and immune response [33]. Several reports suggest that inflammation could be controlled when PARP-1 activity is blocked, possibly by modulating the activation of transcription factors such as NF-κB, AP-1, or HIF-1 [50–52]. PARP-1 inhibition has also been shown to be therapeutic in inflammatory animal models such as chronic colitis, hemorrhagic shock, cerebral ischemia, autoimmune nephritis, and LPS-induced septic shock [53–55]. T-cell activation requires transcriptional regulation by PARP-1 [56], which also modulates the Th1/Th2 balance and regulates NFAT [57, 58]. Based on these data, we next evaluated if inhibition of PARP-1 might be effective in regulating host immune response against scAAV vectors. Indeed, we found that PARP-1 blockade results in marked attenuation of the expression of various NF-κB responsive proinflammatory factors (Fig. 3). A direct impact on NF-κB pathway was evident by suppression of the RelA, a key molecule in canonical pathway. Most of the Toll-like receptor (TLR) proteins were also downregulated by PARP-1 inhibition. PJ-34, the PARP-1 inhibitor significantly downregulated TLRs, including TLR9 that has been shown to be a major endosomal sensing molecule of scAAV genomes during hepatic gene transfer [36]. Thus, our current studies demonstrate the beneficial effect of targeting DNA damage response protein such as PARP-1 in minimizing the vector-induced inflammatory response. In particular, PARP-1 inhibition has a specific effect on various inflammatory cytokine and other genes related to NF-κB signaling in murine liver. This possibly implies that PARP-1 interacts with NF-κB pathway, supported by previous studies where PARP-1 has been shown to be a coactivator of this transcription factor [26]. However, it must be noted that PARP-1 can modulate the activation of other transcription factors such as AP-1 and HIF-1 as well [50, 51]. The phenotype of PARP KO mice is different from that of mice lacking NF-κB subunit ($p65^{-/-}$ mice), which is embryonically lethal [38]. Thus it can be inferred that though PARP-1 and NF-κB interact, in the context of immune response they can still be mutually exclusive. Moreover NF-κB is a widely expressed inducible transcription factor and the activation of its downstream target genes requires multiple coactivators and cofactors [59]. In addition, other transcription factors such as AP1, ETS, C/EBP, STAT-1, and p53 might also influence the expression of NF-κB-dependent genes [33], suggesting that only a subset of NF-κB target genes would be affected by PARP-1. Along these lines, it would be reasonable to investigate the effect of a combined inhibition of PARP-1 and NF-κB signaling on the host immune response against AAV.

As speculated, we found that the combined inhibition of PARP-1 and NF-κB in vivo showed better modulation of the expression of several proinflammatory and cytokine genes induced by AAV infection (Fig. 4). Relative expressions of proinflammatory markers belonging to TLR family, TNF receptors, NF-κB subunits, and other mediators of inflammation induced by AAV2 infection were particularly suppressed in murine liver upon the combined inhibition, in comparison to inhibition of either NF-κB pathway or PARP-1 alone. This effect was more profound when the combination of clinically tested drugs, Bo and ABT was used (Fig. 4). Bo (PS-314) is an FDA-approved drug for clinical use in the treatment of multiple myeloma [60]. It is a proteasome inhibitor that targets the catalytic 20S core of proteasome and induces apoptosis in cancer cells [61]. The antitumor activity of Bo is attributed to its inhibitory effect on NF-κB, which has been implicated in pathogenesis of cancers by regulating genes involved in cancer cell proliferation, survival, and drug resistance [62]. Previous studies have demonstrated that Bo improves the transduction AAV vectors encoding large FVIII transgene, resulting in long-term phenotypic correction of hemophilia A canine models [63]. Bo is shown to be partially effective in abrogating the preexisting immunity to AAV in mice [64]. ABT (Veliparib), a PARP-1 inhibitor has been successfully tested in numerous Phase II/III clinical trials for the treatment of different cancers such as ovarian cancer, breast cancer, solid tumors, lung cancer, pancreatic cancer, lymphoma, and so on either as a monotherapy or in conjugation with other chemotherapeutic drugs [43]. Nevertheless in the context of AAV-mediated gene therapy, it was tested for the first time in the present studies. It must be also noted that we have used various strains of mice to measure immunogenic response to AAV vectors. As our primary aim was to delineate the effect of PARP-1 inhibition on immune response, we initially used a more immunogenic strain of mice such as BALB/c. In our next set of experiments we wished to examine if a similar effect would be seen in other strains such as C57BL6 mice, which incidentally is also of the same genetic background as hemophilia B mice. In short, the attenuation of immune response with inhibitors targeting PARP and NF-κB in different strains of mice demonstrates the widespread utility of this strategy.

Furthermore our data demonstrated that the combined administration of Bo and ABT not only effectively suppressed the proinflammatory response, but also the adaptive $CD8^+$ T-cell immune response to scAAV vectors. PARP-1/NF-κB combined inhibition markedly attenuated the AAV capsid-driven IFN-γ response in mice, without altering the transgene expression (Figs. 5 and 6). The end point of the study was chosen as 4 weeks because it has been shown that AAV2 capsid degrades slowly and induces the activation and proliferation of $CD8^+$ T cells over a period of several weeks [65]. Booster dosing of the vectors at Day 14 was performed to heighten the AAV2 capsid-specific response from

Ag-primed T cells [66]. Since the primary aim of this part of the study was to examine the immunomodulatory effect of the drug combination, we monitored the LUC expression only after 4 weeks. This was done, to minimize the exposure of mice to stressors (isofluorane anesthesia, luciferin substrate) on Day 13/14. Nonetheless, a more comprehensive study to investigate the effect of these drugs on the transgene expression and Cytotoxic T lymphocyte (CTL) response over an early time point such as 2 weeks after primary gene transfer and prior to booster administration may provide additional insights into the contribution of vector load in this process.

Consistent to the data obtained in normal mice, we also found that the IFN-γ secretion from activated T cells was significantly decreased in AAV2-FIX vector administered hemophilia B mice upon treatment with inhibitors targeting PARP-1 and NF-κB (Fig. 7). Taken together, these results suggest that the synergistic inhibition of NF-κB signaling and PARP-1 molecules offers an alternate strategy for evading immune challenges to AAV vectors during gene therapy. However, its relevance remains to be assessed in higher animal models.

Materials and methods

Animal studies

All animal experiments were performed according to the institutional guidelines for animal care specified at Christian Medical College (Vellore, India). Mice (BALB/c, C57BL/6, and hemophilia B) were purchased from Jackson Laboratory (Bar Harbour, ME). Experimental mice were housed at 22–24°C in individually ventilated cages with free access to water and food.

Cell lines and reagents

Human cervical carcinoma cell line (HeLa) and the packaging cell line AAV-293 were purchased from the American Type Culture Collection (ATCC, Rockville, MD, USA) and Stratagene (Santa Clara, CA, USA), respectively. These cell lines were maintained at 37°C and 5% CO_2 in IMDM (Life Technologies, Carlsbad, CA, USA) supplemented with 10% FBS, 1.2 g/L of sodium bicarbonate, and 1% (by volume) of 100× stock solution of antibiotics (10 000 U penicillin + 10 000 mg streptomycin). A small molecule inhibitor of PARP-1, PJ-34 was obtained from Sigma Aldrich (St Louis, MO, USA) and the clinically tested PARP-1 inhibitor, ABT was from Enzo Life Sciences (Farmingdale, NY, USA). The NF-κB inhibitor, Bay11-7085 was sourced from Calbiochem (Darmstadt, Germany). PARP-1 siRNA was purchased from Cell Signaling Technology (Boston, MA, USA) and D-luciferin substrate was purchased from BioVision Inc (Milpitas, CA). Bo was a kind gift from NATCO Pharma Ltd (Hyderabad, India).

Generation of recombinant AAV vectors

Highly purified stocks of AAV vectors were generated by triple transfection of AAV-293 cells as described previously [67]. For vector preparation, three types of transgenes were used: AAV-CB-EGFP (EGFP gene driven by chicken β-actin promoter), AAV-CB-LUC (LUC gene driven by chicken β-actin promoter), and AAV-LP1-hFIX (human FIX gene driven by LP1 promoter). The AAV-CB-EGFP vectors were generated as either ss or self-complementary forms while the other two transgene-based vectors were based on scAAV backbones. The physical particle titers of the vectors were quantified by slot blot hybridization as previously described [68]. The EGFP and LUC-based reporter plasmids used for the vector generation were kind gifts from Dr. Arun Srivastava, University of Florida, Gainesville, USA while the FIX transgene containing plasmid was a kind gift by Dr. Amit Nathwani, UCL, London, UK.

Recombinant AAV2 vector transduction assays in vitro

Approximately 1.6×10^5 HeLa cells were seeded in a single well of a 12-well plate. Cells in the test condition were transfected with 100 nM of PARP-1 siRNA or scrambled siRNA using Lipofectamine (Life Technologies). Twenty-four hours post siRNA or mock transfection, cells were transduced with scAAV2-EGFP or ssAAV2-EGFP vectors at an multiplicity of infection of 2000 vgs per cell. Forty-eight hours postinfection, EGFP expression was measured by fluorescence microscopy (Leica DMI6000B, Germany). Images from five visual fields were quantitatively analyzed by Adobe Photoshop CS2 software and expressed as mean pixels per visual field. Student's *t*-test was used to calculate the statistical significance.

Recombinant AAV2 vector transduction studies in vivo

To study the effect of PARP-1 inhibition on AAV-mediated transgene expression, groups ($n = 4$ per group) of 8–12 weeks old BALB/c mice were administered with PJ-34 (10 mg/kg body weight) i.p. in a 100 μL volume diluted in sterile water at 24 h (Day 0) and 30 min prior to vector injection and subsequently once a week till the animals were euthanized. On Day 1, these animals were mock injected (PBS) or injected with $\sim 5 \times 10^{10}$ vgs of scAAV2-EGFP vectors or $\sim 1 \times 10^{11}$ vgs of ssAAV2-EGFP vectors or $\sim 5 \times 10^{10}$ vgs of ssAAV8-EGFP vectors per animal in a 200 μL suspension via the tail vein. Four weeks after vector administration, mice were euthanized. Cross-sections from three hepatic lobes of the mock-injected and vector- injected groups were assessed for EGFP expression by fluorescence microscopy as described above. Student's *t*-test was used to calculate the statistical significance.

For the combined inhibition of PARP-1 and NF-κB in vivo, groups of 8–12 weeks old C57BL/6 mice ($n = 4$) were administered with 1 mg/kg Bo (for NF-κB inhibition) and 12.5 mg/kg ABT (for PARP-1 inhibition) followed by i.v. administration of scAAV2-LUC vector at a dose of 1×10^{11} vgs/mouse. Bo was administered i.v. 1 day prior to vector administration while ABT was injected

into the peritoneal cavity about 2 h before the vector administration. Two weeks later the drugs were reinjected along with a booster dose of vector to heighten the immune response, if any. All animals were euthanized at 4 weeks time point and the following parameters were analyzed: LUC expression and IFN-γ response by ELISPOT assay. The LUC gene expression was measured by serial imaging of the mice after administration of D-luciferin (Bio-Vision Inc; 2.5 mg in 100 μL for 20 g mouse body weight) in an IVIS Spect-CT small animal imaging system (Perkin Elmer, Caliper Life Sciences, Hopkinton, MA). The bioluminescence captured was quantitatively expressed as photons per second. For validation study in a therapeutic model, groups of 8–12 weeks old hemophilia B mice ($n = 3$) pretreated with 1 mg/ kg Bo and 12.5 mg/ kg ABT were injected with 5×10^{10} vgs of scAAV2-LP1-hFIX vector i.v. After 10 days, a booster injection of the drugs and vectors was given and the animals euthanized a week later. Thereafter, the FIX gene levels in the liver tissue were measured by quantitative real-time PCR and the cytotoxic T-cell response against the vector was assessed by performing ELISA.

Western blot analysis

Nuclear fractions were isolated from HeLa cells using the NE-PER kit as per the manufacturer's protocol (Thermo Scientific–Pierce Biotechnology, Rockford, USA). Normalized amounts of protein lysates from HeLa cells were resolved by SDS-PAGE in 4–20% Tris-HCl gradient gels (Biorad Laboratories, Hercules, CA, USA), transferred to Immobilon-P membranes (Millipore, Bedford, MA), and probed with the following antibodies: polyclonal rabbit anti-PARP-1 or monoclonal mouse anti-Lamin A/C (Cell Signaling Technology, Boston, MA, USA). The immunoreactive bands were detected by anti-idiotype, HRP-linked anti-rabbit IgG or anti-mouse IgG antibodies (Cell Signaling Technology), visualized using chemiluminescence detection kit (ECL-Plus, GE Healthcare, WI, USA), and documented in ImageQuant 400 imager (GE Healthcare).

Gene-expression analysis by real-time quantitative PCR

For assessing the modulation of the proinflammatory response to AAV vectors, mice ($n = 4$–5) pretreated with appropriate compounds (Bay11-7085, PJ34, Bo, or ABT) as single agents or in combination were either mock injected or injected with ~5×10^{10} vgs of scAAV2 vectors and euthanized 2 h post PBS or AAV administration. The dosage and timing of drug intervention was as described above for in vivo transduction assays. Bay11-7085 was administered at 20 mg/kg i.p dose 1 day prior to infusion of vector. Hepatocyte RNA was extracted using the RNeasy mini kit (Qiagen, Valencia, CA). One microgram of RNA was reverse transcribed to cDNA using RT^2 First Strand kit (Qiagen) according to the manufacturer's protocol. The cDNA was profiled by the NF-κB RT-PCR Profiler array (Qiagen, SABiosciences, Frederick, MD, USA) to determine the relative gene expression of 84 key genes related to NF-κB-mediated signal transduction and innate immune response. The data were analyzed using an ABI Prism 7500 Sequence Detection System version 1.1 (Life Technologies, Applied Biosystems). Gene expression was measured by the comparative threshold cycle ($\Delta\Delta$Ct) method and analyzed by the SABiosciences web-based software www.sabiosciences.com/pcr/arrayanalysis.php.

ELISPOT assay and ELISA to measure the T-cell response

To perform the ELISPOT assay, freshly isolated mouse splenocytes were subjected to RBC lysis, following which they were seeded at a density of 1×10^6 cells/well in RPMI media (Life Technologies) containing 10% FBS. Average yield of cells from the spleen of one mouse was about 1×10^8 cells/ mL. These cells were then treated with 2 μg/mL of T-cell epitope peptide, specific to AAV2 serotype and C57BL/6 mouse strain (sequence SNYNKSVNV) (JPT Peptide Technologies, GmbH, Germany). Plates precoated with anti-IFN-γ antibodies (MABTECH, Ohio, USA) were used for the ELISPOT assay. The assay was done as per the manufacturer's protocol. Concanavalin A (ConA) at a concentration of 2 μg/mL was added as a positive control. After about 30 h of incubation, the plates were developed by using BCIP/NBT and the spot forming units were enumerated in an ELISPOT reader (AID reader, GmbH, Germany). Images of the wells of the developed ELISPOT plate was also captured using the ELISPOT reader. The number of distinct spots formed corresponds to the IFN-γ secretion by activated CD8$^+$ T cells. Student's *t*-test was used to calculate the statistical significance between the test and control groups.

To perform IFN-γ ELISA, freshly isolated splenocytes were seeded in normal 96-well plates with seeding densities and other conditions similar to ELISPOT assay. After the incubation period of about 30 h, the cell culture supernatant was collected from each well, diluted, and analyzed using ELISA kit for mouse IFN-γ (MABTECH, Ohio, USA) as per the manufacturer's protocol. Briefly, the samples were added to ELISA plates precoated with anti-mouse IFN-γ mAb. After incubation, biotinylated detection Ab and streptavidin-HRP conjugate was added. Addition of a chromogen enzyme substrate (TMB enzyme) resulted in a colored product whose intensity was directly proportional to the IFN-γ concentration in the sample. The absorbance was read in a microplate reader at 450 nm wavelength. A standard curve ranging from 1 to 1000 pg/mL was prepared by serially diluting the reconstituted IFN-γ cytokine standard stock solution (1 μg/mL) and plotting the concentrations against the 450 nm absorbance values. A sigmoidal standard curve was generated and the sample values were extrapolated from it using the Graph Pad Prism 6 software. The final IFN-γ protein concentrations of the samples (dilution factor multiplied) were determined and compared across the treatment groups.

Histological examinations

Liver tissues from PBS-injected mice or those injected with either AAV2-EGFP/AAV8-EGFP vectors alone or in combination with

PJ-34 were collected 4 weeks postinjection, fixed in 10% buffered formalin, and processed for microscopy. Three micron thick sections were cut and stained with H&E. The degree of lobular and portal inflammation was scored (inflammation score) by a certified hepatopathologist, who was blinded to the experimental conditions. Inflammatory scores were graded as 0—no inflammation, 1—mild inflammation, 2—moderate inflammation, 3—severe inflammation, for both lobular and portal inflammation.

Acknowledgments: G.R.J. is supported by research grants from Department of Science of Technology, Government of India (Swarnajayanti Fellowship 2011), Department of Biotechnology (DBT), Government of India (Senior Innovative Young Biotechnologist award 2010: BT/03/IYBA/2010; Grant BT/PR5021/MED/30/757/2012; Grant: BT/PR8599/AGR/36/783/2013; and an initiation grant (2014-256) from IIT, Kanpur. Author Contribution: S.H. and B.R. performed the experiments, G.R.J. conceptualized and designed the study, S.H. and G.R.J. wrote the manuscript.

Conflict of interest: The authors declare no commercial or financial conflict of interest.

References

1 **Mingozzi, F. and High, K. A.**, Therapeutic in vivo gene transfer for genetic disease using AAV: progress and challenges. *Nat. Rev. Genet.* 2011. **12**: 341–355.

2 **Ginn, S. L., Alexander, I. E., Edelstein, M. L., Abedi, M. R. and Wixon, J.**, Gene therapy clinical trials worldwide to 2012—an update. *J. Gene Med.* 2013. **15**: 65–77.

3 **Cideciyan, A. V., Hauswirth, W. W., Aleman, T. S., Kaushal, S., Schwartz, S. B., Boye, S. L., Windsor, E. A. et al.,** Vision 1 year after gene therapy for Leber's congenital amaurosis. *N. Engl. J. Med.* 2009. **361**: 725–727.

4 **Maguire, A. M., Simonelli, F., Pierce, E. A., Pugh, E. N., Jr., Mingozzi, F., Bennicelli, J., Banfi, S. et al.,** Safety and efficacy of gene transfer for Leber's congenital amaurosis. *N. Engl. J. Med.* 2008. **358**: 2240–2248.

5 **Manno, C. S., Pierce, G. F., Arruda, V. R., Glader, B., Ragni, M., Rasko, J. J., Ozelo, M. C. et al.,** Successful transduction of liver in hemophilia by AAV-factor IX and limitations imposed by the host immune response. *Nat. Med.* 2006. **12**: 342–347.

6 **Mingozzi, F., Maus, M. V., Hui, D. J., Sabatino, D. E., Murphy, S. L., Rasko, J. E., Ragni, M. V. et al.,** CD8(+) T-cell responses to adeno-associated virus capsid in humans. *Nat. Med.* 2007. **13**: 419–422.

7 **Gao, G. P., Lu, Y., Sun, X., Johnston, J., Calcedo, R., Grant, R. and Wilson, J. M.**, High-level transgene expression in nonhuman primate liver with novel adeno-associated virus serotypes containing self-complementary genomes. *J. Virol.* 2006. **80**: 6192–6194.

8 **Nathwani, A. C., Tuddenham, E. G., Rangarajan, S., Rosales, C., McIntosh, J., Linch, D. C., Chowdary, P. et al.,** Adenovirus-associated virus vector-mediated gene transfer in hemophilia B. *N. Engl. J. Med.* 2011. **365**: 2357–2365.

9 **Kelkar, S., De, B. P., Gao, G., Wilson, J. M., Crystal, R. G. and Leopold, P. L.**, A common mechanism for cytoplasmic dynein-dependent microtubule binding shared among adeno-associated virus and adenovirus serotypes. *J. Virol.* 2006. **80**: 7781–7785.

10 **Hirosue, S., Senn, K., Clement, N., Nonnenmacher, M., Gigout, L., Linden, R. M. and Weber, T.**, Effect of inhibition of dynein function and microtubule-altering drugs on AAV2 transduction. *Virology* 2007. **367**: 10–18.

11 **Balakrishnan, B., Sen, D., Hareendran, S., Roshini, V., David, S., Srivastava, A. and Jayandharan, G. R.**, Activation of the cellular unfolded protein response by recombinant adeno-associated virus vectors. *PLoS One* 2013. **8**: e53845.

12 **Gabriel, N., Hareendran, S., Sen, D., Gadkari, R. A., Sudha, G., Selot, R., Hussain, M. et al.,** Bioengineering of AAV2 capsid at specific serine, threonine, or lysine residues improves its transduction efficiency in vitro and in vivo. *Hum. Gene Ther. Methods* 2013. **24**: 80–93

13 **Mowat, F. M., Gornik, K. R., Dinculescu, A., Boye, S. L., Hauswirth, W. W., Petersen-Jones, S. M. and Bartoe, J. T.**, Tyrosine capsid-mutant AAV vectors for gene delivery to the canine retina from a subretinal or intravitreal approach. *Gene Ther.* 2014. **21**: 96–105.

14 **Petrs-Silva, H., Dinculescu, A., Li, Q., Deng, W. T., Pang, J. J., Min, S. H., Chiodo, V. et al.,** Novel properties of tyrosine-mutant AAV2 vectors in the mouse retina. *Mol. Ther.* 2011. **19**: 293–301.

15 **Sen, D., Gadkari, R. A., Sudha, G., Gabriel, N., Sathish Kumar, Y., Selot, R., Samuel, R. et al.,** Targeted modifications in adeno-associated virus (AAV) serotype -8 capsid improves its hepatic gene transfer efficiency in vivo. *Hum. Gene Ther. Methods* 2013. **24**: 104–116

16 **Mingozzi, F., Meulenberg, J. J., Hui, D. J., Basner-Tschakarjan, E., Hasbrouck, N. C., Edmonson, S. A., Hutnick, N. A. et al.,** AAV-1-mediated gene transfer to skeletal muscle in humans results in dose-dependent activation of capsid-specific T cells. *Blood* 2009. **114**: 2077–2086.

17 **Hareendran, S., Balakrishnan, B., Sen, D., Kumar, S., Srivastava, A. and Jayandharan, G. R.**, Adeno-associated virus (AAV) vectors in gene therapy: immune challenges and strategies to circumvent them. *Rev. Med. Virol.* 2013. **23**: 399–413.

18 **Chambon, P., Weill, J. D. and Mandel, P.**, Nicotinamide mononucleotide activation of new DNA-dependent polyadenylic acid synthesizing nuclear enzyme. *Biochem. Biophys. Res. Commun.* 1963. **11**: 39–43.

19 **D'Amours, D., Desnoyers, S., D'Silva, I. and Poirier, G. G.**, Poly(ADP-ribosyl)ation reactions in the regulation of nuclear functions. *Biochem. J.* 1999. **342**(Pt 2): 249–268.

20 **Underhill, C., Toulmonde, M. and Bonnefoi, H.**, A review of PARP inhibitors: from bench to bedside. *Ann. Oncol.* 2011. **22**: 268–279.

21 **Ohsaki, E., Ueda, K., Sakakibara, S., Do, E., Yada, K. and Yamanishi, K.**, Poly(ADP-ribose) polymerase 1 binds to Kaposi's sarcoma-associated herpesvirus (KSHV) terminal repeat sequence and modulates KSHV replication in latency. *J. Virol.* 2004. **78**: 9936–9946.

22 **Tempera, I., Deng, Z., Atanasiu, C., Chen, C. J., D'Erme, M. and Lieberman, P. M.**, Regulation of Epstein-Barr virus OriP replication by poly(ADP-ribose) polymerase 1. *J. Virol.* 2010. **84**: 4988–4997.

23 **Muthumani, K., Choo, A. Y., Zong, W. X., Madesh, M., Hwang, D. S., Premkumar, A., Thieu, K. P. et al.,** The HIV-1 Vpr and glucocorticoid receptor complex is a gain-of-function interaction that prevents the nuclear localization of PARP-1. *Nat. Cell. Biol.* 2006. **8**: 170–179.

24 **Jayandharan, G. R., Aslanidi, G., Martino, A. T., Jahn, S. C., Perrin, G. Q., Herzog, R. W. and Srivastava, A.**, Activation of the NF-kappaB pathway by adeno-associated virus (AAV) vectors and its implications in immune response and gene therapy. *Proc. Natl. Acad. Sci. USA* 2011. **108**: 3743–3748.

25 **Ullrich, O., Diestel, A., Eyupoglu, I. Y. and Nitsch, R.**, Regulation of microglial expression of integrins by poly(ADP-ribose) polymerase-1. *Nat. Cell Biol.* 2001. **3**: 1035–1042.

26 **Hassa, P. O., Buerki, C., Lombardi, C., Imhof, R. and Hottiger, M. O.**, Transcriptional coactivation of nuclear factor-kappaB-dependent gene expression by p300 is regulated by poly(ADP)-ribose polymerase-1. *J. Biol. Chem.* 2003. **278**: 45145–45153.

27 **Giansanti, V., Dona, F., Tillhon, M. and Scovassi, A. I.**, PARP inhibitors: new tools to protect from inflammation. *Biochem. Pharmacol.* 2010. **80**: 1869–1877.

28 **Abdelkarim, G. E., Gertz, K., Harms, C., Katchanov, J., Dirnagl, U., Szabo, C. and Endres, M.**, Protective effects of PJ34, a novel, potent inhibitor of poly(ADP-ribose) polymerase (PARP) in in vitro and in vivo models of stroke. *Int. J. Mol. Med.* 2001. **7**: 255–260.

29 **Haddad, M., Rhinn, H., Bloquel, C., Coqueran, B., Szabo, C., Plotkine, M., Scherman, D. et al.,** Anti-inflammatory effects of PJ34, a poly(ADP-ribose) polymerase inhibitor, in transient focal cerebral ischemia in mice. *Br. J. Pharmacol.* 2006. **149**: 23–30.

30 **Scott, G. S., Kean, R. B., Mikheeva, T., Fabis, M. J., Mabley, J. G., Szabo, C. and Hooper, D. C.**, The therapeutic effects of PJ34 [N-(6-oxo-5,6-dihydrophenanthridin-2-yl)-N,N-dimethylacetamide.HCl], a selective inhibitor of poly(ADP-ribose) polymerase, in experimental allergic encephalomyelitis are associated with immunomodulation. *J. Pharmacol. Exp. Ther.* 2004. **310**: 1053–1061.

31 **Jagtap, P. and Szabo, C.**, Poly(ADP-ribose) polymerase and the therapeutic effects of its inhibitors. *Nat. Rev. Drug Discov.* 2005. **4**: 421–440.

32 **Phulwani, N. K. and Kielian, T.**, Poly (ADP-ribose) polymerases (PARPs) 1–3 regulate astrocyte activation. *J. Neurochem.* 2008. **106**: 578–590.

33 **Hassa, P. O. and Hottiger, M. O.**, The functional role of poly(ADP-ribose)polymerase 1 as novel coactivator of NF-kappa B in inflammatory disorders. *Cell. Mol. Life. Sci.* 2002. **59**: 1534–1553.

34 **Hassa, P. O., Covic, M., Hasan, S., Imhof, R. and Hottiger, M. O.**, The enzymatic and DNA binding activity of PARP-1 are not required for NF-kappa B coactivator function. *J. Biol. Chem.* 2001. **276**: 45588–45597.

35 **Hassa, P. O., Haenni, S. S., Buerki, C., Meier, N. I., Lane, W. S., Owen, H., Gersbach, M. et al.,** Acetylation of poly(ADP-ribose) polymerase-1 by p300/CREB-binding protein regulates coactivation of NF-kappa B-dependent transcription. *J. Biol. Chem.* 2005. **280**: 40450–40464.

36 **Martino, A. T., Suzuki, M., Markusic, D. M., Zolotukhin, I., Ryals, R. C., Moghimi, B., Ertl, H. C. et al.,** The genome of self-complementary adeno-associated viral vectors increases Toll-like receptor 9-dependent innate immune responses in the liver. *Blood* 2011. **117**: 6459–6468.

37 **Wu, T., Topfer, K., Lin, S. W., Li, H., Bian, A., Zhou, X. Y., High, K. A. et al.,** Self-complementary AAVs induce more potent transgene product-specific immune responses compared to a single-stranded genome. *Mol. Ther.* 2012. **20**: 572–579.

38 **Beg, A. A., Sha, W. C., Bronson, R. T., Ghosh, S. and Baltimore, D.**, Embryonic lethality and liver degeneration in mice lacking the RelA component of NF-kappa B. *Nature* 1995. **376**: 167–170.

39 **Martin-Oliva, D., Aguilar-Quesada, R., O'Valle, F., Munoz-Gamez, J. A., Martinez-Romero, R., Garcia Del Moral, R., Ruiz de Almodovar, J. M. et al.,** Inhibition of poly(ADP-ribose) polymerase modulates tumor-related gene expression, including hypoxia-inducible factor-1 activation, during skin carcinogenesis. *Cancer Res.* 2006. **66**: 5744–5756.

40 **Berenson, J. R., Yang, H. H., Sadler, K., Jarutirasarn, S. G., Vescio, R. A., Mapes, R., Purner, M. et al.,** Phase I/II trial assessing bortezomib and melphalan combination therapy for the treatment of patients with relapsed or refractory multiple myeloma. *J. Clin. Oncol.* 2006. **24**: 937–944.

41 **Juvekar, A., Manna, S., Ramaswami, S., Chang, T. P., Vu, H. Y., Ghosh, C. C., Celiker, M. Y. et al.,** Bortezomib induces nuclear translocation of IkappaBalpha resulting in gene-specific suppression of NF-kappaB–dependent transcription and induction of apoptosis in CTCL. *Mol. Cancer Res.* 2011. **9**: 183–194.

42 **Ludwig, H., Khayat, D., Giaccone, G. and Facon, T.**, Proteasome inhibition and its clinical prospects in the treatment of hematologic and solid malignancies. *Cancer* 2005. **104**: 1794–1807.

43 **Lupo, B. and Trusolino, L.**, Inhibition of poly(ADP-ribosyl)ation in cancer: old and new paradigms revisited. *Biochim. Biophys. Acta* 2014. **1846**: 201–215.

44 **Nathwani, A. C., Reiss, U. M., Tuddenham, E. G., Rosales, C., Chowdary, P., McIntosh, J., Della Peruta, M. et al.,** Long-term safety and efficacy of factor IX gene therapy in hemophilia B. *N. Engl. J. Med.* 2014. **371**: 1994–2004.

45 **McIntosh, J. H., Cochrane, M., Cobbold, S., Waldmann, H., Nathwani, S. A., Davidoff, A. M. and Nathwani, A. C.**, Successful attenuation of humoral immunity to viral capsid and transgenic protein following AAV-mediated gene transfer with a non-depleting CD4 antibody and cyclosporine. *Gene Ther.* 2012. **19**: 78–85.

46 **Unzu, C., Hervas-Stubbs, S., Sampedro, A., Mauleon, I., Mancheno, U., Alfaro, C., de Salamanca, R. E. et al.,** Transient and intensive pharmacological immunosuppression fails to improve AAV-based liver gene transfer in non-human primates. *J. Transl. Med.* 2012. **10**: 122.

47 **Song, S., Lu, Y., Choi, Y. K., Han, Y., Tang, Q., Zhao, G., Berns, K. I. et al.,** DNA-dependent PK inhibits adeno-associated virus DNA integration. *Proc. Natl. Acad. Sci. USA* 2004. **101**: 2112–2116.

48 **Cervelli, T., Palacios, J. A., Zentilin, L., Mano, M., Schwartz, R. A., Weitzman, M. D. and Giacca, M.**, Processing of recombinant AAV genomes occurs in specific nuclear structures that overlap with foci of DNA-damage-response proteins. *J. Cell Sci.* 2008. **121**: 349–357.

49 **Romanova, L. G., Zacharias, J., Cannon, M. L. and Philpott, N. J.**, Effect of poly(ADP-ribose) polymerase 1 on integration of the adeno-associated viral vector genome. *J. Gene Med.* 2011. **13**: 342–352.

50 **Martinez-Romero, R., Martinez-Lara, E., Aguilar-Quesada, R., Peralta, A., Oliver, F. J. and Siles, E.**, PARP-1 modulates deferoxamine-induced HIF-1alpha accumulation through the regulation of nitric oxide and oxidative stress. *J. Cell. Biochem.* 2008. **104**: 2248–2260.

51 **Oliver, F. J., Menissier-de Murcia, J. and de Murcia, G.**, Poly(ADP-ribose) polymerase in the cellular response to DNA damage, apoptosis, and disease. *Am. J. Hum. Genet.* 1999. **64**: 1282–1288.

52 **Roebuck, K. A., Rahman, A., Lakshminarayanan, V., Janakidevi, K. and Malik, A. B.**, H2O2 and tumor necrosis factor-alpha activate intercellular adhesion molecule 1 (ICAM-1) gene transcription through distinct cis-regulatory elements within the ICAM-1 promoter. *J. Biol. Chem.* 1995. **270**: 18966–18974.

53 **Cohen, J.**, The immunopathogenesis of sepsis. *Nature* 2002. **420**: 885–891.

54 **Jog, N. R., Dinnall, J. A., Gallucci, S., Madaio, M. P. and Caricchio, R.**, Poly(ADP-ribose) polymerase-1 regulates the progression of autoimmune nephritis in males by inducing necrotic cell death and modulating inflammation. *J. Immunol.* 2009. **182**: 7297–7306.

55 **Roesner, J. P., Vagts, D. A., Iber, T., Eipel, C., Vollmar, B. and Noldge-Schomburg, G. F.**, Protective effects of PARP inhibition on liver microcirculation and function after haemorrhagic shock and resuscitation in male rats. *Intens. Care Med.* 2006. **32**: 1649–1657.

56 **Saenz, L., Lozano, J. J., Valdor, R., Baroja-Mazo, A., Ramirez, P., Parrilla, P., Aparicio, P. et al.,** Transcriptional regulation by poly(ADP-ribose) polymerase-1 during T cell activation. *BMC Genomics* 2008. **9**: 171.

57 **Olabisi, O. A., Soto-Nieves, N., Nieves, E., Yang, T. T., Yang, X., Yu, R. Y., Suk, H. Y. et al.,** Regulation of transcription factor NFAT by ADP-ribosylation. *Mol. Cell. Biol.* 2008. **28**: 2860–2871.

58 **Oumouna, M., Datta, R., Oumouna-Benachour, K., Suzuki, Y., Hans, C., Matthews, K., Fallon, K. and Boulares, H.,** Poly(ADP-ribose) polymerase-1 inhibition prevents eosinophil recruitment by modulating Th2 cytokines in a murine model of allergic airway inflammation: a potential specific effect on IL-5. *J. Immunol.* 2006. **177**: 6489–6496.

59 **Sheppard, K. A., Rose, D. W., Haque, Z. K., Kurokawa, R., McInerney, E., Westin, S., Thanos, D. et al.,** Transcriptional activation by NF-kappaB requires multiple coactivators. *Mol. Cell. Biol.* 1999. **19**: 6367–6378.

60 **Richardson, P. G., Barlogie, B., Berenson, J., Singhal, S., Jagannath, S., Irwin, D., Rajkumar, S. V. et al.,** A phase 2 study of bortezomib in relapsed, refractory myeloma. *N. Engl. J. Med.* 2003. **348**: 2609–2617.

61 **Shah, J. J. and Orlowski, R. Z.,** Proteasome inhibitors in the treatment of multiple myeloma. *Leukemia* 2009. **23**: 1964–1979.

62 **Hideshima, T., Chauhan, D., Richardson, P., Mitsiades, C., Mitsiades, N., Hayashi, T., Munshi, N. et al.,** NF-kappa B as a therapeutic target in multiple myeloma. *J. Biol. Chem.* 2002. **277**: 16639–16647.

63 **Monahan, P. E., Lothrop, C. D., Sun, J., Hirsch, M. L., Kafri, T., Kantor, B., Sarkar, R. et al.,** Proteasome inhibitors enhance gene delivery by AAV virus vectors expressing large genomes in hemophilia mouse and dog models: a strategy for broad clinical application. *Mol. Ther.* 2010. **18**: 1907–1916.

64 **Karman, J., Gumlaw, N. K., Zhang, J., Jiang, J. L., Cheng, S. H. and Zhu, Y.,** Proteasome inhibition is partially effective in attenuating pre-existing immunity against recombinant adeno-associated viral vectors. *PLoS One* 2012. **7**: e34684.

65 **Li, H., Tuyishime, S., Wu, T. L., Giles-Davis, W., Zhou, D., Xiao, W., High, K. A. et al.,** Adeno-associated virus vectors serotype 2 induce prolonged proliferation of capsid-specific $CD8^+$ T cells in mice. *Mol. Ther.* 2011. **19**: 536–546.

66 **Chen, J., Wu, Q., Yang, P., Hsu, H. C. and Mountz, J. D.,** Determination of specific CD4 and CD8 T cell epitopes after AAV2- and AAV8-hF.IX gene therapy. *Mol. Ther.* 2006. **13**: 260–269.

67 **Ling, C., Lu, Y., Cheng, B., McGoogan, K. E., Gee, S. W., Ma, W., Li, B. et al.,** High-efficiency transduction of liver cancer cells by recombinant adeno-associated virus serotype 3 vectors. *J. Vis. Exp.* 2011. doi: 10.3791/2538.

68 **Kube, D. M. and Srivastava, A.,** Quantitative DNA slot blot analysis: inhibition of DNA binding to membranes by magnesium ions. *Nucleic Acids Res.* 1997. **25**: 3375–3376.

Abbreviations: **AAV**: adeno-associated virus · **ABT**: ABT-888 · **Bo**: bortezomib · **EGFP**: enhanced green fluorescent protein · **PARP-1**: poly(ADP-ribose) polymerase-1 · **vgs**: viral genomes

Full correspondence: Dr. G. R. Jayandharan, Department of Biological Sciences and Bioengineering, Indian Institute of Technology, Kanpur 208 016, Uttar Pradesh, India
Fax: +91-512-2594010
e-mail: jayrao@iitk.ac.in

Received: 16/6/2015
Revised: 4/9/2015
Accepted: 30/9/2015
Accepted article online: 7/10/2015

HUMAN GENE THERAPY METHODS 24:80–93 (April 2013)

DOI: 10.1089/hgtb.2012.194

Bioengineering of AAV2 Capsid at Specific Serine, Threonine, or Lysine Residues Improves Its Transduction Efficiency *in Vitro* and *in Vivo*

Nishanth Gabriel,[1*] Sangeetha Hareendran,[2*] Dwaipayan Sen,[1*] Rupali A. Gadkari,[3] Govindarajan Sudha,[3] Ruchita Selot,[2] Mansoor Hussain,[2] Ramya Dhaksnamoorthy,[2] Rekha Samuel,[2] Narayanaswamy Srinivasan,[3] Alok Srivastava,[1,2] and Giridhara R. Jayandharan[1,2]

Abstract

We hypothesized that the AAV2 vector is targeted for destruction in the cytoplasm by the host cellular kinase/ubiquitination/proteasomal machinery and that modification of their targets on AAV2 capsid may improve its transduction efficiency. *In vitro* analysis with pharmacological inhibitors of cellular serine/threonine kinases (protein kinase A, protein kinase C, casein kinase II) showed an increase (20–90%) on AAV2-mediated gene expression. The three-dimensional structure of AAV2 capsid was then analyzed to predict the sites of ubiquitination and phosphorylation. Three phosphodegrons, which are the phosphorylation sites recognized as degradation signals by ubiquitin ligases, were identified. Mutation targets comprising eight serine (S) or seven threonine (T) or nine lysine (K) residues were selected in and around phosphodegrons on the basis of their solvent accessibility, overlap with the receptor binding regions, overlap with interaction interfaces of capsid proteins, and their evolutionary conservation across AAV serotypes. AAV2-EGFP vectors with the wild-type (WT) capsid or mutant capsids (15 S/T→alanine [A] or 9 K→arginine [R] single mutant or 2 double K→R mutants) were then evaluated *in vitro*. The transduction efficiencies of 11 S/T→A and 7 K→R vectors were significantly higher (~63–90%) than the AAV2-WT vectors (~30–40%). Further, hepatic gene transfer of these mutant vectors *in vivo* resulted in higher vector copy numbers (up to 4.9-fold) and transgene expression (up to 14-fold) than observed from the AAV2-WT vector. One of the mutant vectors, S489A, generated ~8-fold fewer antibodies that could be cross-neutralized by AAV2-WT. This study thus demonstrates the feasibility of the use of these novel AAV2 capsid mutant vectors in hepatic gene therapy.

Introduction

Recombinant adeno-associated viral (AAV) vectors based on serotype 2 have been used successfully for *in vivo* gene transfer in numerous preclinical animal models (Mingozzi and High, 2011). AAV2 vectors have shown sustained clinical benefit when targeted to immune-privileged sites such as for Leber's congenital amaurosis (Simonelli *et al.*, 2010). However, their therapeutic efficiency when targeted to other organ systems, such as during hepatic gene transfer in patients with hemophilia B, is suboptimal because of the $CD8^+$ T cell response directed against the AAV capsid particularly at higher administered vector doses ($\geq 2\times10^{12}$ viral genomes [VG]/kg) (Manno *et al.*, 2006). A similar theme of vector dose-dependent immunotoxicity has emerged from the use of alternative AAV serotypes in other clinical trials as well (Stroes *et al.*, 2008). More recently, in the recombinant AAV8-mediated gene transfer for hemophilia B (Nathwani *et al.*, 2011), two patients who received the highest dose (2×10^{12} VG/kg) of vector required glucocorticoid therapy to attenuate a capsid-specific T cell response developed against capsid. Therefore, irrespective of whether an alternative AAV serotype (other than AAV2) or an immune suppression protocol is used, it is important to develop novel AAV vectors that provide enhanced gene expression at significantly lower vector doses to achieve successful gene transfer in humans.

[1]Department of Hematology, Christian Medical College, Vellore 632004, Tamil Nadu, India.
[2]Centre for Stem Cell Research, Christian Medical College, Vellore 632002, Tamil Nadu, India.
[3]Molecular Biophysics Unit, Indian Institute of Science, Bengaluru 560012, India.
*N.G., S.H., and D.S. contributed equally to this work.

Although conventional wild-type AAV2 (AAV2-WT) vectors can transduce a variety of cell types and tissues, the onset of gene expression is slow and they typically require several weeks to achieve sustained, steady state levels of transgene expression (Buning *et al.*, 2008). The AAV capsid has been reported to influence transduction efficiency at many steps, including vector binding to cell surface receptors, internalization, cytoplasmic trafficking to the nuclear membrane, and viral uncoating (Nonnenmacher and Weber, 2012). It has been shown that epidermal growth factor receptor protein tyrosine kinase (EGFR-PTK)-mediated tyrosine phosphorylation of capsid surface-exposed AAV2 residues leads to ubiquitination and proteasomal degradation of viral particles (Jayandharan *et al.*, 2008; Zhong *et al.*, 2008b). The use of proteasomal inhibitors is known to result in an ~2-fold increase in gene expression from AAV vectors (Monahan *et al.*, 2010). However, systemic administration of these proteasomal inhibitors leads to severe side effects (Rajkumar *et al.*, 2005). Alternatively, altering the enzymatic (kinase/ubiquitin ligase) targets on AAV capsid may be a rational approach to circumvent capsid ubiquitination and increase the transduction efficiency of these vectors.

AAV capsid is composed of three proteins—VP1, VP2, and VP3—generated from a single *cap* gene by alternative splicing (Becerra *et al.*, 1985; Trempe and Carter, 1988). Specific residues/motifs on AAV capsid are known to interact with viral receptors on the cell membrane, help in the endosomal escape of the vector (Girod *et al.*, 2002), and, importantly, determine the serotype of the vector. Hence it is but logical to assume that capsid mutagenesis of AAV vectors can introduce functional changes in the vector. To this end, the generation of hybrid serotypes by capsid fusion of multiple serotypes and capsid mutations has been reported (Choi *et al.*, 2005; Koerber *et al.*, 2008). Earlier studies, wherein random capsid mutations of AAV2 were introduced, have demonstrated that such modifications could alter the efficiency of vector packaging, receptor binding, intracellular trafficking, or transgene expression (Kern *et al.*, 2003; Opie *et al.*, 2003; Lochrie *et al.*, 2006). More recently, site-specific mutagenesis of AAV2 capsid to generate tyrosine-mutant AAV2 vectors has demonstrated increased gene expression *in vitro* and *in vivo* (Zhong *et al.*, 2008b; Li *et al.*, 2010). However, because serine (8%), threonine (7.2%), and lysine (4%) residues are more abundant on AAV2 capsid than are tyrosine residues (3.5%), we hypothesized that mutating amino acids other than tyrosines on AAV2 capsid may provide further opportunities to augment AAV-mediated gene expression. This hypothesis is supported by several studies. Targeted inhibition of the serine/threonine kinase phosphorylation of a cellular protein, FK506-binding protein 52 (FKBP52), improves AAV-mediated gene transfer by 30-fold compared with the ~5-fold increase seen by inhibition of tyrosine kinases alone (Zhao *et al.*, 2006). It is also known that lysine residues are direct targets for host cell ubiquitination (Hatakeyama *et al.*, 2005) and therefore modifying them is likely to reduce vector ubiquitination and subsequent proteasome-mediated degradation. On the basis of these data, the present study was designed to test the *in vitro* and *in vivo* efficacy of novel AAV2 vectors that are modified at critical serine/threonine/lysine residues of the vector capsid.

Materials and Methods

Cell lines and reagents

Human cervical carcinoma cell line HeLa and human embryonic kidney cell line HEK-293 were obtained from the American Type Culture Collection (ATCC, Manassas, VA). The packaging cell line for the vectors, AAV-293, was obtained from Stratagene/Agilent Technologies (Palo Alto, CA). Cells were maintained as monolayer cultures in Iscove's modified Dulbecco's medium (Life Technologies, Carlsbad, CA) supplemented with 10% fetal bovine serum (Sigma-Aldrich, St. Louis, MO), 1% by volume of a 100× stock solution of antibiotics (penicillin–streptomycin), and sodium bicarbonate (1.2 g/liter; Sigma-Aldrich). Small-molecule inhibitors of protein kinase A (PKA) (PKA inhibitor fragment 6–22 amide), PKC (inhibitor Gö 6983), and casein kinase II (CKII) (inhibitor TBB) were purchased from Sigma-Aldrich. Fragment 6–22 amide is derived from the active portion of the heat-stable PKA inhibitor protein PKI. Go6983 is a direct inhibitor of L type Ca^{2+} channel and can selectively inhibit several PKC isozymes. TBB (4,5,6,7-tetrabromobenzotriazole) is a highly selective, ATP/GTP-competitive inhibitor of casein kinase II.

Structural analysis of AAV2 capsid

The three-dimensional structure of the AAV2 capsid from the Protein Data Bank (Berman *et al.*, 2000) (PDB accession number 1LP3) (Xie *et al.*, 2002) was analyzed extensively. Protein–protein interaction interface residues on the capsid proteins were determined by a distance-based method using computer programs described elsewhere (De *et al.*, 2005). Briefly, a residue pair from the adjacent subunits is said to be in the interaction interface if the distance between the two interacting atoms is greater than the sum of their van der Waals radii plus 0.5 Å. Solvent accessibility values of the residues were determined with the NACCESS program (Hubbard and Thornton, 1993). Phosphorylation sites in capsid proteins were predicted with NetPhosK (http://www.cbs.dtu.dk/services/NetPhosK/), Phosida (Phosphorylation Site Database; http://www.phosida.com/), KinasePhos (http://kinasephos.mbc.nctu.edu.tw/), and Scansite (http://scansite.mit.edu/) prediction servers whereas ubiquitination sites were predicted with UbiPred (http://iclab.life.nctu.edu.tw/ubipred/), Composition of *k*-Spaced Amino Acid Pairs (CKSAAP_UbSite; http://protein.cau.edu.cn/cksaap_ubsite/), and Prediction of Ubiquitination Sites with Bayesian Discriminant Method (BDM-PUB; http://bdmpub.biocuckoo.org/index.php) prediction servers.

Structures were visualized with the PyMOL software package (DeLano, 2002). To assess the conservation of the predicted phosphorylation as well as ubiquitination sites, multiple sequence alignment of the VP1 sequence across the 10 serotypes was generated with ClustalW (Chenna *et al.*, 2003). The nomenclature of the target amino acids is based on the AAV2 VP1 reference sequence in the NCBI database (accession number NC_001401).

Site-directed mutagenesis

Serine (S)→alanine (A), threonine (T)→A (alanine), and lysine (K)→arginine (R) mutations were introduced into the AAV2 *rep/cap* plasmid (p.ACG2; a kind gift from A. Srivastava, University of Florida, Gainesville, FL) with a QuikChange II XL site-directed mutagenesis kit (Stratagene/

Agilent Technologies) in accordance with the manufacturer's protocol. Briefly, a one-step PCR amplification of the target sites was performed for 18 cycles with the primers (Supplementary Table S1; supplementary data are available online at http://www.liebertpub.com/hgtb) followed by *Dpn*I digestion for 1 hr. Two microliters of this digested PCR product was then transformed into XL10-Gold ultracompetent cells (Stratagene/Agilent Technologies). After plasmid isolation, the presence of the desired point mutation was verified by restriction digestion analysis and DNA sequencing (Applied Biosystems 3130 genetic analyzer; Life Technologies, Warrington, UK).

Generation of recombinant vectors

Highly purified stocks of self-complementary (sc) AAV2-WT or 26 capsid mutants of AAV2 vectors or AAV8-WT vector carrying the enhanced green fluorescent protein (EGFP) gene driven by the chicken β-actin promoter were generated by polyethyleneimine-based triple transfection of AAV-293 cells (Ling *et al.*, 2011). Briefly, forty 150-mm^2 dishes 80% confluent with AAV-293 cells were transfected with AAV2 *rep/cap* (p.ACG2), transgene (dsAAV2-EGFP), and AAV-helper free (p.helper) plasmids. Cells were collected 72 hr post-transfection, lysed, and treated with Benzonase nuclease (25 units/ml; Sigma-Aldrich). Subsequently, the vectors were purified by iodixanol gradient ultracentrifugation (OptiPrep; Sigma-Aldrich) (Zolotukhin *et al.*, 1999) followed by column chromatography (HiTrap SP column; GE Healthcare Life Sciences, Pittsburgh, PA). The vectors were finally concentrated to a final volume of 0.5 ml in phosphate-buffered saline (PBS), using Amicon Ultra 10K centrifugal filters (Millipore, Bedford, MA). The physical particle titers of the vectors were quantified by slot-blot analysis and expressed as vector genomes per milliliter (Kube and Srivastava, 1997).

Recombinant AAV2 vector transduction assays in vitro

To assess the effect of pharmacological inhibition of cellular serine/threonine kinases on AAV2 transduction, approximately 1.6×10^5 HeLa cells were mock (PBS)-treated or pretreated with optimal concentrations of PKA inhibitor (25 n*M*), PKC inhibitor (70 n*M*), or CKII inhibitor (1 μM), or with a combination of each of these inhibitors overnight and transduced with AAV2-WT vector at 2×10^3 VG/cell. The safe and effective concentration of kinase inhibitors used was determined by 3-(4,5-dimethylthiazol-2-yl)-2,5-diphenyltetrazolium bromide (MTT) assay, performed with three 10-fold dilutions around the median inhibition constant (IC_{50}) values for these small-molecule inhibitors. Twenty-four hours later, transgene expression was measured by flow cytometry (FACS Calibur; BD Biosciences, San Jose, CA). A total of 1×10^4 events were analyzed for each sample. Mean values of percent EGFP positivity from three replicate samples were used for comparison between treatment groups.

To assess the efficacy of the novel mutant vectors generated, HeLa or HEK-293 cells were mock-infected or infected with either AAV2-WT or AAV2 S/T/K mutant vector (2×10^3 VG/cell). Forty-eight hours post-transduction, transgene expression was quantitated by flow cytometry (FACSCalibur; BD Biosciences) or captured by EGFP imaging. For flow cytometric analysis, HeLa or HEK-293 cells were trypsinized (0.05% trypsin; Sigma-Aldrich) and rinsed twice with PBS (pH 7.4). A total of 1×10^4 events were analyzed for each sample. In total, three independent experiments were performed including three intraassay replicates in each of the experiment. Mean values of percent GFP positivity from these nine replicate samples were used for comparison between AAV2-WT- and AAV2 S/T/K-infected cells.

Recombinant AAV2 vector transduction studies in vivo

C57BL/6 mice were purchased from Jackson Laboratory (Bar Harbor, ME). All animal experiments were approved and carried out according to the institutional guidelines for animal care (Christian Medical College, Vellore, India). Groups ($n=4$ per group) of 8- to 12-week-old C57BL/6 mice were mock-injected or injected with 5×10^{10} VG each of scAAV2-WT or scAAV2 S/T/K mutant vector carrying the EGFP transgene, via the tail vein. Mice were killed 4 weeks after vector administration. Cross-sections from three hepatic lobes of the mock-injected and vector-injected groups were assessed for EGFP expression by fluorescence microscopy.

Estimation of AAV2 vector genome copies and EGFP expression in murine hepatocytes by quantitative PCR analysis

To quantitate the transduction efficiency of AAV2 vectors *in vivo*, liver tissue samples were collected from each of the mice injected with either AAV2-WT or AAV2 S/T/K mutant vector, 4 weeks after vector administration. Genomic DNA was isolated with a QIAamp DNA mini kit (Qiagen, Valencia, CA). Vector genome copy numbers per diploid genome were quantified with TaqMan probes and primers designed against the AAV2 inverted terminal repeat (ITR) sequence and estimated as described previously (Aurnhammer *et al.*, 2011), using a low-ROX quantitative PCR MasterMix according to the protocol of the manufacturer (Eurogentec, Seraing, Belgium).

To measure EGFP transcript levels, total RNA was isolated from murine hepatocytes 4 weeks after vector administration, using TRIzol reagent (Sigma-Aldrich). Approximately 1 μg of RNA was reverse transcribed, using Verso reverse transcriptase according to the manufacturer's protocol (Thermo Scientific, Surrey, UK). TaqMan PCR was done with primers and probe against the EGFP gene (forward primer, CTTCAAGATCCGC CACAACATC; reverse primer, ACCATGTGATCGCGCTTC TC; probe, FAM-CGCCGACCACTACCAGCAGAACACC-TA MRA), according to the manufacturer's protocol (Eurogentec). Glyceraldehyde-3-phosphate dehydrogenase (GAPDH) was used as the housekeeping control gene. Data were captured and analyzed with ABI Prism 7500 sequence detection system version 1.1 software (Life Technologies).

Estimation of neutralizing antibodies against S/T/K AAV2 vectors

Heat-inactivated serum samples from AAV2-WT-injected or S→A and K→R mutant AAV2-injected C57BL/6 mice were assayed for neutralizing antibody (NAb) titers as described previously (Calcedo *et al.*, 2009). Briefly, groups of mice ($n=4$) were administered 5×10^{10} VG of AAV2-WT and AAV2 S/T/K mutant vectors via tail vein injections. Four

weeks after vector delivery, animals were killed and serum was collected. The pooled serum was snap frozen to −80°C. Samples were analyzed by the Immunology Core (Gene Therapy Program, Department of Pathology and Laboratory Medicine, University of Pennsylvania, Philadelphia, PA). The NAb titer was reported as the highest serum dilution that inhibited AAV transduction of Huh7 cells by 50% or more compared with that for the naive serum control.

Ubiquitin conjugation assay and immunoblotting

A ubiquitination assay of viral capsids was done with a ubiquitin–protein conjugation kit according to the protocol of the manufacturer (Boston Biochem, Cambridge, MA). Briefly, 10× energy solution, conjugation fraction A, conjugation fraction B, and ubiquitin were mixed to a final reaction volume of 100 μl. The conjugation reaction was then initiated by adding 3×10^8 heat-denatured AAV2-WT, AAV2 mutant vector, or AAV5 viral particles and incubated at 37°C for 4 hr. Equal volumes of sodium dodecyl sulfate (SDS)-denatured ubiquitinated samples were then resolved on a 4–20% gradient gel. The ubiquitination pattern for the various viral particles was detected by immunoblotting of the samples with mouse anti-ubiquitin monoclonal antibody (P4D1) and horseradish peroxidase (HRP)-conjugated anti-mouse IgG1 secondary (Cell Signaling Technology, Boston, MA). VP1, VP2, and VP3 capsid proteins were detected with AAV clone B1 antibody (Fitzgerald, North Acton, MA) and HRP-conjugated anti-mouse IgG1 secondary antibody (Cell Signaling Technology).

Histological examination

Liver tissues from mock-injected mice or those injected with either AAV2-WT or AAV2 mutant vector were collected 4 weeks postinjection, fixed in 10% buffered formalin, and processed for microscopy. Three-micron-thick liver sections were cut and stained with hematoxylin and eosin. The degree of lobular and portal inflammation was scored (inflammation score, IS) by a pathologist, who was blinded to the experimental conditions. Inflammation scores were based on the degree of lobular and portal inflammation and expressed as follows: 0, no inflammation; 1, minimal inflammation; 2, mild inflammation; 3, moderate inflammation. The median score for each group ($n=3$) was calculated.

Results

Structural analysis of AAV2 capsid to select amino acids for mutagenesis

To select mutation positions in the AAV2 capsid, the three-dimensional structure available for the capsid (Protein Data Bank accession number 1LP3) (Xie *et al.*, 2002), was analyzed extensively. Sites for phosphorylation and the kinases involved in this process as well as ubiquitination sites were predicted with various software tools, as mentioned in Materials and Methods. Most commonly, the sites predicted were probable targets of the kinases PKA, PKC, and CKII. The consensus residues, predicted by most of the prediction tools, were given higher preference and selected as mutation targets.

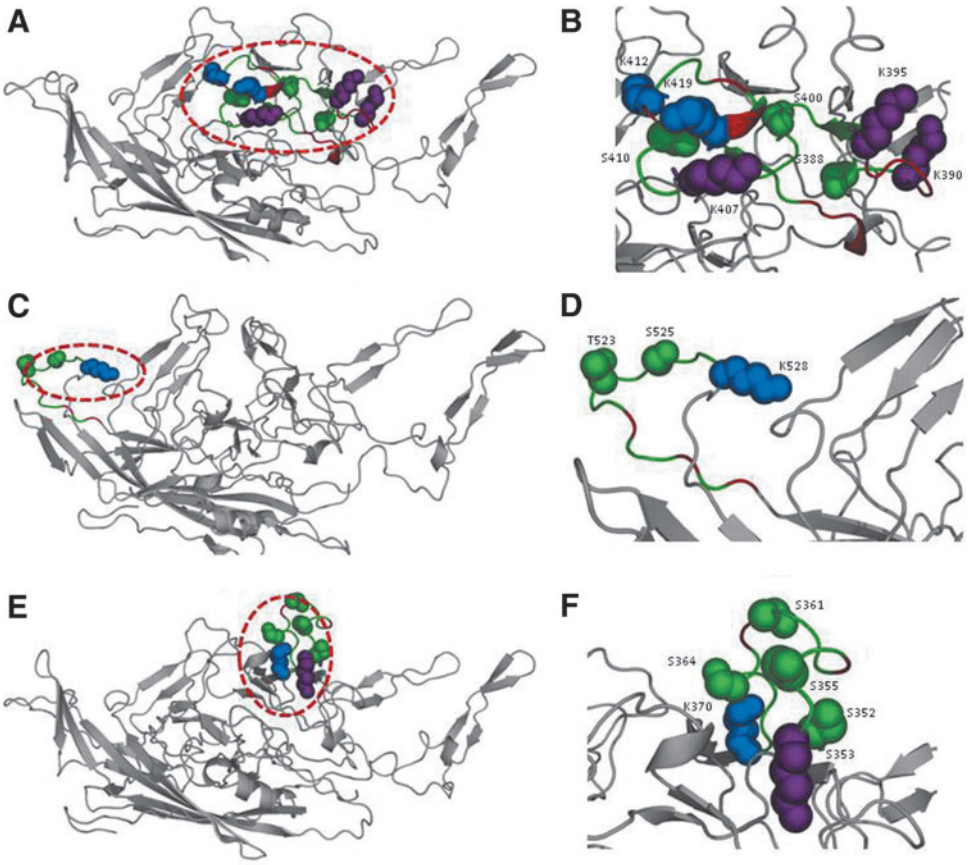

FIG. 1. Structural analysis of phosphodegrons 1–3 in the AAV2 capsid. **(A)**, **(C)**, and **(E)** show phosphodegrons 1, 2, and 3 colored in green, respectively, and corresponding zoomed-in regions of the three phosphodegrons are shown in **(B)**, **(D)**, and **(F)**, respectively. Phosphodegrons in the AAV2 capsid are largely present in the loop regions and are solvent exposed as shown. The phosphorylation and ubiquitination sites in the phosphodegrons are shown as green and blue spheres, respectively. Receptor-binding residues that have also been predicted as ubiquitination sites are shown as purple spheres. The acidic residues in phosphodegrons 1 and 3 and prolines in phosphodegron 2 are colored red whereas the rest of the protein structure is shown in gray. The images were generated with PyMOL software (DeLano, 2002). Color images available online at www.liebertpub.com/hgtb

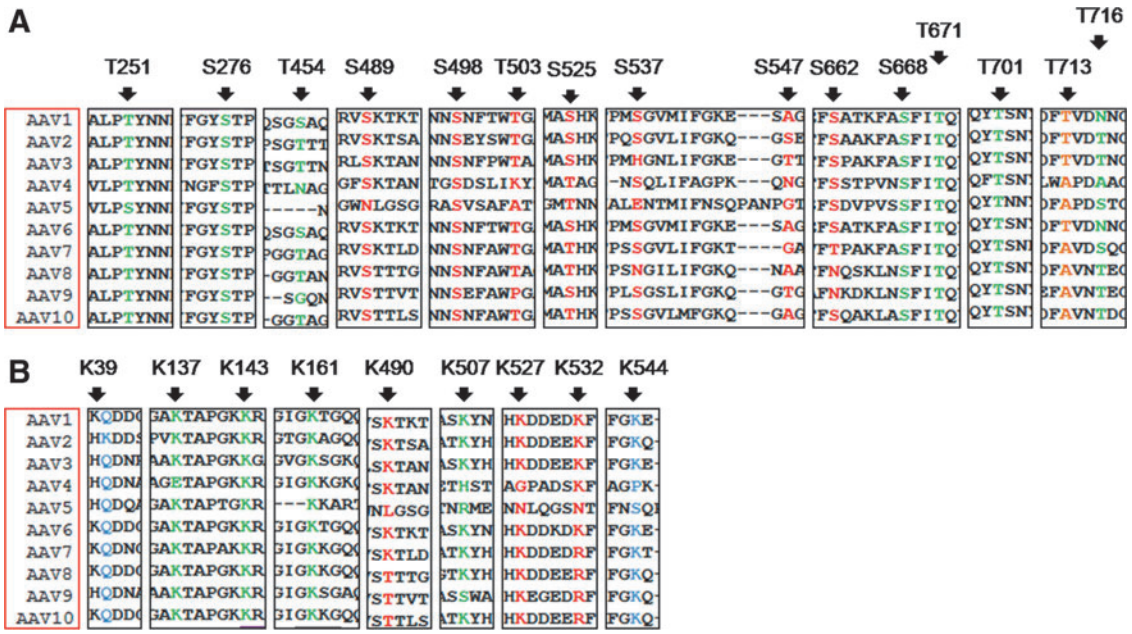

FIG. 2. Schematic representation and conservation status of the various serine (S), threonine (T), and lysine (K) residues mutated in the AAV2 capsid. VP1 protein sequences from AAV serotypes 1 through 10 were aligned with ClustalW and the conservation status of each of the mutated sites is given. S/T residues are shown in **(A)** and lysine residues are shown in **(B)**. S/T/K residues within phosphodegrons 1, 2, and 3 are shown in red whereas those chosen on the basis of evolutionary conservation are shown in green. Those residues that were chosen on the basis of either *in silico* prediction to be a part of a phosphosite or high ubiquitination score with the UbiPred tool are shown in blue. A control threonine mutation shown in brown was chosen as a negative control for the mutation experiments. Color images available online at www.liebertpub.com/hgtb

The phosphorylation and ubiquitination sites forming phosphodegrons were then identified in the AAV2 capsid. It is known that the serine/threonine residues in phosphodegrons reside in the vicinity of lysine residues (within 9–13 residues in the sequence), allowing them to be identified as a degradation signal by the ubiquitin ligase enzyme (Wu *et al.*, 2003). Also, a negative charge often accumulates near the phosphosite and there are multiple phosphosites in one phosphodegron (Wang *et al.*, 2012). The region separating phosphosite and ubiquitination site is largely unstructured and solvent exposed (Inobe *et al.*, 2011). With this information, three phosphodegrons were identified in the AAV2 capsid as shown in Fig. 1. Interactions between the capsid proteins need to be critically maintained to preserve the capsid geometry. Hence, the interaction interfaces were determined from the capsid structure, using both the distance criterion and the accessibility criterion (De *et al.*, 2005), as mentioned in Materials and Methods. Thus, in selecting mutation targets, care was taken that the residues did not belong to these interaction interfaces. A group of positively charged residues on the AAV2 capsid, distributed in three clusters, mediates binding of AAV2 to heparin sulfate receptors (Kern *et al.*, 2003; Opie *et al.*, 2003). Hence, lysines in the receptor-binding regions, if lying in/around phosphodegrons, were still selected and mutated to arginine residues but the serines and threonines were left unaltered. Conservation of a residue across AAV serotypes was considered an added advantage in selection for mutation (Fig. 2). Table 1 summarizes the features of the three phosphodegrons identified and highlights the selected mutation targets within the phosphodegron sequences.

Pharmacological inhibition of cellular serine/threonine kinases improves AAV2-mediated gene expression in vitro

Our *in silico* analysis of the AAV2 capsid structure, using various phosphorylation prediction tools, identified PKA,

Table 1. Location and Amino Acid Sequence of the Three Phosphodegrons in the AAV2 Capsid[a]

Phosphodegron	*Amino acid position (NCBI numbering)*	*Amino acid sequence (N-C terminus)*	*Average solvent accessibility (%)*
1	525–564	**S**hK**D**deekffpq**S**gvlifg**K**qg**S**ektnvdiekvmitdeee	23.6
2	652–665	pvpanpst**T**f**S**aa**K**	35.0
3	489–507	**SK**tsadnnn**S**eysw**T**gat**K**	24.5

[a]The predicted phosphorylation and ubiquitination sites (shown in boldface) that are highly conserved among all the serotypes of AAV within the phosphodegron region (shown enlarged) are listed. All three phosphodegrons are solvent accessible as shown by their high average solvent accessibility.

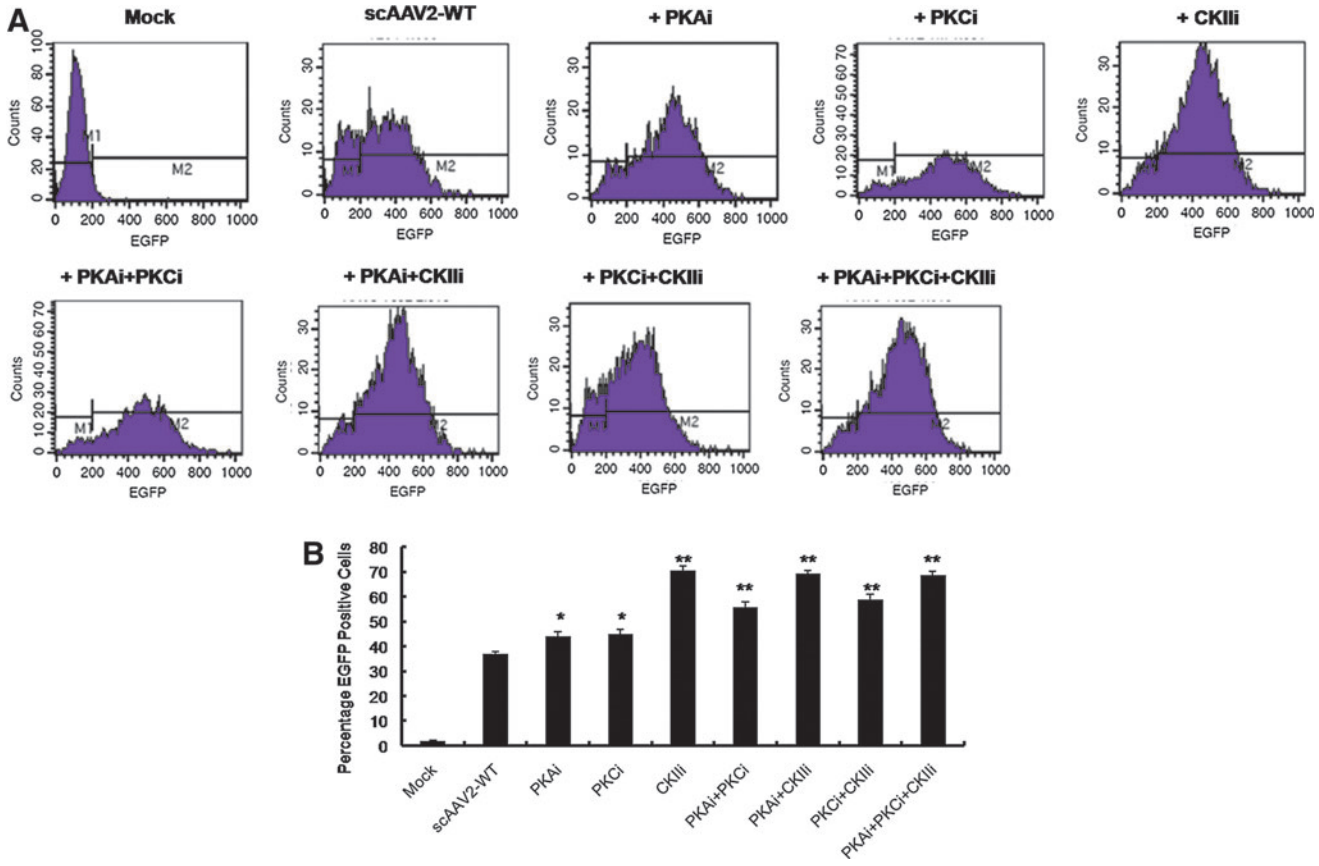

FIG. 3. Effect of pharmacological inhibition of host cellular serine/threonine kinases on AAV2-mediated gene expression. **(A)** HeLa cells were mock (PBS)-treated or pretreated with protein kinase A (PKA), protein kinase C (PKC), and casein kinase II (CKII) inhibitors (PKAi, PKCi, and CKIIi, respectively) either alone or in the combinations shown, 24 hr before transduction with AAV2-EGFP vectors. Twenty-four hours post-transduction, cell suspensions were analyzed for EGFP expression by flow cytometry. **(B)** Quantitative representation of the data from **(A)**. One-way analysis of variance (ANOVA) was used for statistical analysis. $*p<0.05$; $**p<0.01$ versus AAV2-WT-infected cells. Color images available online at www.liebertpub.com/hgtb

PKC, and CKII as major binding partners of phosphodegrons of the AAV2 capsid. Because these enzymes are primarily serine/threonine kinases with an ability to phosphorylate S/T residues, we hypothesized that the inhibition of these viral capsid phosphorylating kinases could augment AAV2 transduction. To test whether the host cellular PKA, PKC, and CKII serine/threonine kinases play a rate-limiting role in AAV2 transduction, we inhibited the kinase activity by specific small-molecule inhibitors and then infected HeLa cells with scAAV2-EGFP vector. As can be seen in Fig. 3A and B, significantly higher gene expression from the AAV2-WT vector was observed when HeLa cells were pretreated with these kinase inhibitors, with a maximal 90% increase seen in cells treated with the CKII inhibitor. This demonstrates that one or more surface-exposed serine and/or threonine amino acids in the AAV2 capsid is phosphorylated within the host cell by PKA, PKC, and CKII serine/threonine kinases and that specific inhibition of this process improves gene expression from the AAV vectors. Because systemic administration of serine/threonine kinase inhibitors in an *in vivo* setting is likely to be toxic (Force and Kolaja, 2011), we instead chose to modify the kinase target substrates in the AAV2 capsid to further improve the transduction efficiency of AAV2 vectors.

Table 2. Physical Particle Packaging Titers (Viral Genomes/ml) of AAV2 Serine/Threonine/Lysine Mutant Vectors

Serine (S)→ Alanine (A)[a]	*Threonine (T)→ Alanine (A)*[a]	*Lysine (K)→ Arginine (R)*[a]
S276A (1.65×10^{10})	T251A (1.8×10^{12})	K39R (2.4×10^{11})
S489A (3.2×10^{12})	T454A (2.5×10^{10})	K137R (3×10^{12})
S498A (1×10^{12})	T503A (5.25×10^{10})	K143R (2.3×10^{12})
S525A (3.2×10^{12})	T671A (1.6×10^{12})	K161R (9×10^{11})
S537A (8×10^{11})	T701A (3.2×10^{12})	K490R (2.3×10^{11})
S547A (1.6×10^{12})	T713A (3.2×10^{12})	K507R (2×10^{11})
S662A (3.2×10^{12})	T716A (5.25×10^{10})	K527R (3.2×10^{11})
S668A (4×10^{11})		K532R (2.4×10^{12})
		K544R (3×10^{11})
		K527R + K532R (6×10^{11})
		K490R + K532R (2×10^{11})

[a]Average packaging titers from at least two packaging experiments. Vectors were generated by polyethyleneimine-based triple transfection of AAV-293 cells. The vectors were purified by iodixanol gradient ultracentrifugation and column chromatography (mentioned in Materials and Methods) and resuspended in a final volume of 0.5 ml of phosphate-buffered saline. The titers of wild-type self-complementary AAV2 vectors ranged between 4×10^{11} and 1×10^{12} VG/ml in the laboratory. VG, viral genomes.

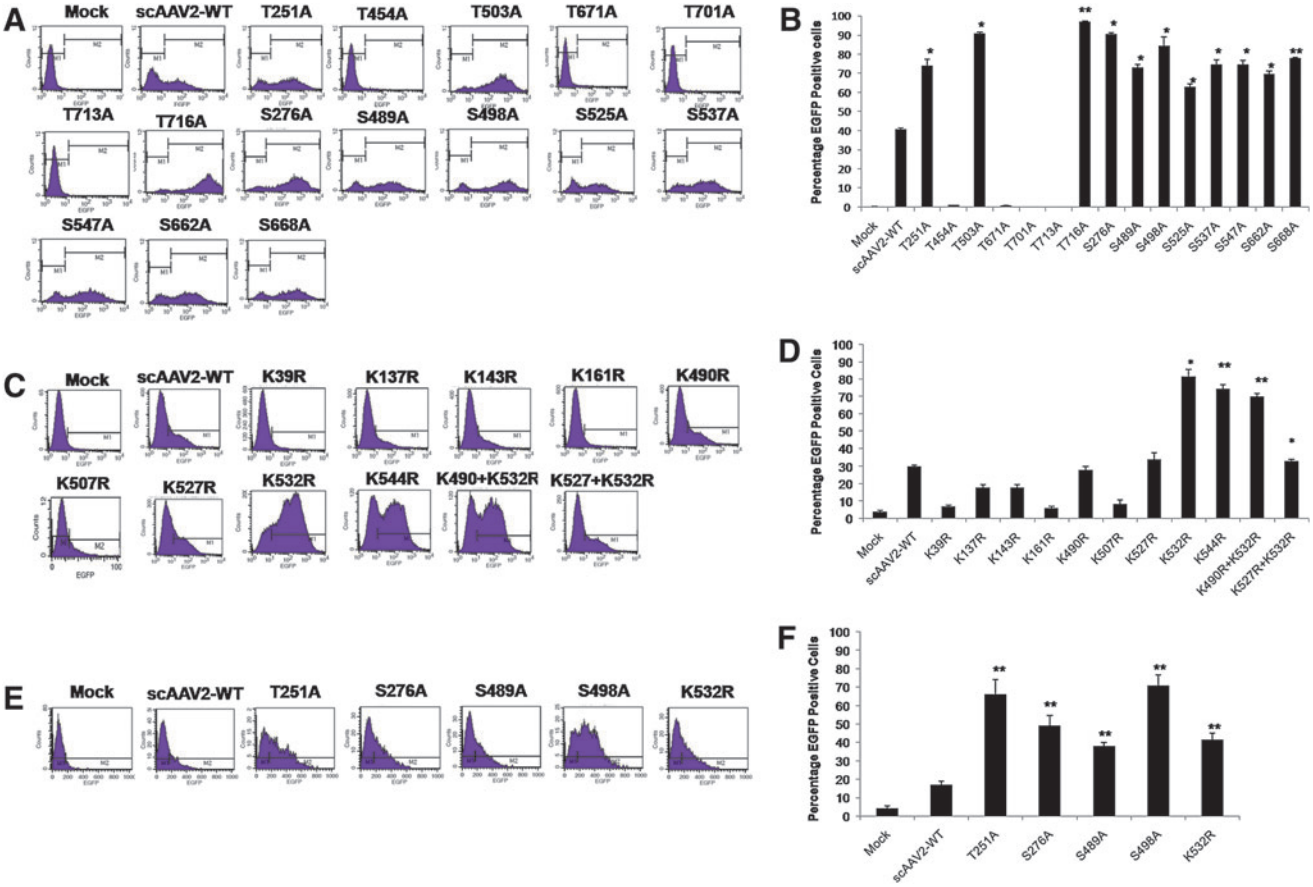

FIG. 4. AAV2 serine/threonine/lysine mutant vectors demonstrate increased transduction efficiency *in vitro.* HeLa cells were either mock-infected or infected at 2×10^3 viral genome (VG)/cell with AAV2-WT or AAV2 S/T→A **(A)** or AAV2 K→R **(C)** mutant vectors and cells were analyzed for EGFP expression 48 hr later by flow cytometry. The percentage of EGFP-positive cells posttransduction with either serine/threonine mutants **(B)** or lysine mutants **(D)** is shown. Similar experiments were carried out in HEK-293 cells with AAV2-WT or AAV2 S/T/K mutant vectors at an MOI of 2×10^3 VG/cell **(E)**. Quantitative analysis of these data by flow cytometric analysis is shown in **(F)**. The data depicted in **(A)**, **(C)**, and **(E)** are representative histograms whereas the data in **(B)**, **(D)**, and **(F)** are means of triplicate analyses. One-way analysis of variance (ANOVA) was used for statistical analysis.*$p<0.05$, **$p<0.01$ versus AAV2-WT-infected cells. Color images available online at www.liebertpub.com/hgtb

AAV2 serine/threonine/lysine mutant vectors demonstrate significantly improved transduction efficiency in vitro

Each of the S/T/K residues identified in the vicinity of phosphodegrons (Figs. 1 and 2) was mutated either as a single mutant ($n=24$) or as a double mutant ($n=2$). The vast majority of these S/T/K mutant capsids did not affect the vector packaging efficiency (Table 2), suggesting that modification of these specific amino acids had negligible effect on the capsid structure. Only four of the mutants generated, S276A (1.65×10^{10} VG/ml), T454A (2.5×10^{10} VG/ml), T503A (5.25×10^{10} VG/ml), and T716A (5.25×10^{10} VG/ml), had consistently 8- to 24-fold lower average packaging titers compared with the AAV2-WT vector and were used only for the *in vitro* transduction studies. Among the 15 S/T→A mutant AAV2 vectors tested for their transduction efficiency at a multiplicity of infection (MOI) of 2000 in HeLa cells, 11 had a significantly higher increase in EGFP-positive cells (63–97%) compared with AAV2-WT vector-infected cells (41%) by FACS analysis (Fig. 4).

We then assessed the transduction potential of the nine single-mutant and two double-mutant AAV2 K→R vectors in HeLa cells at an MOI of 2000. The K532R and K544R single mutants and one double mutant (K490+532R) showed significantly higher transduction compared with the AAV2-WT vector (82–70 vs. 30%) by flow cytometric analysis (Fig. 4C and D). To further rule out the possibility that this increase in transgene expression was cell line specific, the best-performing AAV2 mutant vectors—T251A, S276A, S489A, S498A, and K532R—were further tested in HEK-293 cells, which showed a similar increase in EGFP expression by FACS analysis (38–71 vs. 17%) (Fig. 4E). These data were further corroborated by fluorescence imaging of AAV vector-infected cells, which demonstrated higher EGFP expression with most of the AAV S/T/K mutant vectors (Fig. 5A and B).

AAV2 S/T/K mutant vectors improve hepatic gene transfer in C57BL/6 mice in vivo

To analyze the liver-directed gene expression of the various AAV2 mutant vectors, we next examined their potential efficacy *in vivo*. AAV2 S/T/K mutant vectors that package as

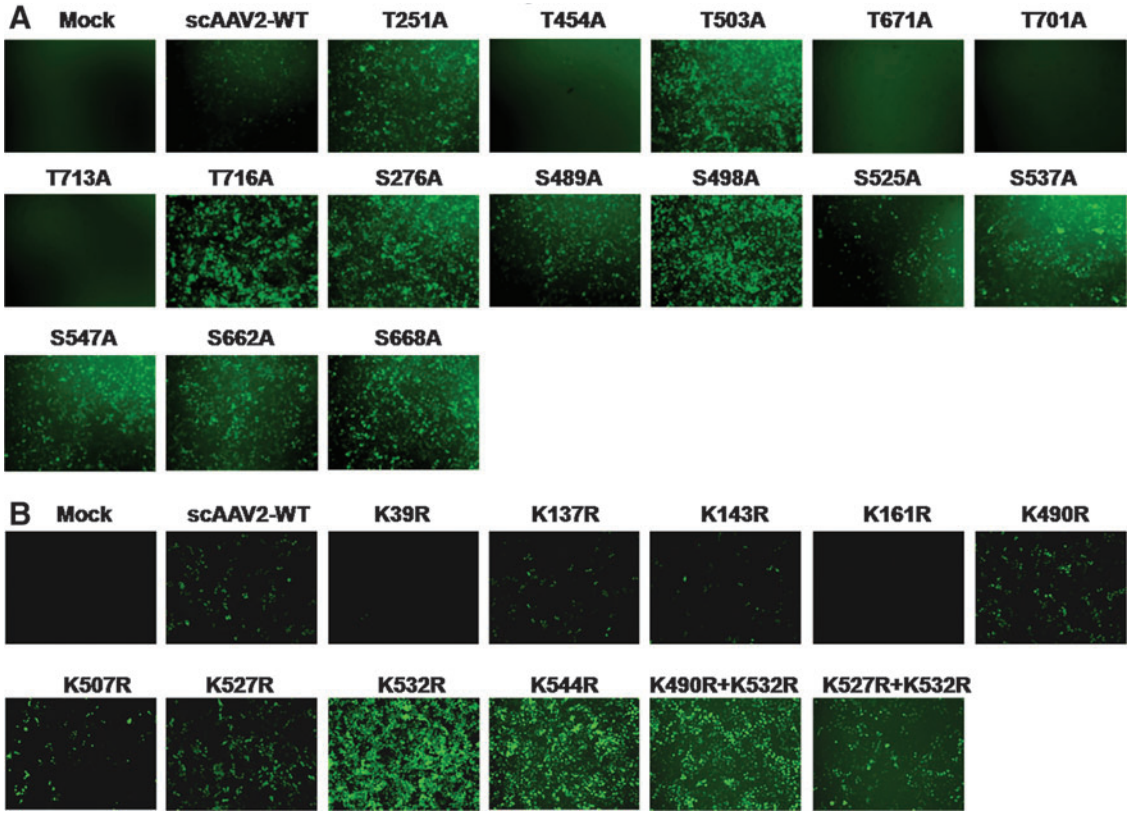

FIG. 5. Fluorescence imaging of HeLa cells infected with AAV2 wild-type or S/T/K mutant vectors. HeLa cells were either mock-infected or infected with AAV2-WT or AAV2 S/T/K mutant vectors at 2×10^3 VG/cell. Forty-eight hours later, the cells were analyzed by fluorescence microscopy. **(A)** Visual comparison of AAV2 S/T→A mutants compared with AAV2-WT vectors. **(B)** Visual comparison of AAV2 K→R mutants compared with AAV2-WT vectors. Color images available online at www.liebertpub.com/hgtb

efficiently as the AAV2-WT vector and those that showed enhanced transgene expression *in vitro* were administered at a dose of 5×10^{10} VG/animal. Consistent with our *in vitro* studies, liver tissues of mice administered the four S→A mutants (S489A, S498A, S662A, and S668A) and the T251A mutant showed higher levels of EGFP reporter when compared with animals injected with AAV2-WT vector and analyzed by fluorescence microscopy (Fig. 6A). A similar increase in EGFP levels was noted after hepatic gene transfer with the AAV2 lysine mutants K532R, K544R, and K490R+K532R (Fig. 7A). To confirm this phenomenon, we then measured AAV vector genome copy numbers in the liver tissue of vector- or mock-injected mice. As shown in Figs. 6B and 7B, a significant increase in vector copies per diploid genome (up to 4.9-fold) was observed in animals injected with S/T/K mutant vectors in comparison with animals that received the AAV2-WT vector alone. To further corroborate these data, we then measured the transcript levels of EGFP in hepatic RNA isolated from these mice. Our studies demonstrate higher levels of transgene transcript expression (up to 14-fold) after hepatic gene transfer, in AAV2 S/T/K mutant-administered mice in comparison with AAV2-WT vector-injected animals (Figs. 6C and 7C). In all these studies, AAV8-injected animals were used as a control group for hepatic gene transfer. Taken together, our data clearly suggest that select S/T→A and K→R mutations can augment the transduction efficiency of AAV2 vectors *in vivo.*

AAV2 S489A mutant vector demonstrates significantly lower neutralizing antibody formation in vivo

Serially diluted serum samples from animals injected with AAV2-WT or with AAV2 S489A, S525A, S537A, S547A, or S662A vector were assayed for neutralizing antibody formation against these vectors (Table 3). The S489A vector-injected group had an 8-fold lower neutralization antibody titer compared with animals injected with AAV2-WT vector. These results imply that the S→A mutation at amino acid position 489 in AAV capsid generated fewer antibodies that could be cross-neutralized by AAV2-WT vectors. Interestingly, the S489A vector also demonstrated 14-fold higher EGFP transcript levels over AAV2-WT vectors in transduced liver (Fig. 6C).

Targeted mutagenesis of lysine residue on AAV2 reduces ubiquitination of AAV vectors

To understand whether the improved transduction achieved with the lysine mutant vectors is due to decreased ubiquitination of viral capsid, we performed an *in vitro* ubiquitination assay followed by Western blotting to detect the levels of mono- and polyubiquitin moieties in the AAV2 capsid. As can be seen in Fig. 8, the AAV2 K532R mutant vector demonstrated significantly reduced ubiquitination compared with either the AAV2-WT or AAV5-WT vector. Interestingly, AAV5 capsid had higher ubiquitination than

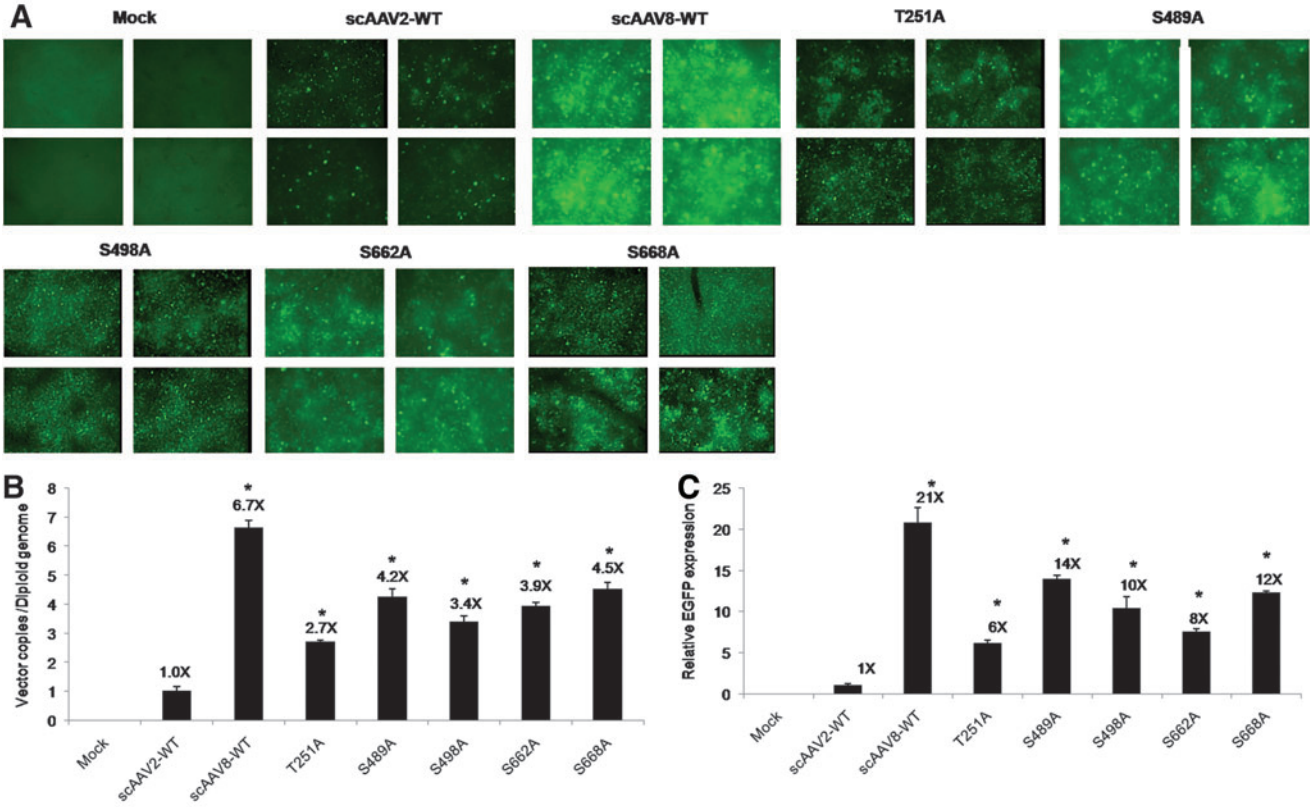

FIG. 6. AAV2 serine/threonine mutant vectors exhibit enhanced transduction on hepatic gene transfer *in vivo.* **(A)** Transgene expression was detected by fluorescence microscopy 4 weeks post-injection of scAAV2-EGFP, scAAV8-EGFP, or AAV2 mutant S/T vectors at 5×10^{10} vector particles per animal. Representative images of hepatic tissues from four different animals in each group are shown. **(B)** Estimation of vector genome copies in liver after AAV-mediated gene transfer. Genomic DNA was isolated from the liver tissue of C57BL/6 mice 4 weeks after vector administration and viral copy numbers were estimated by quantitative PCR as described in Materials and Methods. **(C)** Analysis of EGFP transcript levels by real-time quantitative PCR. Hepatic RNA isolated from animals injected with AAV2-WT, AAV8-WT, or AAV2 S/T vector was analyzed for EGFP expression; the data are normalized to the GAPDH reference gene. One-way analysis of variance (ANOVA) was used for the statistical comparisons. *$p<0.05$ versus AAV2-WT-injected animals. Color images available online at www.liebertpub.com/hgtb

did AAV2-WT capsid, a phenomenon that has been reported previously (Yan *et al.*, 2002). These data provide direct evidence that the superior transduction achieved with the AAV2 K532R mutant vector is due to reduced ubiquitination of the viral capsid, which possibly results in rapid intracellular trafficking of the virus and improved gene expression, as has been suggested previously for the AAV2 tyrosine mutant vectors (Zhong *et al.*, 2008a).

AAV2 S/T/K mutant vectors do not cause any adverse event in C57BL/6 mice

The *in vivo* administration of AAV2 S/T/K mutant vectors did not lead to any significant histological abnormalities in the livers of C57BL/6 mice 4 weeks after vector administration. Livers of mice injected with either AAV2-WT or AAV2 S/T/K mutant vectors were grossly normal with comparable inflammation scores. A set of representative data, shown in Fig. 9, corroborate that AAV2 S/T/K mutant vectors were generally nontoxic and that no adverse events were evident at the 4-week post-injection time point.

Discussion

The collective experience from various AAV2-mediated clinical trials suggests that strategies to improve the transduction efficiencies of these vectors are needed to circumvent the dose-dependent immune response directed against them and to achieve successful long-term gene transfer (Jiang *et al.*, 2006; Jayandharan *et al.*, 2008). Consequently, there has been tremendous interest in evaluating other naturally occurring isolates of AAV (AAV1 through AAV12) or bioengineered AAV strains (Choi *et al.*, 2005; Zincarelli *et al.*, 2008) for gene transfer, each validated for their own desirable properties such as tissue tropism or other clinically relevant challenges. Despite this, AAV2 remains the predominant serotype vector currently in use in human gene therapy applications (High, 2011) as it is the best characterized in terms of vector toxicology. However, its optimal use is contingent on a thorough understanding of the fundamental steps in virus–host cell interactions, which include viral binding and entry (Summerford and Samulski, 1998), intracellular trafficking (Duan *et al.*, 1999), nuclear transport, uncoating (Shi *et al.*, 2006), and viral second-strand DNA synthesis. As previously noted,

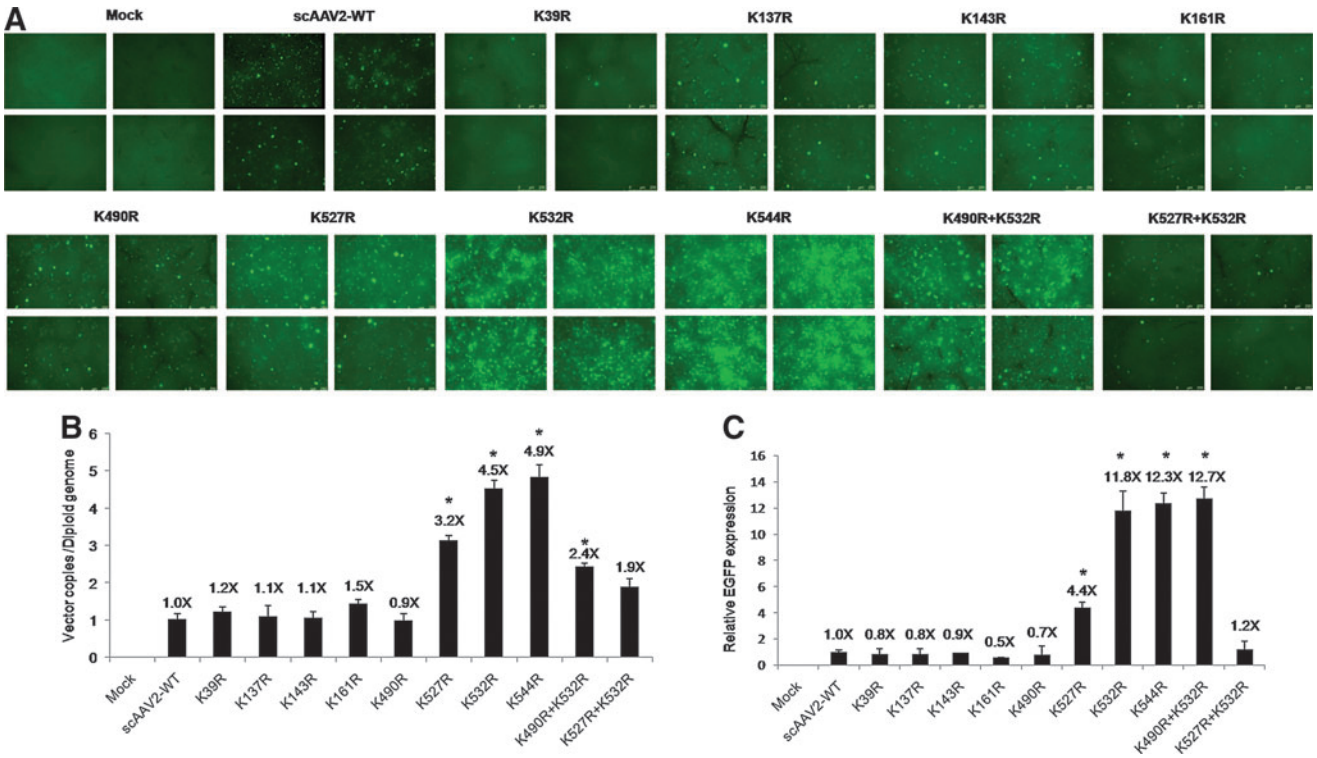

FIG. 7. Analysis of AAV2 lysine mutant vector-mediated EGFP expression in hepatocytes of normal C57BL/6 mice in comparison with wild-type AAV2 vector-mediated EGFP expression. **(A)** Transgene expression was detected by fluorescence microscopy 4 weeks post-injection of scAAV2-EGFP or AAV2 K→R mutant vector at 5×10^{10} vector particles per animal. Representative images of hepatic tissues from four different animals in each group are shown. **(B)** Estimation of vector genome copies in liver after AAV-mediated gene transfer. Genomic DNA was isolated from the liver tissue of C57BL/6 mice 4 weeks after vector administration and the viral copy numbers were estimated by quantitative PCR as described in Materials and Methods. **(C)** Analysis of EGFP transcript levels by real-time quantitative PCR. Hepatic RNA isolated from animals injected with AAV2-WT or K→R mutant vector was analyzed for EGFP expression; the data are normalized to the GAPDH reference gene. One-way analysis of variance (ANOVA) was used for the statistical comparisons. *$p<0.05$ versus AAV2-WT-injected animals. Color images available online at www.liebertpub.com/hgtb

viral intracellular trafficking is an important rate-limiting step that directly influences the efficiency of transgene expression (Sanlioglu *et al.*, 2001). Because it is known that this process is regulated largely by host cellular phosphorylation of the viral capsid, strategies aimed at reversing this block by concurrent administration of pharmacological inhibitors may possibly work, as demonstrated in our present and previous studies (Monahan *et al.*, 2010). However, their applicability in human gene therapy is likely to be limited because of toxicity concerns (Ding *et al.*, 2006). Alternatively, to scale up this approach for possible use in liver-directed human gene therapy, modification of specific phosphorylation targets is likely to be a viable strategy.

Table 3. Neutralizing Antibody Titers: AAV2 S→A Vectors Compared with AAV2-WT[a]

Serum no.	*Group*	*Reciprocal NAb Titer*
1	scAAV2-WT	5,120
2	S489A	640
3	S525A	5,120
4	S537A	5,120
5	S547A	5,120
6	S662A	5,120
7	Anti-AAV2 rabbit control serum	81,920

[a]AAV2 S489A vector demonstrates lower neutralization antibody titers compared with the WT-AAV2 vector. Pooled serum samples from WT-AAV2- or AAV2 mutant-injected mice ($n=4$ per group) were analyzed for neutralizing antibodies 4 weeks after vector administration. Values are the reciprocal of the serum dilution at which relative luminescence units (RLUs) were reduced 50% compared with virus control wells (no test samples).

The concept of mutagenesis of the AAV capsid sequence has been previously employed to generate novel AAV vectors either by targeted evolution or by targeted design. Directed evolution of AAV vectors to generate chimeric AAVs with enhanced gene transfer to the airway epithelia, CNS tissue, or retina has been reported. Similarly, rationally designed AAV strains with robust abilities to transfer genes into muscle (AAV2.5) or with enhanced immunogenic profiles to act as vaccine candidates (Lin *et al.*, 2009) are also available. Mutagenesis of the surface-exposed tyrosines (Y) to phenylalanine (F) has been shown to substantially improve gene expression by up to severalfold in a variety of tissues such as the liver, retina, and musculoskeletal targets (Zhong *et al.*, 2008b; Petrs-Silva *et al.*, 2009, 2011). However, the transduction efficiency of these tyrosine mutants varies according to the target cell type. For example, the AAV2 Y730F mutant shows enhanced gene transfer into

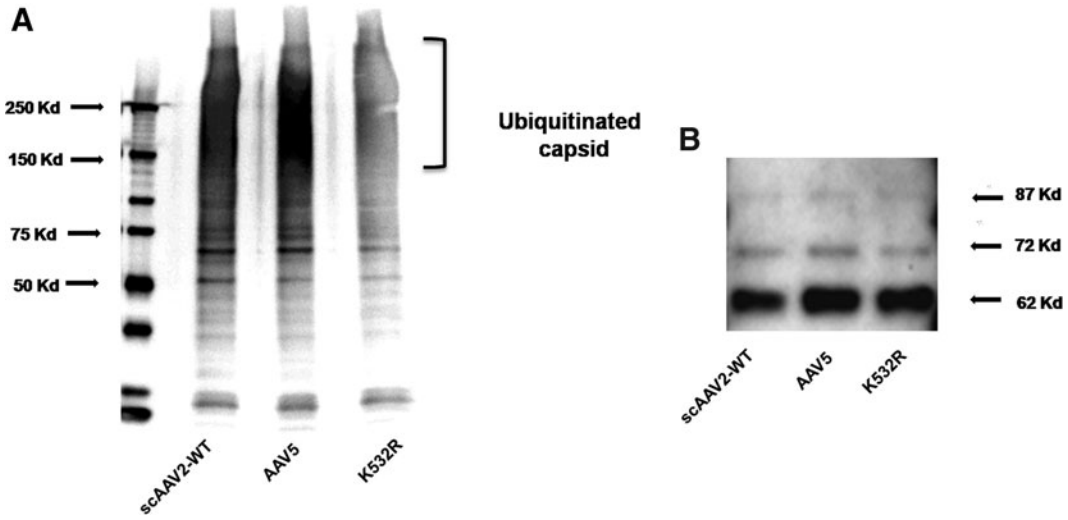

FIG. 8. AAV2 lysine mutant K532R demonstrates reduced ubiquitination compared with the AAV2-WT and AAV5-WT vectors. **(A)** Approximately 3×10^8 viral particles of AAV2-WT, AAV5-WT, and AAV2 K532R vectors were denatured at 95°C for 5 min. The denatured viral particles were then used to perform the ubiquitin conjugation assay according to the manufacturer's protocol. The processed samples were electrophoresed on a 5–20% denaturing polyacrylamide gel and the ubiquitination pattern was detected by immunoblotting with an anti-ubiquitin antibody. The mono- to-polyubiquitin conjugates were detected as a smear at molecular mass >150 kDa. **(B)** Capsid VP1, VP2, and VP3 proteins were used as loading control.

hepatocytes but when directed to stem cells or the retina, its efficiency is modest (Kauss *et al.*, 2010; Ryals *et al.*, 2011). This may possibly be due to varying levels of tyrosine kinase activity in these tissues or to the differential accessibility of the cellular tyrosine kinase to the tyrosines on the AAV2 capsid, the surface exposure of which may be determined in part by specific receptor and coreceptor binding as well as by the varied endosomal processing in these tissues (Qing *et al.*, 1999; Kaludov *et al.*, 2001; Kashiwakura *et al.*, 2005; Seiler *et al.*, 2006). However, we reasoned that apart from targeting tyrosine kinase targets on the AAV capsid, modifying other kinase targets such as S/T residues or ubiquitination targets such as K residues on the AAV2 capsid is likely to further improve its gene delivery. It is important to note that phosphorylation of the viral capsid serves as a trigger for uncoating and release of viral nuclear material inside the host cell. Hence, phosphorylation sites must be mutated more strategically and cannot be replaced at random. Keeping this in mind, a thorough analysis of viral capsid structure was carried out. Three phosphodegron sequences were identified in the AAV2 capsid. The phosphorylation sites within the phosphodegrons were thought to be effective and safer

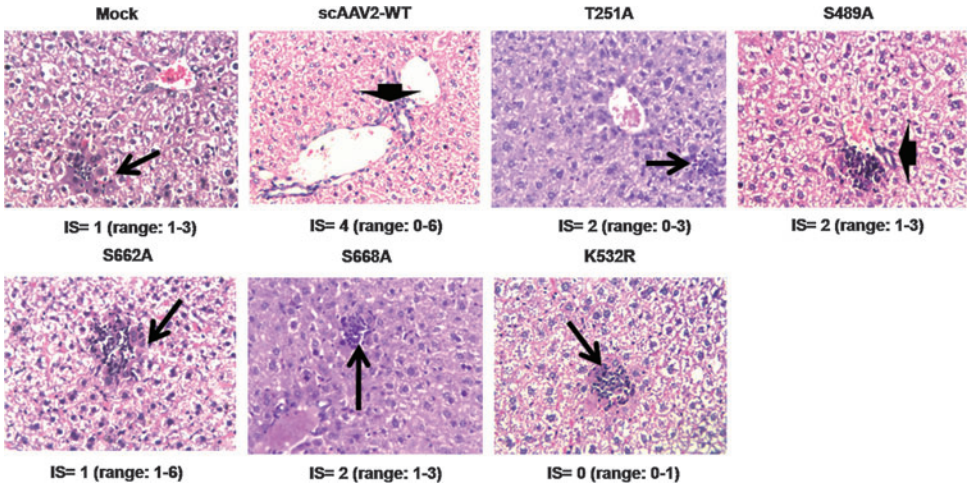

FIG. 9. Histological examination of C57BL/6 liver samples 4 weeks postinjection of AAV2-WT or mutant vector. Hepatic sections were fixed in 10% buffered formalin and stained with hematoxylin–eosin. The median inflammation score (IS) for each group is indicated below the images (original magnification, ×40) with the range of values given within parentheses. Arrowheads and arrows denote portal and focal lobular inflammation, respectively. A representative image of one animal liver from each group ($n = 3$) is shown. Color images available online at www.liebertpub.com/hgtb

targets to mutate as they are the ones used by the host as a signal for clearance of the virus. These residues are thus expected to have minimal influence on the capsid-uncoating processes, essential for the virus inside the host cell. Also, to preserve capsid geometry, only those residues that lie outside the interaction interfaces in the phosphodegron were selected for mutagenesis.

Our hypothesis was further supported by our preliminary studies, in which specific inhibition of CKII serine/threonine kinase increased the transduction profile of AAV2-WT vectors. Subsequently, 24 single S/T/K residues in and around phosphodegrons were selected as targets for site-directed mutagenesis, and our data show that selective modification of these targets on the AAV2 capsid substantially improved gene expression from AAV2 vectors both *in vitro* (up to 97%) and *in vivo* (up to 14-fold). The enhanced transduction seen with the S→A mutants in our study is similar to that with S→V (valine) mutations, which have been shown to be efficacious in gene delivery into dendritic cells *in vitro*. (Aslanidi *et al.*, 2012). As highlighted in Table 2 and Fig. 2, residues S489 and S498 are located in phosphodegron 3, residues S662 and S668 are in/near phosphodegron 2, and residue K532 is part of phosphodegron 1. The effect of these mutations thus corroborates our selection process for the mutagenesis targets. Further ongoing studies with the optimal S/T/K-mutant AAV2 vectors expressing human coagulation factor IX in preclinical models of hemophilia B will demonstrate the feasibility of the use of these novel vectors for potential gene therapy of hemophilia B.

Interestingly, previous mutations at the K532 residue have shown disparate effects on vector infectivity and heparin binding. Opie and colleagues (2003) demonstrated that substitution of K532/K527 with alanine had a modest effect on heparin binding but that the mutant was ~5 logs less infectious than AAV2-WT. Kern and colleagues (2003) have shown that the K532A mutant had similar infectivity but reduced heparin binding. In the present study, the packaging titer of the K532R mutant was 10 times higher and ~6-fold higher infectivity was seen when compared with the AAV2-WT vector (Kern *et al.*, 2003). Taken together, these data suggest that AAV2 K532 might not be as important as other basic residues (R585 and R588) for effective heparin binding (Opie *et al.*, 2003). This can be further substantiated by the fact that both AAV1 (which binds poorly to heparin) and AAV3 (which binds to heparin effectively) have conserved K532. However, it is possible that our choice to replace the lysine amino acid with a structurally compatible arginine instead of alanine perhaps contributed to the observed increase in packaging titers and also its infectivity by minimizing the charge switch on the AAV2 capsid surface. It has been demonstrated that AAV2 capsid mutants generated with various amino acid substitutions can have varied transduction efficiencies (Aslanidi *et al.*, 2012). Hence, the choice of amino acid for mutagenesis has a significant effect on AAV2 vector packaging and transduction efficiency.

The availability of superior AAV2 S/T/K mutant vectors presents several possibilities. First, about ~30% of the S/T/K residues that we mutated are conserved in AAV serotypes 1–10. It is therefore tempting to speculate that S/T/K mutations on other AAV serotypes (1–12) are likely to increase the transduction capabilities of these vectors as well. Second, multiple combinations of these AAV S/T/K mutants are also possible and this is likely to further minimize the overall phosphorylation and ubiquitinated amino acid content of the AAV capsid. Further ongoing studies on the above-mentioned strategies are likely to offer a vast repertoire of these S/T/K mutants and a tool kit of superior AAV vectors.

Acknowledgments

The authors thank Dr. R. Sumathy and Mr. Y. Sathish (Laboratory Animal Core Facility, Centre for Stem Cell Research, Vellore) for animal care. G.R.J. is supported by research grants from the Department of Science and Technology, Government of India (Swarnajayanti Fellowship 2011); the Department of Biotechnology (DBT), Government of India (Innovative Young Biotechnologist award 2010: BT/03/IYBA/2010; grant BT/PR14748/MED/12/491/2010; grant BT/01/COE/08/03); and an early career investigator award (2010) from the Bayer Hemophilia Awards program (Bayer). R.A.G. is supported by a grant under the Women Scientists Programme from the Department of Science and Technology (New Delhi, India). G.S. is supported by a Ph.D. student fellowship from the DBT (New Delhi, India). N.S. acknowledges the support of the DBT, Government of India.

Author Disclosure Statement

No competing financial interests exist.

References

Aslanidi, G.V., Rivers, A.E., Ortiz, L., *et al.* (2012). High-efficiency transduction of human monocyte-derived dendritic cells by capsid-modified recombinant AAV2 vectors. Vaccine 30, 3908–3917.

Aurnhammer, C., Haase, M., Muether, N., *et al.* (2011). Universal real-time PCR for the detection and quantification of adeno-associated virus serotype 2-derived inverted terminal repeat sequences. Hum. Gene Ther. Methods 23, 18–28.

Becerra, S.P., Rose, J.A., Hardy, M., *et al.* (1985). Direct mapping of adeno-associated virus capsid proteins B and C: A possible ACG initiation codon. Proc. Natl. Acad. Sci. U.S.A. 82, 7919–7923.

Berman, H.M., Westbrook, J., Feng, Z., *et al.* (2000). The Protein Data Bank. Nucleic Acids Res. 28, 235–242.

Buning, H., Perabo, L., Coutelle, O., *et al.* (2008). Recent developments in adeno-associated virus vector technology. J. Gene Med. 10, 717–733.

Calcedo, R., Vandenberghe, L.H., Gao, G., *et al.* (2009). Worldwide epidemiology of neutralizing antibodies to adeno-associated viruses. J. Infect. Dis. 199, 381–390.

Chenna, R., Sugawara, H., Koike, T., *et al.* (2003). Multiple sequence alignment with the Clustal series of programs. Nucleic Acids Res. 31, 3497–3500.

Choi, V.W., McCarty, D.M., and Samulski, R.J. (2005). AAV hybrid serotypes: Improved vectors for gene delivery. Curr. Gene Ther. 5, 299–310.

De, S., Krishnadev, O., Srinivasan, N., and Rekha, N. (2005). Interaction preferences across protein–protein interfaces of obligatory and non-obligatory components are different. BMC Struct. Biol. 5, 15.

DeLano, W. (2002). The PyMOL molecular graphics system. Available at: http://www.pymol.org/

Ding, Q., Dimayuga, E., Markesbery, W.R., and Keller, J.N. (2006). Proteasome inhibition induces reversible impairments in protein synthesis. FASEB J. 20, 1055–1063.

Duan, D., Sharma, P., Dudus, L., *et al.* (1999). Formation of adeno-associated virus circular genomes is differentially regulated by adenovirus E4 ORF6 and E2a gene expression. J. Virol. 73, 161–169.

Force, T., and Kolaja, K.L. (2011). Cardiotoxicity of kinase inhibitors: The prediction and translation of preclinical models to clinical outcomes. Nat. Rev. Drug Discov. 10, 111–126.

Girod, A., Wobus, C.E., Zadori, Z., *et al.* (2002). The VP1 capsid protein of adeno-associated virus type 2 is carrying a phospholipase A2 domain required for virus infectivity. J. Gen. Virol. 83, 973–978.

Hatakeyama, S., Matsumoto, M., and Nakayama, K.I. (2005). Mapping of ubiquitination sites on target proteins. Methods Enzymol. 399, 277–286.

High, K.A. (2011). Gene therapy for haemophilia: A long and winding road. J. Thromb. Haemost. 9(Suppl. 1), 2–11.

Hubbard, S.J., and Thornton, J.M. (1993). NACCESS. Department of Biochemistry and Molecular Biology, University College London, London, UK.

Inobe, T., Fishbain, S., Prakash, S., and Matouschek, A. Defining the geometry of the two-component proteasome degron. Nat. Chem. Biol. 7, 161–167.

Jayandharan, G.R., Zhong, L., Li, B., *et al.* (2008). Strategies for improving the transduction efficiency of single-stranded adeno-associated virus vectors *in vitro* and *in vivo*. Gene Ther. 15, 1287–1293.

Jiang, H., Lillicrap, D., Patarroyo-White, S., *et al.* (2006). Multiyear therapeutic benefit of AAV serotypes 2, 6, and 8 delivering factor VIII to hemophilia A mice and dogs. Blood 108, 107–115.

Kaludov, N., Brown, K.E., Walters, R.W., *et al.* (2001). Adeno-associated virus serotype 4 (AAV4) and AAV5 both require sialic acid binding for hemagglutination and efficient transduction but differ in sialic acid linkage specificity. J. Virol. 75, 6884–6893.

Kashiwakura, Y., Tamayose, K., Iwabuchi, K., *et al.* (2005). Hepatocyte growth factor receptor is a coreceptor for adeno-associated virus type 2 infection. J. Virol. 79, 609–614.

Kauss, M.A., Smith, L.J., Zhong, L., *et al.* (2010). Enhanced long-term transduction and multilineage engraftment of human hematopoietic stem cells transduced with tyrosine-modified recombinant adeno-associated virus serotype 2. Hum. Gene Ther. 21, 1129–1136.

Kern, A., Schmidt, K., Leder, C., *et al.* (2003). Identification of a heparin-binding motif on adeno-associated virus type 2 capsids. J. Virol. 77, 11072–11081.

Koerber, J.T., Jang, J.H., and Schaffer, D.V. (2008). DNA shuffling of adeno-associated virus yields functionally diverse viral progeny. Mol. Ther. 16, 1703–1709.

Kube, D.M., and Srivastava, A. (1997). Quantitative DNA slot blot analysis: Inhibition of DNA binding to membranes by magnesium ions. Nucleic Acids Res. 25, 3375–3376.

Li, M., Jayandharan, G.R., Li, B., *et al.* (2010). High-efficiency transduction of fibroblasts and mesenchymal stem cells by tyrosine-mutant AAV2 vectors for their potential use in cellular therapy. Hum. Gene Ther. 21, 1527–1543.

Lin, J., Calcedo, R., Vandenberghe, L.H., *et al.* (2009). A new genetic vaccine platform based on an adeno-associated virus isolated from a rhesus macaque. J. Virol. 83, 12738–12750.

Ling, C., Lu, Y., Cheng, B., *et al.* (2011). High-efficiency transduction of liver cancer cells by recombinant adeno-associated virus serotype 3 vectors. J. Vis. Exp. 49, 2538.

Lochrie, M.A., Tatsuno, G.P., Christie, B., *et al.* (2006). Mutations on the external surfaces of adeno-associated virus type 2 capsids that affect transduction and neutralization. J. Virol. 80, 821–834.

Manno, C.S., Pierce, G.F., Arruda, V.R., *et al.* (2006). Successful transduction of liver in hemophilia by AAV-Factor IX and limitations imposed by the host immune response. Nat. Med. 12, 342–347.

Mingozzi, F., and High, K.A. (2011). Therapeutic *in vivo* gene transfer for genetic disease using AAV: Progress and challenges. Nat. Rev. Genet. 12, 341–355.

Monahan, P.E., Lothrop, C.D., Sun, J., *et al.* (2010). Proteasome inhibitors enhance gene delivery by AAV virus vectors expressing large genomes in hemophilia mouse and dog models: A strategy for broad clinical application. Mol. Ther. 18, 1907–1916.

Nathwani, A.C., Tuddenham, E.G., Rangarajan, S., *et al.* (2011). Adenovirus-associated virus vector-mediated gene transfer in hemophilia B. N. Engl. J. Med. 365, 2357–2365.

Nonnenmacher, M., and Weber, T. (2012). Intracellular transport of recombinant adeno-associated virus vectors. Gene Ther. 19, 649–658.

Opie, S.R., Warrington, K.H., Jr., Agbandje-McKenna, M., *et al.* (2003). Identification of amino acid residues in the capsid proteins of adeno-associated virus type 2 that contribute to heparan sulfate proteoglycan binding. J. Virol. 77, 6995–7006.

Petrs-Silva, H., Dinculescu, A., Li, Q., *et al.* (2009). High-efficiency transduction of the mouse retina by tyrosine-mutant AAV serotype vectors. Mol. Ther. 17, 463–471.

Petrs-Silva, H., Dinculescu, A., Li, Q., *et al.* (2011). Novel properties of tyrosine-mutant AAV2 vectors in the mouse retina. Mol. Ther. 19, 293–301.

Qing, K., Mah, C., Hansen, J., *et al.* (1999). Human fibroblast growth factor receptor 1 is a co-receptor for infection by adeno-associated virus 2. Nat. Med. 5, 71–77.

Rajkumar, S.V., Richardson, P.G., Hideshima, T., and Anderson, K.C. (2005). Proteasome inhibition as a novel therapeutic target in human cancer. J. Clin. Oncol. 23, 630–639.

Ryals, R.C., Boye, S.L., Dinculescu, A., *et al.* (2011). Quantifying transduction efficiencies of unmodified and tyrosine capsid mutant AAV vectors *in vitro* using two ocular cell lines. Mol. Vis. 17, 1090–1102.

Sanlioglu, S., Monick, M.M., Luleci, G., *et al.* (2001). Rate limiting steps of AAV transduction and implications for human gene therapy. Curr. Gene Ther. 1, 137–147.

Seiler, M.P., Miller, A.D., Zabner, J., and Halbert, C.L. (2006). Adeno-associated virus types 5 and 6 use distinct receptors for cell entry. Hum. Gene Ther. 17, 10–19.

Shi, X., Fang, G., Shi, W., and Bartlett, J.S. (2006). Insertional mutagenesis at positions 520 and 584 of adeno-associated virus type 2 (AAV2) capsid gene and generation of AAV2 vectors with eliminated heparin-binding ability and introduced novel tropism. Hum. Gene Ther. 17, 353–361.

Simonelli, F., Maguire, A.M., Testa, F., *et al.* (2010). Gene therapy for Leber's congenital amaurosis is safe and effective through 1.5 years after vector administration. Mol. Ther. 18, 643–650.

Stroes, E.S., Nierman, M.C., Meulenberg, J.J., *et al.* (2008). Intramuscular administration of AAV1-lipoprotein lipase S447X lowers triglycerides in lipoprotein lipase-deficient patients. Arterioscler. Thromb. Vasc. Biol. 28, 2303–2304.

Summerford, C., and Samulski, R.J. (1998). Membrane-associated heparan sulfate proteoglycan is a receptor for adeno-associated virus type 2 virions. J. Virol. 72, 1438–1445.

Trempe, J.P., and Carter, B.J. (1988). Alternate mRNA splicing is required for synthesis of adeno-associated virus VP1 capsid protein. J. Virol. 62, 3356–3363.

Wang, Y., Guan, S., Acharya, P., *et al.* Multisite phosphorylation of human liver cytochrome P450 3A4 enhances Its gp78- and CHIP-mediated ubiquitination: A pivotal role of its Ser-478 residue in the gp78-catalyzed reaction. Mol. Cell. Proteomics 11, M111.010132.

Wu, G., Xu, G., Schulman, B.A., *et al.* (2003). Structure of a β-TrCP1-Skp1-β-catenin complex: Destruction motif binding and lysine specificity of the SCF(β-TrCP1) ubiquitin ligase. Mol. Cell 11, 1445–1456.

Xie, Q., Bu, W., Bhatia, S., *et al.* (2002). The atomic structure of adeno-associated virus (AAV-2), a vector for human gene therapy. Proc. Natl. Acad. Sci. U.S.A. 99, 10405–10410.

Yan, Z., Zak, R., Luxton, G.W., *et al.* (2002). Ubiquitination of both adeno-associated virus type 2 and 5 capsid proteins affects the transduction efficiency of recombinant vectors. J. Virol. 76, 2043–2053.

Zhao, W., Zhong, L., Wu, J., *et al.* (2006). Role of cellular FKBP52 protein in intracellular trafficking of recombinant adeno-associated virus 2 vectors. Virology 353, 283–293.

Zhong, L., Li, B., Jayandharan, G., *et al.* (2008a). Tyrosine-phosphorylation of AAV2 vectors and its consequences on viral intracellular trafficking and transgene expression. Virology 381, 194–202.

Zhong, L., Li, B., Mah, C.S., *et al.* (2008b). Next generation of adeno-associated virus 2 vectors: Point mutations in tyrosines lead to high-efficiency transduction at lower doses. Proc. Natl. Acad. Sci. U.S.A. 105, 7827–7832.

Zincarelli, C., Soltys, S., Rengo, G., and Rabinowitz, J.E. (2008). Analysis of AAV serotypes 1–9 mediated gene expression and tropism in mice after systemic injection. Mol. Ther. 16, 1073–1080.

Zolotukhin, S., Byrne, B.J., Mason, E., *et al.* (1999). Recombinant adeno-associated virus purification using novel methods improves infectious titer and yield. Gene Ther. 6, 973–985.

Address correspondence to:
Dr. G.R. Jayandharan
Department of Hematology and
Centre for Stem Cell Research
Christian Medical College
Vellore-632004, Tamil Nadu
India

E-mail: jay@cmcvellore.ac.in

Received for publication October 8, 2012;
accepted after revision January 31, 2013.

Published online: February 4, 2013.

9. APPENDICES

9.1 Maps of the plasmids used for recombinant AAV production

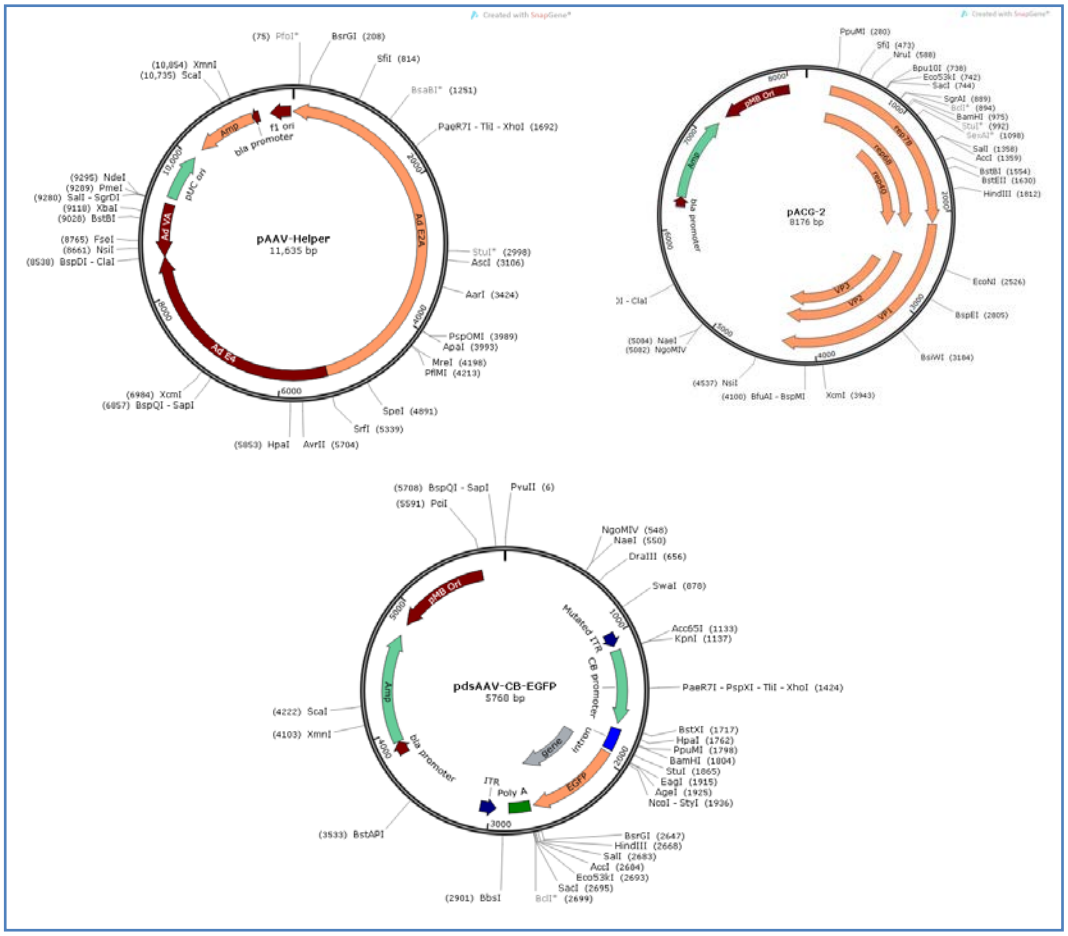

Figure 42: ***Maps of the plasmids used for packaging of scAAV2-EGFP vectors.*** *The maps of the three plasmids used for packaging of scAAV2-EGFP vectors namely AAV2 rep-cap plasmid (pACG2), Helper plasmid (pAAV-Helper) and scAAV-EGFP (pdsAAV-CB-EGFP) are shown.*

9.2 Sequencing primers of AAV2 cap gene

Primer	Sequence (5'-3')
AAV2cap1	GGATGACTGCATCTTTGAACAATAA
AAV2cap2	CTTGAACCTCTGGGCCTGGT
AAV2cap3	CAGCCAATCAGGAGCCTCGA
AAV2cap4	TGGAGTACTTTCCTTCTCAG
AAV2cap5	GGACGATGAAGAAAAGTTTT
AAV2cap6	TGCGGCAAAGTTTGCTTCCT

Table 7: Primers used for sequencing of AAV2 cap gene within the rep-cap plasmid.